



Feedback Regulation Loop Between Bone  
Morphogenetic Proteins and their  
Antagonists in Prostate Cancer and the  
Implication in Bone Metastasis

---

---

By

Jeyna Resaul

Cardiff China Medical Research Collaborative

Cardiff University School of Medicine

October 2018

Thesis submitted to Cardiff University for the degree of Doctor of Philosophy

## Acknowledgements

The path for the completion of this thesis has been challenging but it could not have been achieved without the constant encouragement from the team at CCMRC and Cardiff University and my family.

Firstly, I would like to expression my sincerest gratitude to my supervisors, Doctor Lin Ye and Professor Wen Jiang for their undying and continued support, patience and guidance through my PhD study.

Besides this, I would like to thank Miss Fiona Ruge, Doctor Nicola Jordan, Doctor Andrew Sanders, Doctor Tracey Martin, Doctor Ping-Hui Sun, Doctor Sioned Owen and Doctor Hoi Ping Weeks, for their invaluable help and advice. I would also like to thank Mr Aled Holt who has been incredibly understanding and supportive throughout this whole process.

Finally, I would like to express my gratitude to my fellow PhD students, who have continuously made me laugh through the difficult times. Robyn Bradbury, David Feng, Bethan Frugtniet, Bruno Bastos, Sarah Koushyar, Emily Telford, Ben Lanning, Ross Collins and Valentina Flamini, I will forever be grateful for your friendship, I could never have wished for a better bunch of people to share these years with.

To my family, there are no words that could express how utterly thankful I am to you. Mum and Dad, your continued faith in me is the reason behind this thesis. Thank you.

## Summary

Bone morphogenetic proteins (BMP) have been heavily implicated in prostate cancer and bone metastasis. With various studies demonstrating a feedback loop between BMPs and their regulators, BMP antagonists, we aimed to investigate the role of this interplay in prostate cancer and osteoblastic bone lesion formation.

We assessed the expression of BMPs, their antagonists, and their signalling components in different prostate cancer cell lines in the absence and presence of a bone matrix extract (BME) by RNA-Seq and qPCR. We also analysed GEO data from a prostate cancer cell line expression study, and microarray studies of LNCaP-osteoblast co-cultures and prostate cancer bone metastases. From these, we demonstrated evidence of a BMP/BMP antagonist feedback loop, especially between BMP-2 and Gremlin isoforms, GREM1 and GREM2. BMP antagonists Noggin, Follistatin isoform FST344, and Gremlin were then overexpressed in DU145 using the pEF6/V5-HIS-TOPO<sup>®</sup> TA vector and the resultant cell lines DU145<sup>PEF</sup>, DU145<sup>NOG</sup>, DU145<sup>FST344</sup> and DU145<sup>GREM</sup> were subjected to functional assays examining cell proliferation, invasion, adhesion and migration. Results demonstrated that Noggin and FST344 may have a protective effect against prostate cancer bone metastasis due to their inhibition of cell growth and migration, and stimulation of adhesion, although FST344 also caused an increase in invasion in BME. In contrast, DU145<sup>GREM</sup> showed an increase in cell growth and migration, with minimal effects from BME. qPCR analyses and the GEO data gave more evidence of a BMP/BMP antagonist relationship affecting EMT status and MMP expression profile of cancer cells, with further indication of a BMP-2/Gremlin interplay.

Our study demonstrates the importance of a BMP/BMP antagonist interplay in the establishment of prostate cancer bone metastases. While further experimentation is required to decipher the precise molecular mechanisms underlying this interplay, this could present a novel therapeutic target for the prevention or treatment of prostate cancer and its related bone metastasis.

## Publications

Shi L, Resaul J, Owen S, Ye L, Jiang WG (2016). Clinical and Therapeutic Implications of Follistatin in Solid Tumours. *Cancer Genomics Proteomics*. 13(6): 425-435

Zabkiewicz C, Resaul J, Hargest R, Jiang WG, Ye L (2017). Bone Morphogenetic Proteins, Breast Cancer, and Bone Metastases: Striking the Right Balance. *Endocrine-Related Cancer*. 24(10):349-366

Zabkiewicz C, Resaul J, Hargest R, Jiang WG, Ye L (2017). Increased Expression of Follistatin in Breast Cancer Reduces Invasiveness and Clinically Correlates with Better Survival. *Cancer Genomics Proteomics*. 14(4): 241-251

## Contents

Chapter 1.....	1
1.1 Prostate cancer .....	2
1.2 Diagnosis .....	5
1.2.1 PSA testing .....	5
1.2.2 Digital Rectal Examination .....	6
1.2.3 Biopsy .....	6
1.3 Staging of Prostate Cancer .....	7
1.3.1 Gleason Grading System .....	7
1.3.2 TNM Staging .....	10
1.4 Pathophysiology of Prostate Cancer .....	12
1.4.1 ASAP .....	12
1.4.2 PIN and High-Grade PIN .....	13
1.4.3 Androgen Independence .....	13
1.5 Cancer Metastasis .....	15
1.5.1 Local Invasion .....	15
1.5.2 Cell migration .....	16
1.5.3 Intravasation and Survival in the Circulation .....	17
1.5.4 Extravasation and Colonisation of Distant Sites .....	18
1.6 Prostate Cancer Metastasis .....	20
1.6.1 The Bone .....	21
1.6.2 Pathophysiology of Bone Metastasis .....	24
1.7 BMPs .....	28
1.7.1 Biochemical properties of BMP proteins .....	28
1.7.2 Structure of BMPs .....	29
1.8 BMP Receptors.....	31
1.9 BMP signalling.....	33
1.9.1 The Smad-dependent pathway.....	34
1.9.2 The Smad-independent pathway.....	36
1.10 Regulation of BMP Signalling .....	38
1.11 BMP Signalling in the Bone .....	39
1.12 Aberrance of BMPs and their Implications in Prostate Cancer.....	40
1.13 BMP antagonists .....	43
1.13.1 Noggin .....	45

1.13.2	Follistatin.....	46
1.13.3	Gremlin.....	47
1.14	BMP antagonists and Prostate Cancer.....	47
1.15	Aims.....	48
Chapter 2.....		51
2.1	General Materials .....	52
2.1.1	Cell lines .....	52
2.1.2	Primers .....	52
2.2	Standard reagents and solutions .....	57
2.2.1	Solutions for use in Cell Culture.....	57
2.2.2	Solutions for use in Molecular Biology .....	59
2.2.3	Solutions for use in Cloning .....	60
2.3	Cell Culture, Maintenance, Storage and Transfection .....	60
2.3.1	Preparation of Growth Media.....	60
2.3.2	Cell Maintenance .....	61
2.3.3	Adherent Cell Trypsinisation and Cell Counting .....	61
2.3.4	Transfection of Cells by Electroporation.....	63
2.3.5	Storage of Cell Stocks in Liquid Nitrogen .....	63
2.3.6	Cell Resuscitation .....	64
2.4	Methods for RNA Detection.....	64
2.4.1	mRNA Isolation .....	64
2.4.2	RNA Quantification .....	66
2.4.3	Reverse Transcription .....	66
2.4.4	Reverse Transcription Polymerase Chain Reaction .....	67
2.4.5	Agarose Gel Electrophoresis .....	68
2.4.6	Quantitative Polymerase Chain Reaction .....	69
2.4.7	RNA sequencing .....	72
2.5	Alteration of Gene Expression in Prostate Cancer Cell Lines.....	74
2.5.1	TOPO Gene Cloning and Generation of Stable Transfectants .....	74
2.5.2	Gene Overexpression.....	75
2.5.3	Extraction of PCR products from Agarose Gel .....	76
2.5.4	TOPO TA Gene Cloning.....	77
2.5.5	Transformation of Chemically Competent <i>E. coli</i> .....	79
2.5.6	Colony Selection and Orientation Analysis .....	79
2.5.7	Vector Amplification, Purification and Quantification.....	81
2.5.8	Establishment of Stably Transfected Mammalian Cell Lines .....	82
2.6	<i>In vitro</i> Functional Assays.....	83

2.6.1	Cell Proliferation Assay .....	84
2.6.2	Matrigel Invasion Assay .....	85
2.6.3	Matrigel Adhesion Assay.....	87
2.6.4	Migration Assay (Wound Assay) .....	89
2.6.5	ECIS.....	89
2.7	Database Research.....	91
2.8	Statistical analysis .....	92
Chapter 3.....		94
3.1	Introduction .....	95
3.2	Materials and Methods.....	98
3.2.1	Cell lines and Treatments.....	98
3.2.2	RNA isolation and cDNA synthesis .....	98
3.2.3	RT-PCR.....	99
3.2.4	RNA-Seq .....	99
3.2.5	GEO Database .....	99
3.3	Results.....	100
3.3.1	Expression of BMPs in Prostate Cancer Cell Lines .....	100
3.3.2	Expression of BMP antagonists in Prostate Cancer Cell Lines .....	101
3.3.3	Expression of BMPRs in Prostate Cancer Cell Lines .....	103
3.3.4	Expression of Smads in Prostate Cancer Cell Lines .....	104
3.4	Discussion.....	105
Chapter 4.....		111
4.1	Introduction .....	112
4.2	Materials and Methods.....	115
4.2.1	Cell lines and Treatments.....	115
4.2.2	RNA isolation and cDNA synthesis .....	115
4.2.3	qPCR .....	116
4.2.4	RNA-Seq .....	116
4.2.5	GEO database.....	116
4.3	Results.....	117
4.3.1	Expression of BMPs in Prostate Cancer Bone Metastasis.....	117
4.3.2	Expression of BMP antagonists in Prostate Cancer Bone Metastasis.....	120
4.3.3	Expression of BMPRs in Prostate Cancer Bone Metastasis .....	124
4.3.4	Expression of Smads in Prostate Cancer Bone Metastasis .....	126
4.4	Discussion.....	129
Chapter 5.....		135
5.1	Introduction .....	136

5.2	Materials and Methods.....	138
5.2.1	Materials .....	138
5.2.2	Cell lines and Treatments.....	138
5.2.3	Amplification of Noggin, Follistatin and Gremlin Coding Sequences .....	139
5.2.4	Cloning of Noggin, FST344 and Gremlin into pEF6/V5-HIS-TOPO® TA vectors	139
5.2.5	Prostate Cancer Cell Transfection and Generation of Stable Transfectants ....	140
5.2.6	RNA isolation, cDNA synthesis, RT-PCR and qPCR .....	140
5.2.7	<i>In vitro</i> Cell Proliferation Assay .....	141
5.2.8	<i>In vitro</i> Invasion Assay.....	141
5.2.9	<i>In vitro</i> Adhesion Assay .....	142
5.2.10	<i>In vitro</i> Migration Assay .....	142
5.2.11	ECIS.....	143
5.3	Results.....	143
5.3.1	Overexpression of BMP Antagonists in DU145.....	143
5.3.2	BMP Antagonist Overexpression Affects Prostate Cancer Cell Growth .....	144
5.3.3	Overexpression of BMP Antagonists Affects DU145 Cell Invasion .....	146
5.3.4	BMP Antagonist Overexpression Affects DU145 Cell Adhesion .....	148
5.3.5	BMP Antagonist Overexpression and DU145 Cell Migration.....	150
5.4	Discussion.....	152
Chapter 6	.....	157
6.1	Introduction .....	158
6.2	Materials and Methods.....	161
6.2.1	Materials .....	161
6.2.2	Cell lines and Treatments.....	161
6.2.3	RNA isolation and cDNA synthesis .....	161
6.2.4	RNA-Seq .....	162
6.2.5	qPCR .....	162
6.2.6	GEO Database .....	162
6.3	Results.....	163
6.3.1	Differential Expression of EMT markers and MMPs in Osteolytic and Osteoblastic Cell Lines .....	163
6.3.2	Expression Profiles of EMT Markers and MMPs in Osteoblastic and Osteolytic Bone Lesions .....	165
6.3.3	Differential Expression of MMPs in Osteoblastic and Osteolytic Bone Lesions	167
6.3.4	The MMP Expression Profile of the BMP Antagonist Overexpression Cell Lines	169
6.3.5	The BMP/BMP Antagonist Feedback Loop in the Bone Environment.....	170

6.3.6	The EMT Marker Profile of BMP Antagonist Overexpression Cell Lines in the Bone Microenvironment.....	173
6.4	Discussion.....	174
Chapter 7.....		180
<b>Bibliography.....</b>		<b>187</b>
Appendix .....		212

## List of Figures

Figure		Page
1.1	Age-specific incidence of prostate cancer (UK)	3
1.2	Gleason Grading	7
1.3	The four phases of bone remodelling	23
1.4	The steps involved in cancer cell metastasis to the bone	27
1.5	Schematic of BMP activation	29
1.6	The structure of BMP-2 and BMPR-IA extracellular interaction	33
1.7	The Smad-dependent and the Smad-independent signalling pathways	37
1.8	Inhibition of BMPs by BMP antagonists	45
2.1	Diagram depicting the principle behind qPCR using the Amplifluor™ Universal Detection System	71
2.2	Schematic representation of the Ion Torrent sequencing workflow	73
2.3	Flow-chart depicting the TOPO® TA cloning procedure	74
2.4	Schematic of the pEF6/V5-HIS TOPO® vector	77
2.5	Verifying the insert orientation of newly generated Noggin, Follistatin and Gremlin overexpression vectors	81
2.6	Crystal Violet dilution curve	84
2.7	Schematic illustration of the <i>in vitro</i> Matrigel invasion assay	86
2.8	Representative image of Crystal Violet-stained cells attached to a Matrigel-coated well during an adhesion assay	88
3.1	Expression of BMPs in Prostate Cancer Cell Lines	100
3.2	Expression of BMP antagonists in Prostate Cancer Cell Lines	102
3.3	Expression of BMPRs in Prostate Cancer Cell Lines	103
3.4	Figure 3.4: Expression of Smads in Prostate Cancer Cell Lines	104

4.1	Expression of BMPs in BME-treated Prostate Cancer Cell Lines and in Prostate Cancer Bone Metastasis Samples	118
4.2	BMP expression profile during LNCaP-hOB co-culture	119
4.3	Expression of BMP antagonists in BME-treated Prostate Cancer Cell Lines and in Prostate Cancer Bone Metastasis Samples	121
4.4	The differential expression of BMPs in osteoblastic and osteolytic bone metastatic lesions	122
4.5	BMP antagonist expression profile during LNCaP-hOB co-culture	123
4.6	Expression of BMPRs in BME-treated Prostate Cancer Cell Lines and in Prostate Cancer Bone Metastasis Samples	124
4.7	BMPR expression profile during LNCaP-hOB co-culture	125
4.8	Expression of Smads in Prostate Cancer Cell Lines and in Prostate Cancer Bone Metastasis Samples	127
4.9	Smad expression profile during LNCaP-hOB co-culture	128
5.1	Overexpression of BMP antagonists in the DU145 cell line	144
5.2	Effects of BMP antagonist overexpression on DU145 cell growth	145
5.3	Effects of BMP antagonist overexpression on DU145 cell invasion	147
5.4	Effects of BMP antagonist overexpression on DU145 cell adhesion	149
5.5	Effects of BMP antagonist overexpression on DU145 cell migration	151
6.1	Differential Expression of EMT markers and MMPs between osteolytic and osteoblastic cell lines	164
6.2	The EMT expression profile of osteoblastic and osteolytic bone lesions	165
6.3	The MMP expression profile in osteoblastic and osteolytic prostate cancer bone lesions	168
6.4	BMP-mediated expression of MMPs	169
6.5	The BMP/BMP antagonist feedback loop behind cancer cell behaviour in the bone environment	172

6.6	The EMT profile of the BMP Antagonist Overexpression Cell Lines in the Bone Environment	174
-----	--	-----

## List of Tables

<b>Table</b>		<b>Page</b>
1.1	Gleason Grading for Prostate Cancer	9
1.2	The 2017 TNM Classification for prostate adenocarcinoma	11
2.1	Details of prostate cancer cell lines used in this study	53
2.2	Primers used for conventional RT-PCR	54
2.3	Primers used for qPCR	55
2.4	Primers used for the cloning of Noggin, FST344 and Gremlin vectors	56

## Abbreviations

3D: 3-dimensional

A: deoxyadenosine

aa: amino acid

ActR-IA: type-IA activin receptor

ActR-IIA: type-IIA activin receptor

ActR-IIB: type-IIB activin receptor

ADT: androgen deprivation therapy

AJCC: American Joint Committee on Cancer

ALK: Activin like kinase receptor

Ang: angiopoietin

AR: androgen receptor

ARE: androgen responsive element

BAMBI: BMP and activin membrane-bound inhibitor

BISC: bone morphogenetic protein-induced signalling complexes

BM: basement membrane

BME: bone matrix extract

BMEC: bone marrow endothelial cells

BMP: bone morphogenetic protein

BMPR: bone morphogenetic protein receptor

BPH: benign prostatic hyperplasia

BRAM1: bone morphogenetic protein receptor associated molecule 1

BSS: buffered salt solution

CAF: cancer-associated fibroblast

CAM: cell adhesion molecule

Cbfa-1: core-binding factor subunit alpha-1

CCLE: Cancer Cell Line Encyclopaedia

cDNA: complementary deoxyribonucleic acid

co-IP: co-immunoprecipitation

Co-SMAD: common-Smad

CSC: cancer stem-like cell

CTC: circulating tumour cell

CXCL12: C-X-C motif chemokine-12

DAN: differential screening-selected gene aberrative in neuroblastoma

DEPC: diethyl pyrocarbonate

DHT: dihydrotestosterone

Dlx5: distal-less homeobox-5

DMEM: Dulbecco's Modified Eagle's Medium

DRE: digital rectal examination

DTC: disseminated cancer cell

E-Cadherin: epithelial cadherin

ECIS: Electric Cell-substrate Impedance Sensing®

ECM: extracellular matrix

EDTA: ethylebediaminetraacetic acid

emPCR: emulsion polymerase chain reaction

EMT: epithelial to mesenchymal transition

EMT-TFs: EMT-inducing transcription factors

ERK: extracellular signal-regulated kinase

FBS: foetal bovine serum

FGF: fibroblast growth factor

FKBP12: 12kDa FK506-binding protein

FSD: Follistatin Domain

FST: follistatin

FSTL: follistatin-related protein

GAPDH: glyceraldehyde 3-phosphate dehydrogenase

GDF: growth differentiation factor

GEO: Genomic Expression Omnibus

GREM: Gremlin

GTP: guanosine triphosphate

H&E: haematoxylin and eosin

HGPIN: high-grade PIN

hOBs: primary human osteoblast

HPC1: hereditary prostate cancer locus-1

IGF: insulin-like growth factor

I-Smad: inhibitory-Smad

JNK: c-Jun amino-terminal kinase

KLK3: kallikrein-3

*Mad: Mothers against decapentaplegic*

MAPK: mitogen-activated protein kinase

MET: mesenchymal to epithelial transition

MH1: Mad homology 1

MH2: Mad homology 2

miRNA: micro ribonucleic acid

MMP: matrix metalloproteinase

mPCL-TCP: medical grade polycaprolactone-tricalcium phosphate

mRNA: messenger ribonucleic acid

MSC: mesenchymal stem cell

MT1-MMP: membrane type 1 matrix metalloproteinase

N-Cadherin: neuronal-cadherin

NCBI: National Centre for Biotechnology Information

ND: N-terminal Domain

NGS: Next-Generation Sequencing

NK: Natural Killer

NOG: Noggin

OPG: osteoprotegerin

OPN: osteopontin

PBS: phosphate buffer solution

PDGF: platelet-derived growth factor

PFC: pre-formed hetero-oligomeric complexes

PI3 kinase: phosphoinositide 3-kinase

PIN: prostatic intraepithelial neoplasia

PKA: Protein kinase A

PKC: Protein Kinase C

PP: protein phosphatase

PRDC: protein related to DAN and Cerberus

PSA: prostate-specific antigen

PTHrP: parathyroid-hormone-related peptide

qPCR: quantitative polymerase chain reaction

RANKL: receptor activator of nuclear factor- $\kappa$ B ligand

RNA: ribonucleic acid

RNA-Seq: ribonucleic acid sequencing

RNASEL: Ribonuclease L

RPMI: Roswell Park Memorial Institute

R-Smad: receptor-regulated Smad

RT: reverse transcription

RT-PCR: reverse transcription polymerase chain reaction

Runx2: runt-related transcription factor 2

SCID: severe combined immunodeficient mice

SD: standard deviation

SDF1: stromal cell-derived factor-1

sEcad: E-cadherin

SEM: standard error of the mean

SHBG: sex hormone-binding globulin

Smurf1: Smad ubiquitination regulatory factor-1

SOC: Super Optimal broth with Catabolite repression

T: deoxythymidine

TAB1: TAK1 binding protein

TAK1: TGF- $\beta$  activated kinase 1

TBE: tris-boric-acid

TEB: human tissue engineered bone construct

TEM: transendothelial migration

TF: transcription factor

TGF- $\beta$ : transforming growth factor- $\beta$

TIMP-1: tissue inhibitor of metalloproteinases-1

TNF: tumour necrosis factor

TNM: Tumour Nodal Metastasis

TRUS: transrectal ultrasound-guided biopsy

UICC: Union Internationale Contre le Cancer

USAG-1: uterine sensitization-associated gene-1

v: variant

VEGF: vascular endothelial growth factor

WT: wild-type

XIAP: X-linked inhibitor of apoptosis protein

Zeb1: zinc finger E-box binding homeobox 1

Chapter 1.

# Introduction

## **1.1 Prostate cancer**

Prostate cancer is the most diagnosed male cancer in the developed world and is the second leading cause of cancer-related deaths in the UK, after lung cancer (ONS 2015, Bray, Ferlay et al. 2018). A number of risk factors have been recognised to influence the development of this disease, the most significant factors of which include age, ethnicity, family history, geography and diet.

Age is undoubtedly the most determining risk factor, with prostate cancer increasing in incidence in men over 50. Indeed, there seems to be a consistent trend whereby the probability of developing invasive prostate cancer increases directly with age. Prostate cancer statistics show that in the US for instance, men under the age 49 very rarely develop this disease, demonstrating odds of 0.2% only. However, this percentage sharply rises to 1.7% in 50 to 59-year-olds, 4.8% in 60 to 69-year-olds and 8.2% in 70-year-olds and over (Siegel, Miller et al. 2018). This is a trend that is reflected in mortality rates, with 41% of prostate cancer-related deaths occurring in men aged between 75 and 84, and the 30% occurring in men aged 85 years and over (Wright and Lange 2018).

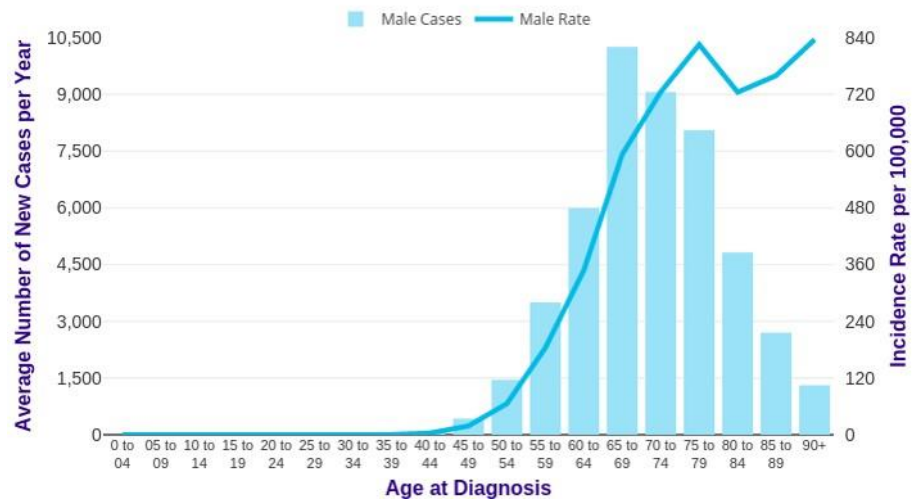


**Figure 1.1: Age-specific incidence of prostate cancer (UK).** Data was obtained from Cancer Research UK and represents the average number of new cases of prostate cancer per year for each age group between 2013 and 2015 (Cancer Research UK, 2018).

The incidence of prostate cancer can also vary by race and ethnicity. Black men, in particular, seem to be disproportionately prone to this disease, so much so that incidence rates in Black populations (120.8 to 247.9 cases per 100,000) are more than double that of White populations (96.0 to 99.9 cases per 100,000) (CRUK 2014). Typically, a geographical variation is also seen in prostate cancer incidence rates, whereby rates in developed countries far exceed that of less developed ones, with rates varying more than 25-fold worldwide. In 2012, approximately 70% of prostate cancer cases occurred in the more developed countries. For example, Australia/New Zealand and North America had the highest prevalence with rates of 111.6 and 97.2 per 100,000 respectively. In contrast, less developed countries like Eastern and South-Central Asia demonstrated a much lower prevalence at 13.9 and 5.0 per 100,000 respectively (Bray, Ferlay et al. 2018). Despite this trend in incidence rates, there is much less variation in mortality rates worldwide, with more developed countries having higher survival rates. These geographical disparities between incidence and mortality rates can mainly be attributed to the standard of medical care and detection by prostate-specific antigen (PSA) testing in these more developed countries.

It is possible that geographical and racial influences on prostate cancer incidence may be overridden by environmental and lifestyle factors. For example, although prostate cancer incidence is relatively low in native Asian populations, it is greatly increased in Asian populations living in more developed countries (Shimizu, Ross et al. 1991, Ito 2014). This indicates that certain factors encountered in those countries may help drive the development of this disease. For instance, several studies have demonstrated a positive association between high fat and dairy product consumption and the risk of developing prostate cancer (Wynder 1979, Chan, Stampfer et al. 2001). Although the exact mechanisms in play are uncertain, the high calcium content in dairy products, for instance, is thought to act by suppressing the production of the most active form of vitamin D,  $1,2,3(OH)_2D_3$ . The latter, along with other micronutrients, like vitamin E, lycopene, selenium, and soya milk have been shown to inversely correlate with prostate cancer risk (Dagnelie, Schuurman et al. 2004, Hwang, Kim et al. 2009). This may explain why Asian populations, which tend to have lower fat and higher soy protein intake, have lower prostate cancer incidence rates than Western populations.

Genetics have been shown to be another important factor to consider in prostate cancer risk. The familial aggregation of this disease was first reported by Morganti and colleagues in 1956, who identified a higher prostate cancer risk in men with relatives affected by this disease (Morganti, Gianferrari et al. 1956). Indeed, men with first-degree relatives affected with prostate cancer have a two or three-fold increased risk of developing prostate cancer - a probability that increases to tenfold if three or more members of the family are affected (Steinberg, Carter et al. 1990, Lesko, Rosenberg et al. 1996). Family history is estimated to be a deciding factor in 5% to 10% of all prostate cancers, with 40% of those cancers being diagnosed in men aged below 55 (Carter, Beaty et al. 1992, Bratt 2002). Several candidate genes have been identified to be potentially associated with prostate cancer. Prostate susceptibility was first mapped to *Ribonuclease L (RNASEL)* and named hereditary prostate cancer locus-1 (HPC1)

(Smith, Freije et al. 1996). Other studied polymorphisms are in the vitamin D-receptor, androgen receptor, *ELAC/HPC2*, *SRD5A2* (5 $\alpha$ -reductase) and *CYP17* (17 $\alpha$ -hydroxylase).

## 1.2 Diagnosis

Typically, prostate cancer is a slow growing cancer, especially in older men. In fact, most prostate cancers remain at a very early stage, where they do not cause any symptoms. However, prostate cancers that do display symptoms most commonly involve nocturia, bladder outlet obstruction, difficulty passing urine and deficiency in emptying the bladder. Advanced or metastatic cases are usually associated with pain in the back, hips, pelvis and other bony areas or haematuria. Three main strategies are used to detect prostate cancer, namely, prostate-specific antigen (PSA), digital rectal examination (DRE) or biopsy.

### 1.2.1 PSA testing

PSA, also known as gamma-seminoprotein or kallikrein-3 (KLK3), is a serine glycoprotein that is produced by prostate epithelial cells. It is believed to act as a liquefying agent in ejaculated seminal fluid, allowing spermatozoa to navigate freely through the uterus (Lilja 1985). During the prostate cancer process, PSA is released into the circulatory system, causing its serum levels to increase up to 10<sup>6</sup>-fold, therefore aiding in the diagnosis of advanced prostate cancer (Lilja, Ulmert and Vickers, 2008). PSA circulates in the blood in different forms, with 70-90% of serum PSA comprising of PSA that is complexed with protease inhibitors termed complexed PSA. The remaining free PSA has three free distinct isoforms: inactive PSA, BPSA and proenzyme-PSA (Özen and Sözen 2006). In general, men with PSA levels of around 5 ng/ml or above are usually referred for further tests. However, diagnosis using PSA can be difficult as its levels can be

affected by various factors, such as age, race, prostatitis, benign prostatic hyperplasia (BPH), as well as urine infections, recent prostate biopsies, prostate or bladder surgery, prostatic massage and recent prostate biopsies. This is because whilst PSA is a prostate specific marker, it is not prostate cancer specific. This raises controversy about its the efficacy of using this method for prostate cancer detection.

### 1.2.2 Digital Rectal Examination

Digital rectal examination (DRE) was the first established method of prostate cancer detection. It is a relatively simple procedure that involves inserting a gloved and lubricated finger into the rectum of a patient to inspect the shape, size and surface of the prostate. Should any irregularities be found, such as hard or bumpy areas, patients are usually referred for further evaluation to assess whether these areas are cancerous or not. DRE, however, lacks sensitivity as only the posterior and lateral sections of the prostate are accessible to the examining finger. Although most prostate cancers arise in these areas, approximately 25-30% of cancers, located in the inaccessible areas, will be missed (McNeal, Bostwick et al. 1986). Moreover, it is possible that cancers that are palpable during DRE may be at more advanced stages.

### 1.2.3 Biopsy

The most common test used for biopsies is transrectal ultrasound-guided biopsy (TRUS). During a TRUS biopsy, an ultrasound probe is inserted in the patient's rectum to build an image of the prostate. The resulting image is then used to direct a spring-loaded 18-gauge biopsy needle to the abnormal areas in order to take small samples.

### 1.3 Staging of Prostate Cancer

In order to decide on the best treatment course for prostate cancer patients, the aggressiveness of the disease first needs to be established. With the results from biopsies, the cancer can be graded and classified through the use of the Gleason grading system and Tumour Nodal Metastasis (TNM) classification.

#### 1.3.1 Gleason Grading System

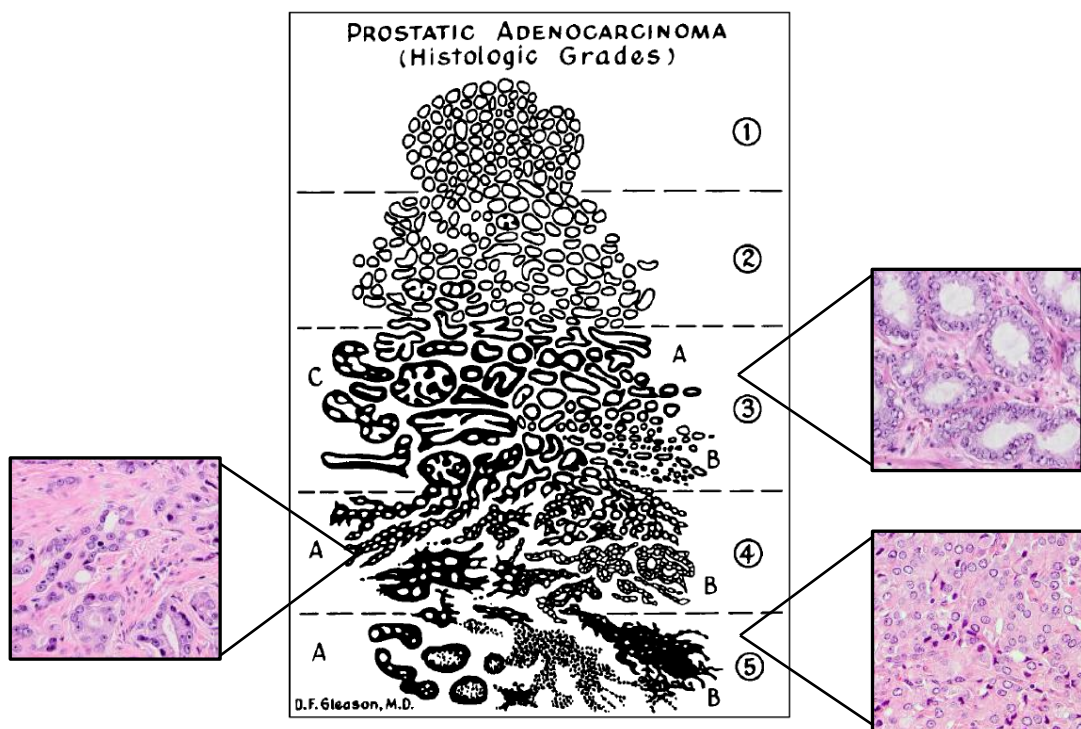


**Figure 1.2: Gleason Grading.** The schematic depicts the Gleason grading system with histological representations of the different grades (adapted from Humphrey 2004 and Koliijn, Verhoef et al. 2015)

In 1966, Dr Donald F Gleason, a pathologist in Minnesota, developed a unique system of grading prostate carcinoma that is based entirely on the architecture of the tumour (Mellinger, Gleason et al. 1967, Gleason and Mellinger 1974, Humphrey 2004). This practice, which is still widely used throughout the world today, examines the histological pattern of prostate carcinoma cells in haematoxylin and eosin (H&E) prostatic tissue sections and categorises the disease by the extent of glandular differentiation and by the growth pattern of the tumour in the prostatic stroma (Gleason 1992).

Based on an initial sample of 270 patients, Dr Gleason described five basic grade patterns (see figure 1.2), classified as ranging from 1 (least aggressive) to 5 (most aggressive). From these, the Gleason histological score, ranging from 2 to 10, is generated by adding the grades of the two most common patterns within the tissue sections, namely the primary and secondary patterns. However, if only one pattern is observed in the tissue sample, or if the secondary pattern is represented by less than 3% of the total tumour, the primary grade is doubled to obtain the corresponding Gleason score (Humphrey 2004).

Despite the grading system, the histomorphological appearance of prostatic carcinoma is quite heterogenous. Therefore, each grade from grade 3 onwards is divided into different subpatterns to help with the recognition of the disease grade. Complete descriptions of the different patterns that can be observed are listed in table 1.1.

<b>Pattern</b>	<b>Tumour Shape and Borders</b>	<b>Stromal Invasion</b>	<b>Tumour Cell Arrangements</b>	<b>Gland Size</b>
1	Nodular with well-defined and smooth edges	Pushing	Single, separate, closely packed, round to oval glands	Medium
2	Less defined and less confined masses	Some gland separation at tumour edge	Single, loosely packed, round to oval glands of variable shape and size with stromal separation	Medium
3A	Ill-defined infiltrating edges	Irregular extension	Single, separate glands of variable shape and size, with elongated, angular and twisted forms, typically with wide stromal separation	Medium
3B	Ill-defined infiltrating edges	Irregular extension	Similar to 3A but with smaller glands	Small to very small
3C	Masses and cylinders with smooth, rounded edges	Expansile	Papillary and cribriform epithelium with no necrosis	Medium to large
4A	Raggedly infiltrative	Diffusely permeative	Fused glands that create masses, cords, or chains	Small, medium, or large
4B	Raggedly infiltrative	Diffusely permeative	Same as 4A, but cells have cleared cytoplasm (hypernephromatoid)	Small, medium, or large
5A	Smooth and rounded cylinders	Expansile	Cribriform, papillary, or solid masses with central necrosis (comedocarcinoma)	Variable
5B	Raggedly infiltrative	Diffusely permeative	Masses and sheets of anaplastic carcinoma, with a few tiny glands or signet ring cells	Small

**Table 1.1: Gleason grading system for prostate cancer** (adapted from Humphrey 2004)

### 1.3.2 TNM Staging

Although the TNM classification for the staging of cancer was developed in the 1940s by Pierre Denoix, it was only in 1992 that the TNM staging system for prostatic carcinoma was first introduced, when the American Joint Committee on Cancer (AJCC) and the Union Internationale Contre le Cancer (UICC) approved a unified TNM staging system for this disease (Greene and Sobin 2002, Cheng, Montironi et al. 2012). This system is based on the evaluation of the primary tumour (T), the regional lymph nodes (N), and the metastatic sites (M), with each category being examined through a series of tests (AJCC 1997). The T category is assessed by clinical examination, imaging, biopsy, endoscopy and biochemical tests, the N category is assessed only by clinical examination and imaging, and the M category is assessed by clinical examination, skeletal studies and biochemical tests (UICC 2017).

Each category serves a specific purpose (see table 1.2). Clinical T staging, for example, describes the size of the primary tumour and whether it has spread beyond the prostatic capsule. In fact, it is the most important prognostic indicator for localised prostate cancer. N describes the spread to the regional lymph nodes and is a strong predictor of progression. The last category, M, describes distant metastasis, which in many advanced stages involved the bone.

<b>T – Primary Tumour</b>	
TX	Primary tumour cannot be assessed
T0	No evidence of primary tumour
T1	Clinically inapparent tumour that is not palpable
T1a	Tumour incidental histological finding in 5% or less of tissue resected
T1b	Tumour incidental histological finding in more than 5% of tissue resected
T1c	Tumour identified by needle biopsy (e.g., because of elevated PSA)
T2	Tumour that is palpable and confined within prostate
T2a	Tumour involves one half of one lobe or less
T2b	Tumour involves more than one half of one lobe, but not both lobes
T2c	Tumour involves both lobes
T3	Tumour extends through the prostatic capsule
T3a	Extracapsular extension (unilateral or bilateral) including microscopic bladder neck involvement
T3b	Tumour invades seminal vesicle(s)
T4	Tumour is fixed or invades adjacent structures other than seminal vesicles: external sphincter, rectum, levator muscles and/or pelvic wall
<b>N – Regional Lymph Nodes</b>	
NX	Regional lymph nodes cannot be assessed
N0	No regional lymph node metastasis
N1	Regional lymph node metastasis
<b>M – Metastatic Sites</b>	
M0	No distant metastasis
M1	Distant metastasis
M1a	Non-regional lymph node(s)
M1b	Bone(s)
M1c	Other site(s)

**Table 1.2: The 2017 TNM classification for prostate adenocarcinoma** (adapted from UICC 2017)

## 1.4 Pathophysiology of Prostate Cancer

During the process of malignant transformation, cells undergo multiple alterations affecting normal cell function, gradually evolving from a benign to a malignant phenotype (Hanahan and Weinberg 2011). As such, premalignant lesions may be observed and have in fact been commonly described in many cancers, including that of the skin, gastrointestinal tract, bronchus, urothelium, breast and prostate (Brawer 2005). Indeed, premalignant lesions are frequently diagnosed upon prostatic biopsy, depicting this disease as progressing through a series of states, ranging from the premalignant atypical small acinar proliferation (ASAP), prostatic intraepithelial neoplasia (PIN) to invasive cancer, and androgen-independence.

### 1.4.1 ASAP

It is possible, in around 1.5% to 2% of prostate biopsy specimens, to find a collection of atypical glands (Adamczyk, Wolski et al. 2014). These are known as ASAP lesions. Classically defined as a “a focus of small acinar structures formed by atypical epithelial cells”, the diagnosis of ASAP is proposed when is not possible to find certain key changes in cell morphology that would indicate prostate cancer (Koca, Çalışkan et al. 2011, Adamczyk, Wolski et al. 2014). Therefore, with insufficient data to make a benign or malignant diagnosis, the presence of ASAP raises the suspicion of cancer. It has been reported that the rate of prostate cancer diagnosis in the second biopsy following ASAP diagnosis ranges from 17-70% (O'dowd, Miller et al. 2000, Postma, Roobol et al. 2004).

#### 1.4.2 PIN and High-Grade PIN

PIN, which was first referred to as “intraductal dysplasia”, represents the pre-invasive, neoplastic growth of epithelial cells that occurs within the lining of prostatic acini or ducts. Although PIN lesions had been widely observed for many years, with initial references possibly dating back to between the 1920s to 1940s, it was only in 1965 that John E McNeal recognised the possible malignant nature of these neoplastic growths (Oertel 1926, Andrews 1949, McNeal 1965). Thereafter, together with Bostwick, they described PIN as a biological precursor of invasive prostate cancer, and proposed diagnostic criteria for the recognition of these lesions, in the form of a three-grade classification system, PIN1, PIN2 and PIN3 (McNeal, Bostwick et al. 1986). This grading system has since then been modified, whereby low-grade PIN replaced PIN1, and high-grade PIN (HGPIN) replaced PIN2 and PIN3. Since there is high level of interobserver variability in low-grade PIN observations, pathologists do not normally report this finding. In fact, nowadays the term PIN is used interchangeably with HGPIN (Bostwick, Liu et al. 2004, Bostwick and Qian 2004). With numerous studies having confirmed HGPIN as a precursor to some prostate carcinomas, it has become a clinically important finding in prostate biopsies for the prediction of cancer. Indeed, HGPIN is reported in 5-7% of prostate biopsies, with an associated risk of prostate adenocarcinoma varying between 25-79%, and an estimated timeframe to disease progression from initial HGPIN observation of between 29 and 36 months (Borboroglu, Comer et al. 2000, Klink, Miocinovic et al. 2012).

#### 1.4.3 Androgen Independence

Androgens, and the transcriptional programs they trigger through their cognate binding of the androgen receptor (AR), are absolutely critical for normal prostate development, growth and maintenance of post-natal physiological functions. Testosterone, the main circulating androgen,

is primarily secreted by testicular Leydig cells and circulates in the blood bound to albumin and sex hormone-binding globulin (SHBG), with a small fraction remaining freely dissolved in the serum (Dunn, Nisula et al. 1981, Rosner, Hryb et al. 1991). This free, unbound testosterone is able to enter prostate cells, where it is converted by the 5 $\alpha$ -reductase enzyme to dihydrotestosterone (DHT), which has a 5- to 10-fold higher affinity for AR than its testosterone counterpart (Pienta and Bradley 2006). During physiological signalling, DHT, along with testosterone, can bind to ARs in the cytoplasm, inducing the translocation of the receptor-ligand complex to the nucleus. Once there, the AR is able to act as a transcription factor by localising to specific binding sequences known as androgen responsive elements (AREs), leading to the expression of genes involved in cell growth and survival (Feldman and Feldman 2001).

Like with other signalling pathways in the cancer process, it is not surprising that the AR axis can be perverted into facilitating prostate carcinogenesis. Almost all cancers begin as androgen-dependent, whereby AR signalling is required from the growth and survival of cancer cells. Indeed, androgen depletion therapy (ADT), which aims to devoid androgen-sensitive cells of their growth and survival stimulus, remains the most common prostate cancer treatment. Yet, ADT is not curative for all cases of prostate cancer, as a proportion of cancer cells may develop a number of cellular pathways in order to survive and thrive in an androgen-depleted environment. Documented mechanisms by which cells may become androgen-independent include *AR* amplification and mutation and alterations in AR co-regulators which bind the AR to either activate or suppress the expression of target genes (Saraon, Drabovich et al. 2014).

## 1.5 Cancer Metastasis

Metastasis – the spread of cells from the primary neoplasm to distant organs – is one of the most devastating aspects of cancer. This process comprises of a cascade of events that includes multiple major steps: local invasion, cell migration, intravasation and circulation, and extravasation of tumour cells, followed by angiogenesis and colonisation of the secondary site (see figure 1.4).

### 1.5.1 Local Invasion

Local invasion is one of the most crucial steps in the metastatic cascade. In fact, it is during this stage of cancer progression that malignant cells first acquire the subversive abilities they require to overcome the constraints of normal cellular architecture to eventually invade secondary sites. To do so, neoplastic cells must develop invasive potential by undergoing an epithelial and mesenchymal transition (EMT). In the normal prostate, epithelial cells have very limited migratory abilities due to the many different junctions that anchor them to other cells and to the basement membrane. Therefore, when a cell undergoes a malignant transformation to gain a more migratory phenotype, it must downregulate its cell-cell and cell-matrix adhesiveness, more specifically, through the alteration of the cell adhesion molecules (CAMs) (Mol, Geldof et al. 2007). Indeed, one of the major features of EMT is cadherin switching, whereby, epithelial (E) -cadherin (typically expressed in normal epithelial cells) is downregulated, and neuronal (N) -cadherin (typically expressed in mesenchymal cells) is upregulated (Thiery 2002, Hazan, Qiao et al. 2004). This is a molecular occurrence that has been reported in various metastatic cancers. In prostate cancer alone, tumour specimens from patients with high grade prostate cancer were shown to express lower levels of E-cadherin and higher levels of N-cadherin in comparison to patients with lower grade disease (Gravdal, Halvorsen et al. 2007).

In addition to becoming more motile, cancer cells also need to invade surrounding tissue for a tumour to spread. However, the extracellular matrix (ECM), which is comprised of the basement membrane (BM) and connective tissue, presents a dense, cross-linked barrier that tumour cells need to negotiate and overcome. Thus, through the use of various families of enzymes, the most typical of which being the matrix metalloproteinase (MMP) family, the invasive cells partially degrade the components of the ECM (Nagle, Knox et al. 1994, Egeblad and Werb 2002). In fact, both the levels of MMP-9 and ratios MMP-2/MMP-9 to MMP inhibitor, tissue inhibitor of metalloproteinases-1 (TIMP-1), have been associated with high Gleason score and poorer patient survival (Wood, Fudge et al. 1997).

### 1.5.2 Cell migration

In prostate cancer, as well as others, cell motility and migration are integrally linked to guanosine triphosphate (GTP)-binding proteins, such as Ras and Rho. Members of the Ras family, for example, are known oncogenes in a variety of cancers. As they normally act as switches that regulate the signalling for such processes as cytoskeletal integrity, cell proliferation, gene transcription, apoptosis, and invasion (Oxford and Theodorescu 2003, Takashima and Faller 2013), it is of no surprise that alterations in Ras signalling can ultimately lead to cancer. In fact, although quite rare in prostate cancer (3%), Ras mutations are estimated to be present in approximately 30% of solid tumours (Adjei 2001).

The Rho family of GTPases, on the other hand, are best known for their key roles in cytoskeleton dynamics, leading to cell movements. Due to their inherent function, Rho GTPases have thus been linked to tumour cell migration and metastasis (Ridley 2015). In terms of prostate cancer, inhibition of the Rho GTPase, RhoC, has been shown to decrease the directed migration and invasion of the prostate cancer cell line, PC-3 (Yao, Dashner Ej Fau - van Golen et al. , Sequeira, Dubyk et al. 2008).

### 1.5.3 Intravasation and Survival in the Circulation

Like normal tissues, growing tumours require sustenance in the form of oxygen and nutrients, as well as a means to evacuate waste products and carbon dioxide. As such, once they reach a certain size and start to experience hypoxia, they develop a neovasculature that meets their metabolic needs – a process called angiogenesis. Several prolific families of angiogenic factors have been identified as players in tumour-induced vascular growth. Amongst these, members of the vascular endothelial growth factor (VEGF) family and angiopoietins (Ang) are the best characterised, with VEGF being established as the most potent and direct-acting factor and Ang2 expression being correlated with the poor prognosis of several cancers (Shweiki, Itin et al. 1992, Ferrara and Davis-Smyth 1997, Metheny-Barlow and Li 2003).

In addition to providing sustenance to the tumour, the new blood vessels also offer an escape route by which neoplastic cells can enter the body blood system through a process called intravasation. Alternatively, lymphatic intravasation (entry into the lymphatic system) is another pathway by which tumour cells may enter the circulation through the drainage of the lymph vessels into the venous system via the thoracic duct. The process of intravasation, however, is a very inefficient system. Following their dissemination into the circulatory system, the shear stress of blood flow alone may be enough to destroy circulating tumour cells (CTCs). Moreover, other stresses, such as immunological stress and collisions with other cells, like blood cells and endothelial cells lining the vessel wall, could affect CTC survival (Wirtz, Konstantopoulos et al. 2011). In fact, only a tiny fraction of CTCs survive to generate clinically relevant metastases (Tarin, Price et al. 1984). For example, a 1-cm primary tumour (corresponding to approximately  $1 \times 10^9$  cancer cells), can shed  $1 \times 10^6$  cells into the circulatory system per day (Fidler 2005). However, the comparative metastatic colonisation is very limited, with only as few as 0.01% of CTCs ultimately surviving (Fidler 1970).

Thus, metastasis cannot occur unless tumour cells find ways to evade and withstand the stresses mentioned above. Different murine studies have demonstrated one possible approach during which tumour cells directly interact with platelets and leukocytes to enhance their survival. According to these studies, the different associations created between the platelets and the tumour cells form small tumour emboli, which not only shield the tumour cells from shear forces, but also impede immune cell recognition by Natural Killer (NK) cells, thereby contributing to disease progression (Nieswandt, Hafner et al. 1999, Palumbo, Talmage et al. 2005).

#### 1.5.4 Extravasation and Colonisation of Distant Sites

Even in the 1800s, it was apparent to physicians and researchers that the distribution of the secondary growths arising from cancer metastasis were more than just a matter of chance. In 1889, in an attempt to explain this phenomenon, Sir Stephen Paget set forth the 'seed' and 'soil' analogy. According to his theory, like a plant that goes to seed, neoplastic cells or 'seeds' disseminate from the primary tumour and migrate in all directions; but only those that reach specific organ microenvironments or 'soil' will be able to survive and form secondary cancers (Paget 1889). Impressively, after more than 100 years of research on the metastatic process, Paget's concept still holds true.

Following intravasation, for surviving CTCs to exit the circulatory system and colonise compatible sites, they must first bind the endothelium of the blood vessel wall. There are two ways by which CTCs may do so: physical occlusion and cell adhesion - the mechanism employed depending on the diameter of the local blood vessel. For instance, if a CTC enters a vessel whose diameter is less than that of the CTC, then arrest may occur due to the CTC being physically trapped (Chambers, Groom et al. 2002, Wirtz, Konstantopoulos et al. 2011). Extravasation of CTCs from larger blood vessels, however, is more tumour specific as it requires the adhesion of cells through the formation of specific interactions. Various *in vitro* studies have shown a wide range

of ligands and receptors, including cadherins, integrins, CD44, selectins, and immunoglobulin superfamily receptors, to contribute to the adhesion between CTCs and endothelial cells (Bendas and Borsig 2012, Reymond, d'Água et al. 2013).

Once arrested, tumour cells can roll along or proliferate within blood vessels before extravasating (Al-Mehdi, Tozawa et al. 2000, Stoletov, Kato et al. 2010). Alternatively, the arrested cells can also transmigrate directly through the endothelial barrier as single cells during a process called transendothelial migration (TEM), after which, they then invade the BM surrounding the blood vessels (Gassmann, Haier et al. 2009). When tumour cells grow within the primary tumour, their survival is supported by a co-evolving microenvironment that suppresses immunosurveillance. However, once within the secondary site, this support is not immediately available to the cancer cells and thus, most of them die. Otherwise, extravasated tumour cells may follow two different routes: dormancy (whereby the cancer cells survive without any apparent increases in cell numbers), or colony formation (Chambers, Groom et al. 2002). Which paths are followed partly depends on different factors such as interactions between tumour cells and the various constituents of the target organ parenchyma (for example, ECM components and host stromal cells). Indeed, tumour cell-ECM interactions have been established to be key in the establishment of secondary growths. For instance, studies have reported cell attachments mediated by  $\alpha_2\beta_1$  integrins and CD44 to be critical in the adhesion of prostate cancer cells to collagen type I in the bone and bone marrow endothelial cells (BMECs) respectively (Draffin, McFarlane et al. 2004, Lee, Jin et al. 2013, Sottnik, Daignault-Newton et al. 2013), ultimately enabling prostate cancer colonisation of the bone. Furthermore, the multitude of growth factors present in the ECM, such as transforming growth factor- $\beta$  (TGF- $\beta$ ), bone morphogenetic proteins (BMPs) and VEGF may also contribute to the survival and/or proliferation of extravasated tumour cells (Shibue and Weinberg 2011).

## 1.6 Prostate Cancer Metastasis

In the majority of cases, prostate cancer presents itself as a relatively slow-growing tumour, which means that it typically takes a number of years for the tumour to become large enough to be detectable, and even longer for it to spread beyond the prostate. However, a small percentage of men experience more rapidly growing, aggressive forms of the disease. During the early stages of the disease, the tumour remains confined to the prostate gland. However, as cancer cells acquire subversive characteristics as a result of genetic or environmental influences, they become more aggressive and begin to penetrate surrounding tissues like the bladder, seminal vesicles, erectile nerves and rectum. Meanwhile, as with other solid tumours, cancer cells may also colonise distant sites by intravasating into lymphatic or haematogenous routes, creating different metastatic patterns. For example, the lymphatic route may be involved in metastasis to the obturator, external iliac, presacral and presciatic areas while the leading metastatic sites for the haematogenous route is the lung, liver and most importantly, the bone (Golimbu, Morales et al. 1979, Bubendorf, Schöpfer et al. 2000).

As mentioned earlier, it has long been recognised that cancers spread to distant sites with characteristic preference. The bone is the second most frequent site to be affected, with breast cancer and prostate cancer causing up to 70% of skeletal metastases (Cecchini, Wetterwald et al. 2005). Bone metastases are infrequently clinically silent, the most common symptom being severe pain. Other symptoms include pathological fractures due to the weakening of bones, hypercalcaemia and spinal compression, the latter of which may lead to numbness or weakness in the legs. Furthermore, since bone metastasis may involve the replacement of haematopoietic tissues by invading cancer cells, it can also lead to anaemia, therefore increasing the risk of infection. Ultimately, owing to their impact on haematopoiesis and bone structure, bone metastases are a major cause of morbidity (Cecchini, Wetterwald et al. 2005, Logothetis and Lin 2005). Unfortunately, once patients show evidence of secondary bone metastases, the cancer

is deemed incurable, the only treatment options available at present focus on symptom management and slowing down the progression of the established cancer.

### 1.6.1 The Bone

To fully appreciate the bone-prostate cancer microenvironment, an understanding of the basic structure and function of the bone is useful. The skeleton is composed of two main structural types of bone: the cortical bone and the trabecular (or cancellous) bone. The cortical bone, which makes up 80% of the skeleton, is the dense outer layer that surrounds the marrow, while the trabecular bone, which makes up the remaining 20% of the skeleton, is composed of a honeycomb-like network of trabecular plates and rods interspersed in the bone marrow-containing compartments of bones (Clarke 2008, Theriault 2012). Bones are highly dynamic tissues that experience constant turnover in order to maintain bone strength and mineral homeostasis. This is achieved through the balanced contributions of specialised bone cells, osteoclasts and osteoblasts, that mutually carry out the resorption of old bone and formation of new bone respectively (Clarke 2008). Osteoclast and osteoblast activities are tightly coupled (Howard, Bottemiller et al. 1981). Indeed, bone remodelling events require communication between these two types of cells, which may occur in a number of ways: cell-cell contact, gap junctions, or diffusible paracrine factors.

The bone remodelling cycle takes place in four sequential phases in response to stimuli like low blood calcium levels, loss of mechanical loading, or alterations in cytokines and hormones. These phases are activation, resorption, reversal, formation and termination (Rucci 2008). During the activation phase, changes in the bone environment are detected by osteocytes, which through their death, release regulatory factors that recruit precursors of the haematopoietic lineage

which fuse and differentiate into osteoclasts (Al-Dujaili, Lau et al. 2011). Once the osteoclasts are differentiated and activated, they are then able to proceed through to the next phase, resorption. During this phase, osteoclasts secrete enzymes like matrix metalloproteinase (MMP)-9, tartrate-resistant acid phosphatase, cathepsin K, and gelatinase, to digest the organic matrix. This liberates growth factors, including transforming growth factor- $\beta$  (TGF- $\beta$ ), insulin-like growth factor (IGFs), platelet-derived growth factors (PDGFs) and bone morphogenetic proteins (BMPs), and other molecules that are abundant in the bone (Mundy 2002). Termination of this phase occurs with the programmed cell death of osteoclasts, thus ensuring the non-occurrence of excess resorption (Xing and Boyce 2005).

The next phase, reversal, marks the transition from bone resorption to bone formation. Although this phase is still not completely understood, two events are thought to be key. These are the preparation of the freshly resorbed bone surface for the deposition of new bone matrix carried out by cells of an osteoblastic lineage, and the coupling of mechanisms of bone resorption and bone formation. Indeed, with studies showing the balanced loss and accretion of calcium in bone remodelling, this is thought to be a critical period for the osteoclast-osteoblast coupling (Matsuo and Irie 2008). The exact coupling signals linking the two ends of the bone remodelling spectrum are not yet completely elucidated, though it is known to include recruitment and differentiation of osteoprogenitors of the mesenchymal lineage. Candidate factors that may be involved in this process include those released from the bone matrix during bone resorption (Clarke 2008, Kenkre and Bassett 2018).

Once recruited and differentiation, mature osteoblasts lead the remodelling process through to the next phase, formation. As part of this, successive layers of osteoblasts line the eroded bone surface and secrete an organic, type I collagen-rich matrix material termed osteoid. The latter is

mineralised over time, entrapping osteoblasts within the matrix, where they terminally differentiate into osteocytes (Kenkre and Bassett 2018).

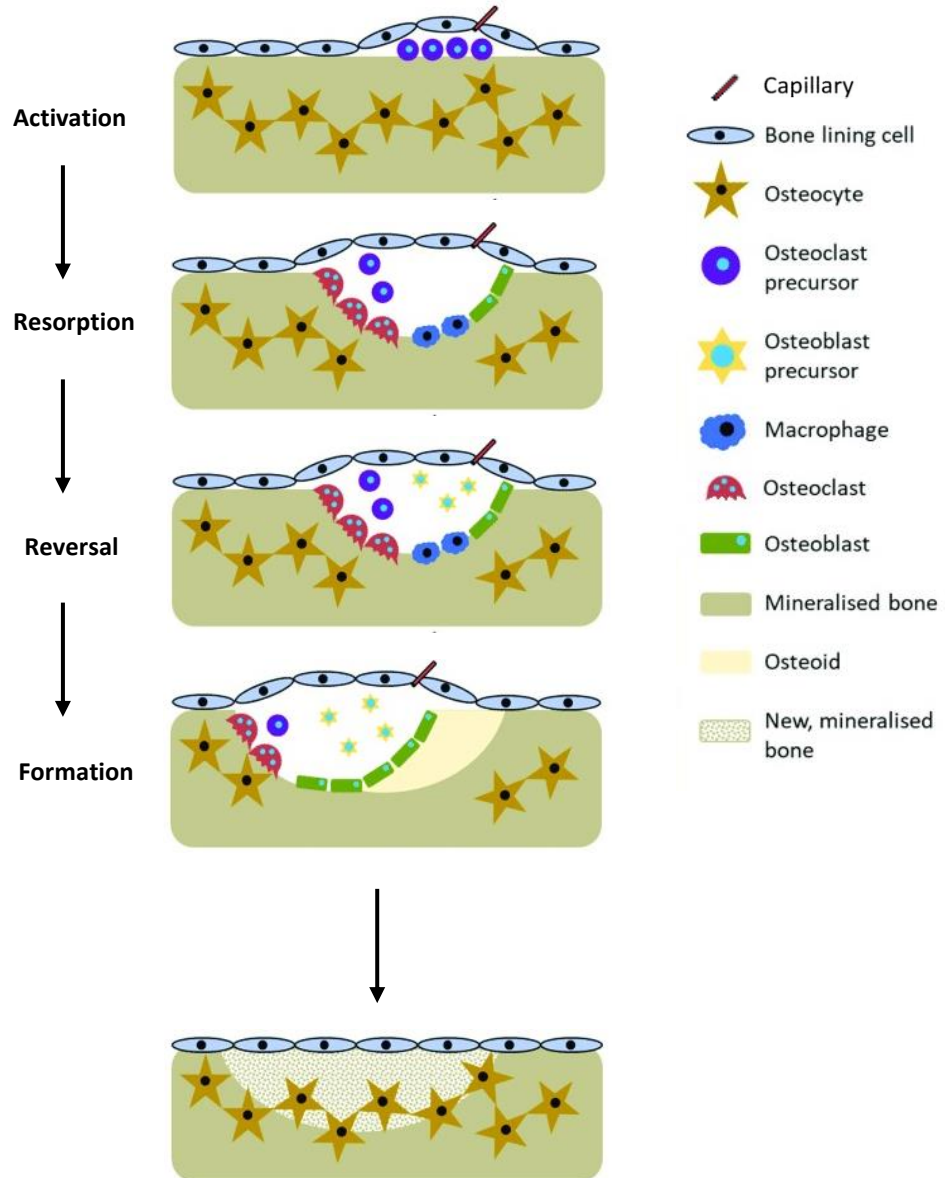


**Figure 1.3: The four phases of bone remodelling.** During the activation phase, apoptosis of osteocytes releases regulatory factors that help differentiate osteoclast precursors into mature osteoclasts. Once differentiated and activated, the osteoclasts are then able to proceed to the resorption phase, during which osteoclasts digest the organic matrix, releasing growth factors from the bone. The following phase, the reversal phase, marks the transition from bone resorption to bone formation. This is made possible through the recruitment and differentiation of osteoblast precursors into mature osteoblasts, a process that is triggered by the growth factors released during the resorption phase. The final phase of the bone remodelling process is the formation phase and involves osteoblasts lining the eroded bone surface to secrete osteoid, which mineralises over time to form new bone (adapted from Owen and Reilly 2018).

### 1.6.2 Pathophysiology of Bone Metastasis

Like with metastasis to other sites, the initial steps in the development of bone metastasis include local invasion of surrounding tissue, intravasation and survival in the circulation and the migration to distant organ sites (see section 1.5 and figure 1.4). However, as a cancer with such high incidences of bone metastasis, advanced prostate cancer metastasis poses an intriguing puzzle: why and how these cancer cells show predilection to the bone rather than other sites. The first attempt in explaining the preferential metastasis of different cancer types came, at the turn of the 20<sup>th</sup> century, from English surgeon, Dr Stephen Paget, when he proposed the 'seed and soil' theory. This concept explains that while cancer cells, much like seeds, disperse in all directions from their primary site, they will only be able to establish where the microenvironment, or soil, is favourable for their survival and growth (Paget 1889).

It is apparent that the anatomical and molecular characteristics the bone possesses make it a favourable target for metastasis (Mastro, Gay et al. 2003). One anatomical characteristic that exemplifies the 'seed and soil' theory is the sluggish blood flow in the sinusoids of the metaphysis that enables initial cancer cell adhesion to the bone marrow endothelium (Phadke, Mercer et al. 2006). With its state of continuous and dynamic turnover, the bone matrix also provides a rich selection of resources, in the form of cells, growth factors, receptors and proteins, that prostate cancer cells can exploit for homing to and colonisation purposes. For instance, the specific homing of CTCs is mediated by the chemokine axis normally employed by haematopoietic stem cells (HSCs) to the bone marrow. By expressing the C-X-C motif receptor (CXCR)-4 and 7, metastatic cancer cells are able to respond to chemotactic gradients of C-X-C motif chemokine-12 (CXCL12), also known as stromal cell-derived factor-1 (SDF1), allowing them to mimic the vascular exit strategy of haematopoietic progenitors upon their return to the bone

marrow from the circulation (Taichman, Cooper et al. 2002, Chinni, Sivalogan et al. 2006, Wang, Shiozawa et al. 2008).

Cross-talk between DTCs and the bone microenvironment is also critical for the establishment secondary colonies. Faced with the highly dense and protective bone matrix, cancer cells need employ a process called the “vicious cycle” to modify their surroundings for survival. As a result of this process, the delicate balance between the resorbing actions of the osteoclasts and the osteogenic functions of the osteoblasts is disrupted, causing a skew towards either extreme of the bone remodelling process. This ultimately results in the formation of osteolytic (bone resorbing) or osteoblastic (bone forming) bone lesions. Various growth factors have been shown to be involved in this process. For instance, during the osteoclastic vicious cycle, tumour cells produce osteoclast-activating factors, the most important of which being the parathyroid-hormone-related peptide (PTHrP), to activate bone resorption (Mundy 2002). With the bone matrix acting as a storehouse for latent growth factors, like members of the TGF- $\beta$ , IGF, PDGF and BMP families, the bone resorption process subsequently causes their release. These are then able to stimulate tumour cell proliferation, further increasing PTHrP levels, thus setting in motion the vicious cycle (Mundy 2002).

Although the term “vicious cycle” is classically used to describe osteolytic lesion formation, a vicious cycle is also known to occur during the development of osteoblastic lesions, whereby prostate cancer cells produce various pro-osteoblastic factors, such as fibroblast growth factors (FGFs), TGF- $\beta$ 1 and TGF- $\beta$ 2, IGF-1 and IGF-2, PDGFs, WNT and BMPs, to induce the recruitment and differentiation of osteoblasts. As a result, the activated osteoblasts mediate the formation of woven bone, all the while secreting growth factors that tumour cells are able to use to potentiate their survival and growth. The growing number of cancerous cells then produce more pro-osteoblastic factors and thus, an osteoblastic vicious cycle is perpetuated. With prostate

cancer producing osteoblastic lesions in more than 95% of cases, this study is more interested in investigating the molecular mechanisms behind the formation of these types of lesions. More, particularly, the role of the pro-osteoblastic factor, BMP, in this process.

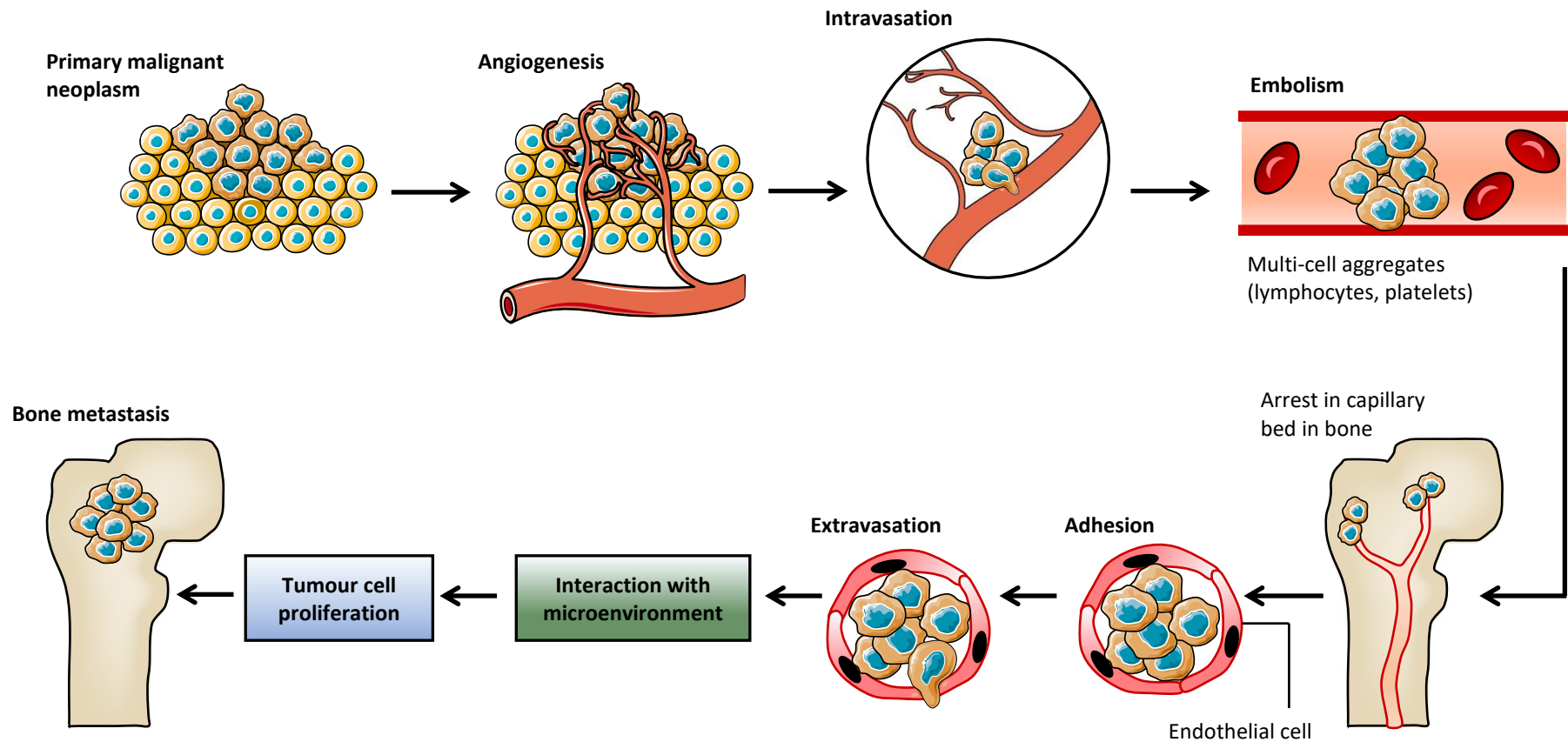


**Figure 1.4: The steps involved in cancer cell metastasis to the bone.** The primary neoplasm invades its immediate surroundings and promotes the formation of new blood vessels. This provides invading cells with an escape route which they can use to enter the circulation. Tumour cells and blood cells may eventually aggregate to form embolisms that arrest in distant capillaries in the bone. Tumour cells eventually adhere to vascular endothelial to extravasate into the bone matrix. In this new environment, they then trigger the “vicious cycle” to support their survival and growth, eventually forming bone metastases (adapted from Mundy 2002).

## 1.7 BMPs

The BMP subfamily of the transforming growth factor- $\beta$  (TGF- $\beta$ ) superfamily was first identified in 1965, by Urist (Ducy and Karsenty 2000), who discovered their ability to induce ectopic bone growth. It was not until the late 1980s, however, when the first BMPs were characterized and cloned, that individual BMPs could be studied biochemically (Wozney, Rosen et al. 1988). Since then, they have been shown to be important morphogens in embryogenesis and development, as well as the regulation of the maintenance of adult tissue homeostasis, by affecting a wide variety of cell types and processes beyond bone and osteogenesis. Indeed, BMP signalling is known to have a crucial role in heart, neural, renal, cartilage and lung development, including airway branching, as well as the maintenance of joint integrity, the initiation of fracture repair, and vascular remodelling by orchestrating cellular processes like cell growth, migration, invasion and adhesion. It is therefore no surprise that anomalies during BMP signalling have been implicated in several human diseases, including development disorders and cancers. In fact, for the last 20 years, BMPs have increasingly been studied in several malignancies, with aberrant expression patterns being reported in various cancers and bone metastases.

### 1.7.1 Biochemical properties of BMP proteins

The BMP subfamily comprises over 20 members. Although they exhibit significant sequence homology, BMPs can be categorised into subgroups, based on their known functions and structural homology. For example, based on phylogenetic similarity, BMP-2 and -4 form the BMP2/4 subgroup, BMP-5, -6, -7 and -8 form the OP-1 subgroup, BMP-9 and -10 form the BMP9/10 subgroup, and BMP-12, -13, -14 (Growth Differentiation Factor; GDF-5, -6 and -7) form the GDF-5 subgroup (Miyazono, Maeda et al. 2005, Wang, Green et al. 2014).

### 1.7.2 Structure of BMPs

Like other members of the TGF- $\beta$  superfamily, BMPs are translated as large precursor proteins consisting of three components. The N-terminal signal peptide sequence, which is composed of 20 amino acids (aa), directs the protein to the secretory pathway. The next region, the pro-domain, whose role has not yet been completely elucidated, varies in length, but normally ranges from 240 to 320 aa. The final region, the C-terminal mature peptide, embodies the functional unit of the BMP protein (Kingsley 1994, Sebald, Nickel et al. 2004).

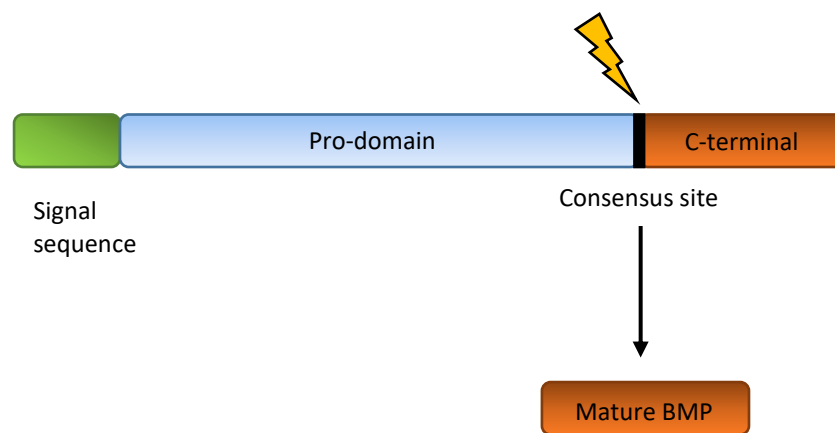


**Figure 1.5: Schematic of BMP activation.** The diagram depicts a simplified view of BMP activation from their large precursor form. The inactive BMP pro-protein consists of three components: the N-terminal signal sequence, the pro-domain and the C-terminal. For the BMP to be functionally active, the precursor needs to be cleaved at the consensus site Arg-X-X-Arg within the pro-domain – a process catalysed by serine endopeptidases.

BMP precursor proteins are formed in the cytoplasm as dimeric pro-protein complexes of about 400 to 500 aa. For the BMP protein to become functionally active however, this precursor needs to be cleaved at the consensus site, Arg-X-X-Arg, present in pro-domain. Cleavage of the proprotein is catalysed by serine endopeptidases with the Trans-Golgi network releasing the C-terminal from the N-terminal – a process that has been shown to be determined by the

downstream amino acid sequence adjacent to the cleavage site (Sieber, Kopf et al. 2009). In TGF- $\beta$ 1, 2 and 3, and myostatin (GDF-8), the pro-domain remains non-covalently attached to the mature peptide, acting as a 'straitjacket' covering all receptor epitopes, hence keeping them in a latent state. In terms of BMPs, although the prodomain has also been reported to remain tethered to the mature forms of BMPs 4, 7, 9, 10, 11 and 12, there is no similar report of the latency effect. In fact, certain studies have observed a role for the proper folding and secretion of certain BMPs (Brown, Zhao et al. 2005, Sopory, Nelsen et al. 2006, Sengle, Ono et al. 2008).

Following activation, the resultant, active, BMP dimer ranges from 50 to 100 aa, with seven highly conserved cysteines in each monomer. Of these seven cysteines, six are stabilised by three intramolecular disulphide bonds, with two pairs forming a ring and the third penetrating the ring, completing a 3-dimensional (3D) structure known as the cysteine knot motif. The seventh cysteine forms the disulphide bond between the BMP monomers, thus forming the biologically active BMP dimer (Butler and Dodd 2003). Bar BMP-3, GDF-9 and BMP-15, which lack a seventh cysteine but are nonetheless biologically active as monomers, all BMPs are biologically active as either homo- or hetero-dimers once processed and activated. For example, heterodimerisation of BMP-2/5, BMP-2/6, BMP-2/7, BMP-4/7 and BMP-7/GDF-7 have been observed *in vitro* and *in vivo*, with certain studies reporting an increase in functional efficiency in these forms in comparison to their respective homodimeric forms.

Several BMPs, including BMP-2 (Scheufler, Sebald et al. 1999, Kirsch, Sebald et al. 2000), BMP-7 (Griffith, Keck et al. 1996, Greenwald, Groppe et al. 2003), BMP-9 (Brown, Zhao et al. 2005) and GDF-5 (Scheufler, Sebald et al. 1999), have been previously crystallised, enabling the elucidation of their structure. The characteristic scaffold of the BMP monomer has been described to be reminiscent of a left hand, with a wrist, thumb and two outstretched fingers (Sebald, Nickel et al. 2004). The structure of the "wrist", also known as the "core" of the protein, is primarily

determined by the seven conserved cysteines. The “thumb” is formed by an  $\alpha$ -helix, whilst the “fingers” are formed by two parallel  $\beta$ -sheets. The fingers, denominated as finger 1 and finger 2, extending in opposite directions within the dimer, with side-chains clustering together at the back, forming the “knuckle” epitope (Slobodan and Sampath 2002). Interestingly, it is the fingers and the  $\alpha$ -helix of the thumb that convey much of the structural variation between BMP family members. The wrists of the ligands are highly structural similar despite their overall sequences being only about 30-40% identical (Brown, Zhao et al. 2005).

### **1.8 BMP Receptors**

Members of the BMP subfamily transduce their signal by interacting with two diverse subfamilies of serine/threonine kinase receptors, termed Type-I and Type-II. Both BMP receptor (BMPR) types are structurally similar, encompassing a cysteine-rich short extracellular domain, a single-spanning transmembrane domain and a highly conserved intracellular serine/threonine kinase domain at their carboxyl-terminal. Although differences exist in the extracellular domains of the two receptor subtypes, it is actually the presence of two additional motifs within the type-I receptor that is used for classification (Mueller and Nickel 2012). The first is a 20 aa juxtamembrane glycine-serine rich regulatory domain (TTSGSGSG motif), known as the GS box, which precedes the kinase domain and is required for phosphorylation (Shi and Massagué 2003, de Caestecker 2004). The second, a short region of 8 aa, is termed the L-45 loop and is found within the type-I receptor kinase (Sieber, Kopf et al. 2009).

For BMP signalling to take place, dimers of both receptor types are required - the wrist epitopes of BMPs is a high affinity binding site for type-I receptors, whilst the knuckle epitope is a low affinity binding site for type-II receptors (Hinck 2012). Mechanistically speaking, as type-I and type-II receptors are single-spanning transmembrane receptors, it is their assembly with their

cognate BMP dimers that induces downstream signalling, as demonstrated by various studies. This is further supported by the fact that type-II receptors are constitutively active. Therefore, bridging both receptor types with ligands would enable the transphosphorylation of the GS box within the type-I receptors by the type-II receptors (Sieber, Kopf et al. 2009).

Overall, for the human TGF- $\beta$  superfamily of ligands, there are a total of seven type I receptors (Activin Like Kinase Receptors, ALK1-7), three of which are known to interact with BMPs: type-IA BMP receptor (BMPR-IA or ALK3), type-IB BMP receptor (BMPR-IB or ALK6), and type-IA activin receptor (ActR-IA or ALK2). Of the five known TGF- $\beta$  family type-II receptors, three bind BMPs: type-II BMP receptor (BMPR-II), type-IIA activin receptor (ActR-IIA), and type-IIB activin receptor (ActR-IIB) (Mueller and Nickel 2012). It is rather surprising therefore, that the number of available receptors has remained so low throughout evolution, despite such a high number of TGF- $\beta$  ligands. With several studies aiming to elucidate this mystery, *in vitro* binding analyses have demonstrated that not only are most TGF- $\beta$  receptors shared between ligands, but one TGF- $\beta$  may also bind to several TGF- $\beta$  receptors. For example, while BMPR-IA, BMPR-IB, and BMPR-II are specific to BMPs, ActR-IA, ActR-IIA, and ActR-IIB can function as receptors for activins, which are also members of the TGF- $\beta$  superfamily. Moreover, the three type-II BMPRs are able to interact similarly with any member of the BMP-2/4, BMP-5/6/7/8 and GDF-5/6/7 subgroups. This phenomenon has been coined “ligand-receptor promiscuity” and has been shown to be particularly present in the BMP subfamily (Mueller and Nickel 2012). However, different type-I and type-II receptor homo- or heterodimer combinations should allow for selectivity and specificity of ligand binding and the consequent intracellular signalling triggered.

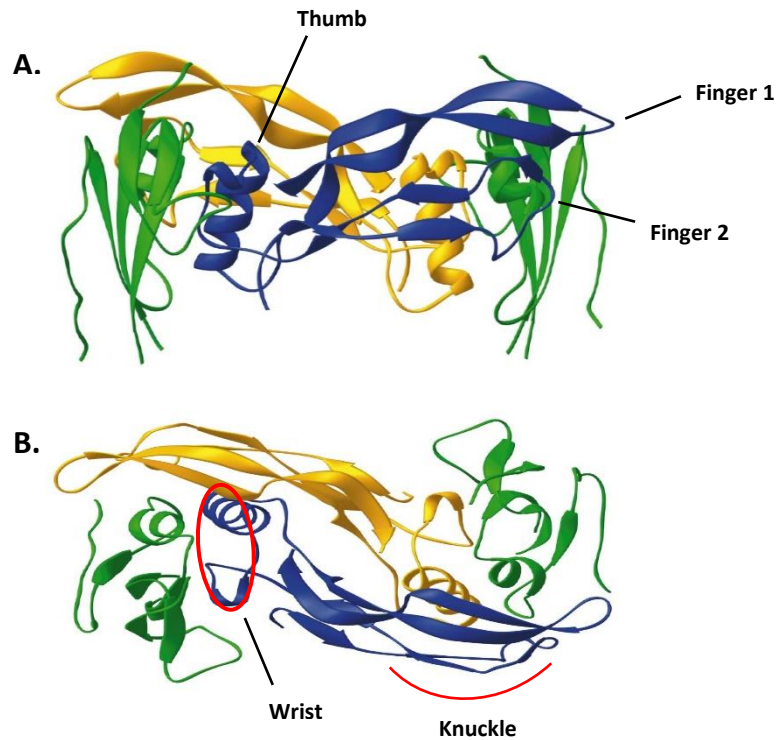


**Figure 1.6: The structure of BMP-2 and BMPR-IA extracellular interaction.** The two monomers (blue and yellow) of BMP-2 homodimer interact with the ectodomains of BMPR-IA (green). **A.** demonstrates the side view of the interaction with annotation of the  $\alpha$ -helix thumb and the two outstretched fingers (1 and 2) formed by parallel  $\beta$ -sheets. **B.** demonstrates the top view of the BMP-2/BMPR-IA interaction. Shown in red are the wrist and knuckle epitopes (adapted from Kirsch, Sebald et al. 2000).

## 1.9 BMP signalling

The classical paradigm of ligand-receptor interaction depicts a ligand-induced receptor-oligomerisation. Although that is still the case during BMP signalling, it is also possible for ligands to bind to preformed oligomeric complexes, the existence of which adds an additional layer of intricacy. Indeed, if the BMP dimer binds to preformed receptor complexes, the Smad-dependent pathway is triggered. In contrast, if the receptor complex is formed as a result of ligand binding, the Smad-independent, p38 mitogen-activated protein kinase pathway (MAPK) is activated (Nohe, Hassel et al. 2002, Nohe, Keating et al. 2004). Figure 1.7 depicts both signalling pathways.

### 1.9.1 The Smad-dependent pathway

The canonical Smad-dependent pathway is the best-studied BMP signalling pathway. Activated by ligands through their interaction with pre-formed hetero-oligomeric complexes (PFC) of type-I and type-II receptor dimers, this pathway requires the participation of transcription factors Smads for the propagation of the intracellular signal.

Smads are a group of related proteins ranging from about 400 to 500 aa that are critical for the downstream intracellular transmission of type-I TGF- $\beta$  and BMP receptor signalling from the cell surface to the nucleus (Attisano and Lee-Hoeflich 2001). The prototypic members of the Smad family were first identified as products of the *Mothers against decapentaplegic (Mad)* and *Sma* genes, respectively found in *Drosophila* and *C. Elegans* (Sekelsky, Newfeld et al. 1995, Kretzschmar and Massagué 1998, Massague 1998). Shortly thereafter, many orthologs were discovered in worms and vertebrates and were named “Smad”, as a contraction of the gene names of the founder members (Attisano and Lee-Hoeflich 2001, Derynck and Zhang 2003).

The human genome encodes eight Smad family members, which can be grouped into three subfamilies based on their structure and function. The first group, the receptor-regulated Smads (R-Smads), includes Smad1, 2, 3, 4, 5 and 8/9, of which Smad1, 5, 8/9 are BMP-specific. The R-Smad group constitutes the only direct substrates of the TGF- $\beta$  superfamily receptors. The second group of Smad proteins, the common Smad (Co-Smads), comprises solely of Smad4, and the third group, termed the inhibitory Smads (I-Smads), comprises Smad6 and Smad7. Typically, Smads consist of an N-terminal Mad homology 1 (MH1), involved in DNA binding (Kim, Johnson et al. 1997), a divergent proline-rich linker segment (L) of variable length, and a C-terminal Mad homology 2 (MH2), involved in Smad oligomerisation, cofactor binding, and receptor interaction

(Attisano and Lee-Hoeflich 2001). The R-Smads and the Co-Smad particularly have a highly conserved MH1. Conversely, the I-Smads have a MH2 domain, but no distinct MH1 domain, which is instead replaced by differing amino-acid termini that contain regions of similarity between members of the I-Smad subgroup (Attisano and Lee-Hoeflich 2001).

Each subgroup of Smad proteins plays a distinct role during Smad-dependent TGF- $\beta$  and BMP signalling. For the signals to be relayed intracellularly from the cell surface, the transphosphorylated type-I receptor first releases a 12 kDa FK506-binding protein (FKBP12), which normally acts as a silencer of kinase activity by binding the unphosphorylated GS regions of the receptor (Okadome, Oeda et al. 1996). Once freed of FKBP12, the GS box is able to recruit and subsequently activate R-Smads (Huse, Muir et al. 2001). Specific R-Smad/receptor interactions are mediated via the aforementioned L45 loop within the type-I receptor and the L3 loop and adjacent  $\alpha$ -helix1 in the MH2 domain of the R-Smad (Chacko, Qin et al. 2001). As such, the different receptors are able to discriminate between the different R-Smads, with TGF- $\beta$  receptors targeting Smad2 and Smad3 specifically, and BMPRs preferentially binding to Smad1, 5 or 8/9. When bound to the type-I receptor, the specific R-Smad is directly phosphorylated on the last two serines of a conserved SSXS motif located at the extreme carboxyl terminus of its MH2 domain (Souchelnytskyi, Tamaki et al. 1997), creating an acidic knob that binds to the MH2 domain of Smad4 or to homologous MH2 domains of other R-Smads (Massagué, 2012). Thus, when the R-Smad dissociates from the type I receptor following phosphorylation at its C-terminal, it is able to form an oligomeric complex with another R-Smad and the Co-Smad, Smad4. This oligomeric complex, with the help of nuclear import and export factors, then transits into the nucleus where it binds to other DNA-binding transcription factors to facilitate target gene recognition and consequently, the regulation of the transcription of the target gene.

### 1.9.2 The Smad-independent pathway

The alternative, non-canonical, signalling pathway that BMPs can also trigger is Smad-independent. During this pathway, BMPs usually first bind to type-I receptors due to their higher affinity for these receptors, and then recruit type-II receptors to form the hetero-oligomeric complex known as BISC (BMP-induced signalling complexes). Once the type-I receptor is phosphorylated by the constitutively active type-II receptor, subsequent signalling typically proceeds through one or more Mitogen-activated protein kinase (MAPK) signalling pathways to indirectly bring about changes in target gene transcription. For instance, it is thought that pathway activation is achieved through the specific interaction of BMPRII with BRAM1 (Bone Morphogenetic Protein Receptor Associated Molecule 1) or XIAP (X-linked Inhibitor of Apoptosis Protein), which mediate the interaction of the receptor with downstream signalling molecules TAK1 (TGF- $\beta$  Activated Kinase 1) and TAB1 (TAK1 binding protein). Both adaptor proteins, BRAM1 and XIAP, interact with BMPRII via its cytoplasmic domain, enabling the recruitment of TAB1, which is crucial for the activation of TAK1. Thereafter, the activated TAK1 can in turn activate the MAPK pathways, such as extracellular signal-regulated kinase (ERK), map kinase p38 and C-jun N-terminal kinase (JNK). The Smad-independent pathway is not as well studied as the Smad-dependent pathway. For example, it is unclear whether there is a causal difference between BRAM1 or XIAP recruiting the TAB1-TAK1 complex to BMPRII. It is also unclear if the adaptor proteins interact with other type I receptors, although XIAP has been reported to interact with ActRII. BMP signal transduction can be complex *in vivo* and although the mode of initiation remains unknown, BMPs have also been reported to trigger and cross-talk with other pathways, for example, phosphoinositide 3-kinase (PI3 kinase), Protein Kinase A (PKA), Protein Kinase C (PKC) (Haÿ, Lemonnier et al. 2001), Wnt and NOTCH signalling pathways (Walsh, Godson et al. 2010).

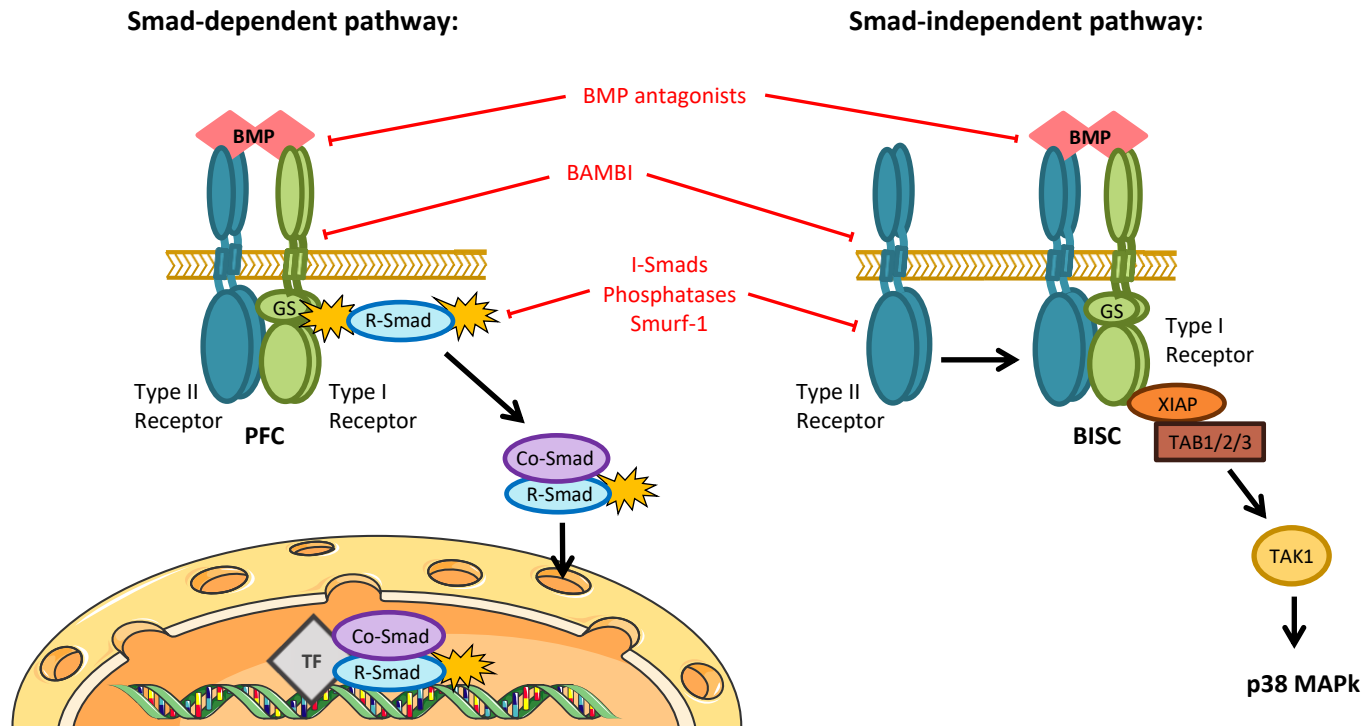


**Figure 1.7: The Smad-dependent and the Smad-independent signalling pathways.** The canonical Smad-dependent pathway is triggered when BMP homo- or hetero-dimers bind to a PFC of type-I and type-II BMPR homodimers. As part of this pathway, the ligation of the BMP ligand to the receptor complex causes the phosphorylation of the GS boxes within the type-I receptors. Phosphorylated GS boxes then recruit and phosphorylate R-Smads 1, 5 or 8/9, which in turn form oligomeric complexes with the Co-Smad, Smad 4. The resulting complexes subsequently transit into the nucleus where they bind to transcription factors (TFs), facilitating target recognition and thus, the regulation of the of target gene transcription. The non-canonical BMP signalling pathway, on the other hand, involves the recruitment of type-II BMPR dimers following the ligation of BMP ligands to type-I receptors. This forms a receptor complex known as BISC. Transduction of this pathway is thought to occur through the interaction of the type-I receptors with XIAP, which mediates the interaction of these receptors with downstream signalling molecules TAB1/2/3 and TAK1. Highlighted in red are different regulators of BMP signalling. Among the intracellular regulators, I-Smads, Smad6 and 7, compete with R-Smads for the binding of type-I receptors, inhibiting their R-Smad phosphorylation. Meanwhile, Smurf-1 specifically targets Smad1 and 5 for ubiquitination, and phosphatases PP-1 and -2A, dephosphorylate activated BMPRs and their associated R-Smads. Extracellular regulators of BMP action include the pseudoreceptor BAMBI, which inhibits BMP signalling by obstructing the formation of functional receptor complexes, and BMP antagonists which attach to and sequester BMP ligands, preventing them from binding to cognate BMPRs.

### 1.10 Regulation of BMP Signalling

Due to their vast roles in embryogenesis, post-natal developmental programs, and homeostasis, BMPs have evolved with numerous multi-level regulatory mechanisms in order to fine-tune signalling outcome (see figure 1.7). Regulation starts in the nucleus where BMP RNA transcript levels may be suppressed via promoter methylation/hypermethylation (Walsh, Godson et al. 2010). These transcripts may then face further silencing in the cytoplasm by action of miRNAs, such as miR-22, which has been shown to regulate BMP-6 and 7 in the kidney (Long, Badal et al. 2013). Intracellular modulation of BMP signalling also occurs through blockade of the different mediators of BMP signalling. For instance, I-Smads, Smad6 and Smad7, compete with R-Smads to bind BMPRs, thereby inhibiting R-Smad phosphorylation by the receptor (Imamura, Takase et al. 1997, Souchelnytskyi, Nakayama et al. 1998). Smad signalling is also targeted by Smad ubiquitination regulatory factor-1 (Smurf1), which specifically targets Smad1 and 5 for ubiquitination, and by protein phosphatases (PP)-1 and 2A, which dephosphorylate activated BMPRs and their associated R-Smads (Zhu, Kavsak et al. 1999, Wrighton, Lin et al. 2009).

On top of these regulatory mechanisms, BMP signalling is also modulated extracellularly. The pseudoreceptor BMP and activin membrane-bound inhibitor (BAMBI) participates in this process by preventing the formation of functional receptor complexes (Onichtchouk, Chen et al. 1999). Furthermore, the BMP signalling pathway is regulated by a key family of structurally diverse, extracellularly secreted antagonists known as BMP antagonists. The latter attach to and sequester BMP ligands, thus preventing them from binding their cognate receptors by blocking their binding sites.

### 1.11 BMP Signalling in the Bone

Among the 20 BMPs that have been identified and characterised, BMP-2, 4, 5, 6, 7 and 9 have all exhibited to have strong osteogenic capacity (Luu, Song et al. 2007, Abula, Muneta et al. 2015). In fact, BMPs are important not only for skeletal development but also for the regeneration and homeostasis of the bone matrix, with numerous studies demonstrating the impairment of skeletal development upon deletion of these growth factors as well as that of the different components of their signalling pathway.

One of the ways BMPs exert their influence on bone and cartilage formation is by stimulating the differentiation of osteoblasts (Itoh, Udagawa et al. 2001, Nishimura, Hata et al. 2008). Many factors are known to be involved in this process, however amongst these, BMPs are uniquely potent. This is because they are able to influence the different stages of differentiation, from the development of pre-osteoblasts to the maturation into osteoblasts (Gazzerro and Canalis 2006). Osteoblasts, like other cells that make up connective tissue (chondrocytes, fibroblasts, myoblasts and adipocytes), are derived from cells of a mesenchymal lineage, known as mesenchymal stem cells (MSCs), with the fate of these pluripotent cells being decided by selective expression of so-called “master transcription regulators” (Grigoriadis, Heersche et al. 1988, Pittenger, Mackay et al. 1999, Jensen, Gopalakrishnan et al. 2010). For the differentiation of osteoblasts, this means the expression of transcription factor runt-related transcription factor 2 (Runx2), also known as core-binding factor subunit alpha-1 (Cbfa-1), a process which is in fact driven by the BMP Smad-dependent and Smad-independent pathways (Wu, Chen et al. 2016). This is not achieved directly, but through the BMP-mediated expression of the transcription factor distal-less homeobox-5 (Dlx5), which in turn induces Runx2 expression (Heo, Lee et al. 2017).

Although indirectly, BMPs may also influence the differentiation of osteoclasts from HSCs. This is due to one of key haematopoietic factors in this process, receptor activator of nuclear factor- $\kappa$ B ligand (RANKL), and its inhibitor osteoprotegerin (OPG) being produced by osteoblasts (Itoh, Udagawa et al. 2001, Boyle, Simonet et al. 2003).

### **1.12 Aberrance of BMPs and their Implications in Prostate Cancer**

Due to the importance and complexity of BMP function in normal physiology, mis-regulation of the various components of their pathway may bring about serious pathophysiological consequences. These may include congenital, bone and cardiovascular diseases, as well as different types of cancer (Bokobza, Ye et al. 2009, Wang, Green et al. 2014). In terms of cancer, the expression BMPs remains controversial due to studies reporting pro-oncogenic or anti-oncogenic roles for specific BMPs. However, there is increasing evidence for the potential of BMPs and their signalling components as novel biomarkers with substantial therapeutic implications for cancer treatment (Bach, Park et al. 2018). Among the various cancers in which BMPs have been implicated, prostate and breast have particularly been represented in cancer studies due to their unique characteristic of metastasis to the bone. In fact, what with the BMPs' innate osteogenic capacities, they have been heavily implied to have a role in the induction of new bone as frequently seen in the lesions formed during prostate cancer. In order to gain insight into the relationship between prostate cancer cells and the bone microenvironment, numerous studies have examined the expression of BMPs in prostate carcinoma and prostate cancer bone metastases.

The first study of this sort was undertaken in the early 90s by Bentley and colleagues, who demonstrated the presence of BMPs 1-6 in prostatic adenocarcinoma and reported BMP-6 to be selectively expressed in bone-scan positive metastatic disease (Bentley, Hamdy et al. 1992).

Thereafter, Bobinac and colleagues, with the aim to investigate the role of BMPs in the different stages of prostate cancer, demonstrated the expression of BMP-2, -4, -5, -6 and -7 in normal prostate tissue, and the predominant expression of BMP-2 and -4 in prostate carcinoma samples, along with significantly decreased levels of BMP-7 (Bobinac, Marić et al. 2005). Another study, by Spanjol et al (2010), reported mostly similar findings by also showing an increased expression of BMP-6 and decreased levels of BMP-7 in localised prostate cancers, and high levels of BMP-2, -4, -6 and -7 in bone metastases. However, slightly conflicting with the data by Bentley et al, Spanjol and colleagues showed decreased expression levels of BMP-2/4, -6 and -7 in metastatic prostate cancer samples. Despite the varying expression patterns highlighted, the overall evidence suggests BMP-2, -4, -6, and -7 to be potential players in the pathophysiology behind skeletal metastases produced by prostate cancer.

This is further supported by findings from other studies. For instance, on top of confirming BMP-2 expression data by Spanjol et al, Horvath et al and Tae et al also reported a negative correlation between BMP-2 expression and Gleason score, describing a decrease in relapse-free survival resulting from a decrease in BMP-2 expression as well. Both studies subsequently concluded that this BMP may serve as a marker of poor prognosis (Horvath, Henshall et al. 2004, Tae, Cho et al. 2018). Furthermore, *in vitro* experimentation have demonstrated that BMP-2 not only contributes to the migration of prostate cancer cells but also, along with BMP-7, may have a role for angiogenesis and protection against apoptosis through the upregulation of SDF1/CXCL12 in cancer-associated fibroblasts (Lai, Fong et al. 2008, Yang, Pham et al. 2008). As for BMP-4, while most studies investigating the role of this BMP in bone metastasis have been focussed on breast cancer, Lee et al demonstrated a potential role in progression of prostate cancer and its related osteogenesis (Lee, Cheng et al. 2011). On the other hand, BMP-6 has been heavily implicated in prostate cancer, most particularly with the more aggressive form of the disease. Indeed, expression studies concentrated on this BMP have confirmed findings by Bentley et al,

describing its expression to be closely associated with high Gleason scores and established secondary skeletal metastases, with studies by Autzen et al, Yuen et al, and Lee et al going as far as to postulate BMP-6 as a potential predictor of prostate cancer metastasis (Hamdy, Autzen et al. 1997, Autzen, Robson et al. 1998, Darby, Cross et al. 2008, Yuen, Chan et al. 2008, Lee, Kang et al. 2014). *In vitro* results supported these findings by demonstrating BMP-6 to promote the migration and invasion of prostate cancer cells, even stimulating the proliferation of these cells in androgen-deprived conditions (Dai, Keller et al. 2005, Darby, Cross et al. 2008, Lee, Kang et al. 2014).

Although the present study will be investigating all the BMPs discussed above, BMP-7 is of particular interest to us. As a BMP that is normally highly expressed in normal prostate tissue, Thomas et al (1998) demonstrated that this expression is dependent upon the presence of testosterone and DHT. However, numerous studies have demonstrated that this expression decreases drastically in early prostate adenocarcinoma, then rises to higher than normal levels in metastatic bone lesions prostate, with Morrissey et al reporting BMP-7 levels to be strikingly increased in castration-resistant prostate cancer in comparison to androgen-dependent prostate cancer (Masuda, Fukabori et al. 2003, Masuda, Fukabori et al. 2004, Buijs, Rentsch et al. 2007, Ye, Lewis-Russell et al. 2007, Morrissey, Brown et al. 2010). Thus, this creates an intriguing overall picture, where the changes in BMP-7 expression could reflect the shift of prostate cancer from an androgen-dependent phenotype to androgen-independent phenotype as the disease gets more aggressive.

Various studies have aimed to study the role of BMP-7 in prostate cancer, with conflicting results. For instance, the *in vivo* study by Buijs et al (2007) demonstrated BMP-7 expression to be significantly correlated with E-cadherin, suggesting a role for BMP-7 in controlling and preserving the epithelial human prostate. Another study, by Kobayashi et al (2011), indicated a

critical role for this BMP in inducing senescence of prostate cancer stem-like cells (CSCs). Thus, both studies suggested the potential therapeutic utility of BMP-7 in the treatment against metastatic prostate cancer. *In vitro* studies have also demonstrated prostate cancer inhibiting abilities of BMP-7, with Miyazaki et al (2004) reporting its inhibition of the proliferation of prostate cancer cell lines, PC-3 and DU145, and previous work from our own laboratory demonstrating the increased motility and invasiveness of PC-3 as a result of decreased BMP-7 expression (Ye, Lewis-Russell et al. 2007). However, other studies have reported differently. Yang et al, for example, demonstrated the BMP-7-mediated induction of EMT in PC-3 cells, as well as inhibition of the serum-starvation-induced apoptosis of prostate cancer cells, LNCaP, and their bone variants, C4-2B cells (Yang, Zhong et al. 2005, Yang, Pham et al. 2008). Dai et al (2004) described a role for BMP-7 in the enhancement of pro-osteoblastic activity of C4-2B through the upregulation of VEGF. Additionally, Lim et al (2011) reported filamentous outgrowths from 3D spheroid PC-3 cultures, which was accompanied with a downregulation of E-cadherin, and an increase in invasiveness through the upregulation of MMP-1 and MMP-13. Although taken together this provides a possible dual mechanism of BMP-7 function in prostate cancer metastasis, it is possible that other signalling molecules that have an impact on BMP function also need to be taken into consideration, such as BMP antagonists.

### **1.13 BMP antagonists**

Out of all the regulators of BMP signalling, BMP antagonists have been shown to be uniquely integral to BMP function. Indeed, the interplay that exists between BMPs and their antagonists has been demonstrated to govern the cellular processes underlying diverse developmental programmes such as limb-bud patterning, joint formation in the skeleton and induction of neural tissue (Reddi 2001, Wessely, Agius et al. 2001, Khokha, Hsu et al. 2003).

Like BMPs, the BMP antagonist structure comprises of a cysteine knot, the size of which is used to classify the antagonists into subfamilies. These are: the CAN family (Cerberus and DAN (differential screening-selected gene aberrative in neuroblastoma); eight-membered ring), twisted gastrulation (nine-membered ring), and Chordin and Noggin (ten-membered ring). The CAN family can also be further divided into four subsets based on a conserved arrangement of additional cysteine residues: Gremlin and protein related to DAN and Cerberus (PRDC); Cerberus and Coco; DAN; and uterine sensitization-associated gene-1 (USAG-1) and Sclerotin (Avsian-Kretchmer and Hsueh 2004). BMP antagonists typically range from 170 to 250 aa in length for the CAN family, while multidomain antagonists like Chordin subfamily of antagonists and Follistatin (FST) are significantly larger. Also consistent with BMPs is the presence of a latent domain in their N-terminus that needs to be cleaved for the antagonists to reach their mature form. In fact, cleavage of the 20 aa propeptide domain enables the N-terminus to form a BMP-interacting domain, known as a clip or finger domain (Groppe, Greenwald et al. 2002).

Although they are canonically known to act as inhibitor of BMP function, more and more evidence has demonstrated the importance of BMP antagonists for proper BMP function. Indeed, some BMP antagonists may actually stimulate BMP action when expressed at low concentrations (Walsh, Godson et al. 2010, Ali and Brazil 2014, Salazar, Gamer et al. 2016). Furthermore, as with BMPs, the expression of BMP antagonists is under tight spatio-temporal control and therefore, alterations to their levels may lead to deformities in limb, bone and kidney development amongst others. For instance, Noggin-mediated BMP antagonism has been shown to be integral in the development of the heart, and prostate (Choi, Stottmann et al. 2007, Cook, Vezina et al. 2007).

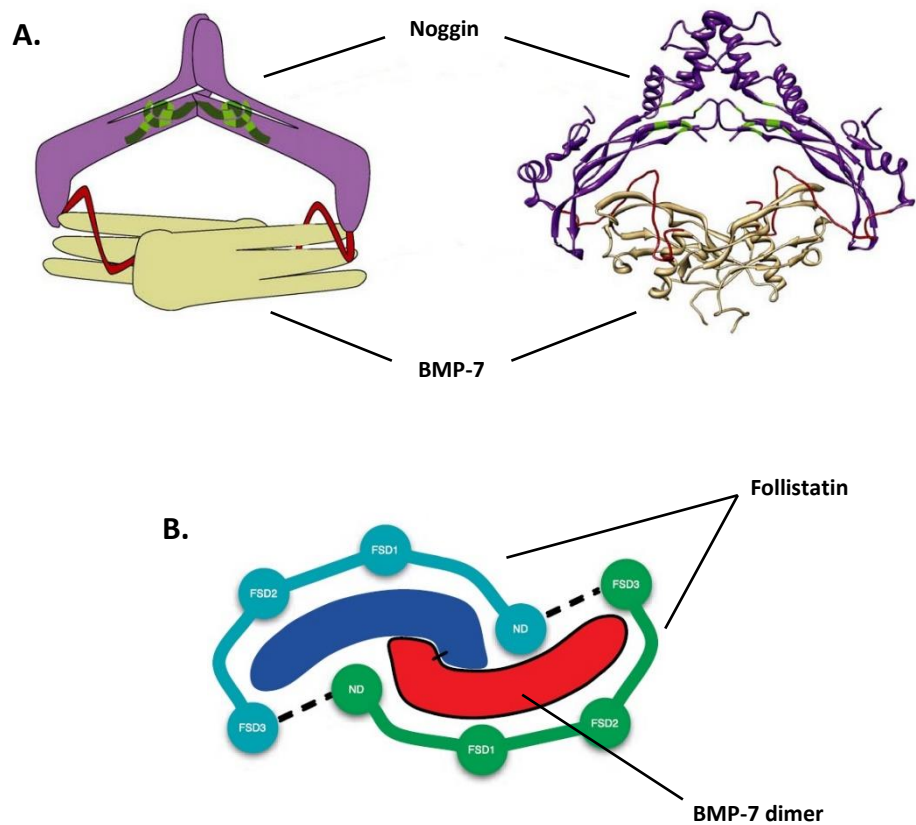


**Figure 1.8: Inhibition of BMPs by BMP antagonists. A.** The diagram depicts the inhibition of BMP-7 by BMP antagonist Noggin. The latter exists as a homodimer (shown in purple) with BMP-interacting domains known as a clip or finger domain (red). Like BMPs, BMP antagonists comprise of a cysteine knot, shown in green. **B.** The schematic demonstrates the inhibition of a BMP-7 ligand dimer by Follistatin. Unlike Noggin, FST monomers completely surround each plane of the target, whereby the head-to-tail contacts between the N-terminal (ND) and the follistatin domain 3 (FSD3) create a neutralised complex (A. was adapted from Walsh, Godson et al. 2010 and B. was adapted from Lin et al 2006).

### 1.13.1 Noggin

Noggin (NOG) is a 67 kDA homodimeric glycoprotein that exists as a dimer of identical subunits. The structure of Noggin has been described as a flat “butterfly-like” shape, with the body of the butterfly represented by the two subunits in close contact, and wings consisting of the  $\beta$ -strands projecting outward at around  $45^\circ$  away from the axis of symmetry of the dimer (see figure 1.8A). Contact with BMPs occurs through the tips of these  $\beta$ -strand loops, therefore with their loops being longer than those in BMPs, Noggin is able to extend over them, obscuring the binding sites

for their cognate receptors (Groppe, Greenwald et al. 2002, Greenwald, Groppe et al. 2003). Like the other BMP antagonists, Noggin is able to bind to a number of BMPs, although with a varying degree of preference. BMPs that Noggin may bind include BMP-2, 4, 6, 7 and 14 (Krause, Guzman et al. 2011).

### 1.13.2 Follistatin

Follistatin (FST) is a multidomain, secreted glycoprotein that may exist as three isoforms. Two isoforms, namely FST288 and FST315, arise from the alternative splicing of the approximately 6 kb *FST* gene precursor from the respective splice variants FST317 and FST344. FST288, the membrane-bound form of FST, comprises of an N-terminal domain (ND) and three FST domains (FSD1, FSD2 and FSD3), while the FST315 isoform represents the serum-circulating form of the antagonist and includes a C-terminal acidic region (Shimasaki, Koga et al. 1988, Shimasaki, Koga et al. 1988). The third FST variant, FST303, is produced from the post-translational truncation of this C-terminus (Sugino, Kurosawa et al. 1993). Interestingly, most FST mRNA corresponds to the FST315 form of the antagonist, with <5% of FST mRNA coding for the FST288 isoform (Schneyer, Wang et al. 2004).

Although FST was originally identified as an Activin antagonist, this antagonist has since been shown to also BMP-2, 4 and 7, with higher affinities for the latter (Iemura, Yamamoto et al. 1998). This antagonist also shares substantial structural and functional homology with antagonists known as Follistatin-Like (FSTL)-1, 3, 4 and 5, that also inhibit BMP action (Sylva, Moorman et al. 2013), with all FST and FSTL antagonists showing the same BMP-inhibiting mode of action. This inhibitory action is actually dissimilar to that of Noggin, in that rather than a clip or finger obscuring the BMPR binding sites within BMPs, FST acts as a peripheral clamp that

completely surrounds one plane of its target ligand, forming head to tail contacts between the N- and C-terminals between each of the FST monomers (Lin, Lerch et al. 2006).

### 1.13.3 Gremlin

Gremlin (GREM) is a 20.7 kDa, highly conserved 184 aa glycoprotein that is part of the DAN family of BMP antagonists. Two isoforms of this antagonist exist, namely Grem1 and Grem2, although the latter is also known as PRDC (Mulloy and Rider 2015). Both isoforms are known to bind BMP-2 and 4, with Grem1 also showing some affinity for BMP-7. Grem1 can exist in both secreted and cell-associated forms, and contrary to the antagonists discussed above, it exerts its BMP inhibitory effects not only by preventing BMP interaction with their cognate receptors but also by blocking BMP secretion and increasing BMP endocytosis (Sun, Zhuang et al. 2006, Wordinger, Zode et al. 2008, Alborzinia, Schmidt-Glenewinkel et al. 2013).

## 1.14 BMP antagonists and Prostate Cancer

Since the dysregulation of BMP function has been linked, in either a pro- or anti-tumourigenic capacity, to cancer, numerous studies have recognised the potential role of BMP antagonists in this process, reporting an effect on basal cell carcinoma, melanoma, colorectal cancer, breast cancer and lung cancer, to name a few. (Sneddon, Zhen et al. 2006, Gao, Chakraborty et al. 2012, Kim, Yoon et al. 2012, Karagiannis, Musrap et al. 2015). However, like with BMPs, conflicting results have been reported in assessing the role of BMP antagonists in prostate cancer and its related bone metastasis.

For instance, suggesting Noggin as a potential therapeutic modality against bone metastasis, Feeley et al (2006) demonstrated the Noggin-mediated inhibition the expansion of osteolytic lesions *in vivo*, while Schwaninger et al (2007) reported its abolishment of the osteoblast response of intraosseous xenografts, blaming a lack of Noggin for the osteoblastic response of prostate cancer bone metastasis. In contrast, studies by Secondini et al (2011) and Al-Shaibi et al (2018) have proposed the suppression of Noggin as a potential anti-bone metastasis therapy due to their results showing a limitation of tumour growth and osteolysis in PC-3 bone xenograft models resulting from Noggin-silencing, and the Noggin-mediated suppression of osteoblast differentiation in bone metastases.

Other than Noggin, FST has also been shown to have a role in prostate cancer. In aiming to investigate keys genes in the progression of prostate cancer to its more aggressive phenotype, Varaala et al (2000) uncovered the increase of FST in the LNCaP androgen-independent variant. These findings are expanded upon by Tumminello et al (2010) who demonstrated a positive correlation between circulating levels of FST and the presence of bone metastases.

### **1.15 Aims**

Taken together, the information outlined in this chapter describes an intimate interplay between BMPs and their antagonists that is critical in various developmental programmes, and that could also be in play a role in pathophysiological conditions during prostate cancer. Previous reports have hinted at this concept, such as Feeley et al (2006) who demonstrated the inhibition of BMP-2 and BMP-4-mediated migration and invasion of PC-3 cells by Noggin. AlShaibi et al (2018) also indicated this BMP/BMP antagonist balance in prostate cancer by describing high levels of BMP-6, in addition to those of Noggin, in prostate cancer cells, a finding which is

confirmed by Haudenschild et al (2004). Van der Poel (2003) additionally reported that an increase in BMP-4, which was induced by rapamycin in their experiments, was accompanied by a decrease in FST levels in PC-3 and DU145 cells. Furthermore, previous work from our own laboratory has demonstrated the decrease of Noggin and FST levels due to BMP-7 knockdown (Ye, Lewis-Russell et al. 2007). As a result of this study, Ye et al suggested that the increased motility and invasiveness of BMP-7-knockdown PC-3 cells, may have been facilitated by the noted decrease of these BMP antagonists.

Therefore, we hypothesised that, due to BMPs being established, powerful osteoinductive factors, the close feedback loop that exists between them and their BMP antagonists has a role in the development of prostate cancer and the related osteoblastic bone metastases.

The aims of the study were:

1. To screen for the baseline levels of BMP-2, 4, 6 and 7, their antagonists, Noggin, FST344, and Gremlin, and related signalling components in prostate cancer cell lines, PC-3, DU145, LNCaP and VCaP so as to assess the differences in gene expression between osteolytic lesion and osteoblastic lesion-causing cell lines.
2. To examine changes in the above gene expression levels when cell lines are within the bone environment as mimicked by a bone matrix extract (BME; see section 2.2.1 for full details), and to assess the differences in these BMP signalling components between osteolytic and osteoblastic bone lesions.
3. To assess the functionality of BMP antagonists, Noggin, FST344 and Gremlin in prostate cancer cell behaviour by overexpressing levels of these antagonists, and investigating the changes incurred within the bone environment (again, as mimicked by BME).

4. To identify key molecular mechanisms underlying the changes in cell behaviour incurred following Noggin, FST344 and Gremlin overexpression.

Chapter 2.

# Materials and Methods

## 2.1 General Materials

### 2.1.1 Cell lines

The current study made use of four prostatic cell lines, PC-3, DU145, LNCaP and VCaP - all of which were obtained from the American Type Culture Collection (ATCC, Rockville, Maryland, USA). Full details are supplied in Table 2.1.

### 2.1.2 Primers

All the primers used in the present study were designed with the use of the program Primer-BLAST available from NCBI, and were synthesized by Sigma-Aldrich (Poole, UK). Primers were diluted in nuclease-free water upon receipt according to the manufacturer's specifications. The forward and reverse primers used for reverse transcription polymerase chain reaction (RT-PCR) and quantitative polymerase chain reaction (qPCR) are shown in Tables 2.2 and 2.3 respectively. Primers used for the amplification of the coding sequences of Noggin, FST344 and Gremlin and the verification of clonal vectors are provided in Table 2.4.

Cell line	Organism	Morphology	Ethnicity	Gender	Age	Disease	Tissue	Features
PC-3	<i>Homo sapiens</i> (Human)	Epithelial	Caucasian	Male	62	Grade IV, Adenocarcinoma	Prostate; derived from metastatic site: Bone	<b>Isolation date:</b> 1979 <b>Culture properties:</b> Adherent <b>Antigen Expression:</b> HLA A1, A9 <b>Androgen Receptor status:</b> -ve <b>Cell type:</b> Osteolytic
DU145	<i>Homo sapiens</i> (Human)	Epithelial	Caucasian	Male	69	Carcinoma	Prostate; Derived from metastatic site: Brain	<b>Isolation date:</b> 1978 <b>Culture properties:</b> Adherent <b>Antigen expression:</b> Blood Type O; Rh+ <b>Androgen Receptor status:</b> -ve <b>Cell type:</b> Osteolytic
LNCaP	<i>Homo sapiens</i> (Human)	Epithelial	Caucasian	Male	50	Carcinoma	Prostate; derived from metastatic site: Left supraclavicular lymph node	<b>Isolation date:</b> 1977 <b>Culture properties:</b> Adherent <b>Cellular Products:</b> human prostatic acid phosphatase; prostate specific antigen <b>Androgen Receptor status:</b> +ve <b>Cell type:</b> Mixed osteolytic/osteoblastic
VCaP	<i>Homo sapiens</i> (Human)	Epithelial	Caucasian	Male	59	Cancer	Prostate; derived from metastatic site: vertebral metastasis	<b>Isolation date:</b> 1997 <b>Culture properties:</b> Adherent <b>Antigen Expression:</b> cytokeratin-18; <i>Homo sapiens</i> , expressed p53 antigen; <i>Homo sapiens</i> , expressed prostate specific antigen (PSA); <i>Homo sapiens</i> , expressed prostatic acid phosphatase (PAP); <i>Homo</i> <i>sapiens</i> , expressed Rb protein; <i>Homo sapiens</i> , expressed <b>Androgen Receptor status:</b> +ve <b>Cell type:</b> Osteoblastic

**Table 2.1.** Details of prostate cancer cell lines used during this study.

Gene	Primer name	Primer sequence	Annealing Temperature	Expected size (bps)
BMP-7	BMP7F8	CTTTCTCAAGGCCACGGAG	55°C	332
	BMP7R8	TTCCGGGTTGATGAAGTGGA		
Noggin	NogginF11	TACAGATGTGGCTGTGGTCTG	55°C	252
	NogginR11	TGCACTCGGAAATGATGGGG		
FST344	FST344F11	TGAGGGAAAGTGTATCAAAGCAAA	55°C	267
	FST344R11	TCGGTGTCTCCGAAATGGAG		
FST317	FST317F11	AAGTGTATCAAAGCAAAGTCCTGT	55°C	267
	FST317R11	ATGGCTCAGTTTTACGGGC		
Gremlin	GremlinF8	CTGCTGAAGGGAAAAGAA	55°C	264
	GremlinR8	GATGGATATGCAACGACACT		
Smad 1	Smad1F8	GTCGTGAGTTTCCTTTTGG	55°C	504
	Smad1R8	CACAGTGTTCCTGTTCT		
Smad 2	Smad2F8	TACAGAACTTCCGCCTC	55°C	495
	Smad2R8	CACTTAGGCACTCAGCAAA		
Smad 3	Smad3F8	CTGGACGACTACAGCCATT	55°C	501
	Smad3R8	GTTGGGAGACTGGACAAAA		
Smad 4	Smad4F8	ATTTCCAATCATCTGCTC	55°C	543
	Smad4R8	GTCATCAACACCAATTCCA		
Smad 5	Smad5F8	CCTGTTGCCTATGAAGAGC	55°C	491
	Smad5R8	TGATATTCTGCTCCCAAC		
Smad 8a	Smad8aF8	CCAGAGAGTCCCTATCAACA	55°C	621
	Smad8bR8	CCAACCTTAACAAAACCTCA		
BMPR-Ia	BMPRIAF8	GACCAGTCACAAAGTTCTGG	55°C	470
	BMPRIAR8	TTTTTGCTCTTTAGGTCTCG		
BMPR-Ib	BMPRIBF8	TGTAGTTTGCTCTTGGTCCT	55°C	501
	BMPRIBR8	CATTGATTTAGCGTCTAGGG		
BMPR-II	BMPR2F8	GCACACCTTTGACTATAGGG	55°C	500
	BMPR2R8	AGTAGGCAGAACATCAGGAA		
ActR1a	ACTRIAF8	TGGTGTAAACAGGAACATCAC	55°C	518
	ACTRIAR8	ATGTCTGAAGCAATGAAACC		
ActR1I	ACTR2F8	ACTTGTTCCAACCTAAGACC	55°C	463
	ACTR2R8	ACTTTTGATGTCCTGTGAG		
ActR1Ib	ACTR2BF8	TCATGTGGACATCCATGAG	55°C	493
	ACTR2BR8	GTCGCTCTTCAGCAATACAT		
GAPDH	GAPDHF10	AGCTTGTCATCAATGGAAAT	55°C	593
	GAPDHR10	CTTCACCACCTTCTTGATGT		

**Table 2.2.** Primers used for conventional RT-PCR.

Gene	Primer name	Primer sequence	Annealing Temp.	Expected size (bps)
BMP-7	BMP7F24	TTCCGGATCTACAAGGACTA	55°C	119
	BMP7Zr24	<b>ACTGAACCTGACCGTACA</b> CTGTGAGCAGGAA GAGAT		
Noggin	NogginF14	AGGGCTAGAGTTCTCCGAGG	55°C	91
	NogginZR14	<b>ACTGAACCTGACCGTACA</b> CGACCACAGCCACAT CTGTA		
FST344	FST344F1	TGAGGGAAAGTGTATCAAAGCAAA	55°C	80
	FST344ZR1	<b>ACTGAACCTGACCGTACA</b> ATTCCTCCTCTTCCTCG GTGT		
Gremlin	GremlinF8	CTGCTGAAGGGAAAAGAA	55°C	89
	GremlinZr	<b>ACTGAACCTGACCGTACA</b> CACGAACTACGCACA AGCAG		
BMP-2	BMP2F1	AGACCACCGTTGGAGAG	55°C	120
	BMP2Zr	<b>ACTGAACCTGACCGTACA</b> GTTGTTTTCCCACTCG TTT		
BMP-4	BMP4F1	CAACACCGTGAGGAGCTT	55°C	134
	BMP4Zr	<b>ACTGAACCTGACCGTACA</b> TGAGGTTAAAGAGG AAACGA		
BMP-6	BMP6F1	AGTCTTACAGGAGCATCAGC	55°C	141
	BMP6Zr	<b>ACTGAACCTGACCGTACA</b> ACAACCCACAGATTG CTAGT		
Snail	SnailF1	CAGAAAGTTTTCCACCAAAG	55°C	106
	SnailZr	<b>ACTGAACCTGACCGTACA</b> AAATGTGAGCAATTC TGCTT		
Slug	SlugF1	ATTCTCAACCCCATCT	55°C	110
	SlugZr	<b>ACTGAACCTGACCGTACA</b> ATTCTCCACTTGATTC CATT		
MMP2	MMP2F1	CAGGGAATGAGTACTGGGTCTATT	55°C	102
	MMP2ZR1	<b>ACTGAACCTGACCGTACA</b> ACTCCAGTTAAAGGC AGCATCTAC		
MMP7	MMP7F1	AAATGGACTTCCAAAGTGGT	55°C	110
	MMP7ZR1	<b>ACTGAACCTGACCGTACA</b> ATTCATACAACTTT CCTG		
MMP9	MMP9F1	AACTACGACCGGGACAAG	55°C	106
	MMP9ZR1	<b>ACTGAACCTGACCGTACA</b> GGAAAGTGAAGGGG AAGA		
MMP12	MMP12F1	ACCCACGTTTTTATAGGACC	55°C	112
	MMP12ZR1	<b>ACTGAACCTGACCGTACA</b> GATAACCAGGGTCCA TCATC		
MMP14	MMP14F1	AACTACGACCGGGACAAG	55°C	105
	MMP14ZR1	<b>ACTGAACCTGACCGTACA</b> ACTCCAGTTAAAGGC AGCATCTAC		
ID1	ID1	TCAACGGCGAGATCAG	55°C	57
	ID1Zr	<b>ACTGAACCTGACCGTACA</b> GATCGTCCGCAGGA A		
GAPDH	GAPDHF	CTGAGTACGTCGTGGAGTC	55°C	93
	GAPDHZr	<b>ACTGAACCTGACCGTACA</b> CAGAGATGATGATG ACCCTTTTG		

**Table 2.3.** Primers used for qPCR. **ACTGAACCTGACCGTACA** represents the Z sequence.

Gene	Primer name	Primer sequence	Expected size (bps)
	T7F	TAATACGACTCACTATAGGG	
	BGHR	TAATACGACTCACTATAGGG	
Noggin	NogginExF1	ATGGAGCGCTGCCCCAGCCTAGGGGTCA	696
	NogginExR1	GCACGAGCACTTGCACTCGGAAATGA	
FST344	FST317ExF1	ATGGTCCGCGCGAGGCA	1299
	FST344ExR1	TTACCACTCTAGAATAGAAGATATAGG	
GREM1V1	GremlinExF1	ATGAGCCGCACAGCCTAC	555
	GremlinExR1	TTAATCCAAATCGATGGATATGCAA	

**Table 2.4.** Primers designed for the cloning of Noggin, FST344 and Gremlin overexpression vectors.

## 2.2 Standard reagents and solutions

### 2.2.1 Solutions for use in Cell Culture

#### *Phosphate Buffer Solution (PBS)*

50 ml of 10X stock solution of PBS (Sigma-Aldrich, Poole, UK) was diluted in 450 ml of distilled water and autoclaved.

#### *Buffered Salt Solution (BSS)*

79.5 g of NaCl (Sigma-Aldrich, Poole, UK), 2.1 g of  $\text{KH}_2\text{PO}_4$  (BDH Chemical Ltd., Poole, UK), 2 g of KCl (Fisons Scientific Equipment, Loughborough, UK) and 1.1 g of  $\text{Na}_2\text{HPO}_4$  (BDH Chemical Ltd., Poole, UK) were dissolved in 10 L of distilled water and the pH was adjusted to 7.4.

#### *0.05 M Ethylenediaminetetraacetic acid (EDTA)*

1 g of KCl (Fisons Scientific Equipment, Loughborough, UK), 5.72 g of  $\text{Na}_2\text{HPO}_4$  (BDH Chemical Ltd., Poole, UK), 1 g of  $\text{KH}_2\text{PO}_4$  (BDH Chemical Ltd), 40 g of NaCl (Sigma-Aldrich, Poole, UK) and 1.4 g of EDTA (Duchefa Biochemie, Haarlem, The Netherlands) were dissolved in 5 L of distilled water and adjusted to pH 7.4. This solution was then autoclaved and stored until needed.

#### *Trypsin/EDTA (25 mg/ml)*

500 mg of trypsin (Sigma-Aldrich, Poole, UK) was dissolved in 20 ml of the 0.05 M EDTA solution detailed above, mixed and filtered through a 0.2  $\mu\text{m}$  minisart filter (Sartorius, Epsom, UK). This solution was split into 250  $\mu\text{l}$  aliquots and stored at  $-20^\circ\text{C}$  for further use. When needed for cell

culture, one aliquot of the trypsin stock was further diluted in 10 ml of 0.05 M EDTA and used as required for the trypsinisation of cells.

#### *100X Antibiotic Cocktail Mix*

5 g of streptomycin, 3.3 g of penicillin, and 12.5 g of amphotericin B in DMSO were dissolved in 500 ml of PBS, filtered and divided into 5 ml aliquots and stored at -20°C for further use. One of the thawed 5 ml aliquots was then directly added to 500 ml bottles of media during the preparation of standard culture medium.

#### *Bone Matrix Extract (BME)*

Femur bone tissues were collected from patients undergoing total hip replacements at the Trauma and Orthopaedic Department of University Hospital of Wales and Llanddough Hospital. The collection was performed after receiving written consent from the donors and was implemented with strict adherence to a protocol ethically approved by the Bro Taf Research Ethics Committee (Panel B) for the Bro Taf Health Board, Cardiff, UK. The proximal femur samples collected consisted of the femoral head and part of the femoral neck. Once removed during the hip replacement process, the bone tissues were placed in sterile containers and stored at -20°C until the end of the operation. The samples were then transferred and stored at -80°C until use or further processing. For the extraction of *BME*, the femur samples first needed to be crushed using a Noviomagus bone mill with +/- 0.5 to 1 mm milling drums (Spierings Orthopaedics B.V., Nijmegen, The Netherlands). The resultant fragments were then further crushed by hand (5ml bone fragments: 20 ml of BSS) using a pestle and mortar, while on ice. 2.5 ml aliquots of the crushed fragments were then transferred to 15 ml centrifuge tubes, to which 10 ml of sterile BSS was added. This mixture was placed in a Bioruptor (Diagenode, Seraing, Belgium) and subjected to 5 minutes of uninterrupted pulses, 30 seconds on, 30 seconds off, in

an ice-cold water bath. Debris were subsequently removed by centrifuging the samples at 3000 rpm at 4°C for 5 minutes and the supernatants were transferred to fresh tubes. This was repeated five times for each sample. Total protein content of the bone extracts was then quantified using a Bio-Rd DC protein assay kit (Bio-Rad Laboratories, Hemel Hempstead, UK) before being standardised to 2 mg/ml. 1ml aliquots were prepared and stored at -80°C.

### 2.2.2 Solutions for use in Molecular Biology

#### *Diethyl pyrocarbonate (DEPC) water*

500 µl of diethylpyrocarbonate (DEPC; Sigma-Aldrich, Poole, UK) was made up to 500 ml using deionised water. The solution was then left overnight and autoclaved.

#### *Tris-Boric-Acid-EDTA (TBE)*

Premixed 10X stock solutions of TBE was purchased from Sigma-Adrich (Poole, UK) and diluted 1:10 in distilled water when needed.

#### *Loading buffer (used for agarose gel electrophoresis)*

25 mg of bromophenol blue and 4 g of sucrose (Fisons Scientific Equipment, Loughborough, UK) were dissolved in 10 ml of distilled water and stored at 4°C until needed.

### 2.2.3 Solutions for use in Cloning

#### *LB agar*

10 g of tryptone (Duchefa Biochemie, Haarlem, The Netherlands), 15 g of agar, 5 g of yeast extract (Duchefa Biochemie) and 10 g of NaCl (Sigma-Aldrich, Poole, UK) were dissolved in 1 L of distilled water. The pH was adjusted to 7.0 and the solution was autoclaved. For the preparation of agar plates, the solidified agar was melted and cooled. Selective antibiotics were then added, and the solution was poured into 10 cm Petri dishes (Bibby Sterilin Ltd, Staffs, UK). The plates were left to cool until the agar hardened and were subsequently inverted and stored at 4°C.

#### *LB broth*

10 g of tryptone (Duchefa Biochemie, Haarlem, The Netherlands), 10 g of NaCl (Sigma-Aldrich, Poole, UK) and 5 g of yeast extract (Duchefa Biochemie) was dissolved in 1 L of distilled water. The pH was then adjusted to 7.0 and the solution was autoclaved and kept at room temperature until needed. Selective antibiotics were then later added as required.

## **2.3 Cell Culture, Maintenance, Storage and Transfection**

### 2.3.1 Preparation of Growth Media

Dubelcco's Modified Eagle's Medium (DMEM/Ham's F-12 with L-glutamine; Sigma-Aldrich, Poole, UK), pH 7.3, containing 2 mM L-glutamine and 4.5 mM NaHCO<sub>3</sub>, supplemented with 10% heat-inactivated Foetal Bovine Serum (FBS; Sigma-Aldrich, Poole, England, UK) and an antibiotic cocktail (described in section 2.2.2), was routinely used to culture the PC-3, DU145 and VCaP cell

lines. Roswell Park Memorial Institute (RPMI) 1640 medium supplemented with 10% FBS and the antibiotic cocktail was used to culture LNCaP cells.

Cell lines transfected with the pEF6/V5-His-TOPO<sup>®</sup> vector (Life Technologies, Paisley, UK) were initially cultured in a “selection” medium, consisting of the cell line’s preferred culture medium supplemented with 5 µg/ml Blastidicin S (Melford Laboratories Limited, Suffolk, UK) for up to 7 days. Surviving cells were then transferred to and grown in a “maintenance” medium containing 0.5 µg/ml Blastidicin S. Resultant cell lines were continuously cultured in the maintenance medium thereafter to ensure that the cells retained the vector for subsequent *in vitro* studies.

### 2.3.2 Cell Maintenance

All cell lines were cultured in 25cm<sup>2</sup> and 75cm<sup>2</sup> tissue culture flasks (Greiner Bio-One Ltd, Gloucestershire, UK) with loosely fitted caps in a humidified incubator at 37°C, 5% CO<sub>2</sub> and 95% humidity. Cell confluency was assessed by visually approximating the percentage of cells covering the culture surface of the tissue culture flask using a light microscope. Once they reached a confluency of approximately 85-90%, cells were then sub-cultured or collected if needed for experimental work, as described in section 2.3.3. All cell work was carried out aseptically, using a Class II Laminar Flow Cabinet (ThermoFisher Scientific, Massachusetts, USA) with sterile and autoclaved equipment and consumables.

### 2.3.3 Adherent Cell Trypsinisation and Cell Counting

Once cells had reached a confluency of approximately 85-90%, the medium was aspirated, and the cells were briefly rinsed with sterile PBS to wash away any traces of serum, which would

otherwise inhibit the effect of trypsin. Depending on the size of the flask cells were cultured in, 0.5-1 ml of Trypsin/EDTA (0.01% trypsin, 0.05% EDTA in BSS) was used to detach adherent cells by incubating them with the trypsin for approximately 5 minutes at 37°C. Once detached, cells were collected in their respective media containing FBS to stop the trypsinisation reaction and transferred to 20 ml universal containers (Greiner Bio-One Ltd, Gloucestershire, UK) before being pelleted at 1,000 rpm for 5 minutes. The supernatant was then aspirated, and the cell pellet was resuspended in the appropriate medium. Cells were either split and transferred to fresh tissue culture flasks for re-culturing or counted using a haemocytometer (Fuchs Rosenthal, Hawksley, UK) and a light microscope at 10X magnification for subsequent use in experimental assays.

Throughout this study, a haemocytometer was used to assess cell count. The haemocytometer allows for the calculation of cell density in a predetermined volume of fluid contained in the counting chamber. This value can be converted to obtain the number of cells per millilitre in the overall cell suspension, from which the volume of cell suspension needed to obtain the appropriate cell concentration for experimental needs. The haemocytometer counting grid is divided into 16 large square areas with dimensions of 1 mm x 1 mm x 0.2 mm (0.2 mm<sup>2</sup>), which are each subdivided into 16 squares. For better accuracy in the determination of cell density, cells were counted in the 4 large corner squares. Cell number was calculated using the following equation:

$$\text{Cell number per ml} = \left( \frac{\text{Total number of cells in 4 corner squares}}{2} / 4 \right) \times 10^4$$

#### 2.3.4 Transfection of Cells by Electroporation

1 - 2 µg of empty control vector, and vectors encompassing the coding sequences of the genes studied were used to transform DU145 cells. Confluent, low passage wild type DU145 cells were detached from tissue culture flasks and resuspended in serum-free medium. A cell suspension of approximately  $1 \times 10^6$  cells in 800µl per transfection was prepared and added to sterile 0.4 cm gap electroporation cuvettes (Eurenetech, Southampton, UK), which were then placed on ice. Subsequently, 5 - 10 µg of purified vector was added to the corresponding cuvette (see section 2.5.8), mixed briefly using the pipette tip before it was subjected to an electrical pulse from a Gene Pulser Xcell™ Electroporation System (Bio-Rad Laboratories, Hemel Hempstead, UK) set to 290 V, 700 µM. Following this pulse, the cell and vector suspension was quickly transferred to a 25 cm<sup>2</sup> tissue culture flask containing 5 ml of pre-warmed medium containing FBS and antibiotics and left in an incubator at 37°C overnight to allow cells to recover and adhere.

#### 2.3.5 Storage of Cell Stocks in Liquid Nitrogen

Cells were trypsinised as described above in section 2.3.3 and resuspended in the appropriate growth medium. 5-10% Dimethyl sulphoxide (DMSO; Sigma-Aldrich, Poole, UK) was added to the cell suspension and 1 ml aliquots were transferred into pre-labelled 1.8 ml cryovials (Nunc, Fisher Scientific, Leicestershire, UK), which were then wrapped in protective tissue paper before being stored at -20°C for approximately 3 hours, then overnight at 80°C, and finally transferred to liquid nitrogen tanks for long term storage, until required.

### 2.3.6 Cell Resuscitation

In order to resuscitate frozen down cells, cryovials were taken from liquid nitrogen storage and placed on dry ice. They were then rapidly thawed in a water bath at 37°C before being transferred into a universal container containing 10 ml of pre-warmed medium to immediately dilute the DMSO present. Traces of the DMSO were removed from the cells by centrifuging them at 1,400 rpm for 10 minutes, and the supernatant was aspirated. The cell pellet was resuspended in 5ml of medium before being transferred to a fresh 25 cm<sup>2</sup> tissue culture flask and maintained in a humidified incubator at 37°C and 5% CO<sub>2</sub>. After 24 hours, the revived cells were examined under the microscope to visually assess the viability of the adherent cells. The medium was aspirated and replaced with fresh, pre-warmed medium to remove any residual DMSO. The flask was returned to the incubator and the previous standard subculture techniques were carried out when necessary.

## 2.4 Methods for RNA Detection

### 2.4.1 mRNA Isolation

TRI reagent® (Sigma-Aldrich, Poole, UK) was used for the extraction of mRNA and the protocol was completed as described by the manufacturer. Cells were grown in a monolayer and allowed to reach a confluency of approximately 85-90% before the medium was aspirated and the cells washed with PBS. TRI reagent® (1 ml per 5-10 x 10<sup>6</sup> cells) was then added to induce cell lysis. To ensure the detachment of cells, the cell monolayer was scraped off using a cell scraper and the homogenate was passed several times through a pipette tip to produce a homogenous lysate, which was then transferred into a 1.5 ml Eppendorf. The lysate was then allowed to incubate at

room temperature for 5 minutes to ensure the complete dissociation of nucleoprotein complexes. This was followed by the addition of 100  $\mu$ l (per 1 ml of TRI reagent<sup>®</sup> used) of 1-bromo-3-chloropropane (Sigma-Aldrich, Poole, UK) and immediate, vigorous shaking for 15 seconds. The homogenate was then left to incubate at room temperature for 15 min before being centrifuged at 12,000 x g for 15 minutes at 4°C (Mikro 200R, DJB labcare, Buckinghamshire, UK). Under these acidic conditions, the homogenate is separated into three phases – a pink lower organic phase containing protein, a white interphase containing DNA, and finally a clear upper aqueous phase containing the RNA. This aqueous phase, which normally constitutes around 40-50% of the total volume, was then carefully removed and transferred into a fresh Eppendorf. 500  $\mu$ l of isopropanol (Sigma-Aldrich, Inc., Poole, UK) was added to the RNA, briefly mixed by inversion and the sample was left to incubate for 10 minutes at room temperature. After centrifugation at 12,000 x g, 4°C for 10 minutes, the RNA precipitate forms as a white pellet on the bottom of the Eppendorf. The supernatant was then discarded, and the RNA pellet was washed by vortexing it with 750  $\mu$ l of 75% ethanol (3:1 ratio of pure ethanol and diethylpyrocarbonate, DEPC water) and subsequently centrifuging the sample at 7,500 x g for 5 minutes at 4°C. Once the ethanol was aspirated, the RNA pellet was briefly dried at 55°C for 5-10 minutes, in a Techne, Hybridiser HB-1D drying oven (Wolf laboratories, York, UK), or air-dried at room temperature, so as to remove any remaining traces of ethanol. The final step was to dissolve the RNA pellet in 20-50  $\mu$ l (depending on pellet size) of DEPC water by vortexing for a short while. Finally, the concentration of the resultant mRNA was assessed using a NanoPhotometer (Implen, München, Germany; see section 2.4.2) and standardised to 0.5  $\mu$ g/ml whenever possible.

#### 2.4.2 RNA Quantification

Once the isolation was complete, 1  $\mu\text{l}$  of the sample was used to measure the concentration and purity of the extracted RNA. This was carried out using a NanoPhotometer (Implen, München, Germany) set to detect single-stranded RNA ( $\mu\text{g}/\mu\text{l}$ ) at the wavelength of 260nm, using DEPC water as a blank. The purity of the RNA was estimated using the A260/A280 nm ratio.

#### 2.4.3 Reverse Transcription

The GoScript™ Reverse Transcription System (Promega, Southampton, UK) was used to convert extracted RNA into first-strand complementary DNA (cDNA). 4  $\mu\text{l}$  of isolated RNA of a known concentration was made up to 5  $\mu\text{l}$  with the Oligo(dT)<sub>15</sub> in a thin-walled 200  $\mu\text{l}$  PCR tube. This mix was then placed at 70°C for 5 minutes, after which it was immediately placed on ice and left to chill for at least 5 minutes. Following this incubation period, samples were centrifuged for 10 seconds, and placed on ice until the reverse transcription (RT) mix was added. The RT mix was made up using the following components:

<i>Component</i>	<i>Volume (<math>\mu\text{l}</math>)</i>
GoScript 5X™ Reaction Buffer	4
1.5 mM MgCl <sub>2</sub>	1.2
PCR Nucleotide Mix	1
Recombinant RNasin® Ribonuclease Inhibitor	0.5
GoScript™ Reverse Transcriptase	1
Nuclease-Free Water	7.3
<b><i>Total</i></b>	<b><i>15</i></b>

The above RT mix was added to each sample and the resultant mix was heated in an Applied Biosystems 2720 Thermal Cycler (Life Technologies, Paisley, UK) using the following conditions:

- Step 1 – Annealing at 25°C for 5 minutes
- Step 2 – Extending at 42°C for 1 hour
- Step 3 – Inactivation of the reverse transcriptase at 70°C for 15 minutes

The cDNA was diluted in nuclease-free water in the ratio needed. cDNA Samples were stored at -20°C.

#### 2.4.4 Reverse Transcription Polymerase Chain Reaction

RT-PCR was carried out using a GoTaq® Green Master Mix (Promega, Southampton, UK).

Reactions were set up in thin walled 200 µl PCR tubes or 96 well plates, as shown below:

<i>Component</i>	<i>Volume (µl)</i>
2X GoTaq® Green Master Mix	8
Forward primer (10 pmol)	1
Reverse primer (10 pmol)	1
Nuclease-free water	5
cDNA template	1
<b>Total</b>	<b>16</b>

Once prepared, the reactions were briefly vortexed and centrifuged. All reactions were run alongside a negative control, which consisted of using nuclease-free water instead of cDNA templates to ensure there was no contamination of the GoTaq® Green Master Mix and primer mix. A loading control probing for GAPDH expression was also run for each sample to confirm

similar concentrations of cDNA were present in each reaction prepared.

The PCR tubes or 96 well plates were sealed, briefly centrifuged, and placed in a 2720 Thermal Cycler (Applied Biosystems, Paisley, UK) and subjected to the following temperature shifts:

- Step 1 – Initial denaturation at 94°C at 5 minutes

Followed by 25-42 cycles of:

- Step 2 – Denaturation at 94°C for 30 seconds
- Step 3 – Annealing at 55°C for 30 seconds
- Step 4 – Elongation at 72°C for 1.5 minutes

And finally:

Step 5 – Final elongation at 72°C for 10 minutes

#### 2.4.5 Agarose Gel Electrophoresis

DNA fragments were fractionated according to size using agarose gel electrophoresis. Samples were loaded onto 0.8% - 2.5% agarose gels, depending on the predicted size of the DNA products. Agarose gels were prepared by adding the required amount of agarose (Melford Chemicals, Suffolk, UK) to the appropriate volume of 1X TBE buffer (Sigma-Aldrich, Poole, UK). The mix was then heated until the agarose was fully dissolved and 1:15000 SYBR safe DNA gel stain (Invitrogen, Paisley, UK) was added. The agarose was left to cool slightly before being poured into the removable gel casting tray and it was allowed to set around the teeth of a plastic comb, creating wells. Once set, the gel was submerged in 1X TBE buffer and the plastic comb was removed. 8 µl of the PCR samples were loaded in each well, alongside 5 µl of a 100 bp or 1 Kb DNA ladder (Genscript, Piscataway, NJ, USA). The samples were subjected to electrophoresis

using a power pack (Gibco, Paisley, UK) at 110 V, 100 mA, 50 W for approximately 1 hour and the gels were finally visualised and imaged using a U:Genius3 gel doc system (Syngene, Cambridge, UK).

#### 2.4.6 Quantitative Polymerase Chain Reaction

Quantitative PCR (qPCR), also known as real-time PCR is a simple and elegant method used to relatively quantify the amount of a target sequence or gene present in a sample. The current study utilised the Amplifluor™ Universal Detection System (Intergen Company, New York, USA), which allows for the simultaneous amplification and detection of the nucleic acid sequence of interest within a closed reaction vessel. This system operates by using two target-specific DNA primers and a universal primer, called the Uniprimer™, to incorporate a fluorescent signal into the PCR product amplified using a qPCR master mix (PrecisionFAST qPCR Master Mix; Integrated Sciences, Sydney, Australia). This is enabled through the addition of an 18-base oligonucleotide tail called the Z sequence (ACTGAACCTGACCGTACA) to the 5' end of one of the target-specific primers, called the Z primer. During the initial stages of amplification, the Z primer is extended following its hybridisation to the target sequence. This creates a new template for the next amplification step, during which the other target specific primer (Primer F; see Figure 2.1) is extended, synthesising a sequence that is complementary to the Z sequence (Z'). Since the Uniprimer™ structure also includes a 3' Z sequence, as well as a 5' hairpin structure linking a fluorophore (FAM) and quencher (DABSYL), it is able to anneal to the Z' sequence of the new template and gets extended. Thus, when this Uniprimer™ amplicon becomes the template for DNA polymerisation in the final cycle of amplification, the 5' to 3' exonuclease activity of the DNA polymerase is able to degrade and unfold the hairpin structure, increasing the distance between the fluorescein and DABSYL moieties, thereby allowing the emission of fluorescence. The resulting fluorescence signal emitted during each PCR cycle can then be directly correlated

to the exponential increase of DNA amplified in this process. The Amplifluor™ qPCR process is illustrated in Figure 2.1.

The cDNA used in qPCR was generated as described in section 2.4.3 and diluted 1:8 using nuclease-free water; this cDNA was then used to make up a reaction mixture outlined below:

<i>Component</i>	<i>Volume (μl)</i>
PrecisionFAST 2X qPCR Master Mix	5
Forward primer (10pmol)	0.3
Reverse Z primer (1pmol)	0.3
UniPrimer™ (10pmol)	0.3
cDNA template and nuclease-free water	4
<b><i>Total</i></b>	<b><i>9.9</i></b>

Each sample was loaded into a 96 well plate (Bio-Rad Laboratories, Hemel Hempstead, UK) in triplicate and sealed with optically clear Microseal (Bio-Rad Laboratories). The qPCR was carried out using StepOnePlus™ Real-Time PCR System (ThermoFisher Scientific Scientific, Massachusetts, USA) set with the following experimental parameters:

- Step 1 – Initial denaturation at 94°C for 5 minutes
- Step 2 – Denaturation at 94°C for 10 seconds
- Step 3 – Annealing at 55°C for 15 seconds
- Step 4 – Elongation at 72°C for 20 seconds

Steps 2-4 were repeated for 100 cycles.

The fluorescent signal was detected at the annealing stage by a camera. A threshold cycle (CT value) was then set at which point the fluorescence in each sample was used to comparatively measure transcript copy numbers between the samples tested. Results were analysed using  $\Delta\Delta\text{CT}$  normalisation to the housekeeping gene glyceraldehyde 3-phosphate dehydrogenase (GAPDH) (Livak and Schmittgen 2001), the levels of which were measured in parallel to the target genes.

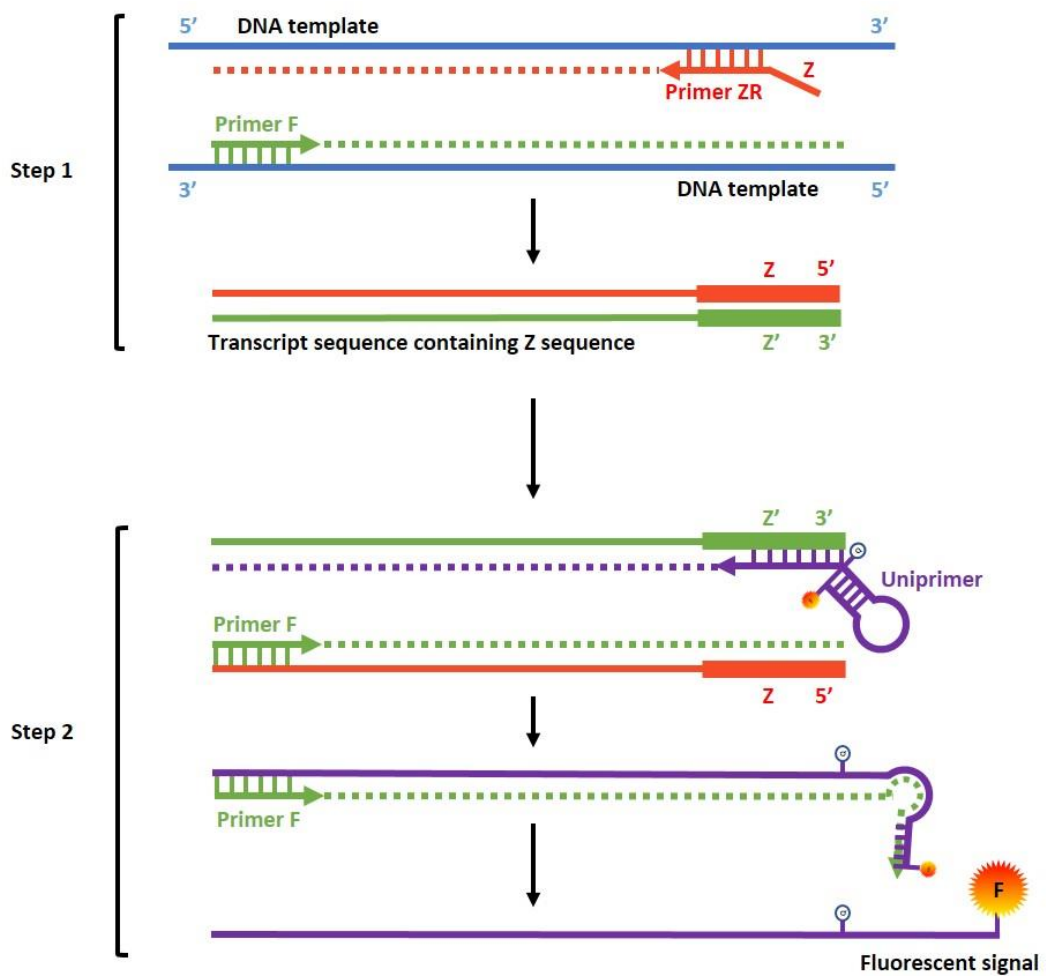
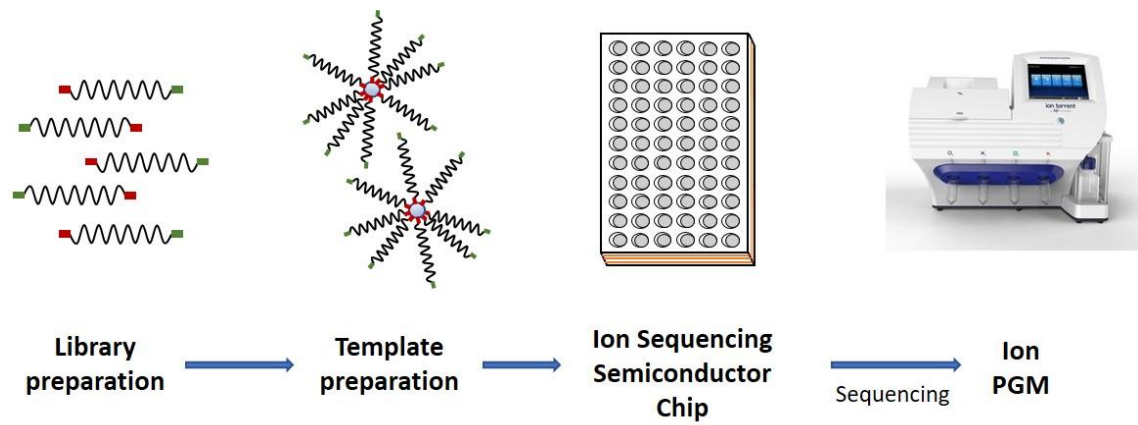


Figure 2.1. Diagram depicting the principle behind qPCR using the Amplifluor™ Universal Detection System.

#### 2.4.7 RNA sequencing

RNA sequencing (RNA-Seq), a revolutionising approach for the study of the transcriptome of cells, refers to high-throughput techniques used to determine the primary sequence and relative abundance of RNA fragments within given samples. In this study, the targeted-sequencing of a selection of prostate cancer cell lines was carried out using the Ion Torrent Personal Genome Machine™ (PGM™; ThermoFisher Scientific, Massachusetts, USA). The Ion Torrent method is a multistep process (see figure 2.2), the first step of which is to generate a barcoded library with the help of the Ion AmpliSeq™ Transcriptome Human Gene Expression Kit. To do so, the SuperScript® VILO™ cDNA Synthesis Kit, supplied as part of the gene expression kit, is used to generate cDNA from mRNA samples. Then, specific cDNA fragments are targeted and amplified by PCR and the products are flanked by Ion Torrent adapters. This creates the barcoded library, which is subsequently purified, quantified and diluted to 100 pM. Following library preparation, the next step is to prepare the templates, whereby, using the Ion PI™ Template OT2 200 v3 Kit, the diluted library fragments are clonally amplified onto Ion Sphere™ particles (ISPs) by emulsion PCR (emPCR). The enriched ISPs are then deposited in the chip wells of an Ion PI™ Chip v2 by a short centrifugation step before placing the chip on the PGM™, and the samples are sequenced using the Ion PI™ Sequencing 200 Kit v3 chemistry.



**Figure 2.2. Schematic representation of the Ion Torrent sequencing workflow.**

For this study, targeted-sequencing of low passage PC-3 WT (passage 4) and VCaP WT (passage 5) was undertaken. These cells were seeded into the wells of a 6-well plate and incubated in DMEM supplemented with 5% FBS and antibiotics overnight. The cells were then incubated with either fresh 5% FBS DMEM or 50 µg/ml BME in 5% FBS DMEM for 3 hours 37°C, 5% CO<sub>2</sub>. Following the incubation period, the media were discarded, and the cells were washed in PBS and subsequently collected in TRI Reagent®. mRNA extraction was then carried out as described in section 2.4.1, and the concentration of the samples was determined using a NanoPhotometer (Implen, München, Germany). 10 ng of total RNA extracted from the prostate cancer cell lines was subsequently used for RNA sequencing.

## 2.5 Alteration of Gene Expression in Prostate Cancer Cell Lines

### 2.5.1 TOPO Gene Cloning and Generation of Stable Transfectants

In order to assess the potential roles that BMP antagonists, Noggin, Follistatin and Gremlin, play in prostate cancer progression and bone metastasis, their gene expression profiles were altered in the mammalian cell line, DU145, using vectors encompassing their coding sequences to assess any consequential phenotypic changes.

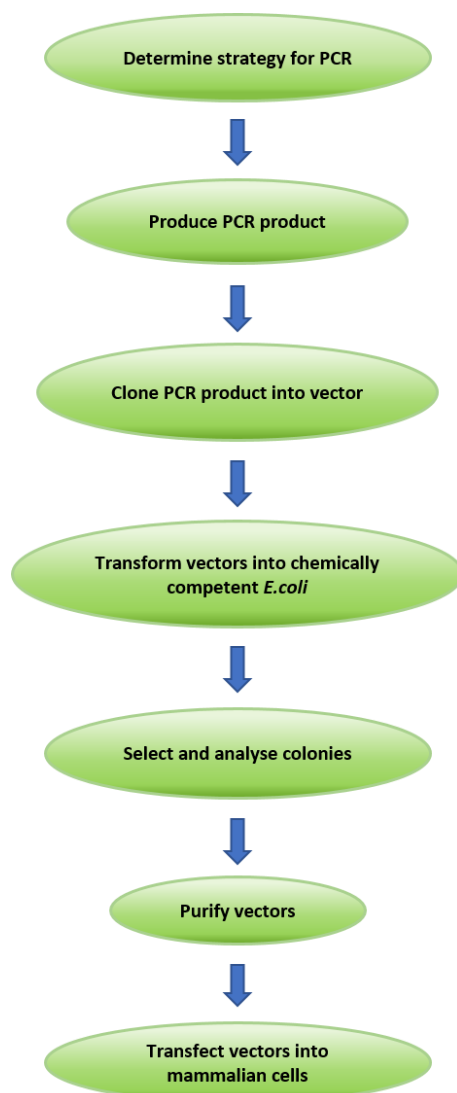


Figure 2.3. Flow-chart depicting the TOPO® TA cloning procedure.

## 2.5.2 Gene Overexpression

The amplification of the coding sequences of Noggin, FST344 and Gremlin was carried out by touchdown PCR using the JumpStart™ AccuTaq™ LA DNA Polymerase Mix (Sigma-Aldrich, Poole, UK). Primers capable of amplifying the complete coding sequences of these BMP antagonists were designed using Primer-BLAST, and cDNA transcribed from normal prostate tissue mRNA was used as a template. The reactions set up for each BMP antagonist were as follows:

<i>Component</i>	<i>Volume (μl)</i>
JumpStart™ AccuTaq™ LA DNA Polymerase Mix	12.5
Forward primer (10 pmol)	1
Reverse primer (10 pmol)	1
Nuclease-free water	9.5
cDNA template	1
<b>Total</b>	<b>25</b>

The touchdown PCR cycling program was then carried out to maximize the specificity of PCR reaction by gradually decreasing the annealing temperature of the reaction every 5 cycles. The cycling conditions were as follows:

- Step 1 – Initial denaturation period, 94°C for 5 minutes
- Step 2 – Denaturation 93°C for 20 seconds
- Step 3 – Annealing at 64°C for 20 seconds, 62°C for 20 seconds, 60°C for 20 seconds and 58°C for 20 seconds
- Step 4 – Elongation 72°C for 1.5 minutes

Steps 2-4 were repeated over 5 cycles for each annealing temperature. The final amplification was as follows:

- Step 5 – Denaturation at 93°C for 20 seconds
- Step 6 – Annealing at 56°C for 30 cycles
- Step 7 – Final elongation at 72°C for 10 minutes

Following the touchdown PCR, 5 µl of loading buffer was added to each reaction and they were run and visualised on a 1.5% agarose gel.

### 2.5.3 Extraction of PCR products from Agarose Gel

Following the agarose gel electrophoresis of the touchdown PCR products (from section 2.6.2), bands corresponding to the expected sizes of the genes of interest were excised from the gel using a clean and sharp scalpel and transferred to tared 1.5 ml Eppendorf tubes, taking care to trim away any excess gel. The GenElute™ Gel Extraction Kit (Sigma-Aldrich, Poole, UK) was then used to extract these PCR products from the agarose gel according to the manufacturer's instructions.

First, the weight of the gel in the tared tubes was determined so that the gel pieces could be resuspended in 300 µl of Gel Solubilisation Solution per 100 mg of agarose gel. Upon addition of the solubilisation solution, the gel slices were then incubated at 55°C for approximately 10 minutes, or until they were dissolved, ensuring complete dissolution of the gel by vortexing the mix every 2-3 minutes throughout the incubation period. Meanwhile, the binding columns were prepared. This was achieved by placing binding columns, GenElute™ Binding Column G, into the provided 2 ml collection tubes, adding 500 µl of the Column Preparation Solution to each

column, and centrifuging them at 14 000 x g for 1 minute. The flow-through was discarded. When the gel slices were completely dissolved, 100 µl of 100% isopropanol (Sigma-Aldrich, Poole, UK) per 100 mg of gel was added to each solubilised gel solution and the mix was loaded into the prepared columns. Following a brief centrifugation period of 1 minute at 14 000 x g, the flow-through was again discarded and the binding columns were washed with 700 µl of Wash Solution. Once more, the flow-through was discarded and the collection tubes were centrifuged again to remove any excess ethanol. Finally, the PCR products were eluted in fresh Eppendorf tubes using 50 µl of Elution Solution and the products were kept at -20°C until needed.

#### 2.5.4 TOPO TA Gene Cloning

The pEF6/V5-HIS-TOPO® TA Expression Kit (Invitrogen, Paisley, UK) provides a highly efficient, one-step cloning strategy for the insertion of selected *Taq* polymerase-amplified PCR products into a vector suited for high-level constitutive expression in mammalian cells.

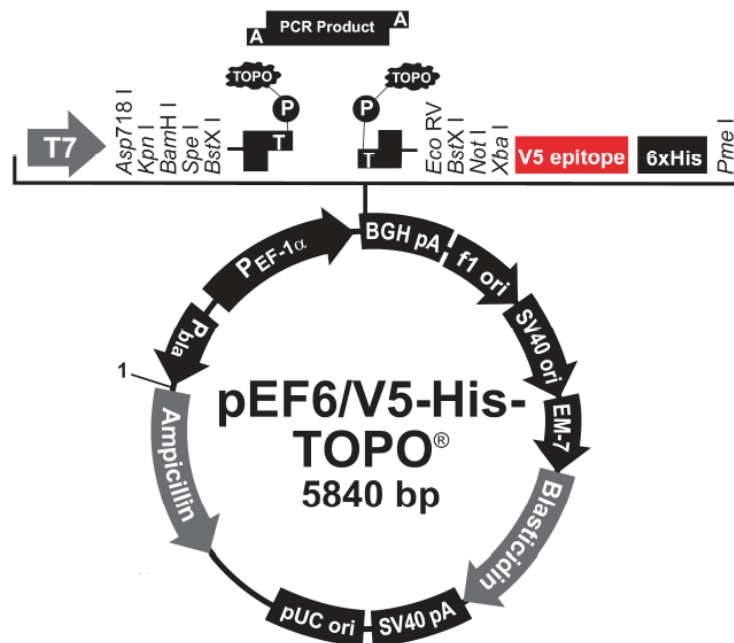


**Figure 2.4. Schematic of the pEF6/V5-HIS TOPO® vector** (taken from the pEF6/V5-HIS-TOPO® TA Expression Kit protocol).

The one-step TOPO TA cloning system offers a direct approach to cloning that does not require the use of any ligases, post-PCR procedures or PCR primers. This is made possible as the pEF6/V5-HIS-TOPO® vector provided in the above expression kit is supplied linearised with single 3' deoxythymidine (T) overhangs and two topoisomerase I enzymes covalently bound to the vector (also referred to as an “activated vectors”; see figure 2.4). As such, since *Taq* polymerase has a non-template-dependent tendency to add single deoxyadenosine (A) residues to the 3' ends of PCR products, these amplified gene sequences are able to efficiently ligate to the 3' T overhangs of the vector.

The cloning procedure was undertaken as specified by the manufacturers. TOPO cloning reactions were in pre-labelled microfuge tubes set up as shown below and the reactions were mixed gently before being incubated for 5 minutes at room temperature.

<i>Component</i>	<i>Volume (μl)</i>
PCR product	4
Salt Solution	1
TOPO vector	1
<b><i>Total</i></b>	<b>6</b>

The cloning reactions were stored on ice until needed for transformation of the vectors into chemically competent *E. coli*.

### 2.5.5 Transformation of Chemically Competent *E. coli*

To transfer the cloned vectors into bacteria, 5 µl of TOPO TA cloning reaction was added to 25 µl of One Shot® TOP10 Chemically Competent *E. coli* (Invitrogen, Paisley, UK) and gently mixed by stirring using the pipette tip. The mix was incubated on ice for 30 minutes, heat-shocked at 42°C for 30 seconds, and immediately transferred back to ice. Then, to each vector-bacteria mix, 250 µl of room temperature Super Optimal broth with Catabolite repression (SOC) medium was added, and the tubes were shaken at 225 rpm on a horizontal orbital shaker (Bibby Stuart Scientific, UK) at 37°C for 1 hour. Following the incubation period, the transformed *E. coli* were spread in different seeding densities on pre-warmed agar petri dishes supplemented with 100 µg/ml ampicillin. Plates were incubated overnight at 37°C.

### 2.5.6 Colony Selection and Orientation Analysis

Since the pEF6/V5-HIS-TOPO® structure includes selection markers that allow cells expressing the vector to grow in the presence of ampicillin and/or blasticidin (see figure 2.4), any *E. coli* colonies which grew on selective agar plates following the transformation procedure were deemed to be positive for the vector. However, to confirm this and to verify the correct orientation of the incorporated PCR product within the vector, further testing was needed. This was achieved by testing 10 colonies on each petri dish and using a primer combination of target specific forward primers and vector specific primers (T7F or BGHR) to run two PCR reactions for each colony. The two reaction mixes set up for each colony are outlined below:

<i>Component</i>	<i>Volume (<math>\mu</math>l)</i>
<i>Reaction 1</i>	
2X GoTaq® Green Master mix	8
Vector specific T7F	1
Target specific forward primer	1
Nuclease-free water	6
<i>Reaction 2</i>	
2X GoTaq® Green Master mix	8
Vector specific BGHR	1
Target specific forward primer	1
Nuclease-free water	6

Once the reaction mixes were combined, samples of colonies were added. To do so, 10 individual colonies were selected and labelled. Then, the reaction mixes were inoculated with the corresponding colony using a sterile pipette tip. The samples were placed in a thermal cycler and subjected to the PCR cycling conditions described above (see section 2.4.6), before being run electrophoretically on a 1% agarose gel. The diagram below demonstrates the results obtained when verifying colonies picked during the process of cloning Noggin, Follistatin and Gremlin overexpression vectors.

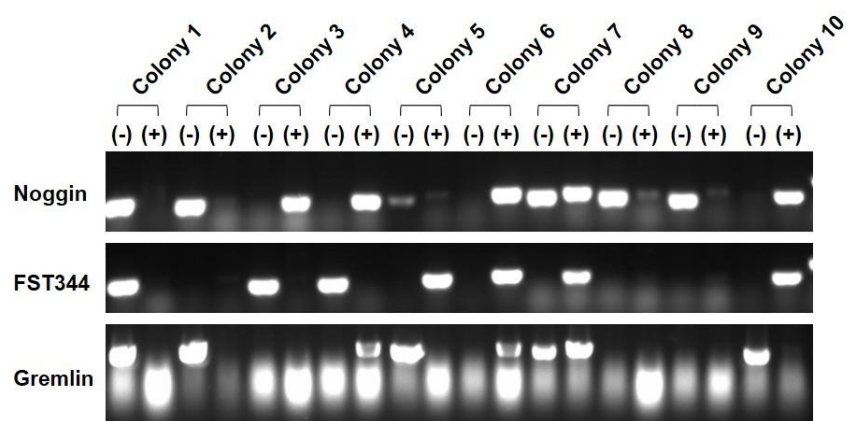


**Figure 2.5. Verifying the insert orientation of newly generated Noggin, Follistatin and Gremlin overexpression vectors.** The (-) lane demonstrate PCR reactions carried out using Noggin, Follistatin or Gremlin forward primers and T7F, while reactions shown in the (+) lane were carried out using the same target specific forward primers and BGHR. Colonies that demonstrated bands in (-) lanes or in both (-) and (+) consisted of cells expressing vectors with inserts in the wrong orientation. Colonies showing bands in the (+) lanes only were selected for amplification and further use in experiments.

#### 2.5.7 Vector Amplification, Purification and Quantification

Following the identification of colonies expressing vectors with correct insert orientation, single colonies were transferred aseptically from the petri dishes and each used to inoculate 10 ml of LB broth supplemented with 100 µg/ml ampicillin. The inoculated broths were then shaken overnight at 220 rpm while incubated at 37°C, and the resultant recombinant *E. coli* cultures were pelleted at 5,000 rpm for 10 minutes, discarding the supernatant.

Vector extraction was undertaken using the GenElute™ Plasmid MiniPrep Kit (Sigma, Poole, UK) based on the protocol provided. Once pelleted, the bacterial cultures were resuspended thoroughly with 200 µl of Resuspension Solution containing RNase A and transferred to 1.5 ml Eppendorf tubes. The resuspended cells were then lysed by adding 200 µl of Lysis Solution and immediately mixed by gentle inversions (6-8 times), all the while ensuring that the lysis reaction did not exceed 5 minutes so as to avoid permanent plasmid denaturation. Lysis of the *E. coli*

cultures using the highly alkaline Lysis Solution creates a white precipitate that consists of large chromosomal DNA, lipids and proteins. Therefore, to remove these cell debris, 350  $\mu$ l of Neutralisation Solution was added to each tube and they were gently inverted 6 times before being centrifuged at 12,000 x g for 10 minutes. Meanwhile, the binding columns were prepared by inserting GenElute Miniprep Binding Columns in microfuge tubes, adding 500  $\mu$ l of Column Preparation Solution to each column and centrifuging them at 12,000 x g for 1 minute. The flow-through was discarded. The clear lysates obtained from the neutralisation step were then transferred to the binding columns and they centrifuged again at 12,000 x g for 1 minute, discarding the flow-through. To clean up the plasmid DNA from any residual salts and debris, 700  $\mu$ l of Wash Solution (containing ethanol) was added to the Miniprep binding columns, which were centrifuged at 12,000 x g for 1 minute before discarding the flow-through. Any excess ethanol from the Wash Solution was removed by centrifugation at 12,000 x g for 1 minute, and the binding columns were transferred to fresh collection tubes. Finally, plasmid DNA was eluted by centrifuging 50  $\mu$ l of Elution Solution through the binding columns at 12,000 x g for 1 minute. The eluted vectors were quantified using a NanoPhotometer set to detect double-stranded DNA ( $\mu$ g/ $\mu$ l), using the Elution Solution as blank. The plasmid DNA was then immediately used or stored at -20°C until needed.

#### 2.5.8 Establishment of Stably Transfected Mammalian Cell Lines

Once the Noggin, Follistatin and Gremlin overexpression vectors were amplified, isolated and quantified, they were ready to be introduced into low passage DU145 cells by electroporation, as outlined in section 2.3.4. Empty pEF6/V5-HIS-TOPO® vectors were also transfected into cells using the same method. To ensure that the transfected cells established stable cell lines carrying these vectors, a selection process was implemented whereby the blasticidin resistance marker of pEF6/V5-HIS-TOPO® was exploited. Following transfection, surviving cells that were left to

adhere and recover overnight were subjected to an initial 7-day period of intense selection by incubating them in DMEM supplemented with 5 µg/ml of Blastidicin S (selection medium). After this initial selection period, cells were transferred to, grown in and continuously cultured in maintenance DMEM containing 0.5 µg/ml of Blastidicin S, therefore ensuring long-term transformation.

All the recombinant cell lines were tested by RT-PCR and qPCR initially and routinely, as well as following cell revival to verify the efficacy and stability of the expression of the overexpression vectors. Once the cell lines had been verified to stably express the desired gene, they were then subjected to various *in vitro* functional assays.

## **2.6 *In vitro* Functional Assays**

To assess the effect of BMP antagonists and the bone microenvironment on prostate cancer progression and metastasis, the generated cell lines, DU145 pEF, DU145 Noggin, DU145 FST344 and DU145 Gremlin, were subjected to *in vitro* functional assays whilst incubated in either Blastidicin S maintenance DMEM or 50 µg/ml BME in maintenance DMEM. As such, the data presented were standardised against the pEF control in maintenance DMEM. With the aim to minimise the inherent effect of growth factors present in FBS on the cells, the FBS content of the maintenance DMEM used in these assays was reduced to 5%, with overnight incubation of the cells in this medium prior to experiments. The cell proliferation, invasion and Matrigel adhesion assays were all carried out using the Crystal Violet method, whereby cells were fixed and stained using the dye, and subsequently subjected to spectrophotometry to obtain relative cell density (Bonnekoh, Wevers et al. 1989).

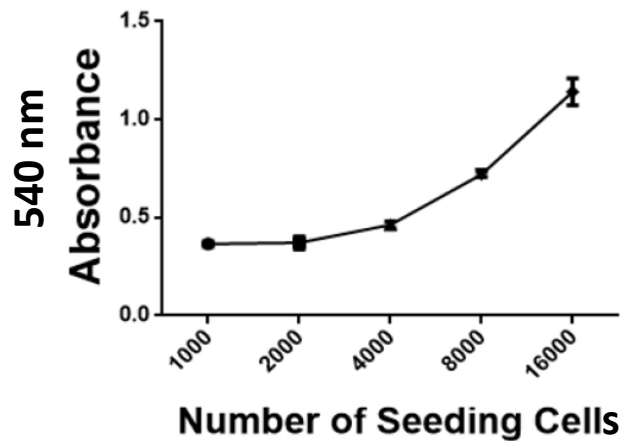


**Figure 2.6: Crystal Violet dilution curve.** The diagram demonstrates the absorbance at 540nm against a known number of seeded cells. The dilution curve demonstrates that the method is quite a sensitive method, as long as cell numbers are not too low.

#### 2.6.1 Cell Proliferation Assay

The overexpression cell lines and the control cell line were trypsinised and cell concentrations (per millilitre) were determined as previously described in section 2.3.3. The cell suspensions were then pipetted into 12 replicate wells of three 96-well plates (NUNC, Greiner Bio-One, Stonehouse, UK) at a seeding density of  $3 \times 10^3$  cells/100  $\mu$ l and topped up with an additional 100  $\mu$ l of maintenance DMEM or BME treatment medium, making up the total volume in each well to 200  $\mu$ l. Plates were subsequently incubated for 1-, 3- or 5-day periods at 37°C with 5% CO<sub>2</sub>, after which, following the appropriate incubation period, the medium was removed and cells were fixed in 4% formaldehyde (v/v) in BSS for 10 minutes. Adhered cells were then stained in 0.5% crystal violet (w/v) in distilled water for 10 minutes, and the excess stain was washed off with water before leaving the plates to dry at room temperature for 24 hours. To determine the cell density in each well, the dye staining fixed cells was solubilised in 200  $\mu$ l of 10% acetic acid and the absorbance was measured at 540 nm using a plate reading spectrophotometer (BIO-TEK, Elx800, UK). Growth rates were then calculated by comparing the absorbance

measurements obtained for the 3-day or 5-day incubation periods against the baseline absorbance taken at day 1. The equation below was used:

$$\text{Growth rate} = \frac{(\text{day 3 or day 5 absorbance}) - \text{day 1 absorbance}}{\text{day 1 absorbance}}$$

### 2.6.2 Matrigel Invasion Assay

The invasive capacity of the cell lines used in this study was determined using an *in vitro* Matrigel invasion assay (modified from (Albini, Iwamoto et al. 1987). This technique aims to mimic an *in vivo* environment, complete with basement membrane, through which the cancer cells are able to invade and migrate. To do so, the assay made use of Transwell inserts (Falcon, 24-well format, Greiner Bio-One, Stonehouse, UK) with a polycarbonate membrane and 8 µm pores, the latter being large to allow cells to migrate through. The surface of this membrane was then coated with a gelatinous protein mixture, Matrigel (BD Matrigel™ Basement Membrane Matrix; BD Biosciences, New Jersey, USA), to form the artificial basement membrane. The following method outlines how the experiment was set up.

Duplicate Transwell inserts per cell line were aseptically placed into the wells of a 24-well plate (NUNC, Greiner Bio-One). Then, once the Matrigel had completely thawed on ice, a stock Matrigel solution of 0.5 mg/ml in serum-free DMEM was prepared. 100 µl aliquots of this Matrigel solution were pipetted into the inserts, bringing the total amount of Matrigel in each insert to 50 µg. The inserts were then placed in a drying oven for approximately 2 hours at 55°C to dry out the Matrigel, forming thin gel layers. The latter were rehydrated prior to use with 100

$\mu\text{l}$  of serum-free medium for 40 minutes at room temperature. When the Matrigel layers were rehydrated, the serum-free medium was then aspirated and replaced with 100  $\mu\text{l}$  of either Blasticidin S maintenance medium or BME treatment medium, to which  $3 \times 10^4$  cells/100  $\mu\text{l}$  of cell suspension was added.  $3 \times 10^4$  cells of each cell line were also added to spare wells of the 24-well plate so as to get a baseline measurement of cell growth during the 72-hour incubation period. 450  $\mu\text{l}$  of maintenance medium was then pipetted into these spare wells as well as the wells containing the inserts in order to sustain any cells that migrated through the insert pores (see figure 2.6). The plates were incubated for 72 hours at 37°C, 5% CO<sub>2</sub> and 95% humidity.

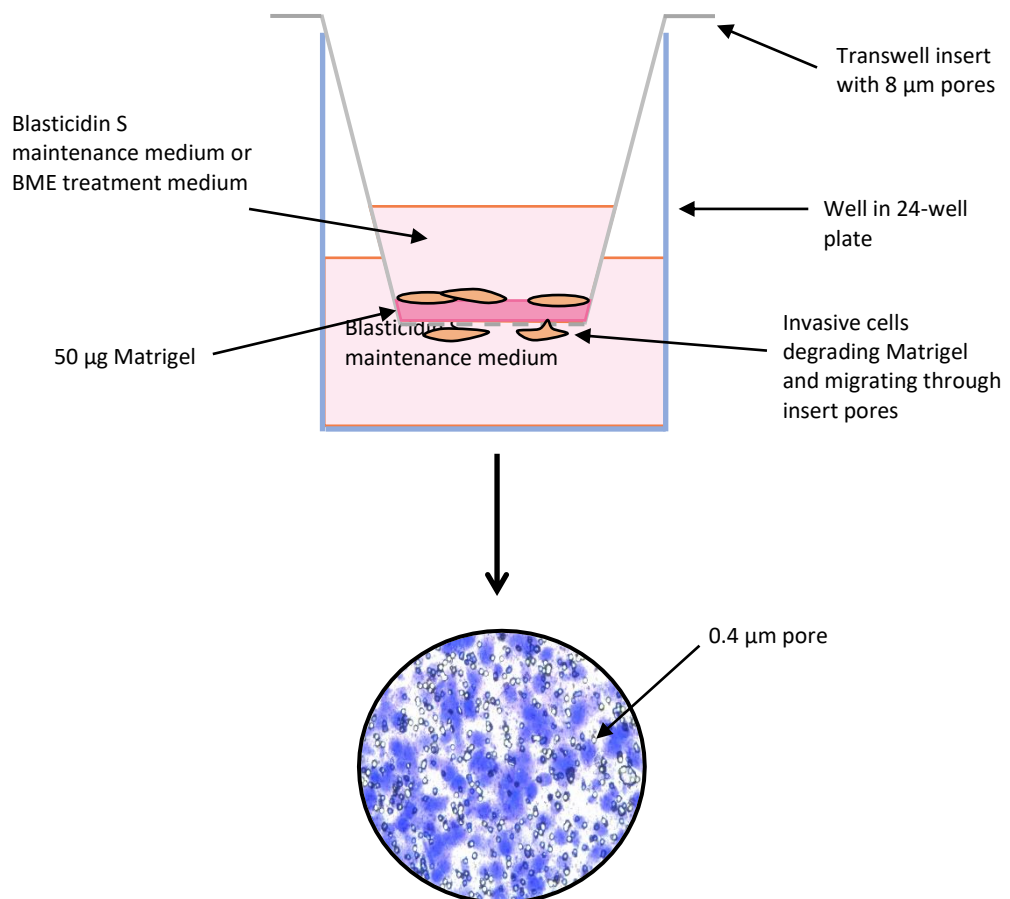


**Figure 2.7. Schematic illustration of the *in vitro* Matrigel invasion assay.** Following an incubation period, during which the cells are allowed to invade through the Matrigel and pores of the inserts, the Matrigel is wiped away and cells adhered to the underside of the insert are fixed and stained using Crystal Violet and viewed under the microscope as seen by the representative image above.

After the 72-hour incubation period, all the media in the inserts and the wells were discarded. The Matrigel together with any non-invaded cells inside the inserts were thoroughly cleaned off using tissue paper and cotton swabs, and the inserts were replaced in their corresponding wells on the 24-well plate. Cells on the underside of the inserts were then fixed in 4% formaldehyde (v/v) in BSS for 10 minutes before being stained in 0.5% crystal violet solution (w/v) in distilled water, also for 10 minutes. Following staining, the excess crystal violet solution was washed off using water and the inserts were left to dry at room temperature for 24 hours. To measure the invasiveness of the cells tested, the crystal violet dye was completely solubilised in 650  $\mu$ l of 10% acetic acid and 100  $\mu$ l aliquots of the resultant solution was subsequently transferred from each well to 6 replicate wells of a 96-well plate. This was also carried out for wells set up for baseline cell growth measurement. Cell density was then measured by spectrophotometry at 540 nm. Invasion rates were calculated by normalising absorbance readings from the insert containing wells against the corresponding baseline cell growth measurements. This was done to eliminate any bias caused by differing growth rates.

### 2.6.3 Matrigel Adhesion Assay

For each cell line tested, 12 replicate wells of a 96-well plate were coated with 5  $\mu$ g of Matrigel in serum-free DMEM and left to dry for approximately 2 hours at 55°C in a drying oven. The dried gel layers were then rehydrated for 40 minutes at room temperature using 100  $\mu$ l of serum-free DMEM, which was subsequently aspirated and replaced with 100  $\mu$ l of maintenance DMEM or BME treatment medium.  $2 \times 10^4$  cells/100  $\mu$ l of cell suspension was seeded in each of the Matrigel-coated wells and the cells were allowed to adhere to the gel layer for 40 minutes at 37°C, 5% CO<sub>2</sub>. After the incubation time, any non-adhered cells were discarded together with the media by gently inverting the plate over a sink, and the wells were washed once with 200  $\mu$ l of BSS, taking care not to wash away the Matrigel layer. The adherent cells were then fixed in

4% formaldehyde (v/v) in BSS for 10 minutes before being stained in 0.5% crystal violet solution (w/v) in distilled water for 10 minutes. The plate was left to dry for at least 24 hours at room temperature. To determine the density of cells adhered to the Matrigel, the crystal violet stain was solubilised in 10% acetic acid and the absorbance was measured by spectrophotometry at 540 nm. To negate the effect of the Matrigel on the cell density measurements, wells without any cell suspension were also set up, fixed, stained and measured at 540 nm along with the experimental wells. Readings from the experimental wells were then normalised against these Matrigel control wells.

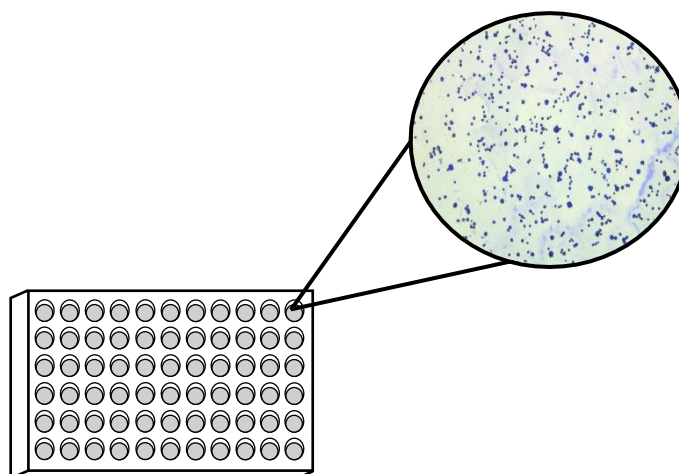


**Figure 2.8: Representative image of Crystal Violet-stained cells attached to a Matrigel-coated well during an adhesion assay.** The Matrigel adhesion assay was carried out as outlined in section 2.6.3, whereby cells were seeded at a density of  $2 \times 10^4$  cells. Following 40 minutes of incubation time, nonadherent cells were washed away, leaving the adhered cells to be fixed and stained using Crystal Violet. Background readings from the stained Matrigel was negated by setting up wells with only Matrigel to be stained and then subtracting these readings from test readings.

#### 2.6.4 Migration Assay (Wound Assay)

Cells were harvested in maintenance DMEM as previously described (section 2.3.3) and seeded into duplicate wells of a 24-well plate at a concentration of  $6 \times 10^5/500 \mu\text{l}$  cells for DU145<sup>PEF</sup>, DU145<sup>NOG</sup> and DU145<sup>GREM</sup>, and  $1 \times 10^6/500 \mu\text{l}$  cells for DU145<sup>FST344</sup>. They were then allowed to attach and reach confluency overnight at 37°C, 5% CO<sub>2</sub>. The following morning, 200  $\mu\text{l}$  pipette tips were used to scratch the cell monolayers, creating a wound, and the medium was aspirated to remove any floating cells. 500  $\mu\text{l}$  of maintenance DMEM or BME treatment medium was then pipetted into the wells and the plate was placed at 37°C, 5% CO<sub>2</sub> for 15 minutes to allow the cells to settle. To image the cell migration across the wound, the 24-plate was then placed in the onstage incubator of an EVOS™ FL Auto Cell Imaging System (ThermoFisher Scientific, Massachusetts, USA) set to image the wound each hour for 20 hours at 37°C, 5% CO<sub>2</sub>. Images were analysed using ImageJ Software (National Institutes of Health, Bethesda, Maryland, USA). The migration rate was calculated using the following equation:

$$\text{Migration rate} = \frac{(\text{Distance at } T_0 - \text{Distance at } T_t)}{\text{Distance at } T_0}$$

#### 2.6.5 ECIS

The Electric Cell-substrate Impedance Sensing® Z $\theta$  instrument (ECIS® Z $\theta$ ; Applied Biophysics, Troy, New York, USA) offers a real-time, *in vitro* approach to monitoring and quantifying the ability of cells to attach to a surface and achieve a spread morphology. As part of this method, cells are seeded and grown in special culture dishes equipped with small gold-film electrodes across which a small constant alternating current is applied. As cells adhere and spread on these

electrodes, their insulating membranes obstruct and constrain the current flow, causing a change in impedance. This change can subsequently be used to infer morphological information on the attached cells. In fact, the two parameters, resistance and capacitance, derived from impedance readings of cells respectively provide information on the quality and function of the cell barrier, and electrode cell coverage. Moreover, ECIS<sup>®</sup> offers the possibility to measure the impedance over a range of frequencies, enabling the study of morphological and functional cell properties based on cell-cell and cell-substrate interactions (Szulcek, Bogaard et al. 2014). The experiment was set up as follows.

A 96-channel array holder was connected to an ECIS Z $\theta$ <sup>®</sup> controller and pre-warmed at 37°C, 5% CO<sub>2</sub> and 95% humidity in an incubator. Meanwhile, 200 $\mu$ l of serum-free DMEM was aseptically pipetted into each well of a 96-well array (Applied Biophysics), which was subsequently secured on the array holder. A connection check and stabilisation were then performed using the Applied BioPhysics-ECIS Software V 1.2.135 (Applied Biophysics). Once this was complete, the serum-free DMEM was aspirated and 12 replicate wells per cell line were seeded with  $6 \times 10^4$  cells/100  $\mu$ l for DU145<sup>PEF</sup>, DU145<sup>NOG</sup> and DU145<sup>GREM</sup>, and  $8 \times 10^4$  cells/100  $\mu$ l for DU145<sup>FST344</sup>. The wells were then supplemented with 100  $\mu$ l of either maintenance DMEM or BME treatment medium. The 96-well array was replaced on the array holder and the software was configured to measure the resistance to the current flow at 4,000 Hz. Data was normalised using the resistance readings from the first time-point.

## 2.7 Database Research

Analysis of Genomic Expression Omnibus (GEO) datasets was performed using the GEO2R function of Pubmed-National Centre for Biotechnology Information (NCBI). The terms “prostate”, “cancer”, “osteoblastic” and “osteolytic” were used as search terms. GEO data from three previous studies was used. Heatmaps were generated using RStudio (see readings and bar graphs in appendix).

The first dataset (GSE36139) was obtained from the Cancer Cell Line Encyclopaedia (CCLE). The latter was generated from a large-scale genomic study of 947 cell lines, complete with pharmacological profiling of 24 compounds across approximately 500 of these cell lines. The CCLE encompasses cell lines relating to 36 tumour types, and mutational information was obtained by Next-Generation Sequencing (NGS) of 1,600 genes and by mass spectrometric genotyping, interrogating 492 mutations in 33 known oncogenes and tumour suppressors (Barretina, Caponigro et al. 2012). By assembling the CCLE, Barretina et al have provided us with the ability to obtain a comprehensive view of BMP signalling across a variety prostate cancer cell lines, against which we can compare or confirm our own findings.

The second dataset (GSE44143) comprised of microarray analyses of LNCaP-primary human osteoblast co-cultures performed by Sieh et (2014). This study aimed to investigate the pathophysiology of bone metastasis by establishing a 3D indirect co-culture model and assessing the paracrine interactions between prostate cancer cells and human primary osteoblasts (hOBs). This was achieved by embedding LNCaP cells within polyethylene glycol hydrogels and co-culturing them with hOBs grown on medical grade polycaprolactone-tricalcium phosphate (mPCL-TCP) scaffolds to form a tissue engineered bone construct (TEB). Microarray gene expression analysis was then performed to assay differences between LNCaP monocultures, hOB monocultures and LNCaP-hOB co-cultures. They accomplished this by hybridising extracted

RNA to a custom Agilent 4x180K oligo array assay (Agilent Technologies, Santa Clara, California) which incorporated the Agilent human gene expression probes with additional probes to detect protein-coding and non-coding RNAs. As a result of this study, Sieh et al have presented a novel 3D *in vitro* model that allows for the study of not only cellular, but also molecular changes occurring in prostate cancer cells and osteoblasts that arise from their cross-talk, the latter being relevant to the metastatic colonisation of the bone. As such, this presents an important of data to incorporate within the present study.

The third dataset (GSE41619) was obtained from Larson et al (2013). As part of this study, the gene expression profiles of 14 prostate cancer metastases from 11 patients were assessed by microarray analysis, with 7 of the samples identified as highly osteoblastic and the remaining 7 as highly osteolytic. These frozen bone core samples were then analysed using Agilent 44K whole human genome expression oligonucleotide microarrays (Agilent Technologies, Santa Clara, California) and pooled equal amounts of RNA isolated from prostate cancer cells, PC-3, DU145, LNCaP and CWR22, were used as a reference standard RNA. This data therefore provides the opportunity to dissect and examine relative changes in gene expression between osteolytic and osteoblastic lesions, enabling the identification of key genes in each type of lesion.

## **2.8 Statistical analysis**

Statistical analysis was performed using GraphPad Prism (GraphPad Software, California, USA). Each experimental protocol was performed at least three times (unless stated otherwise) and data obtained were presented as the mean of the repeats with standard error of the mean (SEM). Unpaired t-test with Welch's correction, unpaired t-test using the Holm-Sidak method, one-way ANOVA and two-way ANOVA were performed to test for statistical significance, with a

*P*-value of  $\leq 0.05$  considered to be statistically significant. Asterisk (\*) notations were used to signify significances: \*  $p \leq 0.05$ , \*\*  $p \leq 0.01$ , \*\*\*  $p \leq 0.001$  and \*\*\*\*  $p \leq 0.0001$ .

## Chapter 3.

# Differential Expression of BMPs and BMP antagonists in Prostate Cancer Cell Lines

### 3.1 Introduction

Advanced-stage prostate cancer is often associated with skeletal complications related to the spread of this disease to its preferred metastatic site, the bone. In fact, approximately 90% of patients that die as a result of prostate cancer have bone metastases (Bubendorf, Schöpfer et al. 2000). Typically, when the disease reaches this stage, a mixed osteolytic/osteoblastic bone response can be seen in the same patient at different metastatic sites (Roudier, Morrissey et al. 2008), although the interactions between the prostate cancer cells and the bone matrix predominantly yield an osteoblastic response. While the pathological events that take place during prostate cancer metastasis are well established, there is only a limited understanding of the exact molecular events involved. So far, studies have implicated a few protein families in this process (Coleman 2006), the BMP family being one of them.

As previously discussed, there are over 20 members of the BMP family which exert their effects through a heteromeric complex of two types of serine threonine kinase transmembrane receptors, termed type-I and type-II (Bragdon, Moseychuk et al. 2011). The extracellular BMP homo- or hetero-dimers utilise three type-I receptors, BMPRIA, BMPRIB and ActRIA, and three type-II receptors, BMPRII, ActRIIA and ActRIIB. When the BMP ligands bind to the BMPRs, they initiate the Smad-dependent or the Smad-independent pathway to subsequently modulate the transcription of target genes affecting key cellular processes like cell survival, apoptosis, migration and differentiation (see figure 1.7 for schematic of signalling pathways). The Smad-dependent pathway is initiated when the BMP dimer binds to a preformed complex of homodimeric type-I and type-II BMPRs, resulting in the phosphorylation of a regulatory domain within the type-I receptor, known as the GS box. The catalytically activate type-I receptor then recruits and phosphorylates BMP-specific intracellular members of the Smad family, R-Smads 1, 5 or 8/9, on their conserved SSXS motif. Once activated, the R-Smads dissociate from the type-I

receptor, presumably due to a change in conformation, and form an oligomeric complex with another R-Smads and a Co-Smad (Smad4), which, with the help of nuclear import and export factors, transits into the nucleus to regulate the transcription of target genes. In addition to this type of pathway, BMP signalling may also exert its effects by completely bypassing the use of Smads via a pathway known as the Smad-independent pathway. For this pathway to be triggered, the BMP dimer needs to interact with just one of the BMPR dimers, triggering the recruitment of a second BMPR dimer for the formation of the heteromeric BMPR complex. This pathway then typically proceeds through one or more MAPK signalling pathways (ERK, p38 or JNK) to indirectly bring about changes in target gene transcription.

Since BMPs are most commonly known for their inherent osteoinductive capacities, many have hypothesised their involvement in osteoblastic lesion formation arising in advanced prostate cancer. This was a theory that was first brought forward by Bentley and colleagues in the early 90s, who, by screening for the mRNA expression of BMPs, demonstrated the presence of BMPs 1-6 in prostatic adenocarcinoma (Bentley, Hamdy et al. 1992). As part of this study, they also compared the expression levels of these BMPs between patients with skeletal metastases and those without, reporting BMP-6 to be selectively expressed in bone-scan positive metastatic disease. Henceforward, the expression of BMPs has been examined in the different stages of prostate cancer to assess their roles in this disease. For example, Bobinac et al (2005) reported the expression of BMP-2, -4, -5, -6 and -7 in normal prostate tissue, while prostate carcinoma samples predominantly expressed BMP-2 and -4, with significantly decreased levels of BMP-7. Spanjol et al (2010) reported mostly similar findings, demonstrating an increased expression of BMP-6 and decreased levels of BMP-7 in localised prostate cancers, and bone metastases expressing high levels of BMP-2, -4, -6 and -7. Contrary to Bentley et al however, Spanjol and colleagues reported decreased expression levels of BMP-2/4, -6 and -7 in metastatic prostate cancers. Thus, despite the slightly conflicting data from these expression studies, the evidence

gathered has indicated BMP-2, -4, -6, and -7 to be potential players in the pathophysiology behind skeletal metastases produced by prostate cancer.

Physiologically, BMPs constitute a pivotal group of morphogenetic signals that orchestrate nearly all of tissue architecture throughout the vertebrate body (Hogan 1996). As such, BMP activity is tightly regulated at different levels of signalling, from the intracellular phosphatases and I-Smads, to the extracellular pseudoreceptor BAMBI, and BMP antagonists. Interestingly, BMP antagonists have been shown to be particularly integral to BMP function, not only due to their canonical inhibitory capacities but also as agonists when present in low concentrations (Walsh, Godson et al. 2010). This dual feedback between BMPs and their antagonists is mainly demonstrated in developmental studies. For instance, while it is well established that BMPs, BMP-2, BMP-4 and BMP-7 more specifically, are critical in limb-bud development, their activity is carefully modulated by their antagonists, with disruptions or alterations in this ligand-antagonist balance leading to congenital malformations (Walsh, Godson et al. 2010, Pignatti, Zeller et al. 2014). Furthermore, BMP antagonist action has also been shown to be crucial in bone formation, with BMP exposure inducing the production of such antagonists as Noggin, Follistatin and Gremlin by osteoblasts, thus binding and sequestering BMP action ultimately enabling proper skeletal development (Gazzerro, Gangji et al. 1998, Pereira, Economides et al. 2000, Abe, Abe et al. 2004). For example, studies on Noggin null mice have reported a failure to initiate joint formation in test mice, as well as excessive cartilage amongst other skeletal anomalies, which were likely brought on due to excessive BMP action (Tylzanowski, Mebis et al. 2006).

Given the information gathered above, we hypothesise that since the feedback between BMPs and BMP antagonists is so crucial in physiological conditions that perturbations in this feedback could also participate in the progression of prostate cancer and more particularly, the spread of

this disease to the bone. Indeed, due to the impact BMPs and their antagonists have on skeletal phenotype, it is possible that alterations in their relationship may have a role in the type of lesions produced during prostate cancer related bone metastasis. The study presented in this chapter aims to investigate this hypothesis by assessing the expression profiles BMP and their antagonists in prostate cancer cell lines associated with different bone lesion phenotypes. By also evaluating the expression profiles of related receptors and some of the intermediate signalling molecules, we also hope to elucidate parts of BMP signalling that could be in play.

## **3.2 Materials and Methods**

### **3.2.1 Cell lines and Treatments**

A total of four prostate cancer cell lines were used in this study. PC-3 WT, DU145 WT and VCaP WT cells were maintained in DMEM with 10% FBS and antibiotics. LNCaP WT cells were maintained in RPMI with 10% FBS and antibiotics. All cell lines were kept at 37°C, 5% CO<sub>2</sub> and 95% humidity. To stabilise BMP signalling, cells were pre-treated with 5% FBS DMEM overnight.

### **3.2.2 RNA isolation and cDNA synthesis**

RNA was extracted from transfected cells using the TRI reagent<sup>®</sup> kit (Sigma-Aldrich, Poole, UK), and synthesised into cDNA by reverse transcription using the GoScript<sup>™</sup> Reverse Transcription System (Promega, Southampton, UK), as respectively described in sections 2.4.2 and 2.4.3.

### 3.2.3 RT-PCR

RT-PCR was carried out using the GoTaq® Green Master Mix (Promega, Southampton, UK) under the following cycling conditions: initial denaturation of 5 minutes at 94°C, 32 cycles of denaturation at 94°C for 30 seconds, annealing at 55°C for 30 seconds and elongation at 72°C for 1.5 minutes, before a final elongation step at 72°C for 10 minutes. The PCR products were then run on a 1% agarose gel and visualised using SYBR safe DNA gel stain (Invitrogen, Paisley, UK).

### 3.2.4 RNA-Seq

For this study, targeted-sequencing of low passage PC-3 WT and VCaP WT was undertaken. Cells were incubated with fresh 5% FBS DMEM for 3 hours 37°C, 5% CO<sub>2</sub>. Following the incubation period, cells were collected in TRI Reagent® and mRNA extraction of the samples was carried out. 10 ng of total RNA extracted from the prostate cancer cell lines was subsequently used for RNA sequencing. Heatmaps were generated using Microsoft Excel.

### 3.2.5 GEO Database

GEO datasets from a study by Barretina et al (2012), who characterised a total of 947 cancer cell lines at the genomic level, was accessed on NCBI using the accession number GSE36139. Expression levels of genes of interest were extracted and heatmaps were generated using RStudio.

### 3.3 Results

#### 3.3.1 Expression of BMPs in Prostate Cancer Cell Lines

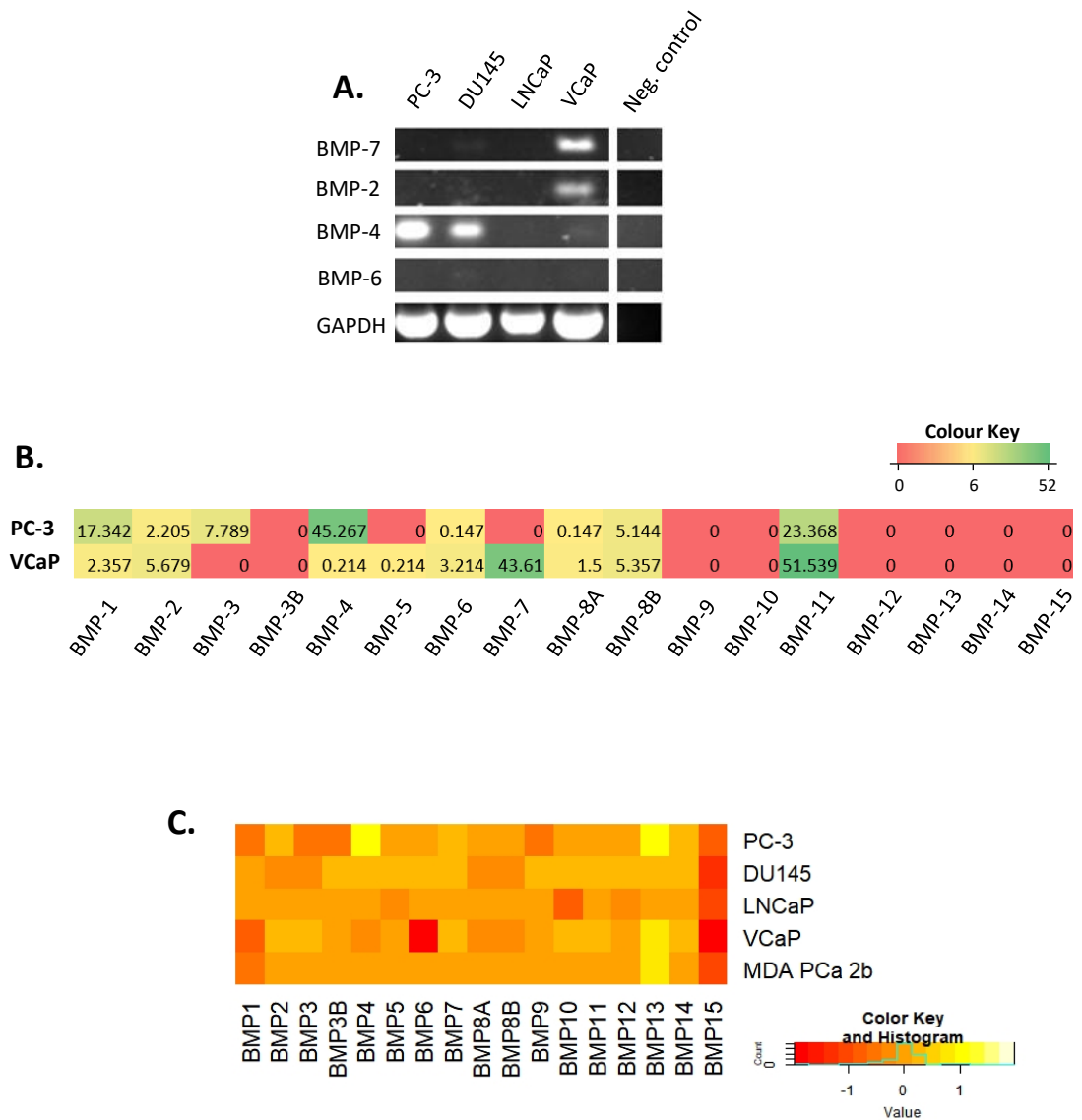


**Figure 3.1: Expression of BMPs in Prostate Cancer Cell Lines.** **A.** Representative RT-PCR images demonstrate the expression of BMP-7, BMP-2, BMP-4 and BMP-6 in prostate cancer lines used in our laboratory. **B.** The heatmap illustrates the expression of BMPs 1 – 15 in PC-3 and VCaP, as shown by Ion Ampliseq™ RNA-Seq of these cell lines. **C.** The heatmap illustrates the expression of BMPs 1 – 15 in the cancer cell lines PC-3, DU145, LNCaP, VCaP and MDA Pca 2b. Data was analysed from the Cancer Cell Line Encyclopaedia GEO database (GSE36139).

The expression of different BMPs was assessed in different prostate cancer cell lines by RT-PCR and RNA-Seq, and results were compared with GEO datasets from the CCLE (GSE36139). The RT-PCR results (see figure 3.1A) demonstrated that cell lines PC-3 and DU145 appeared to express BMP-4 mostly, with DU145 also expressing slight levels of BMP-7 and BMP-6. VCaP cells expressed all of the BMPs tested, with the exception of BMP-6. On the other hand, LNCaP cells did not appear to express any of the BMPs. The findings obtained for PC-3 and VCaP cells were mostly replicated in the RNA-Seq results (figure 3.1B), although they did show VCaP cells to express BMP-6 more intensely than BMP-4, which seems to disagree with the RT-PCR results. Since RNA-Seq is a high throughput method, we were also able to assess the expression of other BMPs, showing that both cell lines expressed BMP-1, BMP-8A, BMP-8B and BMP-11, while BMP-3 was expressed only by PC-3 and BMP-5 was only expressed by VCaP. None of the other BMPs were expressed by the two cell lines. According to the CCLE datasets (see figure 3.1C), PC-3 expressed higher levels of BMP-4 and BMP-13, and slight levels of BMP-2, BMP-7 and BMP-14. DU145 cells expressed slight levels of most BMPs, with the exception of BMP-1, -2, -3, -8A, -8B and -15. VCaP cells expressed higher levels of BMP-13, and slight levels of BMP-2, -3, -7, -10, -11 and -14. MDA PCa 2b cells only appeared to express BMP-13.

### 3.3.2 Expression of BMP antagonists in Prostate Cancer Cell Lines

As seen in figure 3.2A, RT-PCR analyses demonstrated that BMP antagonists were not very well expressed in the different prostate cancer cell lines tested. In fact, out of the cell lines tested, PC-3 expressed Noggin and Gremlin, and VCaP expressed Gremlin only. In contrast, RNA-Seq results (figure 3.2B) demonstrated that neither PC-3 nor VCaP expressed Noggin. They also showed high expression of FST and FSTL1 in PC-3, while VCaP showed high levels of FSTL1 and low levels of FSTL3 and FSTL4. Data from the CCLE (figure 3.2C) seem to corroborate some of the RT-PCR findings. For example, PC-3 expressed higher levels of Noggin and Grem1 and Grem2,

as well as FSTL1. Contrary to our data, DU145 showed expression of antagonists Noggin, FST, FSTL3, FSTL4, Grem1 and Grem2, although at lower levels. LNCaP showed low levels of Grem2 only, while VCaP only expressed FSTL5. MDA PCa 2b cells expressed none of the antagonists.

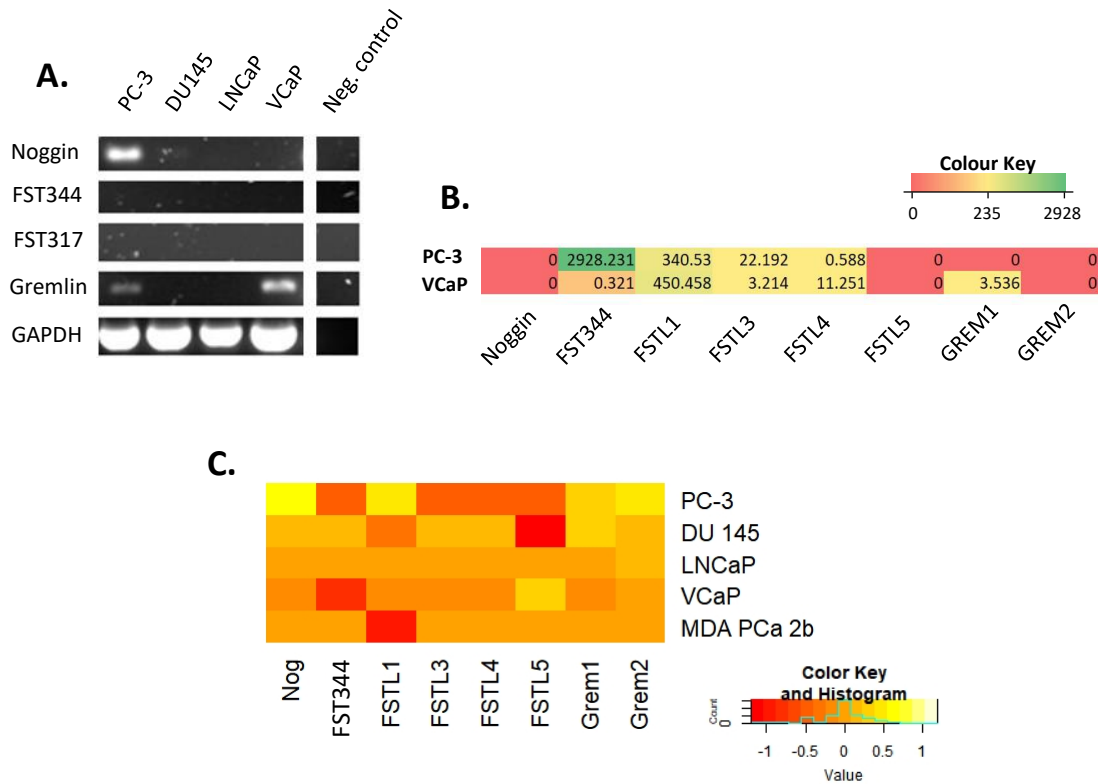


**Figure 3.2: Expression of BMP antagonists in Prostate Cancer Cell Lines.** **A.** Representative RT-PCR images demonstrate the expression of Noggin, FST344, FST317 and Gremlin in prostate cancer lines used in our laboratory. **B.** The heatmap illustrates the expression of Noggin, FST, FSTL1, FSTL3, FSTL4, FSTL5, GREM1 and GREM2 in PC-3 and VCaP, as shown by Ion Ampliseq™ RNA-Seq of these cell lines. **C.** The heatmap illustrates the expression of Noggin, FST, FSTL1, FSTL3, FSTL4, FSTL5, GREM1 and GREM2 in the cancer cell lines PC-3, DU145, LNCaP, VCaP and MDA PCa 2b. Data was obtained from the CCLE (GSE36139).

### 3.3.3 Expression of BMPRs in Prostate Cancer Cell Lines

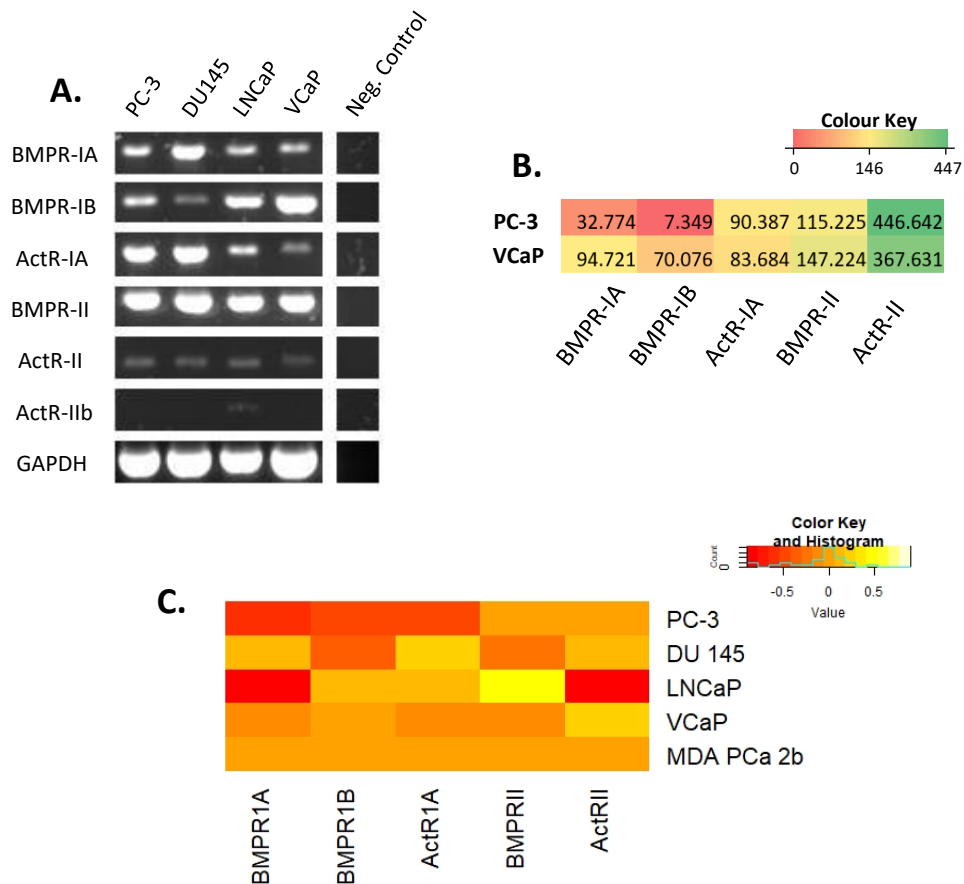


**Figure 3.3: Expression of BMPRs in Prostate Cancer Cell Lines.** **A.** Representative RT-PCR images demonstrate the expression of BMPR-IA, BMPR-IB, ActR-IA in prostate cancer lines used in our laboratory. **B.** The heatmap illustrates the expression of BMPR-IA, BMPR-IB, ActR-IA, BMPR-II and ActR-II in PC-3 and VCaP, as shown by Ion Ampliseq™ RNA-Seq of these cell lines. **C.** The heatmap illustrates the expression of BMPR-IA, BMPR-IB, ActR-IA, BMPR-II and ActR-II in the cancer cell lines PC-3, DU145, LNCaP, VCaP and MDA Pca 2b. Data was obtained from the CCLE (GSE36139).

RT-PCR analyses of the different prostate cancer cell lines in figure 3.3A demonstrated that most of the BMPRs were well expressed, with the exception of ActR-IIb, which seemed to be expressed in LNCaP cells only. RNA-Seq showed some conflicting results (figure 3.3B), with PC-3 showing low levels of BMPR-IB and highest levels of ActR-II. VCaP showed expression of all BMPRs tested, with ActR-II being expressed most strongly, again. The CCLE datasets showed that PC-3 did not seem to express any of the BMPRs (figure 3.3C). According to their data, DU145 appeared to express low levels of BMPR-IA, ActR-IA and ActR-II only and LNCaP appeared

expressed low levels of BMPR-IB and ActR-Ia, and higher levels of BMPR-II. MDA PCa 2b appeared to not express any of the BMPRs tested, while VCaP only seemed to express slight levels of ActR-II.

### 3.3.4 Expression of Smads in Prostate Cancer Cell Lines

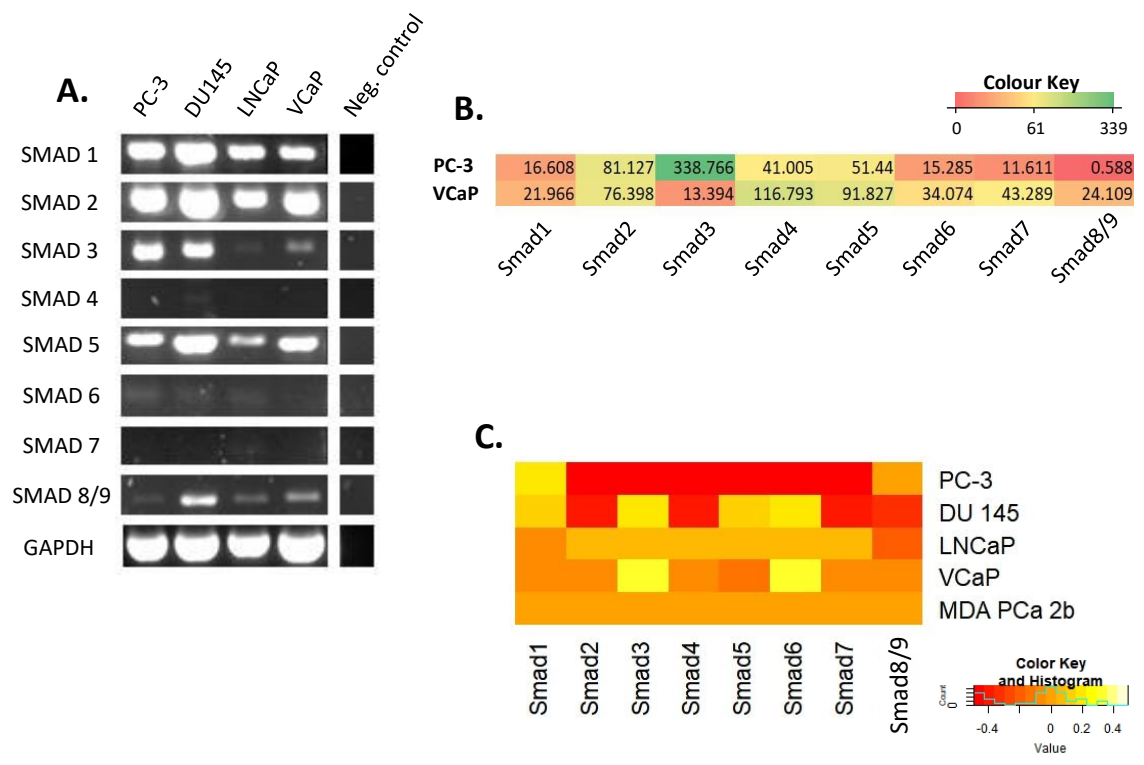


**Figure 3.4: Expression of Smads in Prostate Cancer Cell Lines.** **A.** Representative RT-PCR images demonstrate the expression of Smads 1 – 9 in prostate cancer lines used in our laboratory. **B.** The heatmap illustrates the expression of Smads 1 – 9 in PC-3 and VCaP, as shown by Ion Ampliseq™ RNA-Seq of these cell lines. **C.** The heatmap illustrates the expression of Smads 1 – 9 in the cancer cell lines PC-3, DU145, LNCaP, VCaP and MDA Pca 2b. Data was obtained from the CCLE (GSE36139).

RT-PCR analyses in figure 3.4A demonstrated that most of the Smads were well expressed in the different cell lines. All the cell lines expressed most Smads, except Smad7. Only DU145 seemed to express low levels of Smad4 and only VCaP did not seem to express Smad6. Again, RNA-Seq shown in figure 3.4B seemed to show slightly conflicting data. For example, contrary to the RT-PCR results, RNA-Seq showed that PC-3 expressed Smad4 and very high levels of Smad3, and

VCaP expressed high levels of Smad4 and moderate levels Smad7. Data acquired from the CCLE (figure 3.4C) demonstrated that PC-3 showed high levels of Smad1 and low levels of all the other Smads. Their data also showed that DU145 expressed Smad1, 3, 5 and 6, and that LNCaP expressed low levels of Smad 2 – 7. VCaP, on the other hand, only expressed only Smad3 and 6, while MDA PCa 2b showed no expression of any Smads.

### **3.4 Discussion**

Despite the wealth of studies documenting the potential roles of BMPs during prostate cancer, the exact underpinnings of their effects are as of yet unknown. The study presented in this chapter was aimed to assess the role of the BMP/BMP antagonist relationship in prostate cancer by examining their expression profiles in prostate cancer cell lines representing different characteristics of the disease. With this aim, a range of cell lines, namely PC-3, DU145, LNCaP, VCaP and MDA PCa 2b, were selected for comparison. These were isolated from different sites: PC-3 and MDA PCa 2b were both isolated and established from bone metastases, DU145 was isolated from brain metastasis, LNCaP from lymph node metastasis, and VCaP from vertebral metastasis (Stone, Mickey et al. 1978, Kaighn, Narayan et al. 1979, Horoszewicz, Leong et al. 1983, Navone, Olive et al. 1997, Korenchuk, Lehr et al. 2001). In order to simulate the heterogeneity of prostate cancer, these cell lines comprise of different features, for example, hormone-sensitivity, with PC-3, DU145 and VCaP being androgen-insensitive, and LNCaP and MDA PCa 2b being androgen-sensitive (Stone, Mickey et al. 1978, Kaighn, Narayan et al. 1979, Horoszewicz, Leong et al. 1983, Navone, Olive et al. 1997, Korenchuk, Lehr et al. 2001). The cell lines also differ in the types of bone lesion phenotypes they are associated with, with PC-3 and DU145 causing osteolytic lesions, VCaP and MDA PCa 2b causing osteoblastic lesions and LNCaP causing mixed osteolytic/osteoblastic lesions (Nemeth, Harb et al. 1999, Yang, Fizazi et al. 2001, Kirschenbaum, Liu et al. 2011).

A couple of techniques were used to evaluate the BMP signalling profiles in the different cell lines, namely RT-PCR and RNA-Seq. Expression datasets were also obtained from a large-scale genomic project, the CCLE, for further comparison with our findings. Overall, slight variations in expression levels were observed between the results obtained from the different methods for most of the molecules assessed. In fact, when looking at previous BMP research, fluctuations like these seem to be common between different studies (see table A1). For example, while results by Miyazaki et al (2004) were consistent with the present findings in showing no visible expression of BMP-7 in PC-3, a previous study undertaken in our laboratory (Ye, Lewis-Russell et al. 2007) showed moderate expression of this BMP. There are a number of factors that could contribute to these variations, first being the nature of BMPs themselves. In fact, as growth factors, BMPs could already be present in the FBS supplemented in the growth medium of the different cell lines. Bentley et al (1992) investigated this by evaluating the expression of BMPs 1-6 in PC-3 and DU145 in the presence or absence of serum and found no difference. However, other studies have stated differences cell behaviour following treatment with certain BMPs, such as BMP-7, in the presence or absence of serum (Miyazaki, Watabe et al. 2004, Alarmo, Pärssinen et al. 2009). As such, a routine practise in the study of BMPs is to negate this effect by undertaking their experiments in serum-starvation. Contrary to this, we have opted to limit FBS action by reducing serum levels in our culture medium from 10% to 5% as a compromise between *in vitro* testing of BMP action and a more accurate simulation of the *in vivo* environment of cancer cells.

To begin with, we examined the mRNA expression of different BMPs in the prostate cancer cell lines PC-3, DU145, LNCaP and VCaP by RT-PCR. Since one of the aims of this study is to evaluate prostate cancer-related bone metastasis as a result of BMP signalling, we particularly focussed on the expression of BMP-2, -4, -6 and -7, which have been shown to be of potential importance due to their aberrant expression in prostate cancer bone metastases. According to our RT-PCR,

PC-3 cells only expressed BMP-4, while DU145 cells seemed to express low levels of BMP-7 and high levels of BMP-4. On the other hand, VCaP cells appeared to express all of the BMPs tested, except BMP-6, while LNCaP did not express discernible levels of any BMPs (figure 3.1A). To confirm these findings, we then performed RNA-Seq on two representative cell lines associated with either the osteoblastic or osteolytic bone lesion phenotypes – these were PC-3 and VCaP. As a result of comparing findings from both assays, however, some discrepancies were noted. For instance, while the RNA-Seq data demonstrated the expression of BMP-2 in both cell lines, at levels that are not too dissimilar, the RT-PCR results showed this BMP to be expressed in VCaP cells alone. Furthermore, although the RNA-Seq data showed the expression of BMP-6 in both the cell lines tested, albeit at relatively low levels in the osteolytic PC-3, the RT-PCR analyses demonstrated no expression of the BMP in either cell lines (see figure 3.1). Therefore, this may indicate that, even though both methods aim to assess gene expression levels of target genes, comparing their results poses some limitations. In fact, RT-PCR represents an end-point analysis of cDNA quantification, where relative cDNA levels are assessed by the intensity of bands, which may be manipulated through changing the number of cycles of the protocol used. In contrast, RNA-Seq allows for more absolute expression values when aligned to a reference sequence. As such, an absolute corroboration between the two methods would be difficult.

Further mRNA expression analysis was also performed using the CCLE datasets. These demonstrated that PC-3 slightly overexpressed BMP-2 and BMP-7, while DU145 slightly overexpressed BMP-4, BMP-6 and BMP-7. Like with RT-PCR and RNA-Seq, these datasets demonstrated that BMP levels in LNCaP cells remained unchanged, while VCaP cells slightly overexpressed BMP-2 and BMP-7. Furthermore, through this data, we were also able to evaluate the BMP expression profile in another osteoblastic prostate cancer cell line, MDA PCa 2b, which demonstrated expression unchanged levels of BMP-2, -4, -6 and -7. Similarly to comparing RT-PCR and RNA-Seq results, using data from other laboratories in the form of GEO datasets also

carries its limitations. Indeed, a number variations could easily be incurred when linking data with our own, especially relating to cancer cell lines, due to a number of factors. These could be differences in cell culturing techniques, buffers, passage numbers of cells tested, amongst others.

Cytokine expression profiles between osteolytic and osteoblastic prostate cancer cell lines have already been investigated in a previous study by Lee et al (2003). As part of their study, they examined the expression of BMP-2, -4 and -6 between tumours caused by PC-3 and LAPC-9 and found that LAPC-9 tumours expressed all of the BMPs, while those produced by PC-3 expressed only BMP-4. This is more or less consistent with our current laboratory findings. Their findings also demonstrated that LAPC-9 cells caused purely osteoblastic lesions when injected in the tibias of severe combined immunodeficient (SCID) mice. From this, they supposed that this was in part due to the osteoinductive nature of BMPs.

Since we hypothesise that the interplay between the BMPs and their antagonists may have a role in the spread of prostate cancer to the bone, it is also possible that this interplay may participate in determining the resulting bone lesion phenotype. As such, we also examined the expression of the BMP antagonists Noggin, FST and Gremlin isoforms, GREM1 and GREM2 in the different prostate cancer cell lines. A general overview of the results demonstrates that the osteolytic cell lines express varying levels of the BMP antagonists tested, with Noggin and FST being predominantly expressed by these cell lines. Meanwhile, the only BMP antagonist that appears to be expressed by the osteoblastic cell lines is Gremlin, with LNCaP expressing GREM2 and VCaP expressing GREM1. This could therefore indicate a novel role for Gremlin in the formation of osteoblastic bone lesions. Indeed, a study of GREM1 and Noggin expression in a multitude of normal and cancer samples carried out by Laurila et al (2013) demonstrated that although not widely expressed in the tissues tested, GREM1 was weakly to moderately

expressed in prostate cancer tissues. They also demonstrated that this antagonist was moderately expressed in the bone marrow. With Pereira et al (2000) having previously described a feedback between BMP-2 and Gremlin on osteoblast function, this further hints at the potential importance of the BMP-Gremlin interplay in osteoblastic lesion formation.

Although the expression profiles of Noggin and FST were not completely conclusive from our findings, contrary to Gremlin, these two antagonists have already been implicated in the prostate cancer process. As such, we cannot as of yet completely dismiss the possibility of their involvement in bone metastasis. For instance, a potential of Noggin has been highlighted in osteolytic lesions in particular, with studies demonstrating the inhibitory role of Noggin on BMP-2, BMP-4 and BMP-6 mediated cellular proliferation, invasion and migration of osteolytic prostate cancer cells, PC-3 and DU145 (Haudenschild, Palmer et al. 2004, Feeley, Krenek et al. 2006). Furthermore, on top of also demonstrating the predominant expression of Noggin in osteolytic prostate cancer cell lines, Schwaninger et al (2007) have demonstrated the abolishment of the osteoinductive abilities of prostate cancer cell line, C4-2B, following the forced expression of this antagonist. Previous research focusing on FST has also hinted at its importance in prostate cancer bone metastasis, with the most confounding evidence showing the correlation between FST serum expression with the presence with bone metastases (Tumminello, Badalamenti et al. 2010).

The work presented in this chapter demonstrates the first step in elucidating the potential role of the interplay between BMPs and their antagonists in the formation of osteolytic and osteoblastic prostate cancer bone lesions. From the present findings we were able to assess the differential expression of these cytokines and thus give us an indication of their importance in the bone metastatic process. Additionally, the cytokine profiles obtained provide the baseline

expression of BMP signalling components, which would enable us to assess the underlying signalling pathways in play in subsequent experimentation.

## Chapter 4.

# The Influence of the Bone Environment on the Expression of BMPs and BMP antagonists in Prostate Cancer Cell Lines

#### 4.1 Introduction

The bone is a dynamic tissue that is constantly being remodelled through a balance of bone formation and bone resorption, a process that is regulated by a complex system of endocrine and paracrine growth factors. When cancer spreads to the bone, this balance is disrupted and skewed towards either end of the bone remodelling spectrum, creating osteolytic or osteoblastic bone lesions. Although the two characteristic features of metastatic prostate cancer, namely tropism for the bone and the predominant osteoblastic phenotype of bone lesions formed, were described a long time ago, the mechanisms behind how the lesions are formed remain largely unknown. However, it is believed that prostate cancer cells are able to establish and thrive in the skeleton, and eventually form bone metastases, due to the cross-talk between the cancer cells themselves and the bone microenvironment.

Under normal physiological conditions, the bone is maintained based on the synchronisation of the bone producing cells, the osteoblasts, the calcified matrix resorbing cells, the osteoclasts, and the osteocytes. However, when tumour cells finally reach the bone, they disrupt this synchronisation and divert the bone environment to support their survival and to help their establishment in this new milieu. To do so, they employ a process called the “vicious cycle” (Mundy 2002). This concept brought forward by Mundy (2002) expands on Paget’s “seed and soil” theory to depict how osteolytic bone lesions may develop. According to this theory, with the bone being a highly restrictive and protective environment, tumour cells established in the bone must modify their surroundings for survival. As such, they aim to acquire “bone cell-like” properties by expressing a cytokine profile that would normally be expressed by resident cells of the bone in what is known as “osteomimicry” (Koeneman, Yeung et al. 1999). As a result, this enables the tumour cells to firstly, avoid detection by the immune system and secondly, establish colonies within the bone microenvironment. Indeed, during the osteolytic vicious cycle, tumour cells produce factors like the PTHrP, which, by stimulating the osteoblastic

production of RANKL, indirectly activates osteoclastogenesis, subsequently causing bone resorption (Mundy 2002). This in turn releases and/or activates other factors, including TGF- $\beta$ , IGF, PDGF and BMP family members, from the bone that stimulate tumour cell proliferation, further increasing PTHrP levels and thus setting in motion the vicious cycle (Mundy 2002).

Although not originally described by Mundy, an osteoblastic vicious cycle also exists between tumour cells and bone cells. In fact, the osteolytic vicious cycle still occurs during osteoblastic lesion formation, though, on top of this, cancer cells within the bone also produce factors to stimulate osteoblast differentiation whilst simultaneously inhibiting osteoclasts (Ottewell 2016). Indeed, a number of factors produced by cancer cells are known to directly stimulate osteoblast activity. These are FGFs, TGF- $\beta$ 1 and TGF- $\beta$ 2, IGF-1 and IGF-2, PDGFs, WNT and BMPs (Mundy 2002). However, among these different cytokines, BMPs are uniquely potent: not only do they induce the commitment of bone marrow MSCs, towards the osteoblastic lineage, but they also stimulate the differentiation of osteoprogenitors derived from MSCs into mature osteoblasts (Gazzerro and Canalis 2006). Indeed, when implanted ectopically, BMPs can initiate the complete bone formation cascade, including the stimulation of MSC migration and of osteoblast differentiation, with studies demonstrating BMP-2, 4, 6, 7 and 9 to be particularly effective (Yamaguchi, Ishizuya et al. 1996, Cheng, Jiang et al. 2003, Luu, Song et al. 2007, Geraghty, Kuang et al. 2015). To activate osteoblast differentiation, BMPs bind to and phosphorylate BMPRs on the surface of MSCs, initiating the canonical Smad-dependent pathway and the non-canonical p38 MAPK Smad-independent pathway. These pathways then converge within the nucleus at transcription factors, such as Runx2/Cbfa-1, with which they cooperate to carry out the osteoblast differentiation process, and thus subsequently induce bone formation (Wu, Chen et al. 2016). In fact, as part of the acquisition of osteomimicry by tumour cells, the latter have also been shown to also express Runx2/Cbfa-1 *in vitro*, adding to the osteoblastic vicious cycle.

Still, metastatic tumour cells are not solely responsible for the formation of bone metastases. In fact, this process also depends on the bone environment's influence on the prostate cancer cells. The bone environment is a somewhat vague description for a highly complex biological and structural system which comprises of different lineages of both haematopoietic and mesenchymal cells and whose matrix is extremely rich in growth factors. Many of the latter, as previously mentioned, possess the ability to stimulate the proliferation of metastatic tumour cells within the bone. However, they may also promote the production and release of bone resorbing factors from tumour cells (Yin, Pollock et al. 2005). Resident bone cells also play a role in the bone metastatic process. For instance, although produced during the tumour cell-mediated osteolytic vicious cycle, RANKL is also normally produced by osteoblasts to modulate osteoclast activity, which in a bone environment that is already corrupted by tumour cells, would only add to bone lesion formation. Furthermore, other cell types within the bone may also have a role in this process, like T cells which are known to produce osteoclast-activating factors, including RANKL, as well as TGF- $\beta$ s and tumour necrosis factor (TNF). Aside from the growth factors in the bone environment, a number of non-collagenous bone matrix proteins have been shown to be implicated in the bone metastatic process as well. For example, the secreted adhesive glycoprotein, osteopontin (OPN), has been shown as a potential mediator of prostate cancer growth and progression due to its ability to stimulate the anchorage-independent growth of prostate cancer cell lines LNCaP and C4-2 *in vitro* (Yuen, Kwok et al. 2008).

Taken together, the evidence above reveals the interplay that exists between prostate cancer cells and the bone environment. We have described the vicious cycle that drives the formation of osteolytic bone lesion formation through the initial release of PTHrP and RANKL; however, the osteoblastic vicious cycle is not as well understood. Since numerous studies have demonstrated the aberrant expression of certain BMPs in bone metastases, it is possible that these growth factors be involved in some way in this vicious cycle, which would be as a result of the interplay between prostate tumour cells and their bone environment. As such, it would be

of interest to evaluate the effects that the bone environment might have on their signalling profiles so as to assess any changes to the feedback loop between BMPs and their antagonists from normal conditions.

## **4.2 Materials and Methods**

### **4.2.1 Cell lines and Treatments**

A total of four prostate cancer cell lines were used in this study. PC-3 WT, DU145 WT and VCaP WT cells were maintained in DMEM with 10% FBS and antibiotics. LNCaP WT cells were maintained in RPMI with 10% FBS and antibiotics. All cell lines were kept at 37°C, 5% CO<sub>2</sub> and 95% humidity. To stabilise BMP signalling, cells were pre-treated with 5% FBS DMEM overnight. BME was extracted from femur bone tissues, standardised to 2 mg/ml, and 50 µg/ml in 5% FBS DMEM was used to treat cells.

### **4.2.2 RNA isolation and cDNA synthesis**

RNA was extracted from transfected cells using the TRI reagent® kit (Sigma-Aldrich, Poole, UK), and synthesised into cDNA by reverse transcription using the GoScript™ Reverse Transcription System (Promega, Southampton, UK), as respectively described in sections 2.4.2 and 2.4.3.

#### 4.2.3 qPCR

qPCR was performed using the Amplifluor™ Universal Detection System (Intergen Company, New York, USA) under the cycling conditions detailed in section 2.4.6. CT values obtained were analysed using  $\Delta$ CT normalisation to GAPDH and the relative quantity was calculated using  $2^{-CT}$ . Each reaction was set up in triplicates and the experiments were carried out independently three times. Data analysis was carried out using unpaired t-test with Welch's correction compared to control treatment.

#### 4.2.4 RNA-Seq

Targeted-sequencing of low passage PC-3 and VCaP incubated with either fresh 5% FBS DMEM or 5% FBS DMEM containing 50  $\mu$ g/ml BME for 3 hours 37°C, 5% CO<sub>2</sub> was undertaken. 10 ng of total RNA extracted from the prostate cancer cell lines was subsequently used for RNA sequencing. Heatmaps were generated using Microsoft Excel.

#### 4.2.5 GEO database

In the present study, we utilised the GEO dataset, GSE41619, generated by Larson et al (2013), who performed microarray hybridisation on RNA isolated from osteoblastic and osteolytic bone metastatic cores. Heatmaps of this data were generated using RStudio. Analysis of these samples was also performed by calculating the mean and SEM of these samples, and significance was assessed using unpaired t-test with Welch's correction. These details can be found in the appendix. We also used GEO data (GSGE44143) from microarray gene analyses of monocultures and co-cultures of LNCaP cells and hOBs (Sieh, Taubenberger et al. 2014). This data was analysed

by calculating the means of all the repeats + SEM, and significance was analysed by unpaired t-test using the Holm-Sidak method.

### **4.3 Results**

#### **4.3.1 Expression of BMPs in Prostate Cancer Bone Metastasis**

According to our RNA-Seq results (figure 4.1A), BME treatment of PC-3 and VCaP caused a decrease in expression of most BMPs, with the exception of BMP-4, which was overexpressed in VCaP cells. Slight increases in expression were also seen for BMP-5 in PC-3 and BMP-8A in VCaP, as well as BMP-1 in both PC-3 and VCaP. More importantly, treatment of PC-3 cells caused a decrease in BMP-2, BMP-4 and BMP-6. BMP-7, which according to our findings in Chapter 3, is not normally expressed in PC-3, remains unexpressed following BME treatment. In contrast, its expression was reduced in VCaP cells in BME treatment conditions. We also assessed the expression of BMP-7 in DU145 and LNCaP cells in the absence or presence of BME by qPCR (figure 4.1B). This also demonstrated a decrease in BMP-7 expression following treatment with BME in both cell lines, although only LNCaP showed significance. Since we also posit that BMPs, BMP-7 in particular, have a role in late prostate cancer, especially in the osteoblastic nature of lesions of bone metastases, we aimed to assess their differential expression between osteolytic and osteoblastic lesion samples gathered and tested by Larson et al (2013). The results generated from their GEO dataset indicated that out of the different BMPs, BMP-1, 3, 13 and 15 were downregulated in both types of lesions. The other BMPs on the other hand were all upregulated, with BMP-9 being upregulated in osteoblastic lesions and downregulated in osteolytic lesions. While no significant differences in BMP expression were seen between the different sets of samples (see figure A1), the results showed that BMP-1, 2, 3, 4, 6, 8A, 9 were more highly expressed in osteoblastic lesions than osteolytic lesions.

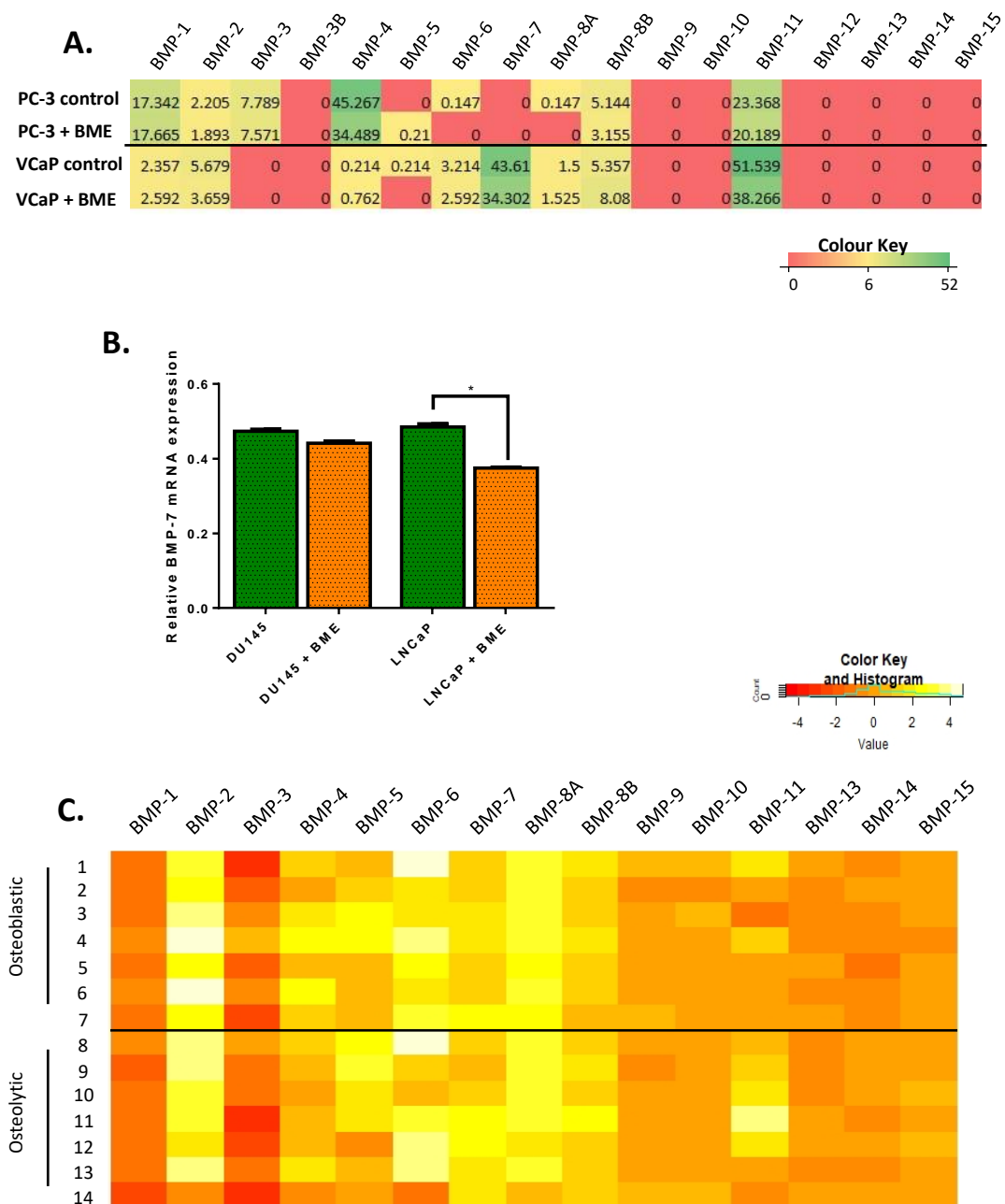


**Figure 4.1: Expression of BMPs in BME-treated Prostate Cancer Cell Lines and in Prostate Cancer Bone Metastasis Samples.** **A.** The RNA-Seq heatmap represent the changes in BMP mRNA expression in PC-3 and VCaP cells in the absence and presence of 50  $\mu\text{g/ml}$  BME. **B.** DU145 and LNCaP cells were treated with either 5% FBS DMEM or 50  $\mu\text{g/ml}$  BME for 3 hours. qPCR was performed to assess changes in BMP-7 mRNA expression. Readings were normalised against GAPDH and the  $\Delta\text{CT}$  method was used to analyse the data. Results shown represents the mean and SEM of three repeats. Significance was assessed by unpaired t-test with Welch's correction (\*  $p \leq 0.05$ ). **C.** The heatmap shown demonstrates the expression profile of BMPs 1-15 in bone metastasis samples. It was generated from GEO data (GSE41619) available on NCBI, with 1-7 representing samples obtained from osteoblastic lesions and 8-14 representing samples obtained from osteolytic lesions. Data was obtained from a bone metastasis study Larson et al (2013).

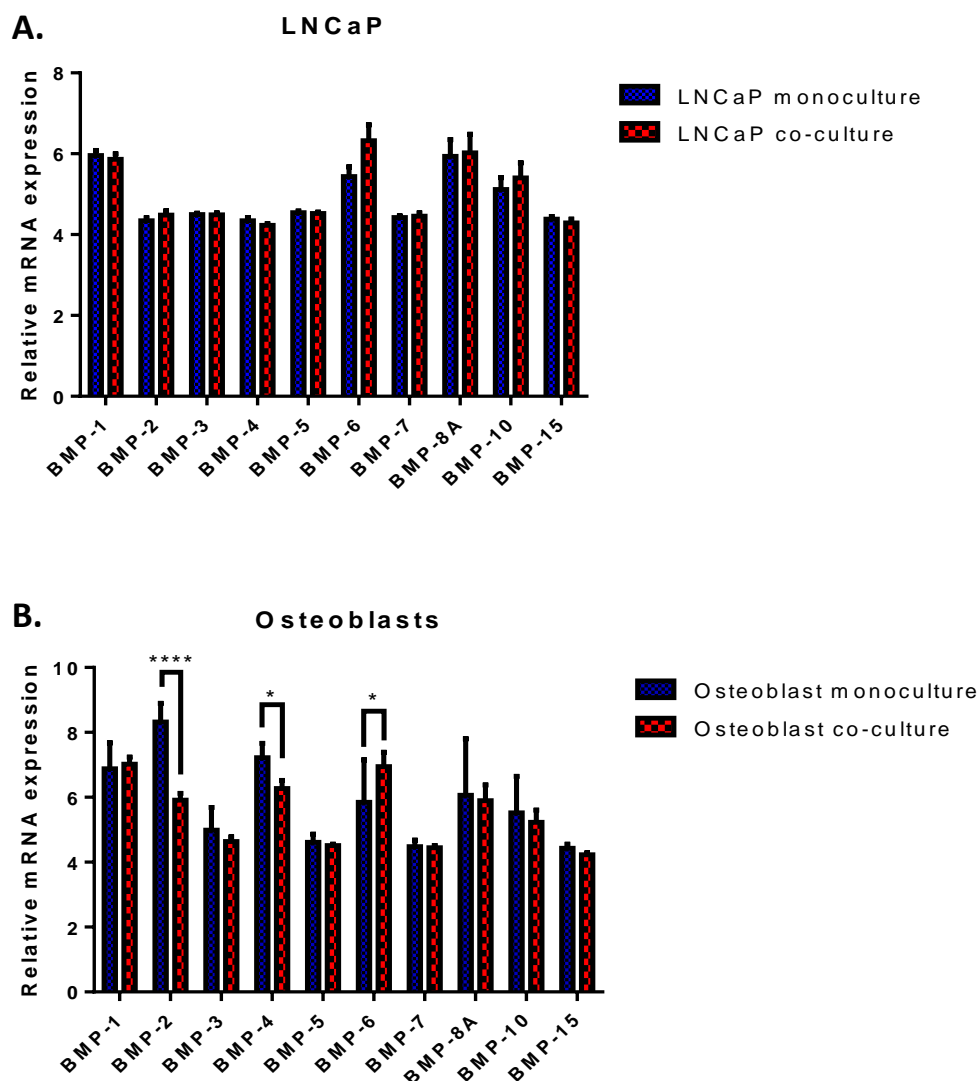


**Figure 4.2: BMP expression profile during LNCaP-hOB co-culture.** The graphs presented here were generated using GEO data (GSE44143) obtained from Sieh et al (2014), who performed microarray gene analysis on both LNCaP cells or hOBs that were either monocultured or co-cultured with each other. The results shown represent the mean + SEM from these assays. Significance was assessed by unpaired ttest using the Holm-Sidak method (\*  $p \leq 0.05$ , \*\*\*\*  $p \leq 0.0001$ ).

We also wanted to assess the how interactions between prostate cancer cells and osteoblasts affected the BMP profiles of both cell types. To do so, we analysed microarray data from LNCaP monocultures, hOB monocultures and LNCaP-hOB co-cultures gathered by Sieh et al (2014) (figure 4.2). These results demonstrated only very slight changes in expression levels of all the BMPs in LNCaP cells when in the LNCaP-hOBs co-cultures. In comparison, hOBs demonstrated

the significant decrease of BMP-2 and BMP-4 ( $p = 1.8481 \times 10^{-5}$  and  $p = 0.0111$  respectively) and the significant increase of BMP-6 ( $p = 0.0494$ ) when co-cultured with LNCaP.

#### 4.3.2 Expression of BMP antagonists in Prostate Cancer Bone Metastasis

As seen in figure 4.3A, RNA-Seq of PC-3 cells showed that BME treatment mostly caused a decrease in the expression of the BMP antagonists tested, with the exception of FSTL1, for which it caused an increase, while BME treatment of VCaP cells caused a decrease in all of the BMP antagonists tested. However, qPCR analyses (figure 4.3B) showed that BME treatment did not cause much effect on Noggin expression in DU145 cells but seemed to cause a very slight decrease in FST344 and Gremlin, although this was not significant. Similarly, BME treatment also cause a decrease in BMP antagonist expression in LNCaP. Although this was at a greater extent than in DU145 cells, it was again not significant. According to the data analysed from the Larson et al (2013) GEO dataset (figure 4.3C), there a low expression of Noggin and FST in both types of metastatic lesions, with FST expression being much lower than the reference sample levels. Overall expression of FSTL1 appeared to be upregulated in osteoblastic lesions and downregulated in osteolytic lesions, while no great change in expression was noted for FSTL4. On the other hand, while there was not much change in FSTL5 expression in osteoblastic lesions, osteolytic lesions showed an overexpression of the antagonist. Both Gremlin isoforms, GREM1 and GREM2, seemed to be well expressed in both lesions. Analysis of the overall data showed significantly higher levels of FSTL3 and GREM2 in osteoblastic lesions in comparison to osteolytic lesions ( $p = 0.0058$  and  $p = 0.0367$  respectively; see figure 4.4).

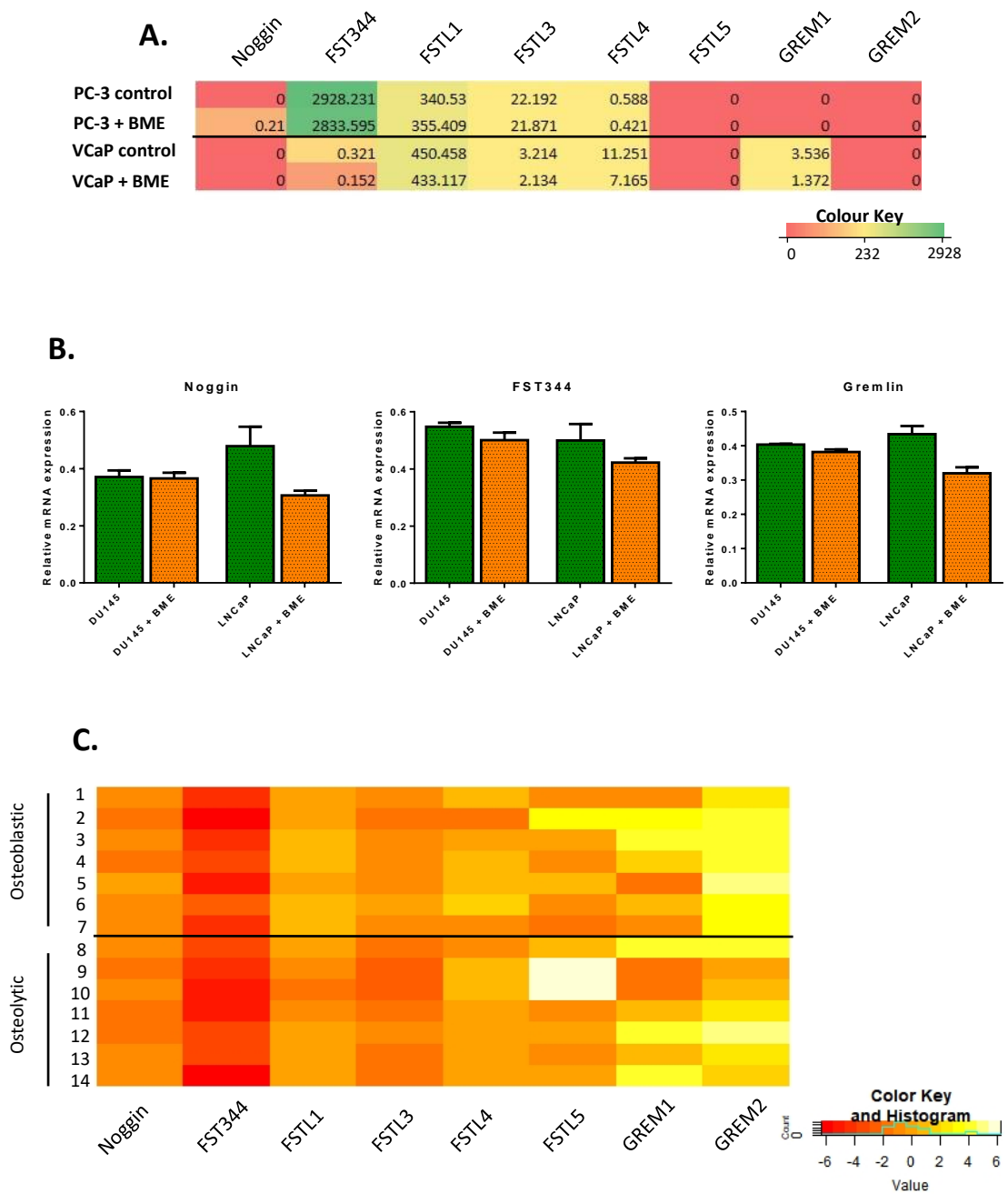


**Figure 4.3: Expression of BMP antagonists in BME-treated Prostate Cancer Cell Lines and in Prostate Cancer Bone Metastasis Samples. A.** The RNA-Seq heatmap represent the changes in BMP antagonist mRNA expression in PC-3 and VCaP cells in the absence and presence of 50  $\mu\text{g}/\text{ml}$  BME. **B.** DU145 and LNCaP cells were treated with either 5% FBS DMEM or 50  $\mu\text{g}/\text{ml}$  BME for 3 hours. qPCR was performed to assess changes in mRNA expression. Readings were normalised against GAPDH and the  $\Delta\text{CT}$  method was used to analyse the data. Results shown represents the mean and SEM of three repeats. Significance was assessed by unpaired t-test with Welch's correction (\*  $p \leq 0.05$ ). **C.** The heatmap was generated from GEO data (GSE41619) obtained from Larson et al (2013), analysing for the expression of BMP antagonists in samples acquired bone metastasis samples. 1-7 represent samples obtained from osteoblastic lesions and 8-14 represent samples obtained from osteolytic lesions.

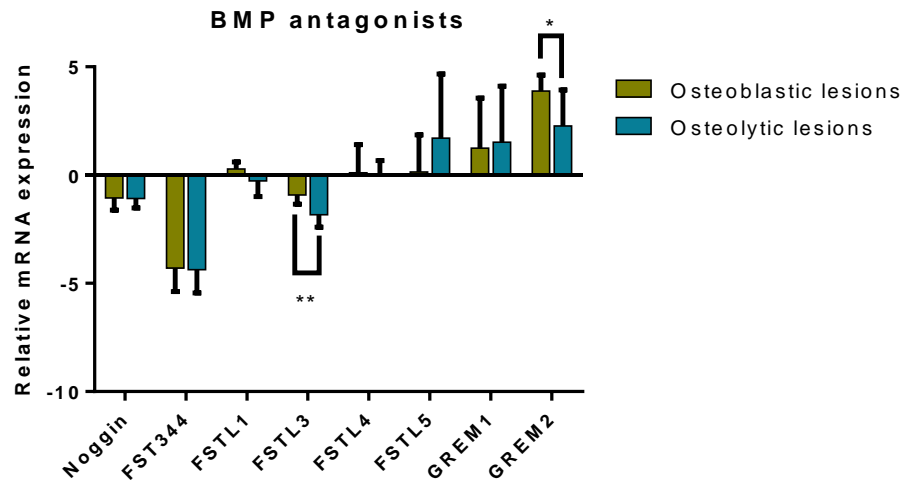


**Figure 4.4: The differential expression of BMPs in osteoblastic and osteolytic bone metastatic lesions.** The data represents mean + SD of BMP expression results from a microarray study by Larson et al (2003; GSE41619). Significance was assessed by t-test using the Holm-Sidak method (\*  $p \leq 0.05$ ).

When assessing the effects of the prostate cancer cell-osteoblast interplay on BMP antagonist expression in LNCaP cell (figure 4.5), the LNCaP microarray data demonstrated an increase in FST, GREM1 and GREM2 levels, while levels in Noggin mRNA were slightly decreased. In fact, a significant increase was observed for FST and GREM1 ( $p = 0.0012$  and  $p = 0.0469$  respectively). The hOBs data, on the other hand, showed that the interactions between the two cell types did not cause much effect on their antagonist expression levels, although a small decrease in FST was noted.

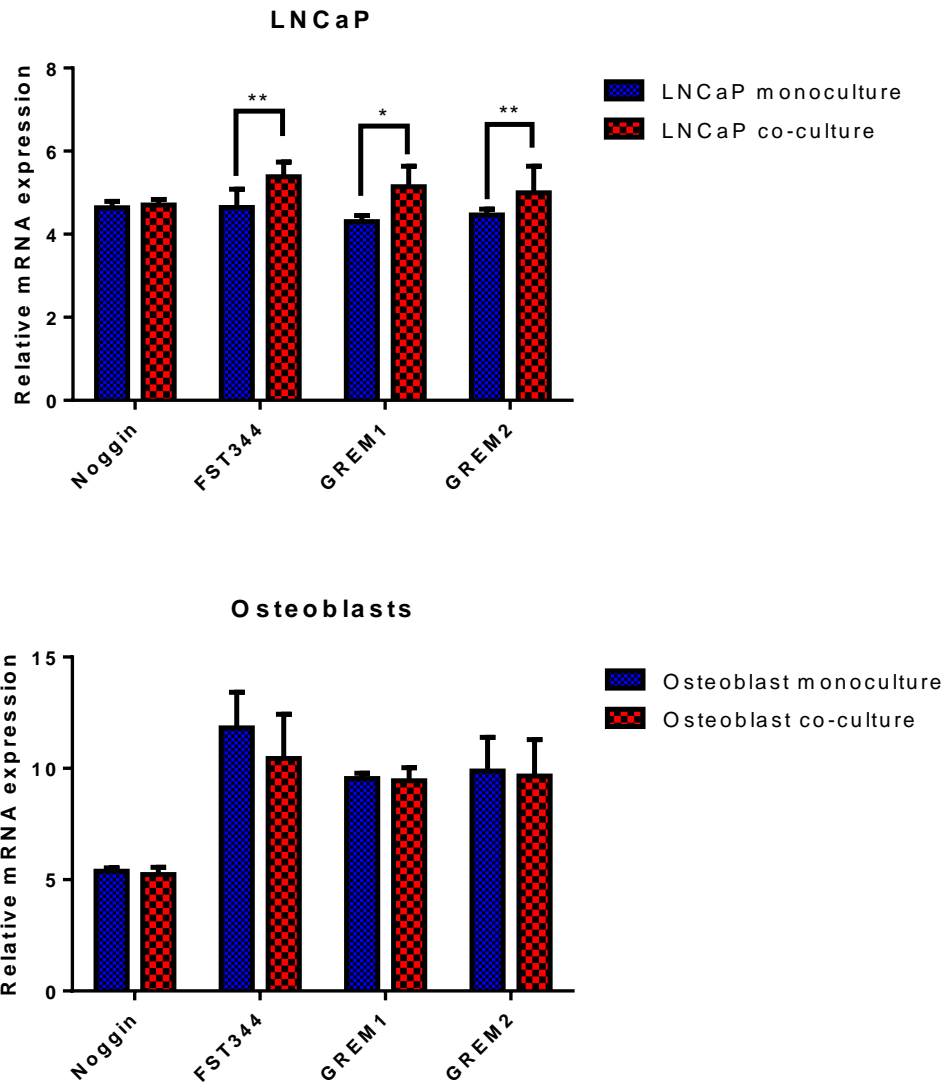


**Figure 4.5: BMP antagonist expression profile during LNCaP-hOB co-culture.** The graphs shown above were generated using GEO data (GSE44143) obtained from Sieh et al (2014), who performed microarray gene analysis on both LNCaP cells or hOBs that were either monocultured or co-cultured with each other. The results shown represent the mean + standard deviation (SD) from these assays. Significance was assessed by unpaired ttest using the Holm-Sidak method (\*  $p \leq 0.05$ , \*\*  $p \leq 0.01$ ).

#### 4.3.3 Expression of BMPRs in Prostate Cancer Bone Metastasis

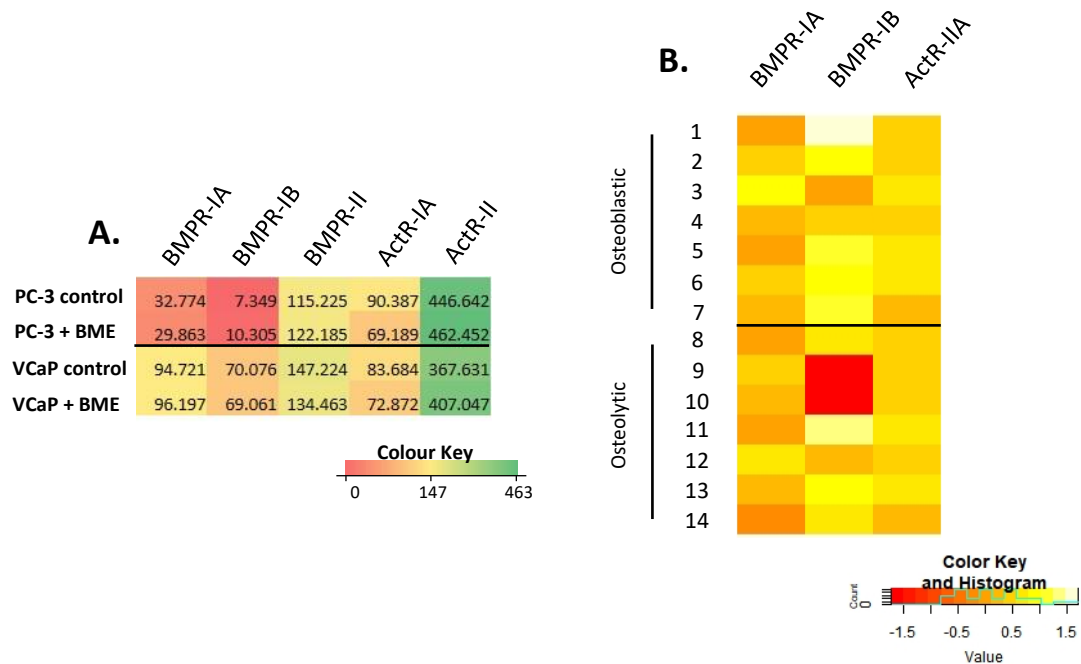


**Figure 4.6: Expression of BMPRs in BME-treated Prostate Cancer Cell Lines and in Prostate Cancer Bone Metastasis Samples. A.** The RNA-Seq heatmap represent the changes in BMPR mRNA expression in PC-3 and VCaP cells in the absence and presence of 50  $\mu\text{g}/\text{ml}$  BME. **B.** The heatmap shown was generated from GEO data (GSE41619) produced by Larson et al (2013) and tested for the expression of BMPR-IA, BMPR-IB and ActR-IIA in samples acquired bone metastasis samples. 1-7 represent samples obtained from osteoblastic lesions and 8-14 represent samples obtained from osteolytic lesions.

RNA-Seq of the samples demonstrated different responses in BMPR expression following BME treatment: PC-3 cells showed a decrease in BMPR-IA and ActR-IA expression, and an increase in BMPR-IB, BMPR-II and ActR-II, and VCaP cells showed a decrease in BMPR-II and ActR-IA expression, and an increase in BMPR-IA and ActR-II expression (figure 4.6A). Data obtained from Larson et al (2013) demonstrated that BMPR-IB was more distributed the bone lesions in comparison to the other receptors tested (see figure 4.6B). Furthermore, it was more distributed in osteoblastic lesions than in osteolytic lesions. BMPR-IA and ActR-IIA seemed to be moderately expressed in both lesion types.

Microarray data (figure 4.7) from the co-cultures of LNCaP with hOBs demonstrated an increase in BMPR-1B and slight decrease in BMPR-2 in the LNCaP cells following co-culture with hOBs. Meanwhile, the latter demonstrated a decrease in both receptors.

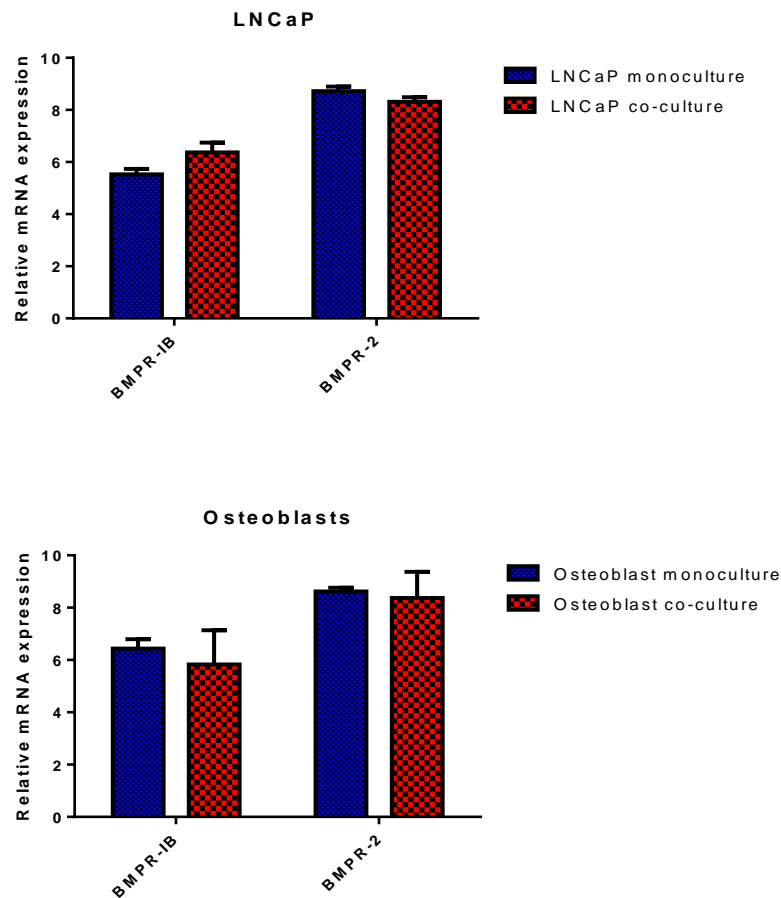


**Figure 4.7: BMPR expression profile during LNCaP-hOB co-culture.** The graphs shown were generated from GEO data (GSE44143) obtained from Sieh et al (2014). Using this data, the expression of BMPR-1A and BMPR-2 was assessed in LNCaP and hOBs that were either monocultured or co-cultured with each other. The results shown represent the mean + SEM from these assays. Significance was assessed by unpaired ttest using the Holm-Sidak method.

#### 4.3.4 Expression of Smads in Prostate Cancer Bone Metastasis

The data obtained from RNA-Seq of PC-3 and VCaP demonstrated different effects on the expression of BMP-specific R-Smads, Smad1, Smad5 and Smad8/9, following BME treatment. For example, in PC-3 cells, BME treatment caused an increase in Smad1 and a decrease in Smad5. It also caused a slight increase in Smad9. In VCaP cells, the treatment caused an increase in Smad5 and Smad9, and a slight decrease in Smad1. On the other hand, expression of the co-Smad, Smad4, was reduced in both cell lines. Interestingly, both I-Smads, Smad6 and Smad7, were increased in PC-3, while only Smad7 was increased in VCaP cells, with Smad6 being reduced. qPCR was performed to assess the expression of the BMP-specific R-Smads and I-Smads. Results showed that BME treatment caused a decrease in all the Smads, in all both DU145 and LNCaP. A significant decrease was observed for Smad1, Smad5 and Smad6 in LNCaP cells. The heatmap generated from data produced from Larson et al (2013) indicated that all the Smads were well expressed in both types of lesions, with Smad8/9 levels being the most pronounced (figure 4.8C). Overall analysis demonstrated that there was a significant upregulation in Smad5 levels and a significant downregulation in Smad6 levels in osteoblastic lesions in comparison to osteolytic lesions ( $p = 0.0179$  and  $p = 0.0250$  respectively; see figure A3).

The LNCaP-hOB microarray data demonstrated that Smad expression was more or less unaffected in LNCaP cells (figure 4.9). However, LNCaP-hOB co-culture caused the decrease of Smad3, Smad6 and Smad7, and a significant increase in Smad8/9 ( $p = 0.0095$ ).

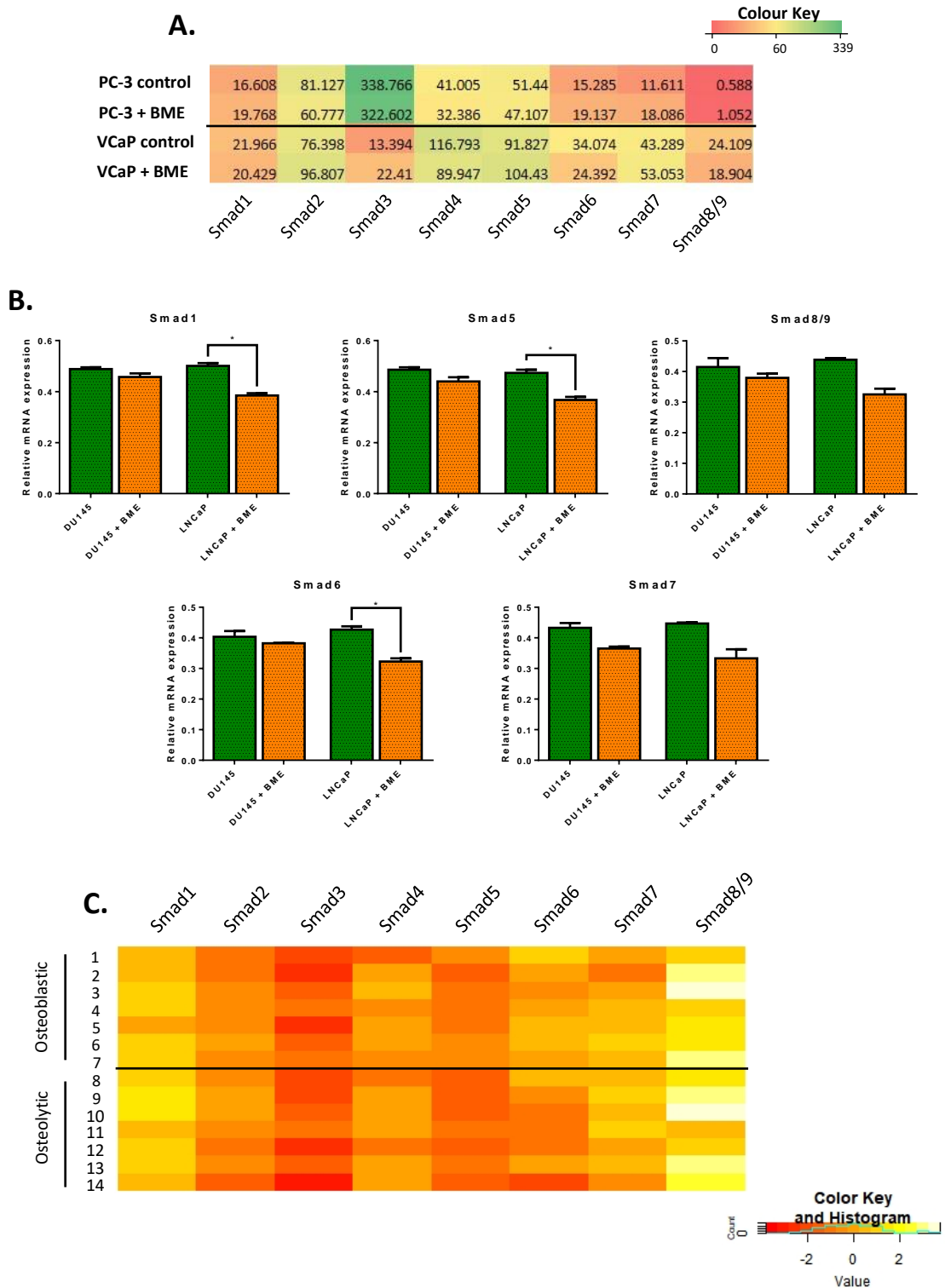


**Figure 4.8: Expression of Smads in Prostate Cancer Bone Metastasis.** **A.** The RNA-Seq heatmap represent the changes in Smad mRNA expression in PC-3 and VCaP cells in the absence and presence of 50  $\mu\text{g/ml}$  BME. **B.** The qPCR results show the changes in Smad expression in DU145 and LNCaP cells in the absence or presence of 50  $\mu\text{g/ml}$  BME. Readings were normalised against GAPDH and the  $\Delta\text{CT}$  method was used to analyse the data. Results shown represents the mean + SEM of three repeats. Significance was assessed by unpaired t-test with Welch's correction (\*  $p \leq 0.05$ ). **C.** The heatmap shown was generated using GEO data (GSE41619) and tested for the expression of Smads in samples acquired bone metastasis samples. 1-7 represent samples obtained from osteoblastic lesions and 8-14 represent samples obtained from osteolytic lesions (Larson et al 2013).

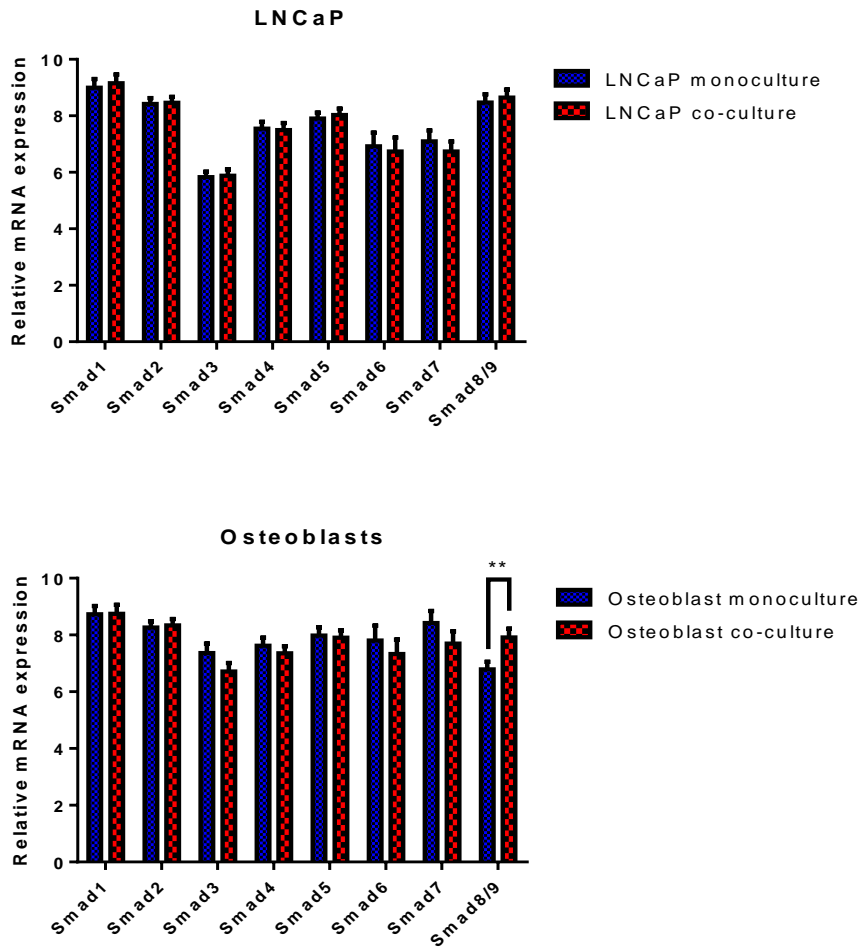


**Figure 4.9: Smad expression profile during LNCaP-hOB co-culture.** Sieh et al (2014) performed microarray gene analysis on LNCaP cells and hOBs that were either monocultured or co-cultured together. The graphs presented here were generated from the GEO data (GSE44143) obtained from this experiment and shows the mean + SEM of the Smads expression readings. Significance was assessed by unpaired ttest using the Holm-Sidak method (\*\*  $p \leq 0.01$ ).

#### 4.4 Discussion

In 1889, Sir Stephen Paget brought forth the 'seed and soil' theory to help explain the preferential metastasis of different cancer types to specific sites. His theory postulates that metastatic cancer cells (the 'seeds') disperse in all directions but can only accomplish metastases where the microenvironment (the 'soil') is permissive for their survival and growth (Paget 1889). While this is still widely accepted as the basic principle of metastasis after more than 120 years of scientific research, studies focussing on prostate cancer metastasis to the bone have since expanded on this theory. Indeed, these studies have shown evidence of bi-directional interactions between cancer cells and the bone that not only attract the cells to bone sites, but that also enables them to adapt and grow in the new, physiologically different environment. With BMPs being one of the family of growth factors through which these interactions occur, the aim of this current study is to investigate the impact of the bone environment on the BMP/BMP antagonist feedback loop and how this may eventually translate to the formation of osteoblastic bone lesions.

In order to investigate the interplay between prostate cancer cells and the bone environment, we wanted a method of simulating the bone which we could use *in vitro*. This was achieved by the crushing and sonication of femoral heads obtained from patients undergoing hip replacements and collecting the supernatant extract, BME. Since we have already established a general idea of the baseline BMP signalling profiles of different prostate cancer cells lines in Chapter 3, the first step of the current study was to utilise this information to assess any changes that may occur within the bone environment, mimicked by treatment with BME, by RNA-Seq and qPCR. For ease of comparison between DMEM and BME RNA-Seq data, we included findings obtained from Chapter 3 alongside those from Chapter 4. Similar to Chapter 3, we utilised GEO data from other studies, which were also investigating the molecular mechanisms underlying prostate cancer bone metastasis, to obtain a more comprehensive overview of the BMP/BMP

relationship in this process. The first study we used, which was completed by Larson et al, provided more translational data, by performing microarray analysis on 14 clinical specimens from prostate cancer bone lesions, divided into the two bone lesion phenotype groups: osteoblastic or osteolytic. Results they obtained were then compared with a reference sample of pooled RNA isolated from prostate cancer cell lines, PC-3, DU145, LNCaP and CWR22. The authors of the second study we used, Sieh et al (2014), utilised a novel 3D, *in vitro* approach to co-culture LNCaP cells with hOBs.

When assessing the BMP expression results (figure 4.1), data yielded from RNA-Seq following BME treatment showed that most of the BMPs that our research is particularly interested in, namely BMP-2, 4, 6 and 7, were downregulated in both the osteolytic PC-3 cells and the osteoblastic VCaP cells, with the exception of BMP-4, that was upregulated in VCaP. qPCR analyses were performed on the osteolytic DU145 and mixed lesion LNCaP cells, and solely focussed on the expression of BMP-7, the latter being reduced in both cell lines. This differs from data we analysed from Larson et al (figure 4.1C), which demonstrated the high expression of all of the BMPs of interest in both types of bone lesions. However, the evaluation of differential BMP expression between the two lesion phenotypes demonstrated higher levels of BMP-2, 4 and 6 in osteoblastic lesions, while BMP-7 was slightly higher in osteolytic ones. Although the BMP-7 expression observations were not statistically significant (see figure 4.2), they were nonetheless surprising. Indeed, being one of the BMPs with the strongest osteogenic activity, various studies have implicated this BMP in the osteoblastic bone metastasis process. For instance, Masuda et al (2003) demonstrated the high expression of BMP-7 in 7 metastatic bone lesion samples in comparison to normal bone tissue. While the phenotypes of the lesion samples were not specified, the authors of this study deduced from their results the likelihood of BMP-7 involvement in osteoblastic lesion formation. Their findings were mirrored in the previously mentioned studies by Spanjol et al (2010), Morrissey et al (2010), Buijs et al (2007), which also demonstrated the high expression of BMP-7 in bone metastatic samples. Despite the current

findings, previous evidence and the current understanding of BMP-7 functions still points towards the involvement of this BMP in the development of prostate cancer osteoblastic lesion. This possibly highlights the need for bigger sample pools for an empirical assessment of key factors in the bone metastasis process. However, analysis of the differential expression data for the other BMPs has brought up some interesting findings, none more so than BMP-11, which demonstrated poor expression in osteoblastic bone lesions and quite a drastic increase in levels in osteolytic lesions. As of yet, it seems that no studies have been performed to investigate the role of this BMP in prostate cancer or bone metastasis, although it has been to stimulate bone formation by mediating the increase in osteoblast function (Li, Zeng et al. 2011). Interestingly, this could tie in with the findings we extrapolated from the Larson et al GEO database.

To help interpret the BMP/BMP antagonist relationship and its role in the establishment of prostate cancer bone metastases, we also assessed the expression levels of BMP antagonists in response to the bone environment. A general overview of these results highlights Noggin and FST to be of particular interest, showing both antagonists to be downregulated in the bone metastasis samples (figure 4.3C), with FST also being downregulated in the *in vitro* bone environment assays (figure 4.3A and figure 4.3B). This seems to agree with previous findings. For instance, although they focussed their research on osteolytic lesion formation, Feeley et al (2006) demonstrated through *in vitro* assays on PC-3 cells and *in vivo* experiments using SCID mice that Noggin inhibited the BMP-mediated formation of osteolytic bone lesions. Furthermore, Schwaninger et al (2007), who also demonstrated the low expression levels of Noggin in osteoblastic lesions, showed that the forced expression of Noggin in osteoblastic prostate cancer cell lines abolished the osteoblast response in *in vivo* intraosseus xenografts. Meanwhile, although FST has drawn more interest lately for its possible role in bone metastasis, its importance and role in this process remains to be ascertained. For example, previous findings from our laboratory on breast cancer progression have demonstrated that higher FST levels correlate with lower grade breast tumours, suggesting a role for this antagonist as a suppressor

of invasion and metastasis (Zabkiewicz, Resaul et al. 2017). In contrast, Tuminello et al (2010) demonstrated that serum FST levels of prostate cancer patients positively correlated with the presence of bone metastases. What was most striking about the current findings was the significant downregulation of GREM2 in osteolytic bone lesions in comparison to osteoblastic lesions ( $p = 0.0367$ , see figure 4.4), since this antagonist has never been previously implicated in the prostate cancer process before. Although no previous literature was seen on GREM2 in relation to this disease or the related bone metastasis, Laurila et al (2013) who, as previously mentioned, investigated the expression of the GREM2 isoform, GREM1, in a multitude of normal and cancer tissues, has demonstrated weak levels of GREM1 in the prostate and moderate levels in the bone marrow. GREM1 levels were then increased to weak to moderate levels in prostate adenocarcinoma. Moreover, GREM2 has been highlighted as a candidate gene in the study of osteoporosis, suggesting its importance in bone health. In combination with the current findings, it indicates the Gremlin isoforms as potential proteins of interest in prostate cancer progression and bone metastasis.

Additional evidence for the importance of BMP signalling in prostate cancer metastasis can be seen through the expression profiles of BMPRs and Smads. Indeed, although the RNA-Seq data demonstrated that BME treatment caused varying effects on BMPR expression, they did show their high distribution throughout in both cell types, in both treatment conditions (figure 4.6A). This was reflected in data we analysed from GSE41619 (Larson, Zhang et al. 2013), which demonstrated the moderate expression of all the BMPRs tested. Of note, the results of both assays both showed the high expression of BMPR-IB in the osteoblastic VCaP cell line and osteoblastic lesions, even showing an increase in PC-3 following BME treatment. Although this contradicts previous studies that demonstrated the correlation between the loss of BMPR-IB and the Gleason score in prostate cancer patients, the current findings may imply the importance of the cognate BMPs of this receptor, namely BMP-2, 4, 6 and/or 7 in the osteoblastic lesion formation (Yamaji, Celeste et al. 1994, Ebisawa, Tada et al. 1999, Kim, Lee et

al. 2000, Lavery, Swain et al. 2008). Furthermore, although BME treatment demonstrated fluctuating changes in co-Smad levels as well as those of the different R-Smads and I-Smads, with the qPCR demonstrating a downregulation in most of the Smads tested, data from Larson et al showed the downregulation of Smad5 and upregulation of Smad6 in osteoblastic lesions. This further indicates that BMP function is in play in the osteoblastic reaction.

When evaluating the LNCaP-hOB interplay on BMP and BMP antagonist expression levels, the overall results co-culture experiments strongly suggest a feedback loop between BMPs and their antagonists (see figures 4.2 and figure 4.5). Indeed, it was observed that these experiments mostly did not affect the expression profile of BMPs in LNCaP cells, only causing an increase BMP-6 levels. However, they did cause significant increases in the expression of BMP antagonists, FST, GREM1 and GREM2. Conversely, although hOBs in the co-cultures demonstrated a slight decrease in FST and minimal changes in levels of the other antagonists, they showed significant changes in BMP levels, causing a decrease in expression levels of both BMP-2 and BMP-4, and an increase in BMP-6 in the hOBs. The increase in BMP-6 ties in with previous findings, which demonstrated the high expression of this BMP with disease progression (Hamdy, Autzen et al. 1997, Autzen, Robson et al. 1998, Thomas and Hamdy 2000). As for the downregulation of BMP-2 and BMP-4, since LNCaP cells are typically associated with the formation of mixed lesions, this could explain the differing levels of the different osteogenic BMPs. Although this co-culture experiment only represents the early phases of metastasis, where cancer cells and resident bone cells would communicate to negotiate survival and the establishment of a secondary colonies, it apparent that part of this interaction occurs through BMP and BMP antagonist interplay. Furthermore, as the formation of osteoblastic lesions is driven by osteoblasts, the present results indicate that their actions are BMP-mediated, hence why the levels of BMP antagonists were mostly unchanged.

Reflecting the BMPR and Smad results discussed above, the analysis of the LNCaP-hOB demonstrated that the tested BMPRs, BMPR-IB and BMPR-II were well expressed in both LNCaP cells and hOBs in monocultures. Again, BMPR-IB levels seemed to be more affected than that of BMPR-II in LNCaP-hOB co-cultures, as evidenced by an increase in LNCaP cells and decrease in hOBs. The subsequently Smad signalling in LNCaP cells was mostly unchanged in co-culture conditions, however, hOBs demonstrated a significant increase in Smad9, supporting the implication that an interaction through BMPs is taking place between the two cell types.

The chapter presented here summarises a wealth of information gathered with the aim to show whether BMP and their antagonists have a role during the initial establishment of prostate cancer cells in the bone and formation of bone lesions. As such, taken together, our data may support the hypothesis that BMP signalling in prostate cancer occurs through an interplay with BMP antagonists. Unfortunately, since our attempts to confirm these results on a protein level were unsuccessful, our data does not reflect any post-translational changes and regulations that could impact on these findings. Due to the level of promiscuity between the BMP antagonists and the BMPs, it is difficult to pinpoint which exact BMP/BMP antagonist interplay are of importance and how it may translate in bone metastasis. Therefore, it would be of interest to see how BMP antagonists impact cancer cell behaviour in subsequent experimentation.

Chapter 5.

**Overexpression of BMP  
antagonists and their  
Regulatory Role in Cellular  
Functions**

## 5.1 Introduction

The progress from normal cell to cancerous growth is a multifaceted affair. Indeed, a cell must acquire a range of subversive characteristics as it evolves in order to escape the constraints of normal cellular physiology. To do so, neoplastic cells utilise the different cellular properties that are typically vital to normal cells and aberrantly activate them. Different cancers present with different combinations of these aberrant properties, although arguably, the most fundamental trait that cancer cells share is the ability to sustain chronic proliferation. Of the other cellular traits that may be corrupted during the cancer process, the adhesive, migratory and invasive properties of cancer cells are also of significance as they all contribute to metastatic potential (Hanahan and Weinberg 2011).

Classically known for their roles in embryonic morphogenesis and postnatal development, BMPs carry out their tasks through the orchestration of cellular processes like the ones mentioned above (Hemmati-Brivanlou and Thomsen 1995, Zou and Niswander 1996, Kobayashi, Lyons et al. 2005, Stewart, Guan et al. 2010). However, during the cancer process, neoplastic cells may hijack signalling mediated by certain BMPs. For example, while normal cells carefully control the production and release of growth-promoting signals, cancer cells in contrast actively deregulate them, and do so largely through the use of growth factors like BMPs (Hanahan and Weinberg 2011). In fact, many have posited a significant role for BMPs in prostate cancer progression, with a number of studies testing this theory by examining the expression of these growth factors in prostatic tissue. As summarised in Chapter 3, the combined evidence of these studies showed the expression patterns of BMP-2, -4, -6, and -7 in the different stages of prostate cancer to be of particular interest as they suggested their implication in the formation of skeletal metastases (Bentley, Hamdy et al. 1992, Masuda, Fukabori et al. 2003, Bobinac, Marić et al. 2005, Spanjol, Djordjević et al. 2010). Of note, each of the BMPs mentioned above are known to have powerful

osteoinductive properties (Lavery, Swain et al. 2008). BMP-4, for example, has been shown to regulate limb development (Selever, Liu et al. 2004). On the other hand, BMP-2 and BMP-7, have already been approved for clinical use as therapeutic options for the treatment of long-bone nonunions (Govender, Csimma et al. 2002, Papanagiotou, Dailiana et al. 2015), while studies are being undertaken to test the viability of BMP-6 as a candidate in bone generation therapies (Mizrahi, Sheyn et al. 2013). Therefore, these BMPs present themselves as ideal candidates for the formation of osteoblastic bone lesions, with studies by Masuda et al implicating BMP-7 in particular having a key role in this process, specifically in prostate cancer (Masuda, Fukabori et al. 2003, Masuda, Fukabori et al. 2004).

Since more and more studies have demonstrated the capacities of BMP antagonists to be beyond their canonical BMP-regulating role, it is possible that the interplay that exists between them and BMPs physiologically may also be in play pathophysiologically. The current study aims to elucidate if this is the case during prostate cancer and its spread to the bone. Thus, in order to achieve this, we decided to induce the overexpression of a number of BMP antagonists in prostate cancer cells and assess any downstream changes in their cellular activities. As different BMP antagonists have varying affinities for different BMPs, we chose to overexpress antagonists that will altogether interact with the BMPs we have identified to possibly be more implicated in bone metastasis, that is, BMP-2, BMP-4, BMP-6 and more importantly, BMP-7. These antagonists are Noggin, FST344 and Gremlin (Re'em-Kalma, Lamb et al. 1995, Yamashita, ten Dijke et al. 1995, Zimmerman, De Jesús-Escobar et al. 1996, Fainsod, Deissler et al. 1997, Hsu, Economides et al. 1998, Iemura, Yamamoto et al. 1998, Merino, Rodriguez-Leon et al. 1999, Haudenschild, Palmer et al. 2004, Zhu, Kim et al. 2006).

Finally, if one were to fully understand the role of BMPs and their antagonists in the formation of osteoblastic lesions, one would also need to consider Stephen Paget's 'seed and soil'

hypothesis. With the bone containing numerous non-collagenous proteins as well as a multitude of growth factors, all of which are able to interact with cancer cells and thus alter cancer cell behaviour, we would need to consider the influence of the bone environment in conjunction with the overexpression of the selected antagonists (Zheng, Zhou et al. 2013). Thus, the phenotypes of the overexpression cell lines under treatment with BME was also examined. Altogether, this study may offer insight into the underpinnings of BMP/BMP antagonist related bone metastasis and how it could be exploited in prostate cancer treatment and the prevention of osteoblastic bone metastasis.

## **5.2 Materials and Methods**

### **5.2.1 Materials**

All the primers used were synthesised and provided by Sigma-Aldrich (Poole, UK). Primer sequences are detailed in tables 2.2 to 2.4.

### **5.2.2 Cell lines and Treatments**

DU145 WT cells maintained in DMEM with 10% FBS and antibiotics at 37°C, 5% CO<sub>2</sub> and 95% humidity were used this chapter. These cells were later transfected, and the stable cell lines produced were cultured in maintenance medium consisting of DMEM supplemented with 10% FBS, antibiotics and 0.5 µg/ml blasticidin thereafter. All cell lines were pre-treated in maintenance medium with 5% FBS and antibiotics overnight, preceding any functional assays. The BME treatment used in this study was prepared as described in section 2.2.1 and 50 µg/ml in 5% FBS DMEM was used to simulate the bone microenvironment.

### 5.2.3 Amplification of Noggin, Follistatin and Gremlin Coding Sequences

Prior to the amplification process, the cDNA template first needed to be generated by reverse transcription of mRNA extracted from normal human prostate tissue using the GoScript™ Reverse Transcription System (Promega, Southampton, UK). The resultant cDNA was then combined with JumpStart™ AccuTaq™ LA DNA Polymerase Mix (Sigma-Aldrich, Poole, UK) and primers that were designed to amplify the entire coding sequences of Noggin, FST344 or Gremlin (see table 2.4). The reaction mixes were subsequently subjected to touchdown PCR, the parameters of which were pre-determined by gradient PCR. In brief, following an initial denaturation at 94°C for 5 minutes, the reaction mixes were subjected to 5 cycles of denaturation at 93°C for 20 seconds, annealing at 64°C, 62°C, 60°C or 58°C for 20 seconds, and elongation 72°C for 1.5 minutes. An additional amplification of 30 cycles was performed, whereby denaturation was carried out at 93°C for 20 seconds, annealing at 58°C for 20 seconds, and elongation 72°C for 1.5 minutes. This was followed by a final extension of 10 minutes at 72°C. The PCR products were then run and visualised on a 1.5% agarose gel with bands corresponding to the expected sizes of the BMP antagonists excised. Extraction of the excised products was carried out as described in section 2.5.3.

### 5.2.4 Cloning of Noggin, FST344 and Gremlin into pEF6/V5-HIS-TOPO® TA vectors

Following their isolation from agarose gel, the selected touchdown PCR products were directly incorporated into the pEF6/V5-HIS-TOPO® TA vector (Invitrogen, Paisley, UK) by TOPO TA cloning, as detailed in section 2.5.4. Then, the resultant vectors were transformed into One Shot® TOP10 Chemically Competent *E. coli* (Invitrogen, Paisley, UK), after which the correct

orientation of PCR products within the vectors expressed by transformants was verified. The correct constructs were then amplified and purified using the GenElute™ Plasmid MiniPrep Kit (Sigma, Poole, UK), based on the protocol provided.

#### 5.2.5 Prostate Cancer Cell Transfection and Generation of Stable Transfectants

Once purified, vectors expressing Noggin, FST344 or Gremlin were transfected into DU145 WT cells using an electroporator (Gene Pulser Xcell™ Electroporation System, Bio-Rad Laboratories, Hemel Hempstead, UK) set to 290 V. Empty pEF6/V5-HIS-TOPO® TA vectors were also electroporated into the prostate cancer cell line to serve as a negative control for subsequent experiments. Following transfection, cells were immediately transferred to 25 cm<sup>2</sup> flasks containing 5 ml of pre-warmed 10% FBS DMEM and left to adhere overnight. A selection process was then implemented during which transfected cells were cultured in 10% FBS DMEM supplemented with 5 µg/ml Blasticidin S (Melford Laboratories Limited, Suffolk, UK) for about a week. Surviving cells were then cultured and maintained in 10% FBS DMEM with a reduced blasticidin concentration of 0.5 µg/ml to create the stably transfected cell lines DU145<sup>PEF</sup>, DU145<sup>NOG</sup>, DU145<sup>FST344</sup> and DU145<sup>GREM</sup>.

#### 5.2.6 RNA isolation, cDNA synthesis, RT-PCR and qPCR

RNA was extracted from transfected cells using the TRI reagent® kit (Sigma-Aldrich, Poole, UK), and synthesised into cDNA by reverse transcription using the GoScript™ Reverse Transcription System (Promega, Southampton, UK), as respectively described in sections 2.4.2 and 2.4.3. The acquired cDNA was then used for RT-PCR or qPCR. RT-PCR was carried out using the GoTaq® Green Master Mix under the following cycling conditions: initial denaturation of 5 minutes at

94°C, 32 cycles of denaturation at 94°C for 30 seconds, annealing at 55°C for 30 seconds and elongation at 72°C for 1.5 minutes, before a final elongation step at 72°C for 10 minutes. The PCR products were then run on an agarose gel and visualised using SYBR safe DNA gel stain (Invitrogen, Paisley, UK). qPCR was performed using the Amplifluor™ Universal Detection System (Intergen Company, New York, USA) under the cycling conditions detailed in section 2.4.6. CT values obtained were analysed using  $\Delta\Delta$ CT normalisation to GAPDH and standardised to the pEF control. Each reaction was set up in triplicates and the experiments were carried out independently three times. Data analysis was carried out using unpaired t-test with Welch's correction compared to DU145<sup>pEF</sup>.

#### 5.2.7 *In vitro* Cell Proliferation Assay

DU145<sup>pEF</sup>, DU145<sup>NOG</sup>, DU145<sup>FST344</sup> and DU145<sup>GREM</sup> were seeded at a density of  $3 \times 10^3$  cells/100  $\mu$ l into 12 replicate wells of three 96-well plates. Cells were either treated with 5% FBS DMEM or 50  $\mu$ g/ml BME in 5% FBS DMEM and incubated for 1, 3 or 5 days. Following the appropriate incubation period, cells were then fixed in 4% formaldehyde and stained with 0.5% crystal violet. Once dried, cells were solubilised with 10% acetic acid and cell densities were determined by spectrophotometry at 540 nm. Growth rates were calculated using the absorbance measured at day 1 as a baseline.

#### 5.2.8 *In vitro* Invasion Assay

8 Transwell inserts with 8  $\mu$ m pores (Greiner Bio-One, Stonehouse, UK) were coated with 50  $\mu$ g of Matrigel (BD Biosciences, New Jersey, USA) and placed into wells of a 24-well plate containing 5% FBS DMEM. The transfected cell lines were seeded into the inserts at a density of  $3 \times 10^4$

cells/100  $\mu$ l and treated with either 5% FBS DMEM or 50  $\mu$ g/ml BME in 5% FBS DMEM. Cells were incubated over 3 days, after which they were fixed and stained, and the density of cells that had migrated through the Matrigel to the underside of the inserts were determined by spectrophotometry at 540 nm as explained above.

#### 5.2.9 *In vitro* Adhesion Assay

12 replicate wells of a 96-well plate were coated with 5  $\mu$ g Matrigel, onto which  $2 \times 10^4$  cells/100  $\mu$ l of DU145<sup>pEF</sup>, DU145<sup>NOG</sup>, DU145<sup>FST344</sup> or DU145<sup>GREM</sup> was pipetted. Cells were treated with either 5% FBS DMEM or 50  $\mu$ g/ml BME in 5% FBS DMEM and incubated for 40 minutes before being fixed and stained. As with previous *in vitro* assays, the number of cells that had adhered to the Matrigel was determined by spectrophotometry at 540 nm. Any background reading from stained Matrigel was negated by measuring the absorbance of wells containing only Matrigel.

#### 5.2.10 *In vitro* Migration Assay

$6 \times 10^5$ /500  $\mu$ l cells of DU145<sup>pEF</sup>, DU145<sup>NOG</sup> and DU145<sup>GREM</sup>, and  $1 \times 10^6$ /500  $\mu$ l cells of DU145<sup>FST344</sup> were seeded into duplicate wells of a 24-well plate. Once grown into a monolayer, cells were scratched and treated with 5% FBS DMEM or 50  $\mu$ g/ml BME in 5% FBS DMEM. Cell migration across the wound was imaged at 37°C, 5% CO<sub>2</sub> using an EVOS™ FL Auto Cell Imaging System (ThermoFisher Scientific, Massachusetts, USA) for each hour over 20 hours. Images were analysed using ImageJ Software (National Institutes of Health, Bethesda, Maryland, USA).

### 5.2.11 ECIS

Cells were seeded at a density of  $6 \times 10^4$  cells/100  $\mu$ l for DU145<sup>pEF</sup>, DU145<sup>NOG</sup> and DU145<sup>GREM</sup>, and  $8 \times 10^4$  cells/100  $\mu$ l for DU145<sup>FST344</sup> into 12 replicate wells of a 96-well array (Applied Biophysics). They were then treated with 5% FBS DMEM or 50  $\mu$ g/ml BME in 5% FBS DMEM, and the resistance of the cells over 20 hours was measured at 4000 Hz using an Applied BioPhysics-ECIS Software V 1.2.135 (Applied Biophysics, Troy, New York, USA). Data was normalised using the resistance readings from the first time-point.

## 5.3 Results

### 5.3.1 Overexpression of BMP Antagonists in DU145

In order to assess the effects of BMP antagonists on the properties of prostate cancer cells, Noggin, FST344 and Gremlin expression was induced in the DU145 cell line by means of mammalian expression constructs. This was achieved by cloning the entire coding sequences of these BMP antagonists into the pEF6/V5-HIS-TOPO<sup>®</sup> vector and transfecting the resulting constructs into DU145 cells by electroporation. Once the stably transfected cell lines were set up, the success of these transfections was then assessed by RT-PCR and qPCR, as seen in figure 5.1. Results from both techniques demonstrated significant increases in expression of the induced BMP antagonists in comparison to the pEF control.

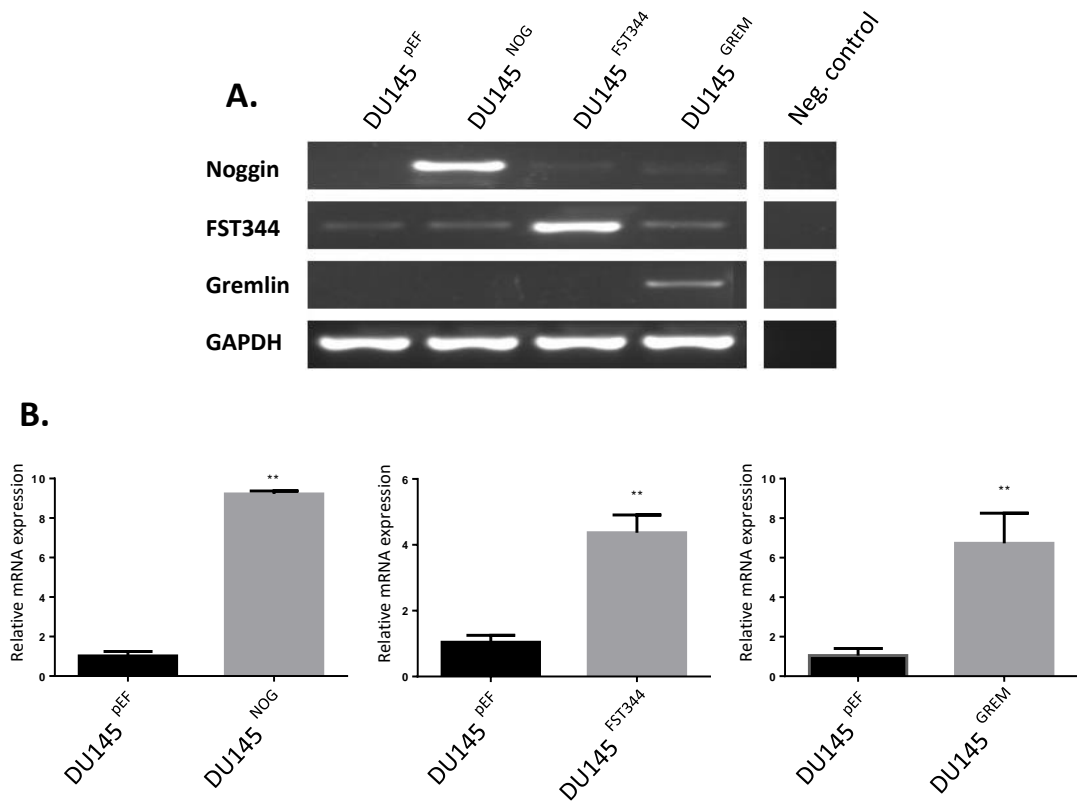


**Figure 5.1: Overexpression of BMP antagonists in the DU145 cell line.** DNA sequences of Noggin, FST344 and Gremlin were cloned into pEF6/V5-His TOPO TA vectors which were then transfected into DU145 cells along with empty vectors to act as control (pEF). **A.** The representative PCR analyses shown demonstrate the increased expression of the target genes in comparison to the pEF control. The negative control used nuclease-free water as replacement for cDNA. **B.** Representative qPCR analyses confirmed significant increase of target gene expression. qPCR readings were normalized against GAPDH and the  $\Delta\Delta C_T$  method was used against pEF for each gene (standardised to 1). Data shown represents mean values of three repeats, error bars represent standard deviation (\*  $p \leq 0.05$ , \*\*  $p \leq 0.01$ ).

### 5.3.2 BMP Antagonist Overexpression Affects Prostate Cancer Cell Growth

The effects of Noggin, FST344 and Gremlin overexpression were assessed in comparison to pEF over 3-day and 5-day periods using the crystal violet method. When only considering DMEM treatment (figure 5.2A), growth readings at Day3 showed that Noggin overexpression had no effect on DU145 cell growth, although interestingly by Day5, it caused a significant decrease ( $p < 0.05$ ). Conversely, at Day3, Gremlin overexpression caused a significant increase in cell growth ( $p < 0.01$ ), but by Day5 it caused no change to DU145 cell growth. On the other hand,

overexpression of FST344 significantly decreased the proliferative ability of DU145 cells at Day3 – an effect that lasted through to Day5 ( $p < 0.05$  and  $p < 0.0001$ , respectively).

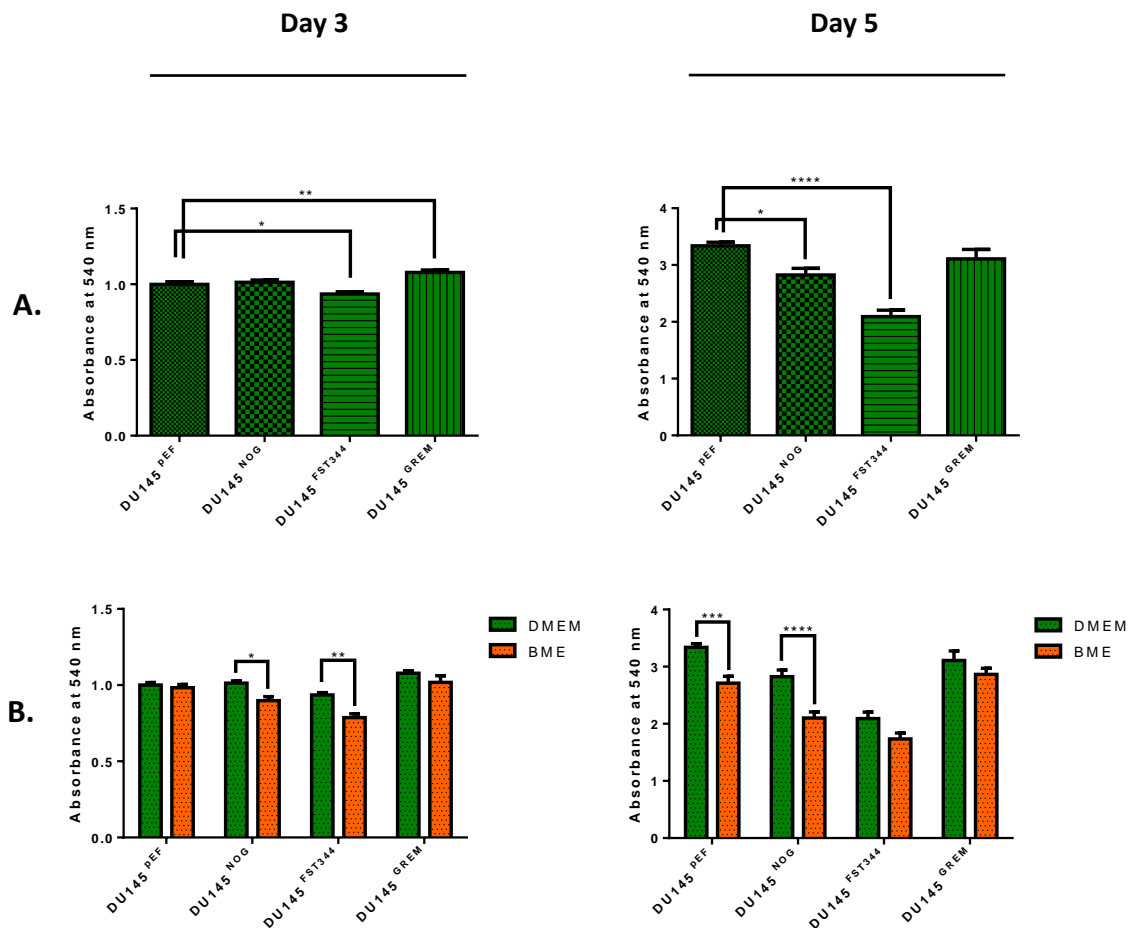


**Figure 5.2: Effects of BMP antagonist overexpression on DU145 cell growth. A.** Proliferation of DU145 cells following Noggin, FST344 and Gremlin overexpression at Day3 and Day5 in maintenance DMEM. One-way ANOVA was performed to test for significance. **B.** Proliferation of DU145 cells following Noggin, FST344 and Gremlin overexpression at Day3 and Day5 in 50  $\mu\text{g/ml}$  BME medium (orange). For ease of comparison between the two growth media, data in A. (green) was replicated in this set of graphs. Two-way ANOVA analysis was performed to test for significance. All the data shown represents mean values of three separate experiments and error bars represent standard error of the mean (SEM). Significance was annotated as follows \*  $p \leq 0.05$ , \*\*  $p \leq 0.01$ , \*\*\*  $p \leq 0.001$ , \*\*\*\*  $p \leq 0.0001$ .

To investigate the influence of the bone microenvironment on the growth of the overexpression cell lines, BME treatment was also included in this assay and readings obtained from these wells were normalised against the pEF control in DMEM. Results (figure 5.2B) demonstrated that BME treatment seemed to decrease the cell growth of all the overexpression cell lines, however it did so significantly only for DU145<sup>NOG</sup> and DU145<sup>FST344</sup> at Day3 ( $p \leq 0.05$  and  $p \leq 0.01$ , respectively). This inhibitory effect was replicated at Day5, with BME treatment significantly affecting DU145<sup>pEF</sup> and DU145<sup>NOG</sup> growth ( $p \leq 0.001$  and  $p \leq 0.0001$ , respectively).

### 5.3.3 Overexpression of BMP Antagonists Affects DU145 Cell Invasion

As seen in figure 5.3, overexpression of all FST344 and Gremlin significantly inhibited the invasive ability of DU145 cells ( $p < 0.01$  for both antagonists), while overexpression of Noggin caused no changes. More broadly, the two-way ANOVA analysis also indicated that there was no significant difference between DMEM and BME treatments.

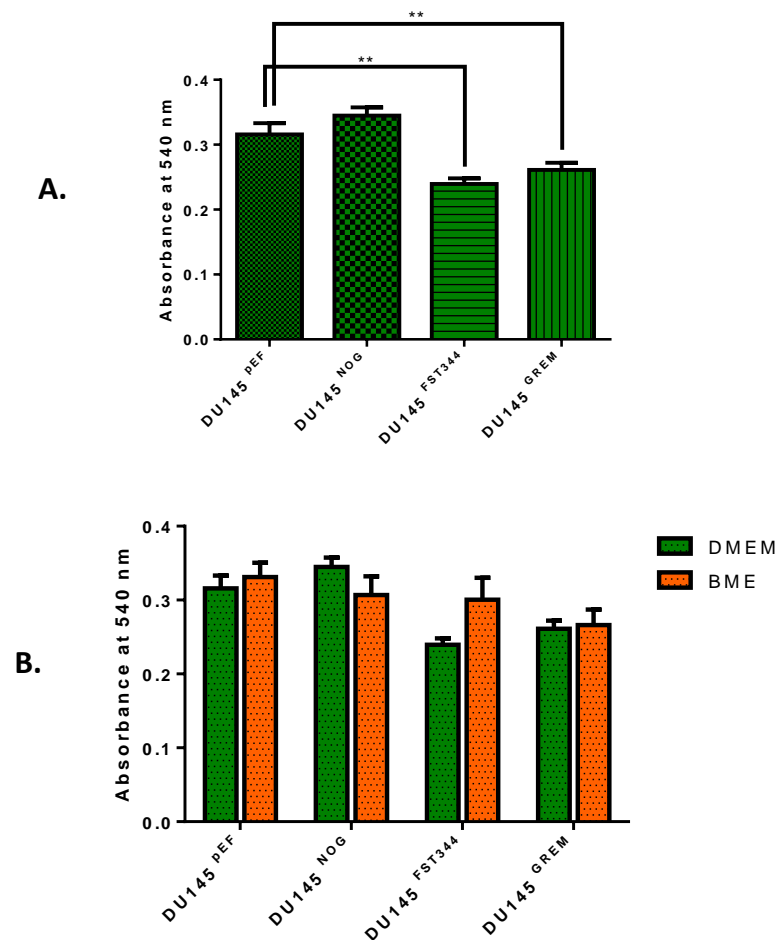


**Figure 5.3: Effects of BMP antagonist overexpression on DU145 cell invasion.** The invasion rate of DU145 cells following Noggin, FST344 and Gremlin overexpression was measured by seeding in Matrigel-coated inserts and letting them migrate through the pores of the inserts over a period of three days. Cells were then fixed and cell density was assessed by cell spectrophotometry. To negate the effect of cell proliferation from the data gathered, readings were normalised against day 3 growth readings obtained from control cell-only wells set up during the experiment and day 3 growth data from the cell proliferation assay. **A.** Invasion rates of the overexpression cell lines when cultured in maintenance DMEM. One-way ANOVA was performed to test for significance. **B.** Invasion rates of overexpression cell lines when treated with 50 µg/ml BME medium (orange). For ease of comparison between the two growth media, data in A. (green) was replicated in this graph. Two-way ANOVA analysis was performed to test for significance. All the data shown represents mean values of three separate experiments and error bars represent standard error of the mean (SEM). Significance was annotated as follows: \*\* p ≤ 0.01.

#### 5.3.4 BMP Antagonist Overexpression Affects DU145 Cell Adhesion

The ability of DU145 overexpression cell lines to adhere to a Matrigel basement membrane was assessed in maintenance DMEM or 50 µg/ml BME (figure 5.4A). Results demonstrated that overexpression of Noggin seemed to decrease adhesion of DU145 cells. In contrast, FST344 and Gremlin overexpression increased their adhesive abilities, with Gremlin overexpression doing so significantly ( $p < 0.01$ ). Treatment with BME seemed to have varying effects on the different cell lines. For example, treatment with BME increased the adhesion of DU145<sup>pEF</sup> (not significant) and DU145<sup>NOG</sup> cells ( $p < 0.01$ ), while it seemed to decrease adhesion of DU145<sup>FST344</sup> and DU145<sup>GREM</sup>. Furthermore, two-way ANOVA analysis indicated that results obtained from BME treatment wells were as a result of an interaction between the BMP antagonist overexpressed and the BME treatment ( $p < 0.01$ ).

The adhesion of the overexpression cell lines was also assessed by ECIS over a period of 20 hours (figure 5.4B). These results demonstrated that overexpression of Noggin and FST344 caused a significant decrease in cell adhesion ( $p < 0.0001$  for both), while overexpression of Gremlin seemed to cause a slight increase in resistance in comparison to DU145<sup>pEF</sup>, which may indicate that cells were more densely packed. Treatment with BME caused a significant increase in DU145<sup>FST344</sup> adhesion ( $p = 0.0018$ ) only.

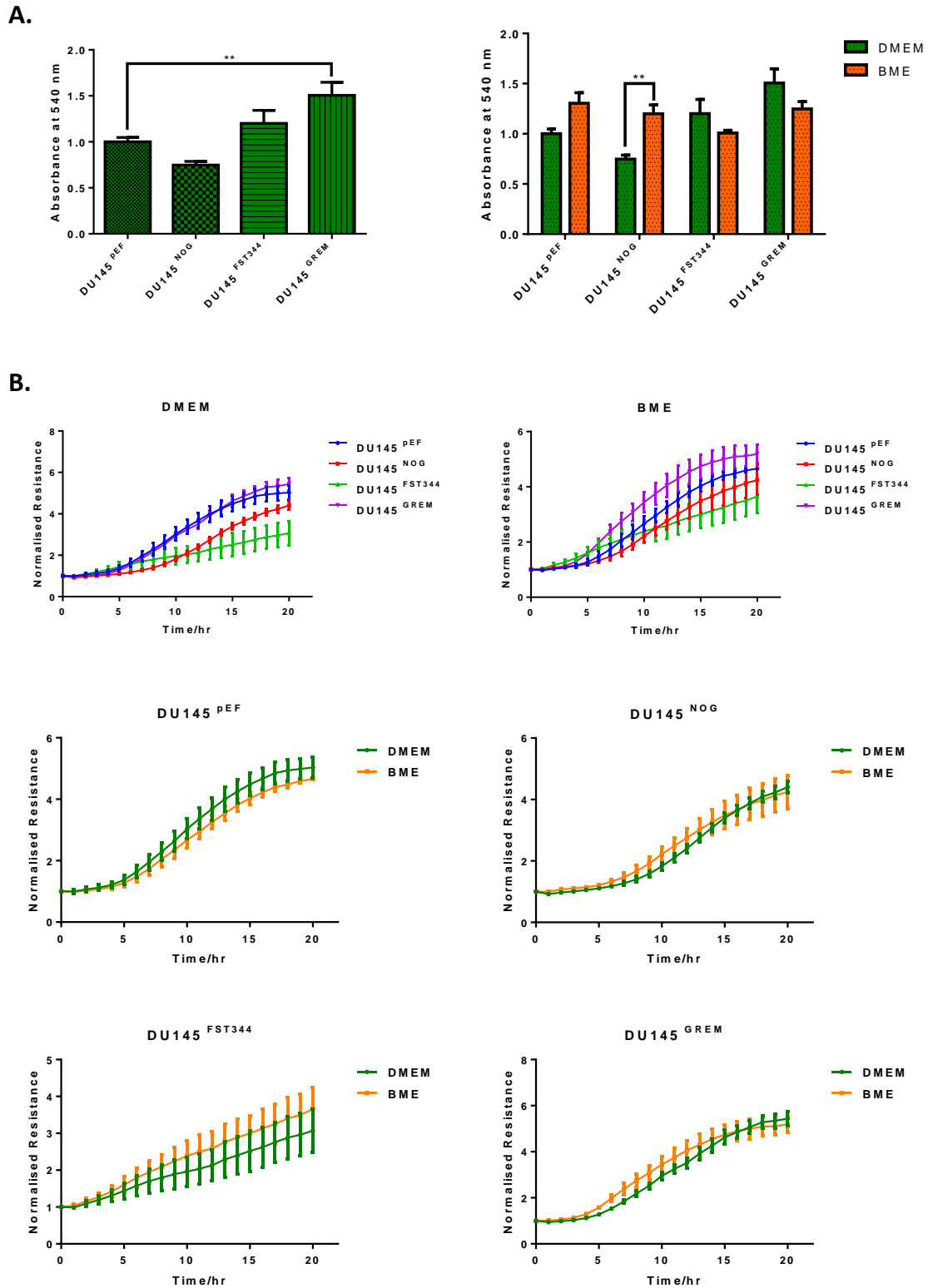


**Figure 5.4: Effects of BMP antagonist overexpression on DU145 cell adhesion.** **A.** Graphs demonstrate the adhesion of overexpression cell lines to Matrigel-coated cells when cultured in maintenance DMEM (green) or 50  $\mu\text{g}/\text{ml}$  BME medium (orange). One-way ANOVA was performed to test for significance between DMEM treated cells and two-way ANOVA analysis was performed to test for significance between the treatment media. Significance was annotated as follows \*\*  $p \leq 0.01$ . **B.** ECIS results demonstrated show the adhesion of the DU145 cell lines in maintenance DMEM or 50  $\mu\text{g}/\text{ml}$  BME medium. The effects of the different treatments on each cell line is also shown. All the data shown represents mean values of three separate experiments and error bars represent standard error of the mean (SEM).

### 5.3.5 BMP Antagonist Overexpression and DU145 Cell Migration

The migration of the transfected DU145 cell lines was assessed in the presence of maintenance DMEM or 50 µg/ml BME. As seen in figure 4.4, the overexpression of Noggin and Gremlin did not have a noticeable effect on the migration rate of DU145 cells, while FST344 overexpression caused a significant decrease in cell migration ( $p < 0.0001$ ). However, Noggin overexpression did hinder the overall migration of the cells since the distance travelled by the cells was significantly lower than that travelled by pEF cells ( $p = 0.0014$ ) by the end of the assay.

In contrast, although BME treatment seemed to decrease overall DU145<sup>NOG</sup> migration, there was not enough evidence to be proven significant. In contrast, the migration rate of DU145<sup>FST344</sup> cells was shown to be significantly different between the two treatment media ( $p = 0.0242$ ), which was denoted by an initial increase in migration rate, followed by a decreased migration rate in comparison to DU145<sup>pEF</sup> cells, while the overall migration seemed unchanged. There was no noticeable change in DU145<sup>GREM</sup> cell migration caused by the presence or absence of 50 µg/ml BME.

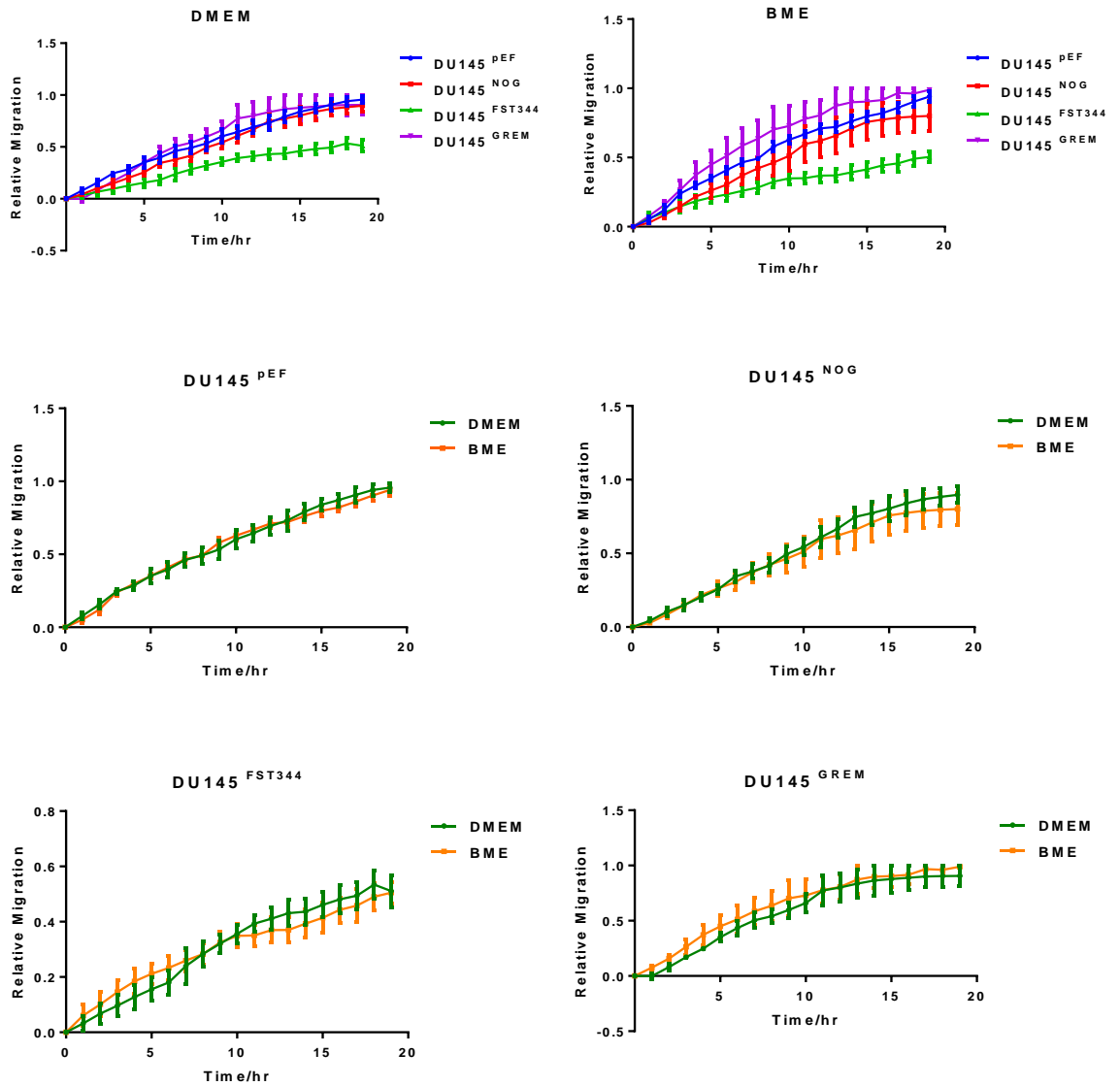


**Figure 5.5: Effects of BMP antagonist overexpression on DU145 cell migration.** The top two graphs show the migration of DU145 overexpression cell lines across a wound when treated with either maintenance DMEM or 50  $\mu\text{g/ml}$  BME. The graphs underneath show the different responses that each individual cell line had to the different treatment media. The data above represents mean  $\pm$  SEM from 4 individual experiments and any significant differences between the responses were assessed by linear regression.

## 5.4 Discussion

For a primary tumour to form and progress to secondary sites, it is crucial for cells to gain certain aberrant characteristics to override the constraints of physiological cell architecture. In fact, cancer cells are defined by two heritable properties: (1) the ability to reproduce in defiance of the normal restraints on cell growth and division, and (2) the ability to invade and colonise territories normally reserved for other cells; both properties being a result the distortion of vital cellular processes such as, cell growth, invasion, adhesion and migration. This chapter aims to assess the role of the feedback loop that exists between BMPs, more specifically BMP-7, and their antagonists in these cellular processes and to investigate how it may relate to prostate cancer progression and metastasis to the bone.

To help with the aim of this study, we decided to overexpress levels of BMP antagonists within prostate cancer cells and assess any resulting impact on their behaviour. However, due to the reported implication of various BMPs in the prostate cancer process, as well as the promiscuity that exists between BMP antagonists and the BMPs they inhibit, we opted to overexpress a selection of these antagonists in a prostate cancer cell line. We based our decision of which antagonists to overexpress on previous literature to ascertain whether they are able to inhibit BMP-2, 4, 6 and 7. Additionally, we also took into consideration preliminary expression profile work (Chapter 3 and Chapter 4) to gauge which BMP antagonist could be key in process cancer and bone metastasis. As a result, we selected BMP antagonists, Noggin, the FST isoform, FST344, and Gremlin for overexpression.

As part of this study, the BMP antagonist overexpression cell lines were generated through the transfection of DU145 cells. This cell line was used since attempts at transfecting other cells also

used in this study were unfortunately unsuccessful. Still, as DU145 cells do not appear to inherently express very high levels of the selected BMP antagonists (see figure 3.2) enabling us to ascertain that any changes in cell phenotype would be due to BMP antagonist overexpression. Once the candidate BMP antagonists were identified, the next step was to then create stable cell lines that would constitutively express them throughout the duration of the intended functional assays. As such, Noggin, FST344 and Gremlin overexpression vectors were generated by cloning using the pEF6/V5-HIS-TOPO® TA vector and these were subsequently electroporated in DU145 cells. Following a period of antibiotic selection, we were eventually able to obtain cell lines that significantly overexpressed the selected BMP antagonists as proven by RT-PCR and qPCR analyses. Again, we were unable to prove the downregulation of the BMP antagonists by Western Blot, despite many attempts.

The most typical characteristic of cancer cells is their ability to proliferate uncontrollably. Therefore, once the stable cell lines were acquired, we aimed to elucidate if the overexpression of the BMP antagonists entailed a change in DU145 cell proliferation over a 3-day and 5-day period (figure 5.2). Results yielded demonstrated that at Day3, overexpression of Noggin did not seem to have any noticeable effect on cell growth, which seems to agree with a study by Secondini et al (2011) that demonstrated that knock down of Noggin did not have any effect on the cell growth of PC-3 cells. By Day5 however, overexpression of Noggin caused a significant decrease in cell proliferation. Since studies have demonstrated that BMP action may be time-dependent (Ye, Lewis-Russell et al. 2008), it is also possible that the feedback caused by Noggin overexpression is also time-dependent. Overexpression of FST344, on the other hand, caused a significant decrease in cell growth at Day3, through to Day5. Sepporta et al (2013), despite focussing on the Activin/FST system, have highlighted a role for the FST in prostate cancer by demonstrating that the FST344 isoform, FST288, may have a stimulating effect on DU145 cell growth. This disagrees with our current findings. Interestingly, Gremlin overexpression caused a

significant increase in DU145 cell proliferation at Day3. This is supported by a study by Kim et al (2012) who demonstrated that Gremlin was able to promote cell proliferation of different cancer cell lines, although they did demonstrate that this occurred in a BMP-independent manner. Of note, BME caused a decrease in proliferation of all the overexpression cell lines, implying the need for BMP action in the cell proliferation of prostate cancer cells within the bone environment.

The invasion of DU145 cells was also assessed as a result of BMP antagonist overexpression (see figure 5.3). Interestingly, the invasion of DU145<sup>FST344</sup> and DU145<sup>GREM</sup> was significantly decreased in comparison to DU145<sup>DEF</sup>, and a slight increase was noted in DU145<sup>NOG</sup>. In terms of Noggin, these results seem to disagree with Feeley and colleagues (2006) who demonstrated that Noggin significantly inhibited cell invasion mediated by BMP-2. Furthermore, previous literature implied that FST and Gremlin may induce cell invasion, which contradicts the current findings (Kim, Yoon et al. 2012, Sepporta, Tumminello et al. 2013). Treatment with BME caused no significant changes in cell invasion, although it did appear to cause a noticeable stimulatory effect on DU145<sup>FST344</sup> cells. This could potentially paint an interesting picture translationally, whereby FST344 in conjunction with the growth factors in the bone environment could increase the invasion capabilities of prostate cancer cells.

Morphologically speaking, the loosening of cell-cell and cell-ECM contacts is crucial for carcinomas to progress. In fact, the loss of these restraints creates permissive conditions for the cells to migrate and invade through the ECM (Coman 1944, McCutcheon, Coman et al. 1948, Birchmeier and Behrens 1994). The adhesion of DU145 stable cell lines was examined using two methods, namely the *in vitro* Matrigel adhesion assay and ECIS (figure 5.4). The Matrigel assay, which indicated the differences in the initial adhesion of the different cell lines, demonstrated that DU145<sup>GREM</sup> adhesion was significantly enhanced in comparison to DU145<sup>DEF</sup> in normal

culture conditions, while DU145<sup>NOG</sup> adhesion was decreased. Interestingly, this loss in adhesion caused by Noggin overexpression was overcome by treatment with BME, as shown by a significant upregulation of adhesive abilities of DU145<sup>NOG</sup> cells. This could be quite telling in terms of prostate cancer metastasis: high levels of this antagonist would enable cancer cells to sever their attachments, thus allowing them to migrate. Therefore, the adhesion results obtained from treatment with BME could indicate that once the migrating cancer cells reach the bone, the growth factors and non-collagenous proteins within that environment would induce re-attachment of the cancer cells. ECIS, in comparison, demonstrated the adhesion of the cell lines over a period of 20 hours. These results demonstrated that the overexpression FST344 caused a drastic decrease in cell adhesion and reflected the Matrigel adhesion assay results in terms of a decrease in adhesion following Noggin overexpression. This is supported by studies that have implicated Noggin and FST344 in the prostate cancer metastasis (Tumminello, Badalamenti et al. 2010, Secondini, Wetterwald et al. 2011, Sepporta, Tumminello et al. 2013).

Once cells have lost their cell-cell and cell-ECM contacts, they are able to migrate to distant sites and establish secondary sites. Only the overexpression of FST344 caused a significant decrease in cell migration. However, treatment with BME caused an increase in migration which indicates that although FST344 overexpression may have a protective effect on prostate cancer metastasis, it may be overridden by the presence of growth factors present in the bone microenvironment.

Altogether, the data yielded in this chapter describes potentially important roles for each of the BMP antagonists in prostate cancer and its progression to the bone. In fact, overexpression of all the BMPs induced some cellular behavioural reaction that could impact on prostate cancer progression. For instance, while most of the behavioural effects caused by Noggin overexpression could be deemed as defensive against cancer, adhesion results demonstrated a

potential role of this BMP in the bone metastasis process. Meanwhile, we described novel, potentially protective roles implications for Gremlin in prostate in terms of its ability to decrease invasion and increase adhesion abilities of DU145 cells. However, the data from FST344 overexpression assays were quite striking. Indeed, although it seems to have an inhibitory effect on most pro-cancer activities, once treated with BME, the effect seems to reverse to a pro-cancer stance. This effect needs further analysis as to whether this may be as a result of a BMP/FST344 feedback loop.

Chapter 6.

**Molecular Mechanisms  
underlying the Changes in  
Cell Behaviour Mediated by  
BMP Antagonists**

## 6.1 Introduction

It has long been recognised that metastasis is inherently a very inefficient process (Weiss 1990). Indeed, by the time CTCs reach a secondary site that is suitable for their needs of survival and growth, they have already had to survive and escape haemodynamic forces, immunological stress and collisions with other cells (Key 1983, Weiss, Dimitrov et al. 1985, Wirtz, Konstantopoulos et al. 2011). Still, once they reach and extravasate into the new site, the disseminated cancer cells (DTCs) are faced with a yet another obstacle: the dense, cross-linked ECM of a physiologically different environment. In fact, only a minority of DTCs are able to negotiate and invade through this barrier to form macro-metastases (Luzzi, MacDonald et al. 1998).

Unspoken by Paget was the concept that even in their preferred metastatic sites, DTCs must still undergo certain phenotypic and morphological adaptations in order to colonise them. Indeed, several steps must be completed by DTCs to change their plasticity, one of the most important steps being EMT. The latter is a highly conserved and reversible process that involves the loss of cell-cell adhesion and apical-basal polarisation, the reorganisation of the cytoskeleton architecture, changes in the signalling programmes that convey cell shape, and the reprogramming of gene expression, all with the aim to bestow onto epithelial cells increased motility, invasiveness and the ability to degrade the ECM (Thiery 2002, Thiery, Acloque et al. 2009, De Craene and Berx 2013, Lamouille, Xu et al. 2014). In fact, EMT should be more precisely described as a 'group' of biological programmes, all of which are orchestrated and networked by a group EMT-inducing transcription factors (EMT-TFs). The most studied and potent EMT-TFs are by far master EMT-TFs Snail, zinc finger E-box binding homeobox 1 (Zeb1) and Twist.

One fundamental hallmark of EMT is the 'cadherin switch', whereby expression of E-cadherin, an essential component of adherens junctions, is transcriptionally repressed by Snail and Twist, and the expression of the mesenchymal marker, N-cadherin, is upregulated (Batlle, Sancho et al. 2000, Vesuna, van Diest et al. 2008, De Craene and Berx 2013). This not only leads to the disassembly of adherens junctions, due to the loss of E-cadherin, but also the rearrangement of the cytoskeleton, lamellipodia formation, and the induction of pro-migratory and invasive signalling cascades by action of N-cadherin (Hazan, Phillips et al. 2000, Li, Satyamoorthy et al. 2001, Shih and Yamada 2012). Another mechanism by which EMT may induced is by proteolytic degradation of E-cadherin by MMPs. While this process disrupts E-cadherin-mediated cell-cell adhesion, cleavage of the cadherin also yields an 80 kDa soluble E-cadherin (sEcad) fragment, which is capable of inducing EMT, invasion and proliferation in its own rights (Nawrocki-Raby, Gilles et al. 2003, David and Rajasekaran 2012). In fact, sEcad levels are significantly heightened in the sera and urine of cancer patients and are associated with invasive disease and/or poor prognosis in a variety different tumour types, including prostate cancer (Katayama, Hirai et al. 1994, Kuefer, Hofer et al. 2003, De Wever, Derycke et al. 2007).

Beyond their EMT-inducing functions, MMPs have a much broader role in the metastatic process and have a profound effect on the ability of cancer cells to colonise a secondary site. Indeed, as the members of the cancer degradome that are able to digest virtually any component of the ECM and basal membrane component, MMPs are the principle mediators of changes observed in the cancer microenvironment (Egeblad and Werb 2002, Kessenbrock, Plaks et al. 2010). Even during bone metastasis, MMPs can be derived from a number of cellular sources, however none more so than by the key players of this process, that is, the DTCs, the osteoblasts and the osteoclasts (Lynch 2011). While it would seem counterintuitive that osteoblasts would ever secrete proteinases given their role in bone formation, it seems that both types of bone cells, the osteoblasts and the osteoclasts, require MMPs for normal function. This notion is supported

by various studies, one of which demonstrated impaired skeletogenesis in MMP2 null mice (Mosig, Dowling et al. 2007). Therefore, it is unsurprising that MMP action would be involved in prostate cancer progression to the bone. In fact, MMP2, 3, 9, 12, 13 and 14 have all been detected in the prostate cancer bone microenvironment (Nemeth, Yousif et al. 2002, Chinni, Sivalogan et al. 2006, Bonfil, Dong et al. 2007, Nabha, dos Santos et al. 2008).

While they are all necessary for normal physiology, the aberrant, combined action of disrupted cell-cell junctions, cytoskeletal readjustments and secreted MMPs drive cancer creates a perfect storm for cancer cell invasion through the stroma. As such, assessing for expression of the different components of these processes provides a good insight in the invasive capabilities, and thus aggressiveness of a cancer. For instance, the Snail, Twist and E-cadherin axis has been described in the majority of cancer types investigated so far, including breast, pancreas, liver, lung and prostate (Sánchez-Tilló, Liu et al. 2012). Therefore, our aim was to screen for these telling signs of EMT and invasion to get a better insight into the molecular mechanisms underlying the formation of osteolytic and osteoblastic lesions. Furthermore, having accumulated data on the phenotypic behaviour of prostate cancer cells under the influence of BMP overexpression, we also endeavoured to decipher which BMP-BMP antagonist interplay could be in play.

## **6.2 Materials and Methods**

### **6.2.1 Materials**

All the primers used were synthesised and provided by Sigma-Aldrich (Poole, UK). Primer sequences are detailed in tables 2.2 to 2.4.

### **6.2.2 Cell lines and Treatments**

Stably transfected overexpression cell lines were cultured in maintenance medium consisting of DMEM supplemented with 10% FBS, antibiotics and 0.5 µg/ml blasticidin. All cell lines were pre-treated in the maintenance medium with 5% FBS and antibiotics overnight, preceding any treatment experiments. The BME treatment used in this study was prepared as described in section 2.2.1, and 50 µg/ml in 5% FBS DMEM was used to treat cells.

### **6.2.3 RNA isolation and cDNA synthesis**

RNA was extracted from the cells using the TRI reagent<sup>®</sup> kit (Sigma-Aldrich, Poole, UK), and synthesised into cDNA by reverse transcription using the GoScript<sup>™</sup> Reverse Transcription System (Promega, Southampton, UK), as respectively described in sections 2.4.2 and 2.4.3.

#### 6.2.4 RNA-Seq

Targeted-sequencing of low passage PC-3 and VCaP incubated with either fresh 5% FBS DMEM or 5% FBS DMEM containing 50 µg/ml BME for 3 hours 37°C, 5% CO<sub>2</sub> was undertaken. 10 ng of total RNA extracted from the prostate cancer cell lines was subsequently used for RNA sequencing. Heatmaps were generated using Microsoft Excel.

#### 6.2.5 qPCR

qPCR was performed using the Amplifluor™ Universal Detection System (Intergen Company, New York, USA) under the cycling conditions detailed in section 2.4.6. CT values obtained were analysed using  $\Delta\Delta CT$  normalisation to GAPDH and the relative quantity was calculated using  $2^{-\Delta CT}$ . Data analysis was carried out using unpaired t-test with Welch's correction compared to the pEF control for the DMEM data. Two-way ANOVA was performed to assess significance in the BME data.

#### 6.2.6 GEO Database

In the present study, we utilised data from the GEO dataset (GSE41619) generated by Larson et al (2013), who performed microarray hybridisation on RNA isolated from osteoblastic and osteolytic bone metastatic cores. Expression data for genes of interest were extracted from the GSE41619 and heatmaps of this data were generated using RStudio. Analysis of these samples was also performed by calculating the mean and SEM of these samples, and significance was assessed using unpaired t-test with Welch's correction. These details can be found in the appendix. We also extracted expression data from a GEO dataset produced from the microarray

gene analyses of LNCaP cells and primary hOBs monocultures and co-culture (Sieh, Taubenberger et al. 2014). This data was analysed by calculating the means of all the repeats + SEM, and significance was analysed by unpaired t-test using the Holm-Sidak method.

## **6.3 Results**

### **6.3.1 Differential Expression of EMT markers and MMPs in Osteolytic and Osteoblastic Cell Lines**

RNA-Seq analysis was run on PC-3 and VCaP cells to assess their invasiveness and EMT status (see figure 6.1A). According to these results, PC-3 appeared to express more of the mesenchymal markers, that is, Snail, Slug, Twist and N-cadherin, in comparison to VCaP, with the latter not even expressing Twist1. Upon BME treatment however, most of the markers that PC-3 expressed were downregulated, with the exception of Snail, which was upregulated. Twist1 levels remained more or less the same. Similarly, although VCaP expressed very low levels of the mesenchymal markers, they were all further downregulated following BME treatment. Both cell types expressed high levels of epithelial marker, E-cadherin, although VCaP less so than PC-3. BME treatment also reduced levels of the marker in both PC-3 and VCaP.

When assessing the levels MMPs in the different cell lines (figure 6.1B), we observed that PC-3 expressed a higher proportion of the proteinases, and in generally higher levels than VCaP. In fact, PC-3 cells expressed MMP1, 2, 3, 7, 8, 9, 11, 13, 15, 16, 17, 23, 24, 25, 28 and extremely high levels of MMP14. Along with MMP21, VCaP expressed the same MMPs, with the exception of MMP3, 9, 16 and 23. BME treatment induced fluctuating changes to the levels of the different MMPs, however the most expressed ones were upregulated in both cell lines.

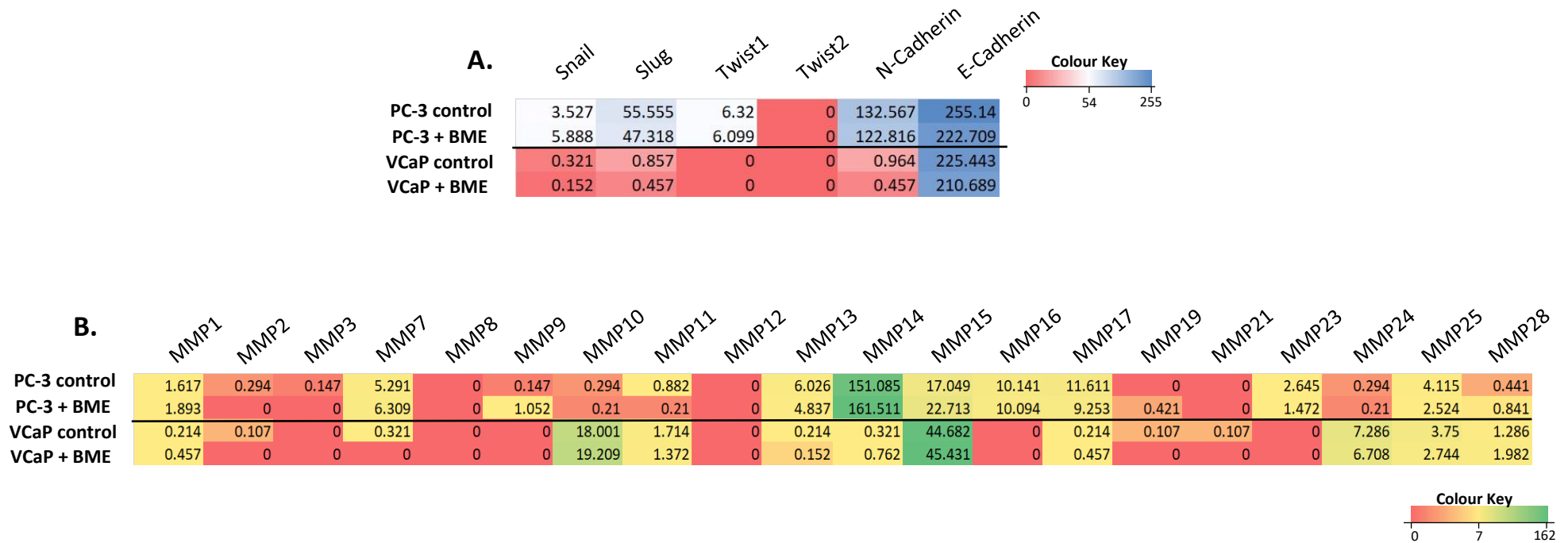


**Figure 6.1: Differential Expression of EMT markers and MMPs between osteolytic and osteoblastic cell lines.** The osteolytic cell line, PC-3, and the osteoblastic cell line, VCaP, were treated with 5% FBS DMEM or 5% FBS DMEM containing 50 µg/ml BME. RNA was extracted from the cells and RNA-Seq was performed on the samples. **A.** The heatmap presented demonstrates the changes in expression of the EMT markers, Snail, Slug, Twist1, Twist2, N-Cadherin and E-Cadherin in both cell lines following BME treatment. **B.** We also analysed the differing levels of MMPs between the cell lines, in the absence and presence of 50 µg/ml BME.

6.3.2 Expression Profiles of EMT Markers and MMPs in Osteoblastic and Osteolytic Bone Lesions

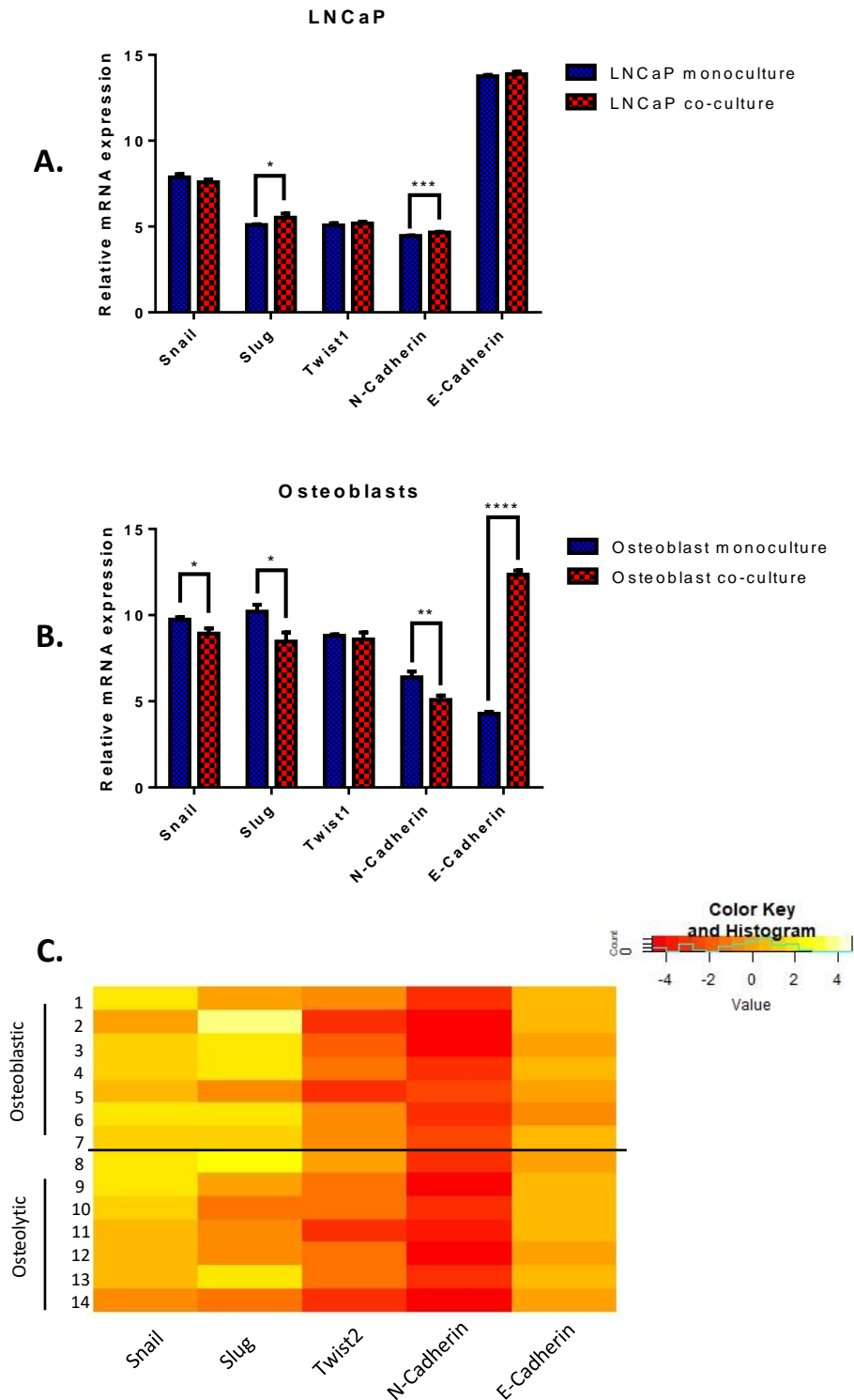


**Figure 6.2: The EMT expression profile of osteoblastic and osteolytic bone lesions.** **A.** Data was extracted from GEO data (GSE44143) produced by Sieh et al (2014) who performed microarray gene analysis of LNCaP cells and hOBs that were monocultured or co-cultured. The data shown represents mean + SD and significance was assessed by unpaired t-test using the Holm-Sidak method. **B.** The heatmap generated represents EMT marker expression data extracted from the GSE41619 microarray analysis of osteoblastic (1-7) and osteolytic lesions (8-14) (Larson et al 2013).

Using GEO data from Sieh et al (2014) and Larson et al (2013), we analysed the differential expression of EMT markers in the osteoblastic and osteolytic bone lesions (figure 6.2). Data from Sieh et al demonstrated that LNCaP cells expressed much higher levels of E-Cadherin in comparison to the mesenchymal markers. This was still the case following co-culture with hOBs, although levels of the Slug and N-cadherin were significantly increased ( $p = 0.0346$  and  $p = 0.0009$ , respectively). In contrast, Snail levels seemed to be decreased. hOBs demonstrated a different EMT profile altogether by expressing higher levels of all the mesenchymal markers in comparison to E-cadherin. However, this was reversed following co-culture with LNCaP, with Snail, Slug and N-cadherin showing significant downregulation ( $p = 0.0119$ ,  $p = 0.0106$  and  $p = 0.0057$ , respectively) and E-cadherin being considerably upregulated ( $p < 0.0001$ ).

Analysis of EMT marker expression using data acquired from Larson et al demonstrated that while both types of bone lesions exhibited a high expression of Snail and Slug in comparison to the reference pool, N-cadherin was downregulated, and E-cadherin was only slightly upregulated. Twist1, on the other hand, was downregulated in both lesion types. Although not significant, certain differences were observed between the EMT marker levels of osteoblastic and osteolytic lesions (see figure A4). Indeed, an upregulation in levels of all the mesenchymal markers, Snail, Slug, Twist and N-Cadherin, was noted in the osteoblastic lesions when compared to osteolytic lesions. In contrast, levels of E-cadherin were higher in the osteolytic lesions.

### 6.3.3 Differential Expression of MMPs in Osteoblastic and Osteolytic Bone Lesions

Using the same GEO data from section 6.3.2, we analysed the expression of MMP expression profiles of osteoblastic and osteolytic bone lesions (see figure 6.3). From these findings we observed that LNCaP cells expressed all of the MMPs tested, with MMP2 and MMP17 being exhibiting higher levels than the others. Changes to MMP levels were variable following co-culture with hOBs, although it caused a significant decrease in MMP2, 13, 17 and 28 ( $p = 0.0021$ ,  $p = 0.0226$ ,  $p = 0.0181$  and  $p = 0.0178$ , respectively). Similarly, hOBs expressed all of the MMPs tested, with higher levels MMP2 and MMP17. Furthermore, co-culture with LNCaP cells also demonstrated variable changes. For instance, while MMP2, 3, 11, 27 and 28 were all significantly downregulated ( $p = 0.0098$ ,  $p = 0.0406$ ,  $p = 0.0034$ ,  $p = 0.0177$  and  $p = 0.0391$ , respectively), the co-culture experiments also caused a significant increase in MMP10, 15, 16 and 25 ( $p = 0.0001$ ,  $p < 0.0001$ ,  $p = 0.0009$  and  $p = 0.0228$ , respectively).

Again, MMPs were expressed at varying levels in both types of lesions. Overall analysis of the samples (see figure A5) have shown that out of the MMPs tested, levels of MMP1, the two variants (v) of MMP16, MMP16 v1 and MMP16 v2, and MMP17 were lower than that of the reference sample. All the other MMPs were more highly expressed in comparison, with MMP2 and MMP26 showing the highest expression. Further analysis into the differential expression of the two types of lesions has demonstrated that their MMP profiles showed some differences, with MMP13 and MMP15 being significantly more expressed in osteolytic lesions ( $p = 0.0022$  and  $p = 0.0438$ , respectively). Of note, while highly expressed in both lesions, MMP2 was more highly expressed in osteoblastic lesions.

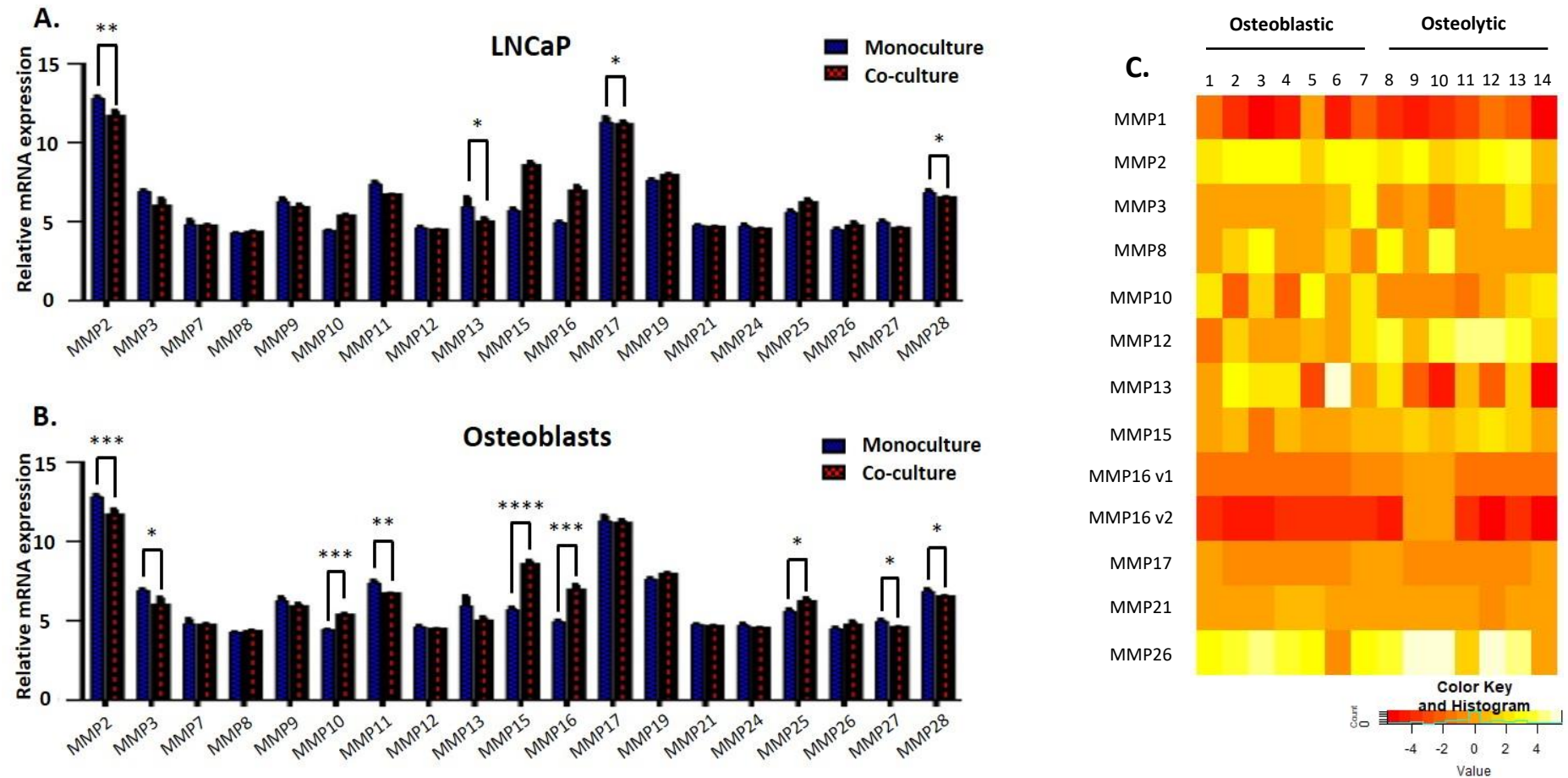


**Figure 6.3: The MMP expression profile in in osteoblastic and osteolytic prostate cancer bone lesions.** **A.** Microanalysis GEO data (GSE44143) obtained from LNCaP-hOB monoculture and co-culture experiments performed by Sieh et al (2014) were analysed, assessing for MMP expression levels. The images above represent the mean + SD and significance was assessed using unpaired t-test using the Holm-Sidak method (\*  $p \leq 0.05$ , \*\*  $p \leq 0.01$ ,  $p \leq 0.001$ , \*\*\*\*  $p \leq 0.0001$ ). The data demonstrates the difference in MMP expression between LNCaP monoculture and their co-culture with hOBs. **B.** The data demonstrates the differential expression of MMPs in hOBs between hOB monoculture and their co-culture with LNCaP cells as obtained from the GSE44143 dataset. **C.** The heatmap was generated from the GSE41619 dataset depicts the differential expression of MMPs between osteoblastic (1-7) and osteolytic (8-14) bone lesions. This data was obtained from Larson et al (2013).

### 6.3.4 The MMP Expression Profile of the BMP Antagonist Overexpression Cell Lines

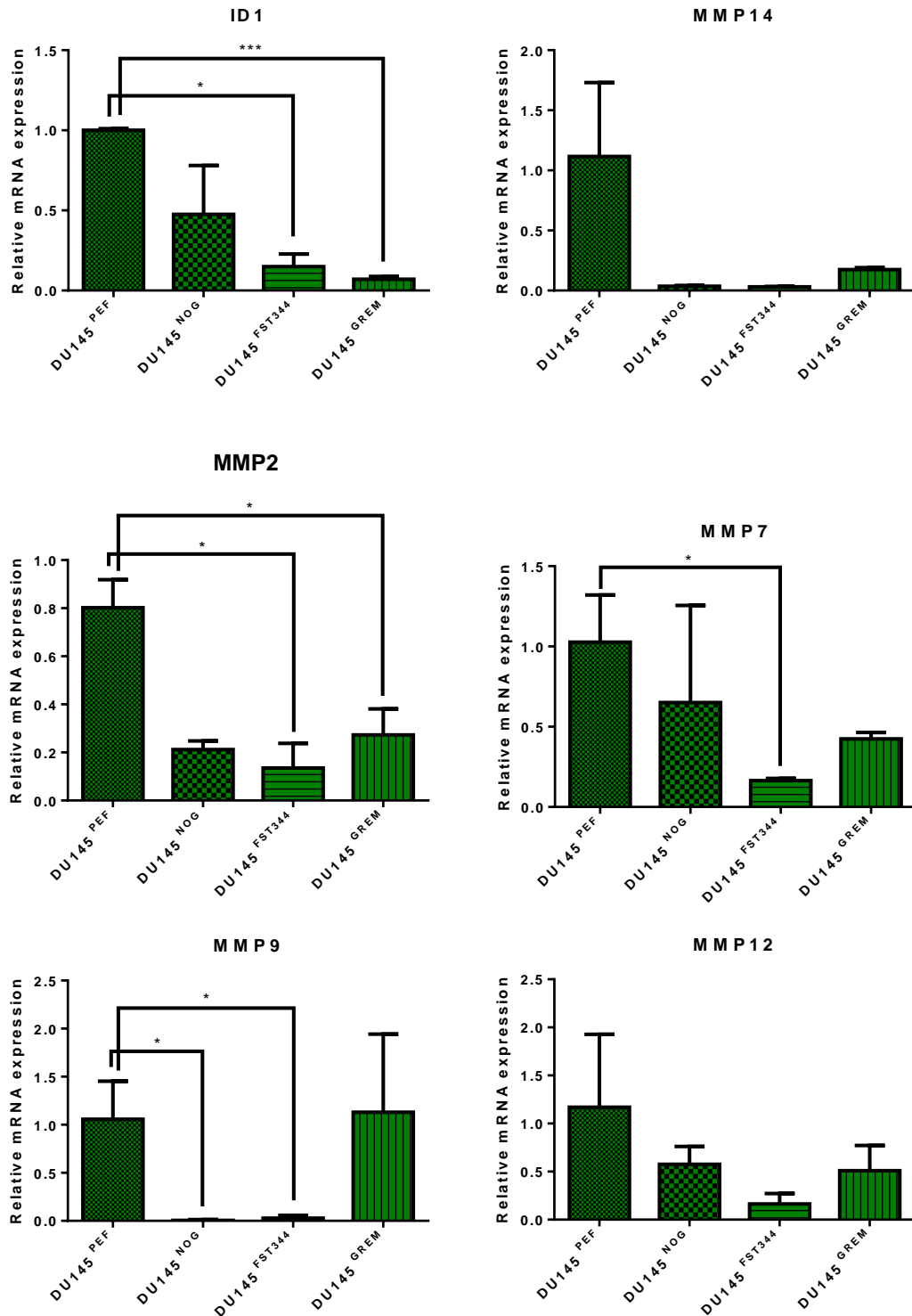


**Figure 6.4: BMP-mediated expression of MMPs.** The expression of ID1 and MMP2, 7, 9, 12 and 14 was assessed in the overexpression cell lines DU145<sup>PEF</sup>, DU145<sup>NOG</sup>, DU145<sup>FST344</sup> and DU145<sup>GREM</sup>, by qPCR. The data represents the mean + SD from one assay. Statistical significance was measured by unpaired t-test with Welch's correction (\*  $p \leq 0.05$ , \*\*\*  $p \leq 0.001$ ).

qPCR analyses (figure 6.4) demonstrated that overexpression of all the BMP antagonists caused a decrease of ID1, with FST344 and Gremlin overexpression causing significant decreases ( $p = 0.0381$  and  $p = 0.0007$ ). BMP antagonist overexpression also caused a decrease in most of the MMPs tested, although Gremlin overexpression seemed less efficient in downregulating MMPs than the other antagonists, even causing an increase in MMP9 levels. MMP2 levels were significantly reduced in both DU145<sup>FST344</sup> and DU145<sup>GREM</sup> ( $p = 0.0270$  and  $p = 0.0426$ ). MMP7 were decreased significantly in DU145<sup>FST344</sup> ( $p = 0.0366$ ) and MMP9 was significantly decreased in both DU145<sup>NOG</sup> and DU145<sup>FST344</sup> ( $p = 0.0441$  and  $p = 0.0449$ , respectively). While both MMP12 and MMP14 were decreased following BMP antagonist overexpression, neither showed any significance.

#### 6.3.5 The BMP/BMP Antagonist Feedback Loop in the Bone Environment

qPCR analyses were performed on the cell lines generated from the experiments outlined in Chapter 5. These were either treated in maintenance medium with reduced FBS content (5%) or with this same medium supplemented with 50  $\mu\text{g/ml}$  for 3 days (see figure 6.5). The data demonstrated that levels of all the BMPs tested were reduced following overexpression of Noggin and FST344, although BMP-4 downregulation by Noggin was minimal. The same could not be said would Gremlin overexpression, which downregulated expression of BMP-2 only, even causing an increase in expression for the other BMPs. Interestingly treatment with BME caused different effects on the levels of the BMPs tested. For instance, BME treatment caused the downregulation of BMP2 and an upregulation of BMP-4 in all the cell lines. BME caused a slight increase of BMP-7 in DU145<sup>PEF</sup> and DU145<sup>NOG</sup> cells, and a slight decrease in DU145<sup>FST344</sup> and DU145<sup>GREM</sup>. In contrast, BMP-6 levels were decreased in DU145<sup>PEF</sup> and DU145<sup>GREM</sup>, and increased in DU145<sup>NOG</sup> and DU145<sup>FST344</sup>. However, two-way ANOVA analysis of the results

indicated these changes in BMP levels did not result from the integrated action of the BMP antagonists and the BME.

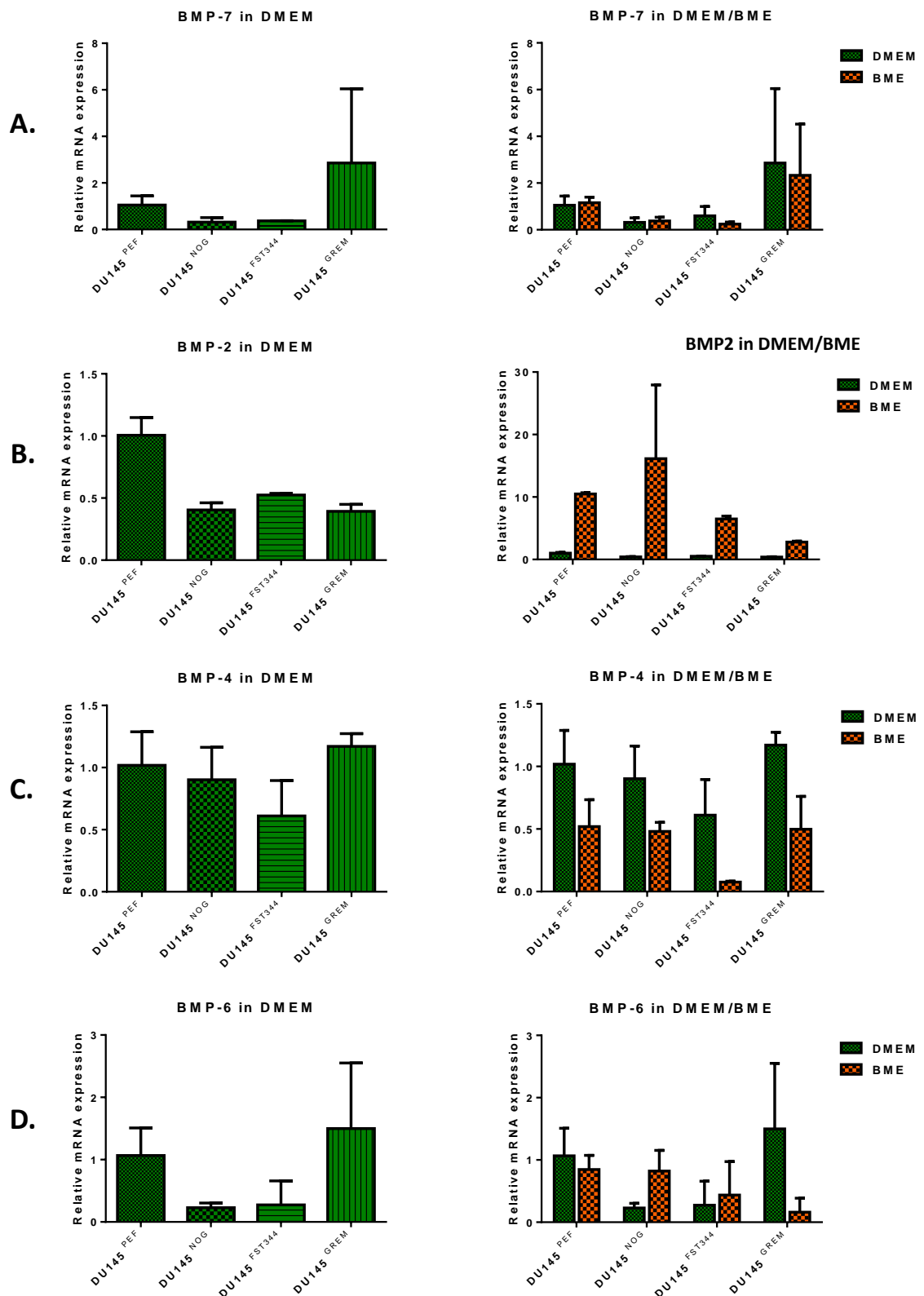


**Figure 6.5: The BMP/BMP antagonist feedback loop behind cancer cell behaviour in the bone environment.** The BMP antagonist overexpression cell lines, DU145<sup>PEF</sup>, DU145<sup>NOG</sup>, DU145<sup>FST344</sup> and DU145<sup>GREM</sup>, were pre-treated overnight in serum-reduced maintenance medium (5% FBS). Cells were then treated for 72 hours with fresh 5% FBS maintenance medium with or without 50  $\mu\text{g}/\text{ml}$  BME. RNA was extracted, and qPCR analyses were carried testing for the levels of BMP-7 (**A**), BMP-2 (**B**), BMP-4 (**C**) and BMP-6 (**D**). The data was analysed using the  $\Delta\Delta\text{CT}$  method against DU145<sup>PEF</sup> in DMEM. The control data (DMEM) was replicated in the treatment graphs for ease of comparison data above show mean + SD from one assay. Statistical significance was measured by unpaired t-test using the Holm-Sidak method (\*  $p \leq 0.05$ ) and two-way ANOVA.

### 6.3.6 The EMT Marker Profile of BMP Antagonist Overexpression Cell Lines in the Bone Microenvironment

The levels of Snail and Slug in the overexpression cell lines following 3 days in a control, reduced FBS medium or in a BME treatment medium were assessed by qPCR (see figure 6.6). The data demonstrated that while in the control medium, Snail levels were decreased in both DU145<sup>FST344</sup> and DU145<sup>GREM</sup>, with DU145<sup>FST344</sup> showing a significant decrease ( $p = 0.0349$ ). DU145<sup>NOG</sup> showed a slight increase. In contrast, levels of Slug were increase in both DU145<sup>FST344</sup> and DU145<sup>GREM</sup>, and reduced in DU145<sup>NOG</sup>. BME treatment demonstrated differing effects on the levels of the EMT markers. Indeed, despite causing an increase in both EMT marker levels in the control cell line, BME treatment caused a decrease in Snail levels and a drastic increase in Slug levels in the overexpression cell lines. Interestingly, while two-way ANOVA of the results demonstrated that the changes shown in Snail levels were not as a result of an interaction between BMP antagonist overexpression and BME treatment, they showed a significant chance that the combined action of these two factors caused changes in Slug expression ( $p < 0.0001$ ).

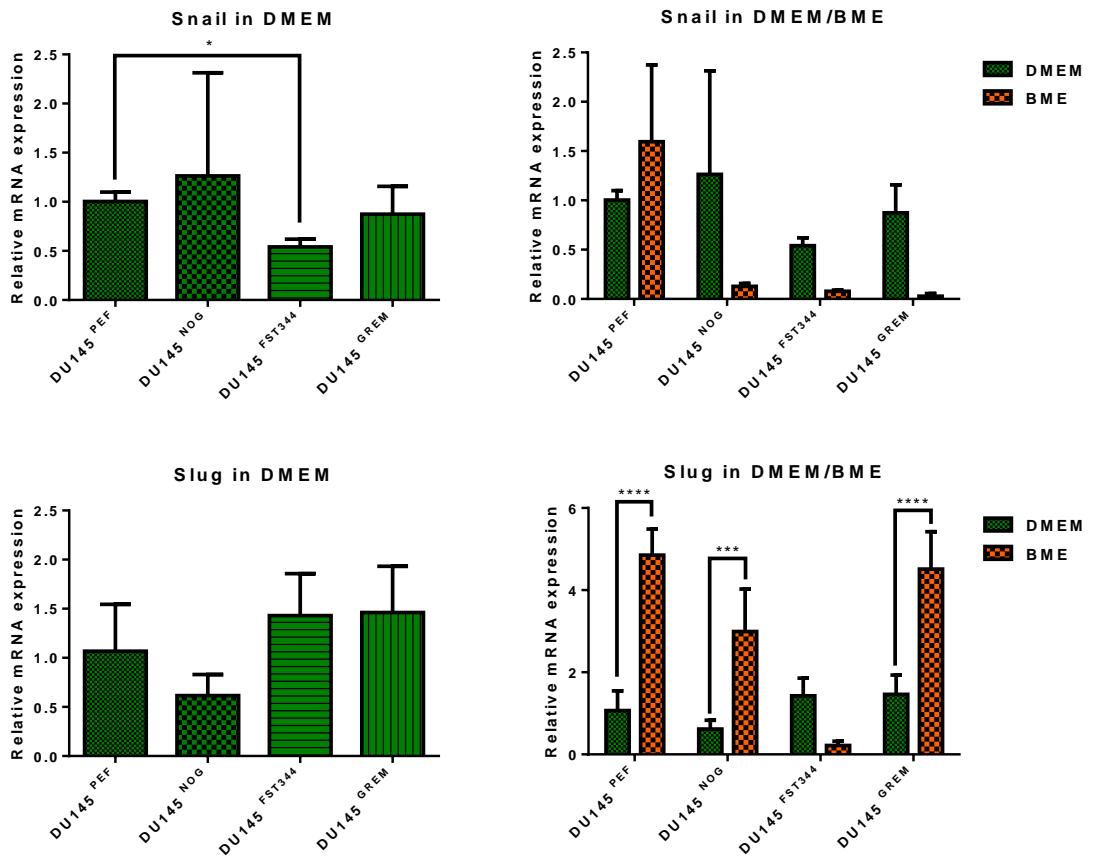


**Figure 6.6: The EMT profile of the BMP Antagonist Overexpression Cell Lines in the Bone Environment.** The cell lines were cultured in reduced FBS (5%) maintenance medium overnight. They were then treated with fresh reduced maintenance medium in the absence or presence of 50  $\mu\text{g/ml}$  BME for 3 days. RNA was extracted, and qPCR was performed on the samples. The data represents mean + SD from one assay. Statistical significance was assessed by unpaired t-test with Welch's correction for the samples in control medium (DMEM) and two-way ANOVA was used on the both set of data.

## 6.4 Discussion

Bone metastasis is by far the most devastating and challenging aspect of prostate cancer. Despite the advances in the diagnosis and management of this disease, once it reaches the bone, the only available options are mainly palliative. Skeletal metastases unfortunately result in significant complications that greatly diminish the quality of life of affected patients, causing such symptoms as bone pain, pathological fractures, symptomatic hypercalcaemia and spinal cord compression (Coleman 1997, Coleman 2006). In spite of these severe complications, there have not been many advances in the development of therapeutic strategies to prevent or treat

these lesions. As such, gaining an understanding of the pathophysiological processes behind the formation of prostate cancer bone metastases is critical. In this study, we aimed to understand the metastatic differences of the osteolytic and osteoblastic lesions and how BMPs and their antagonists participate in this process.

Since it is well recognised that the 'successful' establishment of prostate cancer in the bone depends on interactions between the cancer cells and the bone microenvironment, our first aim for this study was to assess how BME affects the metastatic status of the osteolytic PC-3 and osteoblastic cell lines VCaP cells. In order to do so, we assessed the differential expression of mesenchymal markers, Snail, Slug, Twist isoforms, Twist1 and Twist2, and N-cadherin, as well as the epithelial marker E-cadherin, in the cell lines in the absence and presence of BME (figure 6.1A). From these findings, it was apparent that the PC-3 cell line expressed much higher levels of the mesenchymal markers than VCaP. This could be explained by the fact that this cell line is inherently more aggressive (Tai, Sun et al. 2011). Interestingly, with the exception of Snail which was upregulated in PC-3, all the EMT markers were downregulated in both cell lines. While the decrease in mesenchymal markers could indicate that factors in the BME are inducing a mesenchymal to epithelial transition (MET) response, however this is contradicted by the decrease in the levels of E-cadherin. It is possible that both are happening in parallel. It is generally known that DTCs need to undergo MET to allow adhesion and anchorage for the colonisation of the metastatic niche (Yao, Dai et al. 2011). Still, it is possible that an invasive response is still being triggered, as is manifested by the downregulation of E-cadherin. Although the BME treatment caused varying effects on the levels of the different MMPs (see figure 6.1B), the MMPs that were most highly expressed, that is MMP14 (also known as membrane type 1 matrix metalloproteinase, MT1-MMP) in PC-3 and MMP10 and MMP15 in VCaP, were upregulated in response to BME. This could tie in with the previous suggestion that while some cancer cells are undergoing MET in response to BME, others are retaining their mesenchymal

and invasive phenotype to enable the infiltration of their new environment. Furthermore, the increase in MMP levels could explain the decrease in E-cadherin, due to their ability to degrade the EMT marker to the smaller sEcad fragment (Nawrocki-Raby, Gilles et al. 2003, David and Rajasekaran 2012).

We also wanted to assess the EMT marker status of cancer cells in the early establishment of bone metastasis. This was done by analysing the expression of EMT markers in LNCaP cells in co-culture with hOBs, as carried out by Sieh et al (2014; see figure 6.2A). Although the changes between the monoculture and co-culture conditions were minimal, all the mesenchymal markers, except Snail, were upregulated, along with E-cadherin. Although the pathophysiological conditions simulated in both experiments are different, this data demonstrates could agree with the RNA-Seq data, demonstrating a mixed EMT response. However, the GEO results also indicate that MMP-mediated EMT might not be occurring due to the downregulation of known EMT-inducing MMPs, MMP2, 3, 9, 13 and 28 (Gialeli, Theocharis et al. 2011; see figure 6.3A and B). Part of these MMPs, such as MMP2 and 9 are also known to be implicated prostate cancer cell invasion, thus their decrease could be indicative that co-culture with the hOBs did not induce an osteolytic response (Nemeth, Yousif et al. 2002). Using the data from Larson et al, we also assessed how the prostate cancer cell and osteoblast interplay affect the EMT status of hOBs (figure 6.2B). Interestingly, the data demonstrated that interaction with LNCaP caused the hOBs to undergo EMT, as manifested by the significant decrease of mesenchymal markers and significant increase of E-cadherin. If one were to consider a study by Stewart et al (2010) who investigated zebrafish bone regeneration, this could be reminiscent of the EMT undergone by osteoblasts in order to generate proliferative preosteoblasts following fin amputation. Although this study demonstrated that this process was Wnt-mediated, they also iterated the requirement of BMPs for the osteoblast differentiation. Therefore, altogether, observed findings could be indicative of an osteoblastic

response to the prostate cancer cells. While it is known that osteoblasts express MMPs, the exact mechanism through which these MMPs contribute to osteoblast function remains mostly unknown. However, a study by Johansson et al (1997) have demonstrated the expression of MMP13 by osteoblasts and its importance in endochondral ossification and bone remodelling. With this in mind, the decrease in MMP13 levels in hOBs could indicate that the hOBs are not initiating an ossification process. Johansson et al also demonstrated that expression of BMP-2 inhibited MMP13 expression, therefore it is possible that the decrease of MMP13 observed would be due to the BMP-2 produced by the LNCaP in co-culture.

The analysis of the differential expression of EMT markers between the two types of bone lesions demonstrated that generally (figure 6.2C), osteoblastic lesions expressed higher levels of mesenchymal markers and lower levels of the epithelial markers, indicating that the cells in the lesions are more mobile and invasive in the osteoblastic lesions. This seems to be supported by the high expression of MMP2 and MMP15 (also known as MT2 MMP) in particular, with both MMPs known to be potent metalloproteinases (Nemeth, Yousif et al. 2002, Ito, Yana et al. 2010). Meanwhile, the high expression of MMP13 could be indicative of osteoblast activity. The increase observed in these MMPs could be as a result of BMP-2, 4, and 6 as they were all more highly expressed in osteoblastic lesions. In fact, BMP-4, for instance, has been shown to stimulate breast cancer cell invasion by enhancing MMP2 and MMP9 activity (Cyr-Depauw, Northey et al. 2016). The decrease in MMP2, 7, 9, 12 and 14 following BMP antagonist overexpression as seen by our qPCR analyses indicates that this could indeed be the case, especially with the BMP-responsive ID1 confirming a decrease in BMP activity (see figure 6.4).

In order to assess the BMP/BMP antagonist feedback loop that could be in play during the phenotypic changes observed in Chapter 5, we treated the overexpression cell lines generated with BME. Since most of the functional assays were carried out for up to 3 days and BMP action

has been shown to be time-dependent, we opted to also carry out the treatment for 3 days. From these findings (figure 6.5), we were able to see that although BMP antagonist overexpression are extracellular regulators, their overexpression was also able to trigger a BMP downregulation at the mRNA level, except for Gremlin, which seemed to cause an overexpression of most of the tested BMP. However, treatment with BME caused varying responses in the different BMPs. For instance, it caused an increase in BMP-2 and a decrease in BMP-4 levels in all the stable cell lines. Meanwhile, BME treatment caused a mixed response in the expression of BMP-6, inducing an increase in expression in DU145<sup>NOG</sup> and DU145<sup>FST344</sup>, and a decrease in DU145<sup>GREM</sup>, and did not cause much change in BMP-7 expression, although it show a downregulation of this BMP in DU145<sup>FST344</sup>. Despite not being able properly measure statistical significance due to the low number of observations, the data gives us an idea of the BMP/BMP antagonist interplay in the bone. For instance, the results summarised in Chapter 5 have demonstrated that BME treatment instigated a decrease in growth in DU145<sup>FST344</sup> cells, the qPCR therefore indicate that this could be as a result of BMP-7 downregulation or BMP-6 upregulation. It is also possible that these changes were mediated by BMP-2 and BMP-4, however, one would expect that since the BME treatment caused the same response in the expression of these BMPs in all the cell lines, that they would also incite the same response phenotypically.

Building on this information, we then wondered which BMP/BMP antagonist feedback loop participates in the invasion of prostate cancer cell. As such, we assess the expression of the mesenchymal markers Snail and Slug in the BMP antagonist overexpression cell lines (figure 6.6). These results demonstrated that while BME treatment induced an increase in the expression of Snail in the control DU145<sup>PEF</sup>, it also induced a decrease in the levels of the mesenchymal marker in the overexpression cell lines. Although this was not confirmed by two-way ANOVA, it indicates that BMP antagonist overexpression, together with the influence of BME reduced the

mesenchymal phenotype of the DU145 cells. However, the Slug results indicated otherwise in the DU145<sup>NOG</sup> and DU145<sup>GREM</sup> cell lines. Further experimentation might be needed to confirm these findings, such as assessing N-cadherin and E-cadherin levels as well. Still, with DU145<sup>FST344</sup> exhibiting a decrease in both Snail and Slug, it indicates that this cell line has more of an epithelial phenotype. This is supported by the ECIS and migration data, which both demonstrated a decrease in the adhesive and migratory properties of this cell line following BME treatment.

Having gathered information on the differential expression of BMP and their antagonists in prostate cancer bone metastases in previous chapters, we aimed to evaluate how this translated in the downstream markers of invasive and migratory properties. This chapter summarises these findings, showing that the BMP/BMP antagonist feedback loop has a role in the expression of MMPs and that the bone environment may impact on this relationship, in some cases causing an increase in mesenchymal markers. Further experimentation is required to confirm and build on the current findings.

Chapter 7.

# Discussion

As members of the TGF- $\beta$  superfamily which are known not only for their strong osteoinductive capacities but also for their ability to coordinate cellular functions, such as proliferation, migration, adhesion and invasion, many have suggested a role for BMPs in the formation of the osteoblastic bone lesions typically seen in advanced-stage prostate cancer patients. Since the current understanding of BMP antagonists denotes them as being more than just BMP regulators but also as integral components of BMP function, we hypothesise that the feedback loop that exists between BMPs and their antagonists in normal physiology may also be key during prostate cancer progression and bone metastasis.

In an effort to elucidate BMPs and antagonists of potential importance in the osteoblastic lesion formation, we first aimed to investigate their differential expression in prostate cancer cell lines associated with the different bone lesion phenotypes by RT-PCR, qPCR and by analysing GEO data from a prostate cancer cell line expression study performed by Barretina et al (2012). We especially focussed our attention on the expression of BMP-2, 4, 6 and 7 since previous literature has demonstrated them to be of potential importance due to their aberrant expression in prostate carcinoma and bone metastasis samples (Bentley, Hamdy et al. 1992, Bobinac, Marić et al. 2005, Spanjol, Djordjević et al. 2010). From our laboratory findings we observed that BMP-4 and the antagonists Noggin and FST344 were most highly expressed in osteolytic cell lines, while BMP-2 and 7 and the antagonist Grem1 were mostly expressed in osteoblastic cell lines. Although there were some variations when we compared this data to the GEO data from Barretina et al, from this data we deduced that there may be a feedback loop between BMP-2 and BMP-7 and Gremlin. Furthermore, this feedback loop could be of importance during the formation of osteoblastic lesions, especially with Pereira et al (2000) having shown the interplay between BMP-2 and Gremlin on osteoblast function. Since the osteoblastic VCaP cells demonstrated a high expression of BMP-7, while PC-3 did not exhibit any expression of this antagonist, its importance in the osteoblastic bone lesions is further indicated.

The next step in our study was to put this theory to the test by assessing how the BMP/BMP antagonist interplay may participate in the development of bone metastases. Although Sir Stephen Paget's 'seed and soil' theory is still widely accepted, studies have since built upon this concept, demonstrating it is the dual interaction between cancer cells and the bone environment that enable the establishment of bone metastases. As such, we aimed to see how the bone environment would impact on the BMP/BMP antagonist feedback loop. To do so, we aimed simulate the bone environment *in vitro* by using the extract from femoral heads collected from patients who have undergone hip replacement surgeries. This extract, BME, was then used to treat osteolytic and osteoblastic cell lines, and the effect on BMP signalling was assessed by RNA-Seq and qPCR. These results demonstrated that the expression of BMP-2, 4 and 6 were all downregulated in the osteolytic PC-3 cell line, with BMP-7 remaining unexpressed. Meanwhile, BMP-4 was upregulated in the VCaP cells, while BMP-2, 4 and 7 were downregulated. The upregulation in BMP-4 could show a possible role in osteoblastic lesion formation, however the levels are so low in comparison to other BMPs, especially BMP-7, that it seems unlikely. Like with the BMPs, BME treatment caused a decrease in BMP antagonist expression. We also aimed to assess the BMP/BMP antagonist relationship in early osteoblastic establishment using GEO data from LNCaP-hOB co-culture assays performed by Sieh et al (2014). From this data, we deduced that BMP/BMP antagonist feedback loop was indeed in play between the LNCaP and the hOBs. This was evidenced by the increase in BMP antagonists FST, GREM1 and GREM2 in LNCaP, and the decrease in BMP-2 and 4 and increase of BMP-6 levels in hOBs during co-culture conditions. Since LNCaP cells are known to produce mixed lesions, it is difficult to discern which interplay would be especially key in osteoblastic bone formation. This is why the GEO data by Larson et al (2013) was useful due to its analysis of prostate cancer bone metastases, grouped into osteoblastic and osteolytic lesions. This data demonstrated that the expression of BMP-2, 4 and 6 as well as the antagonists GREM2 were more highly expressed in osteoblastic lesions, while BMP-7 and Noggin were more highly expressed in osteolytic lesions. This ties in with our previous suppositions about the possible involvement of BMP-2 and Gremlin in the

development of osteoblastic lesions. However, the high expression of BMP-7 in osteolytic lesions in comparison to osteoblastic ones goes against the main hypothesis of this study, as well as previous studies who have documented the expression of BMP-7 in prostate cancer bone metastases (Buijs, Rentsch et al. 2007, Morrissey, Brown et al. 2010, Spanjol, Djordjević et al. 2010). Although the phenotypes of the bone lesions processed in these studies were not specified, due to the small number of observations available in the study by Larson et al, we opted not to completely reject our main hypothesis.

Having gathered information on differential expression of BMPs and their antagonists, as well as their signalling components, we aimed to assess the expression EMT markers and MMPs in the LNCaP-hOB culture assays performed by Sieh et al (GSE44143) and the prostate cancer bone metastasis samples analysed by Larson et al (GSE41619). Analysis of these findings suggested that while under the influence of the LNCaP cells, the hOBs seemed to undergo EMT. With our findings having already shown co-culture conditions induced significant changes in BMP expression in hOBs, the EMT changes observed could be as a result of these changes. The differential expression of BMPs and their antagonists in the prostate cancer samples demonstrated that mesenchymal markers were more highly expressed in osteoblastic lesions in comparison to the osteolytic lesions. This too could be due to the higher expression of BMP-2, 4 and 6, although more observations, as well as further experimentation are required to investigate this.

To further investigate the role of BMP/BMP antagonist feedback loop in prostate cancer and its establishment in the bone, we overexpressed BMP antagonists, Noggin, FST344 and Gremlin in the prostate cancer cell line DU145 and subjected the resultant cell lines to different functional assays. This data demonstrated that in general, Noggin overexpression had caused a decrease in cell proliferation, Matrigel and ECIS adhesion, and migration. While BME treatment of the

DU145<sup>NOG</sup> cell line caused further inhibition of most of the tested cellular properties, it also caused an increase in adhesion as shown by the *in vitro* Matrigel assay. When we assessed the downstream target genes by qPCR, we observed the functional data was supported by the downregulation of MMP2, 7, 9, 12 and 14 and the downregulation of mesenchymal marker Snail upon treatment with BME. BME treatment also induced the expression of BMP-2 and 6 in this cell line as well, it is possible that the interplay between these BMPs and Noggin are the cause for this increase in adhesion.

Similar to these results, FST overexpression also caused a decrease in cell proliferation, invasion, ECIS adhesion and migration. However, it also caused an increase in Matrigel adhesion, although this was not statistically significant. BME treatment further inhibited most of these cellular properties, except for invasion and long-term adhesion shown by ECIS. As with DU145<sup>NOG</sup> cells, the inhibition of cellular properties seen in the absence of BME seems to be due to the inhibition of BMP action, as shown by the decrease in the BMP-responsive ID1, and the decrease in invasion was as a result of MMP downregulation. The increase in invasion observed in BME seemed to agree with Slug upregulation in the same treatment conditions, although the other mesenchymal marker tested, Snail, was downregulated. It is possible that both Noggin and FST344 have a protective effect on prostate cancer and bone metastasis. The current observations regarding Noggin are supported by Feeley and colleagues who demonstrated that this antagonist inhibited the development of BMP-mediated osteolytic and osteoblastic prostate cancer lesions (Feeley, Gamradt et al. 2005, Feeley, Krenek et al. 2006). As for FST, studies have described this antagonist as a potential therapeutic target and bone metastasis marker in prostate cancer (Sardana, Jung et al. 2008, Tumminello, Badalamenti et al. 2010, Sepporta, Tumminello et al. 2013), which disagrees with the current findings.

Unlike the other antagonists, Gremlin overexpression showed a stimulation in cell proliferation, adhesion and migration, as well as an inhibition of cell invasion. Furthermore, BME treatment of the DU145<sup>GREM</sup> cell line did not seem to affect cellular function as much as it did for the other cell lines. However, it did appear to cause a decrease in Matrigel adhesion and an increase in ECIS adhesion and migration. The increase in adhesion and migration observed seem to be contradictory. Indeed, the cellular properties needed for adhesion, such as strong cell-cell and cell-matrix contacts, are precisely the ones that cells need to lose in order to migrate. Although this could be explained by different responses shown by the mesenchymal markers to treatment with BME, as with the downstream results obtained for the other cell lines, more observations are needed for confirmation. While overexpression of Gremlin also appeared to inhibit BMP action as seen by the downregulation of ID1, it did not appear to cause a downregulation of all the BMPs tested as the other antagonists did, causing a downregulation of BMP-2 only. This finding would agree with a previous study by Church et al (2015) who described the preferential binding of GREM1 to BMP-2 over BMP-4 and 7. This may bring further evidence to the BMP-2-Gremlin interplay previously described.

### **Future work**

Although the main hypothesis of this study was investigating the role of the BMP-7/BMP antagonist feedback loop in particular and understanding its role in prostate cancer and bone metastasis, we still gathered some promising information a possible BMP-2/Gremlin interplay and the potential protective capacity of Noggin and FST344 in prostate cancer metastasis. Since our study is also primarily focused on osteoblastic lesion formation, the use of the osteolytic DU145 cell line for BMP overexpression and subsequent functional assays was not ideal. However, various attempts at transfecting both the LNCaP and VCaP cell lines using the pEF6/V5-HIS-TOPO<sup>®</sup> TA vector were unsuccessful. Hence, further work might require the use of

osteoblastic cell lines for better representation, the genetic modulation of which could be achieved either through use the use of other methods of transfection, such as lentiviral transfection, or exogenous treatment using recombinant proteins. Furthermore, due to the multiple processes that occur beyond transcription to contribute to the establishment of expression levels of a protein, our current work needs verification at protein levels by Western blot. Indeed, assessing the phosphorylation of downstream Smads would be more conclusive in assessing if the Smad signalling pathway is being triggered. In parallel, examining downstream components of the Smad-independent pathway, such as p38, would also be of interest to help map the signalling of interplay between BMPs and their antagonists.

To further investigate the BMP/BMP antagonist relationship in prostate cancer, future experimentation could involve treatment of the overexpression cell with recombinant BMPs. The results obtained from the recombinant BMP experiments could also be compared with those obtained from BME treatment. A more detailed analysis of BMP/BMP antagonist interplay could be achieved by co-immunoprecipitation (co-IP). By taking samples from the culture medium of the transfected and treated cells and studying them by co-IP, we could ascertain how the BMP/BMP antagonist feedback loop is being affected from genetic modulation and BME treatment. While the functional assays used in this study are acceptable for a preliminary examination of the cellular properties of the overexpression cell lines, more three-dimensional assays could also be used for a better representation of *in vivo* conditions. An example would be a spheroid assay using Matrigel to assess cell invasion as described by Berens et al (2015). Finally, to get a clearer role for the BMP/BMP antagonist interplay in prostate cancer progression and bone metastasis, *in vivo* models would eventually need to be used, potentially through the injection of stable cell lines into immunodeficient mice.

## Bibliography

- Abe, Y., T. Abe, Y. Aida, Y. Hara and K. Maeda (2004). "Follistatin restricts bone morphogenetic protein (BMP)-2 action on the differentiation of osteoblasts in fetal rat mandibular cells." J Bone Miner Res **19**(8): 1302-1307.
- Adjei, A. A. (2001). "Blocking oncogenic Ras signaling for cancer therapy." J Natl Cancer Inst **93**(14): 1062-1074.
- Al-Mehdi, A. B., K. Tozawa, A. B. Fisher, L. Shientag, A. Lee and R. J. Muschel (2000). "Intravascular origin of metastasis from the proliferation of endothelium-attached tumor cells: a new model for metastasis." Nat Med **6**(1): 100-102.
- Alarmo, E. L., J. Pärssinen, J. M. Ketolainen, K. Savinainen, R. Karhu and A. Kallioniemi (2009). "BMP7 influences proliferation, migration, and invasion of breast cancer cells." Cancer Lett **275**(1): 35-43.
- Albini, A., Y. Iwamoto, H. K. Kleinman, G. R. Martin, S. A. Aaronson, J. M. Kozlowski and R. N. McEwan (1987). "A rapid in vitro assay for quantitating the invasive potential of tumor cells." Cancer Res **47**(12): 3239-3245.
- Attisano, L. and S. T. Lee-Hoeflich (2001). "The Smads." Genome Biol **2**(8): Reviews3010.
- Autzen, P., C. N. Robson, A. Bjartell, A. J. Malcolm, M. I. Johnson, D. E. Neal and F. C. Hamdy (1998). "Bone morphogenetic protein 6 in skeletal metastases from prostate cancer and other common human malignancies." Br J Cancer **78**(9): 1219-1223.
- Batlle, E., E. Sancho, C. Francí, D. Domínguez, M. Monfar, J. Baulida and A. García De Herreros (2000). "The transcription factor snail is a repressor of E-cadherin gene expression in epithelial tumour cells." Nat Cell Biol **2**(2): 84-89.
- Bendas, G. and L. Borsig (2012). "Cancer cell adhesion and metastasis: selectins, integrins, and the inhibitory potential of heparins." Int J Cell Biol **2012**: 676731.
- Bentley, H., F. C. Hamdy, K. A. Hart, J. M. Seid, J. L. Williams, D. Johnstone and R. G. Russell (1992). "Expression of bone morphogenetic proteins in human prostatic adenocarcinoma and benign prostatic hyperplasia." Br J Cancer **66**(6): 1159-1163.
- Birchmeier, W. and J. Behrens (1994). "Cadherin expression in carcinomas: role in the formation of cell junctions and the prevention of invasiveness." Biochimica et Biophysica Acta (BBA) - Reviews on Cancer **1198**(1): 11-26.
- Bobinac, D., I. Marić, S. Zorčić, J. Spanjol, G. Dordević, E. Mustačić and Z. Fuckar (2005). "Expression of bone morphogenetic proteins in human metastatic prostate and breast cancer." Croat Med J **46**(3): 389-396.
- Bonfil, R. D., Z. Dong, J. C. Trindade Filho, A. Sabbota, P. Osenkowski, S. Nabha, H. Yamamoto, S. R. Chinni, H. Zhao, S. Mobashery, R. L. Vessella, R. Fridman and M. L. Cher (2007). "Prostate cancer-associated membrane type 1-matrix metalloproteinase: a pivotal role in bone response and intraosseous tumor growth." Am J Pathol **170**(6): 2100-2111.
- Bragdon, B., O. Moseychuk, S. Saldanha, D. King, J. Julian and A. Nohe (2011). "Bone morphogenetic proteins: a critical review." Cell Signal **23**(4): 609-620.
- Brown, M. A., Q. Zhao, K. A. Baker, C. Naik, C. Chen, L. Pukac, M. Singh, T. Tsareva, Y. Parice, A. Mahoney, V. Roschke, I. Sanyal and S. Choe (2005). "Crystal structure of BMP-9 and functional interactions with pro-region and receptors." J Biol Chem **280**(26): 25111-25118.
- Brubaker, K. D., E. Corey, L. G. Brown and R. L. Vessella (2004). "Bone morphogenetic protein signaling in prostate cancer cell lines." J Cell Biochem **91**(1): 151-160.
- Bubendorf, L., A. Schöpfer, U. Wagner, G. Sauter, H. Moch, N. Willi, T. C. Gasser and M. J. Mihatsch (2000). "Metastatic patterns of prostate cancer: an autopsy study of 1,589 patients." Hum Pathol **31**(5): 578-583.
- Buijs, J. T., C. A. Rentsch, G. van der Horst, P. G. van Overveld, A. Wetterwald, R. Schwaninger, N. V. Henriquez, P. Ten Dijke, F. Borovecki, R. Markwalder, G. N. Thalmann, S. E. Papapoulos, R. C. Pelger, S. Vukicevic, M. G. Cecchini, C. W. Löwik and G. van der Pluijm (2007). "BMP7, a

putative regulator of epithelial homeostasis in the human prostate, is a potent inhibitor of prostate cancer bone metastasis in vivo." *Am J Pathol* **171**(3): 1047-1057.

Butler, S. J. and J. Dodd (2003). "A role for BMP heterodimers in roof plate-mediated repulsion of commissural axons." *Neuron* **38**(3): 389-401.

Cecchini, M. G., A. Wetterwald, G. v. d. Pluijm and G. N. Thalmann (2005). "Molecular and Biological Mechanisms of Bone Metastasis." *EAU Update Series* **3**(4): 214-226.

Chambers, A. F., A. C. Groom and I. C. MacDonald (2002). "Dissemination and growth of cancer cells in metastatic sites." *Nat Rev Cancer* **2**(8): 563-572.

Cheng, H., W. Jiang, F. M. Phillips, R. C. Haydon, Y. Peng, L. Zhou, H. H. Luu, N. An, B. Breyer, P. Vanichakarn, J. P. Szatkowski, J. Y. Park and T. C. He (2003). "Osteogenic activity of the fourteen types of human bone morphogenetic proteins (BMPs)." *J Bone Joint Surg Am* **85-A**(8): 1544-1552.

Chinni, S. R., S. Sivalogan, Z. Dong, J. C. Filho, X. Deng, R. D. Bonfil and M. L. Cher (2006). "CXCL12/CXCR4 signaling activates Akt-1 and MMP-9 expression in prostate cancer cells: the role of bone microenvironment-associated CXCL12." *Prostate* **66**(1): 32-48.

Clarke, B. (2008). "Normal bone anatomy and physiology." *Clin J Am Soc Nephrol* **3** Suppl 3: S131-139.

Abe, Y., T. Abe, Y. Aida, Y. Hara and K. Maeda (2004). "Follistatin restricts bone morphogenetic protein (BMP)-2 action on the differentiation of osteoblasts in fetal rat mandibular cells." *J Bone Miner Res* **19**(8): 1302-1307.

Abula, K., T. Muneta, K. Miyatake, J. Yamada, Y. Matsukura, M. Inoue, I. Sekiya, D. Graf, A. N. Economides, V. Rosen and K. Tsuji (2015). "Elimination of BMP7 from the developing limb mesenchyme leads to articular cartilage degeneration and synovial inflammation with increased age." *FEBS Lett* **589**(11): 1240-1248.

Adamczyk, P., Z. Wolski, R. Butkiewicz, J. Nussbeutel and T. Drewa (2014). "Significance of atypical small acinar proliferation and extensive high-grade prostatic intraepithelial neoplasm in clinical practice." *Cent European J Urol* **67**(2): 136-141.

Adjei, A. A. (2001). "Blocking oncogenic Ras signaling for cancer therapy." *J Natl Cancer Inst* **93**(14): 1062-1074.

AJCC (1997). *AJCC Cancer Staging Manual*.

Al-Dujaili, S. A., E. Lau, H. Al-Dujaili, K. Tsang, A. Guenther and L. You (2011). "Apoptotic osteocytes regulate osteoclast precursor recruitment and differentiation in vitro." *J Cell Biochem* **112**(9): 2412-2423.

Al-Mehdi, A. B., K. Tozawa, A. B. Fisher, L. Shientag, A. Lee and R. J. Muschel (2000). "Intravascular origin of metastasis from the proliferation of endothelium-attached tumor cells: a new model for metastasis." *Nat Med* **6**(1): 100-102.

Alarmo, E. L., J. Pärssinen, J. M. Ketolainen, K. Savinainen, R. Karhu and A. Kallioniemi (2009). "BMP7 influences proliferation, migration, and invasion of breast cancer cells." *Cancer Lett* **275**(1): 35-43.

Albini, A., Y. Iwamoto, H. K. Kleinman, G. R. Martin, S. A. Aaronson, J. M. Kozlowski and R. N. McEwan (1987). "A rapid in vitro assay for quantitating the invasive potential of tumor cells." *Cancer Res* **47**(12): 3239-3245.

Alborzina, H., H. Schmidt-Glenewinkel, I. Ilkavets, K. Breitkopf-Heinlein, X. Cheng, P. Hortschansky, S. Dooley and S. Wolfl (2013). "Quantitative kinetics analysis of BMP2 uptake into cells and its modulation by BMP antagonists." *J Cell Sci* **126**(Pt 1): 117-127.

Ali, I. H. A. and D. P. Brazil (2014). "Bone morphogenetic proteins and their antagonists: current and emerging clinical uses." *British journal of pharmacology* **171**(15): 3620-3632.

AlShaibi, H. F., F. Ahmed, C. Buckle, A. C. M. Fowles, J. Awlia, M. G. Cecchini and C. L. Eaton (2018). "The BMP antagonist Noggin is produced by osteoblasts in response to the presence of prostate cancer cells." *Biotechnol Appl Biochem* **65**(3): 407-418.

Andrews, G. S. (1949). "Latent Carcinoma of the Prostate." *Journal of Clinical Pathology* **2**(3): 197-208.

Attisano, L. and S. T. Lee-Hoeflich (2001). "The Smads." *Genome Biol* **2**(8): Reviews3010.

Autzen, P., C. N. Robson, A. Bjartell, A. J. Malcolm, M. I. Johnson, D. E. Neal and F. C. Hamdy (1998). "Bone morphogenetic protein 6 in skeletal metastases from prostate cancer and other common human malignancies." *Br J Cancer* **78**(9): 1219-1223.

Avsian-Kretchmer, O. and A. J. Hsueh (2004). "Comparative genomic analysis of the eight-membered ring cystine knot-containing bone morphogenetic protein antagonists." *Mol Endocrinol* **18**(1): 1-12.

Bach, D. H., H. J. Park and S. K. Lee (2018). "The Dual Role of Bone Morphogenetic Proteins in Cancer." *Mol Ther Oncolytics* **8**: 1-13.

Barretina, J., G. Caponigro, N. Stransky, K. Venkatesan, A. A. Margolin, S. Kim, C. J. Wilson, J. Lehár, G. V. Kryukov, D. Sonkin, A. Reddy, M. Liu, L. Murray, M. F. Berger, J. E. Monahan, P. Morais, J. Meltzer, A. Korejwa, J. Jané-Valbuena, F. A. Mapa, J. Thibault, E. Bric-Furlong, P. Raman, A. Shipway, I. H. Engels, J. Cheng, G. K. Yu, J. Yu, P. Aspesi, Jr., M. de Silva, K. Jagtap, M. D. Jones, L. Wang, C. Hatton, E. Palesscandolo, S. Gupta, S. Mahan, C. Sougnez, R. C. Onofrio, T. Liefeld, L. MacConaill, W. Winckler, M. Reich, N. Li, J. P. Mesirov, S. B. Gabriel, G. Getz, K. Ardlie, V. Chan, V. E. Myer, B. L. Weber, J. Porter, M. Warmuth, P. Finan, J. L. Harris, M. Meyerson, T. R. Golub, M. P. Morrissey, W. R. Sellers, R. Schlegel and L. A. Garraway (2012). "The Cancer Cell Line Encyclopedia enables predictive modelling of anticancer drug sensitivity." *Nature* **483**(7391): 603-607.

Batlle, E., E. Sancho, C. Francí, D. Domínguez, M. Monfar, J. Baulida and A. García De Herreros (2000). "The transcription factor snail is a repressor of E-cadherin gene expression in epithelial tumour cells." *Nat Cell Biol* **2**(2): 84-89.

Bendas, G. and L. Borsig (2012). "Cancer cell adhesion and metastasis: selectins, integrins, and the inhibitory potential of heparins." *Int J Cell Biol* **2012**: 676731.

Bentley, H., F. C. Hamdy, K. A. Hart, J. M. Seid, J. L. Williams, D. Johnstone and R. G. Russell (1992). "Expression of bone morphogenetic proteins in human prostatic adenocarcinoma and benign prostatic hyperplasia." *Br J Cancer* **66**(6): 1159-1163.

Berens, E. B., J. M. Holy, A. T. Riegel and A. Wellstein (2015). "A Cancer Cell Spheroid Assay to Assess Invasion in a 3D Setting." *J Vis Exp*(105).

Birchmeier, W. and J. Behrens (1994). "Cadherin expression in carcinomas: role in the formation of cell junctions and the prevention of invasiveness." *Biochimica et Biophysica Acta (BBA) - Reviews on Cancer* **1198**(1): 11-26.

Bobinac, D., I. Marić, S. Zorčić, J. Spanjol, G. Dordević, E. Mustać and Z. Fuckar (2005). "Expression of bone morphogenetic proteins in human metastatic prostate and breast cancer." *Croat Med J* **46**(3): 389-396.

Bokobza, S. M., L. Ye and W. G. Jiang (2009). "When BMP Signalling Goes Wrong: The Intracellular and Molecular Mechanisms of BMP Signalling in Cancer." *Current Signal Transduction Therapy* **4**(3).

Bonfil, R. D., Z. Dong, J. C. Trindade Filho, A. Sabbota, P. Osenkowski, S. Nabha, H. Yamamoto, S. R. Chinni, H. Zhao, S. Mobashery, R. L. Vessella, R. Fridman and M. L. Cher (2007). "Prostate cancer-associated membrane type 1-matrix metalloproteinase: a pivotal role in bone response and intraosseous tumor growth." *Am J Pathol* **170**(6): 2100-2111.

Bonnekoh, B., A. Wevers, F. Jugert, H. Merk and G. Mahrle (1989). "Colorimetric growth assay for epidermal cell cultures by their crystal violet binding capacity." *Arch Dermatol Res* **281**(7): 487-490.

Borboroglu, P. G., S. W. Comer, R. H. Riffenburgh and C. L. Amling (2000). "Extensive repeat transrectal ultrasound guided prostate biopsy in patients with previous benign sextant biopsies." *J Urol* **163**(1): 158-162.

Bostwick, D. G., L. Liu, M. K. Brawer and J. Qian (2004). "High-Grade Prostatic Intraepithelial Neoplasia." *Reviews in Urology* **6**(4): 171-179.

Bostwick, D. G. and J. Qian (2004). "High-grade prostatic intraepithelial neoplasia." *Mod Pathol* **17**(3): 360-379.

Boyle, W. J., W. S. Simonet and D. L. Lacey (2003). "Osteoclast differentiation and activation." *Nature* **423**(6937): 337-342.

Bragdon, B., O. Moseychuk, S. Saldanha, D. King, J. Julian and A. Nohe (2011). "Bone morphogenetic proteins: a critical review." Cell Signal **23**(4): 609-620.

Bratt, O. (2002). "Hereditary prostate cancer: clinical aspects." J Urol **168**(3): 906-913.

Brawer, M. K. (2005). "Prostatic intraepithelial neoplasia: an overview." Rev Urol **7 Suppl 3**: S11-18.

Bray, F., J. Ferlay, I. Soerjomataram, R. L. Siegel, L. A. Torre and A. Jemal (2018). "Global cancer statistics 2018: GLOBOCAN estimates of incidence and mortality worldwide for 36 cancers in 185 countries." CA: A Cancer Journal for Clinicians **0**(0).

Brown, M. A., Q. Zhao, K. A. Baker, C. Naik, C. Chen, L. Pukac, M. Singh, T. Tsareva, Y. Parice, A. Mahoney, V. Roschke, I. Sanyal and S. Choe (2005). "Crystal structure of BMP-9 and functional interactions with pro-region and receptors." J Biol Chem **280**(26): 25111-25118.

Bubendorf, L., A. Schöpfer, U. Wagner, G. Sauter, H. Moch, N. Willi, T. C. Gasser and M. J. Mihatsch (2000). "Metastatic patterns of prostate cancer: an autopsy study of 1,589 patients." Hum Pathol **31**(5): 578-583.

Buijs, J. T., C. A. Rentsch, G. van der Horst, P. G. van Overveld, A. Wetterwald, R. Schwaninger, N. V. Henriquez, P. Ten Dijke, F. Borovecki, R. Markwalder, G. N. Thalmann, S. E. Papapoulos, R. C. Pelger, S. Vukicevic, M. G. Cecchini, C. W. Löwik and G. van der Pluijm (2007). "BMP7, a putative regulator of epithelial homeostasis in the human prostate, is a potent inhibitor of prostate cancer bone metastasis in vivo." Am J Pathol **171**(3): 1047-1057.

Butler, S. J. and J. Dodd (2003). "A role for BMP heterodimers in roof plate-mediated repulsion of commissural axons." Neuron **38**(3): 389-401.

Carter, B. S., T. H. Beaty, G. D. Steinberg, B. Childs and P. C. Walsh (1992). "Mendelian inheritance of familial prostate cancer." Proceedings of the National Academy of Sciences of the United States of America **89**(8): 3367-3371.

Cecchini, M. G., A. Wetterwald, G. v. d. Pluijm and G. N. Thalmann (2005). "Molecular and Biological Mechanisms of Bone Metastasis." EAU Update Series **3**(4): 214-226.

Chacko, B. M., B. Qin, J. J. Correia, S. S. Lam, M. P. de Caestecker and K. Lin (2001). "The L3 loop and C-terminal phosphorylation jointly define Smad protein trimerization." Nat Struct Biol **8**(3): 248-253.

Chambers, A. F., A. C. Groom and I. C. MacDonald (2002). "Dissemination and growth of cancer cells in metastatic sites." Nat Rev Cancer **2**(8): 563-572.

Chan, J. M., M. J. Stampfer, J. Ma, P. H. Gann, J. M. Gaziano and E. L. Giovannucci (2001). "Dairy products, calcium, and prostate cancer risk in the Physicians' Health Study." Am J Clin Nutr **74**(4): 549-554.

Cheng, H., W. Jiang, F. M. Phillips, R. C. Haydon, Y. Peng, L. Zhou, H. H. Luu, N. An, B. Breyer, P. Vanichakarn, J. P. Szatkowski, J. Y. Park and T. C. He (2003). "Osteogenic activity of the fourteen types of human bone morphogenetic proteins (BMPs)." J Bone Joint Surg Am **85-A**(8): 1544-1552.

Cheng, L., R. Montironi, D. G. Bostwick, A. Lopez-Beltran and D. M. Berney (2012). "Staging of prostate cancer." Histopathology **60**(1): 87-117.

Chinni, S. R., S. Sivalogan, Z. Dong, J. C. Filho, X. Deng, R. D. Bonfil and M. L. Cher (2006). "CXCL12/CXCR4 signaling activates Akt-1 and MMP-9 expression in prostate cancer cells: the role of bone microenvironment-associated CXCL12." Prostate **66**(1): 32-48.

Choi, M., R. W. Stottmann, Y. P. Yang, E. N. Meyers and J. Klingensmith (2007). "The bone morphogenetic protein antagonist noggin regulates mammalian cardiac morphogenesis." Circ Res **100**(2): 220-228.

Church, R. H., A. Krishnakumar, A. Urbanek, S. Geschwindner, J. Meneely, A. Bianchi, B. Basta, S. Monaghan, C. Elliot, M. Strömstedt, N. Ferguson, F. Martin and D. P. Brazil (2015). "Gremlin1 preferentially binds to bone morphogenetic protein-2 (BMP-2) and BMP-4 over BMP-7." Biochem J **466**(1): 55-68.

Clarke, B. (2008). "Normal bone anatomy and physiology." Clin J Am Soc Nephrol **3 Suppl 3**: S131-139.

Coleman, R. E. (1997). "Skeletal complications of malignancy." Cancer **80**(8 Suppl): 1588-1594.

Coleman, R. E. (2006). "Clinical features of metastatic bone disease and risk of skeletal morbidity." *Clin Cancer Res* **12**(20 Pt 2): 6243s-6249s.

Coman, D. R. (1944). "Decreased Mutual Adhesiveness, a Property of Cells from Squamous Cell Carcinomas." *Cancer Research* **4**(10): 625-629.

Cook, C., C. M. Vezina, S. M. Hicks, A. Shaw, M. Yu, R. E. Peterson and W. Bushman (2007). "NOGGIN IS REQUIRED FOR NORMAL LOBE PATTERNING AND DUCTAL BUDDING IN THE MOUSE PROSTATE." *Developmental biology* **312**(1): 217-230.

CRUK. (2014). "Cancer Incidence by Major Ethnic Group." Retrieved 03rd June 2018.

Cyr-Depauw, C., J. J. Northey, S. Tabariès, M. G. Annis, Z. Dong, S. Cory, M. Hallett, J. P. Rennhack, E. R. Andrechek and P. M. Siegel (2016). "Chordin-Like 1 Suppresses Bone Morphogenetic Protein 4-Induced Breast Cancer Cell Migration and Invasion." *Mol Cell Biol* **36**(10): 1509-1525.

Dagnelie, P. C., A. G. Schuurman, R. A. Goldbohm and P. A. Van den Brandt (2004). "Diet, anthropometric measures and prostate cancer risk: a review of prospective cohort and intervention studies." *BJU Int* **93**(8): 1139-1150.

Dai, J., J. Keller, J. Zhang, Y. Lu, Z. Yao and E. T. Keller (2005). "Bone morphogenetic protein-6 promotes osteoblastic prostate cancer bone metastases through a dual mechanism." *Cancer Res* **65**(18): 8274-8285.

Dai, J., Y. Kitagawa, J. Zhang, Z. Yao, A. Mizokami, S. Cheng, J. Nör, L. K. McCauley, R. S. Taichman and E. T. Keller (2004). "Vascular endothelial growth factor contributes to the prostate cancer-induced osteoblast differentiation mediated by bone morphogenetic protein." *Cancer Res* **64**(3): 994-999.

Darby, S., S. S. Cross, N. J. Brown, F. C. Hamdy and C. N. Robson (2008). "BMP-6 over-expression in prostate cancer is associated with increased Id-1 protein and a more invasive phenotype." *J Pathol* **214**(3): 394-404.

David, J. M. and A. K. Rajasekaran (2012). "Dishonorable discharge: the oncogenic roles of cleaved E-cadherin fragments." *Cancer Res* **72**(12): 2917-2923.

de Caestecker, M. (2004). "The transforming growth factor- $\beta$  superfamily of receptors." *Cytokine & Growth Factor Reviews* **15**(1): 1-11.

De Craene, B. and G. Berx (2013). "Regulatory networks defining EMT during cancer initiation and progression." *Nat Rev Cancer* **13**(2): 97-110.

De Wever, O., L. Derycke, A. Hendrix, G. De Meerleer, F. Godeau, H. Depypere and M. Bracke (2007). "Soluble cadherins as cancer biomarkers." *Clin Exp Metastasis* **24**(8): 685-697.

Derynck, R. and Y. E. Zhang (2003). "Smad-dependent and Smad-independent pathways in TGF-beta family signalling." *Nature* **425**(6958): 577-584.

Draffin, J. E., S. McFarlane, A. Hill, P. G. Johnston and D. J. Waugh (2004). "CD44 potentiates the adherence of metastatic prostate and breast cancer cells to bone marrow endothelial cells." *Cancer Res* **64**(16): 5702-5711.

Ducy, P. and G. Karsenty (2000). "The family of bone morphogenetic proteins." *Kidney Int* **57**(6): 2207-2214.

Dunn, J. F., B. C. Nisula and D. Rodbard (1981). "Transport of steroid hormones: binding of 21 endogenous steroids to both testosterone-binding globulin and corticosteroid-binding globulin in human plasma." *J Clin Endocrinol Metab* **53**(1): 58-68.

Ebisawa, T., K. Tada, I. Kitajima, K. Tojo, T. K. Sampath, M. Kawabata, K. Miyazono and T. Imamura (1999). "Characterization of bone morphogenetic protein-6 signaling pathways in osteoblast differentiation." *J Cell Sci* **112** ( Pt 20): 3519-3527.

Egeblad, M. and Z. Werb (2002). "New functions for the matrix metalloproteinases in cancer progression." *Nat Rev Cancer* **2**(3): 161-174.

Fainsod, A., K. Deissler, R. Yelin, K. Marom, M. Epstein, G. Pillemer, H. Steinbeisser and M. Blum (1997). "The dorsalizing and neural inducing gene follistatin is an antagonist of BMP-4." *Mech Dev* **63**(1): 39-50.

Feeley, B. T., S. C. Gamradt, W. K. Hsu, N. Liu, L. Krenek, P. Robbins, J. Huard and J. R. Lieberman (2005). "Influence of BMPs on the formation of osteoblastic lesions in metastatic prostate cancer." J Bone Miner Res **20**(12): 2189-2199.

Feeley, B. T., L. Krenek, N. Liu, W. K. Hsu, S. C. Gamradt, E. M. Schwarz, J. Huard and J. R. Lieberman (2006). "Overexpression of noggin inhibits BMP-mediated growth of osteolytic prostate cancer lesions." Bone **38**(2): 154-166.

Feldman, B. J. and D. Feldman (2001). "The development of androgen-independent prostate cancer." Nat Rev Cancer **1**(1): 34-45.

Ferrara, N. and T. Davis-Smyth (1997). "The biology of vascular endothelial growth factor." Endocr Rev **18**(1): 4-25.

Fidler, I. J. (1970). "Metastasis: quantitative analysis of distribution and fate of tumor emboli labeled with 125 I-5-iodo-2'-deoxyuridine." J Natl Cancer Inst **45**(4): 773-782.

Fidler, I. J. (2005). "Cancer biology is the foundation for therapy." Cancer Biol Ther **4**(9): 1036-1039.

Gao, H., G. Chakraborty, A. P. Lee-Lim, Q. Mo, M. Decker, A. Vonica, R. Shen, E. Brogi, A. H. Brivanlou and F. G. Giancotti (2012). "The BMP inhibitor Coco reactivates breast cancer cells at lung metastatic sites." Cell **150**(4): 764-779.

Gassmann, P., J. Haier, K. Schlüter, B. Domikowsky, C. Wendel, U. Wiesner, R. Kubitz, R. Engers, S. W. Schneider, B. Homey and A. Müller (2009). "CXCR4 regulates the early extravasation of metastatic tumor cells in vivo." Neoplasia **11**(7): 651-661.

Gazzerro, E. and E. Canalis (2006). "Bone morphogenetic proteins and their antagonists." Rev Endocr Metab Disord **7**(1-2): 51-65.

Gazzerro, E., V. Gangji and E. Canalis (1998). "Bone morphogenetic proteins induce the expression of noggin, which limits their activity in cultured rat osteoblasts." J Clin Invest **102**(12): 2106-2114.

Geraghty, S., J. Q. Kuang, D. Yoo, M. LeRoux-Williams, C. T. Vangsness and A. Danilkovitch (2015). "A novel, cryopreserved, viable osteochondral allograft designed to augment marrow stimulation for articular cartilage repair." J Orthop Surg Res **10**: 66.

Gialeli, C., A. D. Theocharis and N. K. Karamanos (2011). "Roles of matrix metalloproteinases in cancer progression and their pharmacological targeting." Febs j **278**(1): 16-27.

Gleason, D. F. (1992). "Histologic grading of prostate cancer: a perspective." Hum Pathol **23**(3): 273-279.

Gleason, D. F. and G. T. Mellinger (1974). "Prediction of prognosis for prostatic adenocarcinoma by combined histological grading and clinical staging." J Urol **111**(1): 58-64.

Golimbu, M., P. Morales, S. Al-Askari and J. Brown (1979). "Extended Pelvic Lymphadenectomy for Prostatic Cancer." J Urol **121**(5): 617-620.

Govender, S., C. Csima, H. K. Genant, A. Valentin-Opran, Y. Amit, R. Arbel, H. Aro, D. Atar, M. Bishay, M. G. Börner, P. Chiron, P. Choong, J. Cinats, B. Courtenay, R. Feibel, B. Geulette, C. Gravel, N. Haas, M. Raschke, E. Hammacher, D. van der Velde, P. Hardy, M. Holt, C. Josten, R. L. Ketterl, B. Lindeque, G. Lob, H. Mathevon, G. McCoy, D. Marsh, R. Miller, E. Munting, S. Oevre, L. Nordsletten, A. Patel, A. Pohl, W. Rennie, P. Reynders, P. M. Rommens, J. Rondia, W. C. Rossouw, P. J. Daneel, S. Ruff, A. Rüter, S. Santavirta, T. A. Schildhauer, C. Gekle, R. Schnettler, D. Segal, H. Seiler, R. B. Snowdowne, J. Stapert, G. Taglang, R. Verdonk, L. Vogels, A. Weckbach, A. Wentzensen, T. Wisniewski and B.-E. i. S. f. T. B. S. Group (2002). "Recombinant human bone morphogenetic protein-2 for treatment of open tibial fractures: a prospective, controlled, randomized study of four hundred and fifty patients." J Bone Joint Surg Am **84-A**(12): 2123-2134.

Gravdal, K., O. J. Halvorsen, S. A. Haukaas and L. A. Akslen (2007). "A switch from E-cadherin to N-cadherin expression indicates epithelial to mesenchymal transition and is of strong and independent importance for the progress of prostate cancer." Clin Cancer Res **13**(23): 7003-7011.

Greene, F. L. and L. H. Sobin (2002). "The TNM system: our language for cancer care." J Surg Oncol **80**(3): 119-120.

Greenwald, J., J. Groppe, P. Gray, E. Wiater, W. Kwiatkowski, W. Vale and S. Choe (2003). "The BMP7/ActRII extracellular domain complex provides new insights into the cooperative nature of receptor assembly." *Mol Cell* **11**(3): 605-617.

Griffith, D. L., P. C. Keck, T. K. Sampath, D. C. Rueger and W. D. Carlson (1996). "Three-dimensional structure of recombinant human osteogenic protein 1: structural paradigm for the transforming growth factor beta superfamily." *Proc Natl Acad Sci U S A* **93**(2): 878-883.

Grigoriadis, A. E., J. N. Heersche and J. E. Aubin (1988). "Differentiation of muscle, fat, cartilage, and bone from progenitor cells present in a bone-derived clonal cell population: effect of dexamethasone." *J Cell Biol* **106**(6): 2139-2151.

Groppe, J., J. Greenwald, E. Wiater, J. Rodriguez-Leon, A. N. Economides, W. Kwiatkowski, M. Affolter, W. W. Vale, J. C. Izpisua Belmonte and S. Choe (2002). "Structural basis of BMP signalling inhibition by the cystine knot protein Noggin." *Nature* **420**(6916): 636-642.

Hamdy, F. C., P. Autzen, M. C. Robinson, C. H. Horne, D. E. Neal and C. N. Robson (1997). "Immunolocalization and messenger RNA expression of bone morphogenetic protein-6 in human benign and malignant prostatic tissue." *Cancer Res* **57**(19): 4427-4431.

Hanahan, D. and R. A. Weinberg (2011). "Hallmarks of cancer: the next generation." *Cell* **144**(5): 646-674.

Haudenschild, D. R., S. M. Palmer, T. A. Moseley, Z. You and A. H. Reddi (2004). "Bone morphogenetic protein (BMP)-6 signaling and BMP antagonist noggin in prostate cancer." *Cancer Res* **64**(22): 8276-8284.

Hazan, R. B., G. R. Phillips, R. F. Qiao, L. Norton and S. A. Aaronson (2000). "Exogenous expression of N-cadherin in breast cancer cells induces cell migration, invasion, and metastasis." *J Cell Biol* **148**(4): 779-790.

Hazan, R. B., R. Qiao, R. Keren, I. Badano and K. Suyama (2004). "Cadherin switch in tumor progression." *Ann N Y Acad Sci* **1014**: 155-163.

Haÿ, E., J. Lemonnier, O. Fromigué and P. J. Marie (2001). "Bone morphogenetic protein-2 promotes osteoblast apoptosis through a Smad-independent, protein kinase C-dependent signaling pathway." *J Biol Chem* **276**(31): 29028-29036.

Hemmati-Brivanlou, A. and G. H. Thomsen (1995). "Ventral mesodermal patterning in *Xenopus* embryos: Expression patterns and activities of BMP-2 and BMP-4." *Developmental Genetics* **17**(1): 78-89.

Heo, J. S., S. G. Lee and H. O. Kim (2017). "Distal-less homeobox 5 is a master regulator of the osteogenesis of human mesenchymal stem cells." *Int J Mol Med* **40**(5): 1486-1494.

Hinck, A. P. (2012). "Structural studies of the TGF-betas and their receptors - insights into evolution of the TGF-beta superfamily." *FEBS Lett* **586**(14): 1860-1870.

Hogan, B. L. (1996). "Bone morphogenetic proteins: multifunctional regulators of vertebrate development." *Genes Dev* **10**(13): 1580-1594.

Horoszewicz, J. S., S. S. Leong, E. Kawinski, J. P. Karr, H. Rosenthal, T. M. Chu, E. A. Mirand and G. P. Murphy (1983). "LNCaP model of human prostatic carcinoma." *Cancer Res* **43**(4): 1809-1818.

Horvath, L. G., S. M. Henshall, J. G. Kench, J. J. Turner, D. Golovsky, P. C. Brenner, G. F. O'Neill, R. Kooner, P. D. Stricker, J. J. Grygiel and R. L. Sutherland (2004). "Loss of BMP2, Smad8, and Smad4 expression in prostate cancer progression." *Prostate* **59**(3): 234-242.

Howard, G. A., B. L. Bottemiller, R. T. Turner, J. I. Rader and D. J. Baylink (1981). "Parathyroid hormone stimulates bone formation and resorption in organ culture: evidence for a coupling mechanism." *Proc Natl Acad Sci U S A* **78**(5): 3204-3208.

Hsu, D. R., A. N. Economides, X. Wang, P. M. Eimon and R. M. Harland (1998). "The *Xenopus* dorsalizing factor Gremlin identifies a novel family of secreted proteins that antagonize BMP activities." *Mol Cell* **1**(5): 673-683.

Humphrey, P. A. (2004). "Gleason grading and prognostic factors in carcinoma of the prostate." *Mod Pathol* **17**(3): 292-306.

Huse, M., T. W. Muir, L. Xu, Y. G. Chen, J. Kuriyan and J. Massagué (2001). "The TGF beta receptor activation process: an inhibitor- to substrate-binding switch." *Mol Cell* **8**(3): 671-682.

Hwang, Y. W., S. Y. Kim, S. H. Jee, Y. N. Kim and C. M. Nam (2009). "Soy food consumption and risk of prostate cancer: a meta-analysis of observational studies." Nutr Cancer **61**(5): 598-606.

Iemura, S., T. S. Yamamoto, C. Takagi, H. Uchiyama, T. Natsume, S. Shimasaki, H. Sugino and N. Ueno (1998). "Direct binding of follistatin to a complex of bone-morphogenetic protein and its receptor inhibits ventral and epidermal cell fates in early *Xenopus* embryo." Proc Natl Acad Sci U S A **95**(16): 9337-9342.

Imamura, T., M. Takase, A. Nishihara, E. Oeda, J. Hanai, M. Kawabata and K. Miyazono (1997). "Smad6 inhibits signalling by the TGF-beta superfamily." Nature **389**(6651): 622-626.

Ito, E., I. Yana, C. Fujita, A. Irifune, M. Takeda, A. Madachi, S. Mori, Y. Hamada, N. Kawaguchi and N. Matsuura (2010). "The role of MT2-MMP in cancer progression." Biochem Biophys Res Commun **393**(2): 222-227.

Ito, K. (2014). "Prostate cancer in Asian men." Nat Rev Urol **11**(4): 197-212.

Itoh, K., N. Udagawa, T. Katagiri, S. Iemura, N. Ueno, H. Yasuda, K. Higashio, J. M. Quinn, M. T. Gillespie, T. J. Martin, T. Suda and N. Takahashi (2001). "Bone morphogenetic protein 2 stimulates osteoclast differentiation and survival supported by receptor activator of nuclear factor-kappaB ligand." Endocrinology **142**(8): 3656-3662.

Jensen, E. D., R. Gopalakrishnan and J. J. Westendorf (2010). "Regulation of gene expression in osteoblasts." BioFactors **36**(1): 25-32.

Johansson, N., U. Saarialho-Kere, K. Airola, R. Herva, L. Nissinen, J. Westermarck, E. Vuorio, J. Heino and V. M. Kähäri (1997). "Collagenase-3 (MMP-13) is expressed by hypertrophic chondrocytes, periosteal cells, and osteoblasts during human fetal bone development." Dev Dyn **208**(3): 387-397.

Kaighn, M. E., K. S. Narayan, Y. Ohnuki, J. F. Lechner and L. W. Jones (1979). "Establishment and characterization of a human prostatic carcinoma cell line (PC-3)." Invest Urol **17**(1): 16-23.

Karagiannis, G. S., N. Musrap, P. Saraon, A. Treacy, D. F. Schaeffer, R. Kirsch, R. H. Riddell and E. P. Diamandis (2015). "Bone morphogenetic protein antagonist gremlin-1 regulates colon cancer progression." Biol Chem **396**(2): 163-183.

Katayama, M., S. Hirai, K. Kamihagi, K. Nakagawa, M. Yasumoto and I. Kato (1994). "Soluble E-cadherin fragments increased in circulation of cancer patients." Br J Cancer **69**(3): 580-585.

Kenkre, J. S. and J. Bassett (2018). "The bone remodelling cycle." Ann Clin Biochem **55**(3): 308-327.

Kessenbrock, K., V. Plaks and Z. Werb (2010). "Matrix metalloproteinases: regulators of the tumor microenvironment." Cell **141**(1): 52-67.

Key, M. E. (1983). "Macrophages in cancer metastases and their relevance to metastatic growth." Cancer Metastasis Rev **2**(1): 75-88.

Khokha, M. K., D. Hsu, L. J. Brunet, M. S. Dionne and R. M. Harland (2003). "Gremlin is the BMP antagonist required for maintenance of Shh and Fgf signals during limb patterning." Nat Genet **34**(3): 303-307.

Kim, I. Y., D. H. Lee, H. J. Ahn, H. Tokunaga, W. Song, L. M. Devreux, D. Jin, T. K. Sampath and R. A. Morton (2000). "Expression of bone morphogenetic protein receptors type-IA, -IB and -II correlates with tumor grade in human prostate cancer tissues." Cancer Res **60**(11): 2840-2844.

Kim, J., K. Johnson, H. J. Chen, S. Carroll and A. Laughon (1997). "Drosophila Mad binds to DNA and directly mediates activation of vestigial by Decapentaplegic." Nature **388**(6639): 304-308.

Kim, M., S. Yoon, S. Lee, S. A. Ha, H. K. Kim, J. W. Kim and J. Chung (2012). "Gremlin-1 induces BMP-independent tumor cell proliferation, migration, and invasion." PLoS One **7**(4): e35100.

Kingsley, D. M. (1994). "The TGF-beta superfamily: new members, new receptors, and new genetic tests of function in different organisms." Genes Dev **8**(2): 133-146.

Kirsch, T., W. Sebald and M. K. Dreyer (2000). "Crystal structure of the BMP-2-BRIA ectodomain complex." Nat Struct Biol **7**(6): 492-496.

Kirschenbaum, A., X. H. Liu, S. Yao, A. Leiter and A. C. Levine (2011). "Prostatic acid phosphatase is expressed in human prostate cancer bone metastases and promotes osteoblast differentiation." Ann N Y Acad Sci **1237**: 64-70.

Klink, J. C., R. Miocinovic, C. Magi Galluzzi and E. A. Klein (2012). "High-Grade Prostatic Intraepithelial Neoplasia." Korean Journal of Urology **53**(5): 297-303.

Kobayashi, A., H. Okuda, F. Xing, P. R. Pandey, M. Watabe, S. Hirota, S. K. Pai, W. Liu, K. Fukuda, C. Chambers, A. Wilber and K. Watabe (2011). "Bone morphogenetic protein 7 in dormancy and metastasis of prostate cancer stem-like cells in bone." J Exp Med **208**(13): 2641-2655.

Kobayashi, T., K. M. Lyons, A. P. McMahon and H. M. Kronenberg (2005). "BMP signaling stimulates cellular differentiation at multiple steps during cartilage development." Proc Natl Acad Sci U S A **102**(50): 18023-18027.

Koca, O., S. Calışkan, M. Oztürk, M. Güneş and M. I. Karaman (2011). "Significance of atypical small acinar proliferation and high-grade prostatic intraepithelial neoplasia in prostate biopsy." Korean J Urol **52**(11): 736-740.

Koenenman, K. S., F. Yeung and L. W. Chung (1999). "Osteomimetic properties of prostate cancer cells: a hypothesis supporting the predilection of prostate cancer metastasis and growth in the bone environment." Prostate **39**(4): 246-261.

Korenchuk, S., J. E. Lehr, M. C. L. Y. G. Lee, S. Whitney, R. Vessella, D. L. Lin and K. J. Pienta (2001). "VCaP, a cell-based model system of human prostate cancer." In Vivo **15**(2): 163-168.

Krause, C., A. Guzman and P. Knaus (2011). "Noggin." Int J Biochem Cell Biol **43**(4): 478-481.

Kretzschmar, M. and J. Massagué (1998). "SMADs: mediators and regulators of TGF- $\beta$  signaling." Current Opinion in Genetics & Development **8**(1): 103-111.

Kuefer, R., M. D. Hofer, J. E. Gschwend, K. J. Pienta, M. G. Sanda, A. M. Chinnaiyan, M. A. Rubin and M. L. Day (2003). "The role of an 80 kDa fragment of E-cadherin in the metastatic progression of prostate cancer." Clin Cancer Res **9**(17): 6447-6452.

Lai, T. H., Y. C. Fong, W. M. Fu, R. S. Yang and C. H. Tang (2008). "Osteoblasts-derived BMP-2 enhances the motility of prostate cancer cells via activation of integrins." Prostate **68**(12): 1341-1353.

Lamouille, S., J. Xu and R. Derynck (2014). "Molecular mechanisms of epithelial-mesenchymal transition." Nat Rev Mol Cell Biol **15**(3): 178-196.

Larson, S. R., X. Zhang, R. Dumpit, I. Coleman, B. Lakely, M. Roudier, C. S. Higano, L. D. True, P. H. Lange, B. Montgomery, E. Corey, P. S. Nelson, R. L. Vessella and C. Morrissey (2013). "Characterization of osteoblastic and osteolytic proteins in prostate cancer bone metastases." Prostate **73**(9): 932-940.

Laurila, R., S. Parkkila, J. Isola, A. Kallioniemi and E. L. Alarmo (2013). "The expression patterns of gremlin 1 and noggin in normal adult and tumor tissues." Int J Clin Exp Pathol **6**(7): 1400-1408.

Lavery, K., P. Swain, D. Falb and M. H. Alaoui-Ismaili (2008). "BMP-2/4 and BMP-6/7 differentially utilize cell surface receptors to induce osteoblastic differentiation of human bone marrow-derived mesenchymal stem cells." J Biol Chem **283**(30): 20948-20958.

Lee, G. T., D. I. Kang, Y. S. Ha, Y. S. Jung, J. Chung, K. Min, T. H. Kim, K. H. Moon, J. M. Chung, D. H. Lee, W. J. Kim and I. Y. Kim (2014). "Prostate cancer bone metastases acquire resistance to androgen deprivation via WNT5A-mediated BMP-6 induction." Br J Cancer **110**(6): 1634-1644.

Lee, Y., E. Schwarz, M. Davies, M. Jo, J. Gates, J. Wu, X. Zhang and J. R. Lieberman (2003). "Differences in the cytokine profiles associated with prostate cancer cell induced osteoblastic and osteolytic lesions in bone." J Orthop Res **21**(1): 62-72.

Lee, Y.-C., C.-J. Cheng, M. A. Bilen, J.-F. Lu, R. L. Satcher, L.-Y. Yu-Lee, G. E. Gallick, S. N. Maity and S.-H. Lin (2011). "BMP4 Promotes Prostate Tumor Growth in Bone through Osteogenesis." Cancer Research **71**(15): 5194-5203.

Lee, Y. C., J. K. Jin, C. J. Cheng, C. F. Huang, J. H. Song, M. Huang, W. S. Brown, S. Zhang, L. Y. Yu-Lee, E. T. Yeh, B. W. McIntyre, C. J. Logothetis, G. E. Gallick and S. H. Lin (2013). "Targeting Constitutively Activated  $\beta$ (1) Integrins Inhibits Prostate Cancer Metastasis." Molecular cancer research : MCR **11**(4): 405-417.

Lesko, S. M., L. Rosenberg and S. Shapiro (1996). "Family history and prostate cancer risk." Am J Epidemiol **144**(11): 1041-1047.

Li, G., K. Satyamoorthy and M. Herlyn (2001). "N-cadherin-mediated intercellular interactions promote survival and migration of melanoma cells." Cancer Res **61**(9): 3819-3825.

Li, Z., F. Zeng, A. D. Mitchell, Y. S. Kim, Z. Wu and J. Yang (2011). "Transgenic overexpression of bone morphogenetic protein 11 propeptide in skeleton enhances bone formation." Biochem Biophys Res Commun **416**(3-4): 289-292.

Lilja, H. (1985). "A kallikrein-like serine protease in prostatic fluid cleaves the predominant seminal vesicle protein." J Clin Invest **76**(5): 1899-1903.

Lim, M., C. M. Chuong and P. Roy-Burman (2011). "PI3K, Erk signaling in BMP7-induced epithelial-mesenchymal transition (EMT) of PC-3 prostate cancer cells in 2- and 3-dimensional cultures." Horm Cancer **2**(5): 298-309.

Lin, S. J., T. F. Lerch, R. W. Cook, T. S. Jardetzky and T. K. Woodruff (2006). "The structural basis of TGF-beta, bone morphogenetic protein, and activin ligand binding." Reproduction **132**(2): 179-190.

Livak, K. J. and T. D. Schmittgen (2001). "Analysis of relative gene expression data using real-time quantitative PCR and the 2(-Delta Delta C(T)) Method." Methods **25**(4): 402-408.

Logothetis, C. J. and S. H. Lin (2005). "Osteoblasts in prostate cancer metastasis to bone." Nat Rev Cancer **5**(1): 21-28.

Long, J., S. S. Badal, Y. Wang, B. H. Chang, A. Rodriguez and F. R. Danesh (2013). "MicroRNA-22 is a master regulator of bone morphogenetic protein-7/6 homeostasis in the kidney." J Biol Chem **288**(51): 36202-36214.

Luu, H. H., W. X. Song, X. Luo, D. Manning, J. Luo, Z. L. Deng, K. A. Sharff, A. G. Montag, R. C. Haydon and T. C. He (2007). "Distinct roles of bone morphogenetic proteins in osteogenic differentiation of mesenchymal stem cells." J Orthop Res **25**(5): 665-677.

Luzzi, K. J., I. C. MacDonald, E. E. Schmidt, N. Kerkvliet, V. L. Morris, A. F. Chambers and A. C. Groom (1998). "Multistep nature of metastatic inefficiency: dormancy of solitary cells after successful extravasation and limited survival of early micrometastases." Am J Pathol **153**(3): 865-873.

Lynch, C. C. (2011). "Matrix metalloproteinases as master regulators of the vicious cycle of bone metastasis." Bone **48**(1): 44-53.

Massague, J. (1998). "TGF-beta signal transduction." Annu Rev Biochem **67**: 753-791.

Mastro, A. M., C. V. Gay and D. R. Welch (2003). "The skeleton as a unique environment for breast cancer cells." Clin Exp Metastasis **20**(3): 275-284.

Masuda, H., Y. Fukabori, K. Nakano, N. Shimizu and H. Yamanaka (2004). "Expression of bone morphogenetic protein-7 (BMP-7) in human prostate." Prostate **59**(1): 101-106.

Masuda, H., Y. Fukabori, K. Nakano, Y. Takezawa, T. CSuzuki and H. Yamanaka (2003). "Increased expression of bone morphogenetic protein-7 in bone metastatic prostate cancer." Prostate **54**(4): 268-274.

Matsuo, K. and N. Irie (2008). "Osteoclast-osteoblast communication." Arch Biochem Biophys **473**(2): 201-209.

McCutcheon, M., D. R. Coman and F. B. Moore (1948). "Studies on invasiveness of cancer; adhesiveness of malignant cells in various human adenocarcinomas." Cancer **1**(3): 460-467.

McNeal, J. E. (1965). "Morphogenesis of prostatic carcinoma." Cancer **18**(12): 1659-1666.

McNeal, J. E., D. G. Bostwick, R. A. Kindrachuk, E. A. Redwine, F. S. Freiha and T. A. Stamey (1986). "Patterns of progression in prostate cancer." Lancet **1**(8472): 60-63.

Mellinger, G. T., D. Gleason and J. Bailar (1967). "The Histology and Prognosis of Prostatic Cancer." The Journal of Urology **97**(2): 331-337.

Merino, R., J. Rodriguez-Leon, D. Macias, Y. Gañan, A. N. Economides and J. M. Hurle (1999). "The BMP antagonist Gremlin regulates outgrowth, chondrogenesis and programmed cell death in the developing limb." Development **126**(23): 5515-5522.

Metheny-Barlow, L. J. and L. Y. Li (2003). "The enigmatic role of angiopoietin-1 in tumor angiogenesis." Cell Res **13**(5): 309-317.

Miyazaki, H., T. Watabe, T. Kitamura and K. Miyazono (2004). "BMP signals inhibit proliferation and in vivo tumor growth of androgen-insensitive prostate carcinoma cells." *Oncogene* **23**(58): 9326-9335.

Miyazono, K., S. Maeda and T. Imamura (2005). "BMP receptor signaling: transcriptional targets, regulation of signals, and signaling cross-talk." *Cytokine Growth Factor Rev* **16**(3): 251-263.

Mizrahi, O., D. Sheyn, W. Tawackoli, I. Kallai, A. Oh, S. Su, X. Da, P. Zarrini, G. Cook-Wiens, D. Gazit and Z. Gazit (2013). "BMP-6 is more efficient in bone formation than BMP-2 when overexpressed in mesenchymal stem cells." *Gene Ther* **20**(4): 370-377.

Mol, A. J., A. A. Geldof, G. A. Meijer, H. G. van der Poel and R. J. van Moorselaar (2007). "New experimental markers for early detection of high-risk prostate cancer: role of cell-cell adhesion and cell migration." *J Cancer Res Clin Oncol* **133**(10): 687-695.

Morganti, G., L. Gianferrari, A. Cresseri, G. Arrigoni and L. G. (1956). "Recherches clinico-statistiques et genetiques sur les neoplasies de la prostate." *Acta Genet Stat Med* **6**: 304-305.

Morrissey, C., L. G. Brown, T. E. Pitts, R. L. Vessella and E. Corey (2010). "Bone morphogenetic protein 7 is expressed in prostate cancer metastases and its effects on prostate tumor cells depend on cell phenotype and the tumor microenvironment." *Neoplasia* **12**(2): 192-205.

Mosig, R. A., O. Dowling, A. DiFeo, M. C. Ramirez, I. C. Parker, E. Abe, J. Diouri, A. A. Aqeel, J. D. Wylie, S. A. Oblander, J. Madri, P. Bianco, S. S. Apte, M. Zaidi, S. B. Doty, R. J. Majeska, M. B. Schaffler and J. A. Martignetti (2007). "Loss of MMP-2 disrupts skeletal and craniofacial development and results in decreased bone mineralization, joint erosion and defects in osteoblast and osteoclast growth." *Hum Mol Genet* **16**(9): 1113-1123.

Mueller, T. D. and J. Nickel (2012). "Promiscuity and specificity in BMP receptor activation." *FEBS Lett* **586**(14): 1846-1859.

Mulloy, B. and C. C. Rider (2015). "The Bone Morphogenetic Proteins and Their Antagonists." *Vitam Horm* **99**: 63-90.

Mundy, G. R. (2002). "Metastasis to bone: causes, consequences and therapeutic opportunities." *Nat Rev Cancer* **2**(8): 584-593.

Nabha, S. M., E. B. dos Santos, H. A. Yamamoto, A. Belizi, Z. Dong, H. Meng, A. Saliganan, A. Sabbota, R. D. Bonfil and M. L. Cher (2008). "Bone marrow stromal cells enhance prostate cancer cell invasion through type I collagen in an MMP-12 dependent manner." *Int J Cancer* **122**(11): 2482-2490.

Nagle, R. B., J. D. Knox, C. Wolf, G. T. Bowden and A. E. Cress (1994). "Adhesion molecules, extracellular matrix, and proteases in prostate carcinoma." *J Cell Biochem Suppl* **19**: 232-237.

Navone, N. M., M. Olive, M. Ozen, R. Davis, P. Troncoso, S. M. Tu, D. Johnston, A. Pollack, S. Pathak, A. C. von Eschenbach and C. J. Logothetis (1997). "Establishment of two human prostate cancer cell lines derived from a single bone metastasis." *Clin Cancer Res* **3**(12 Pt 1): 2493-2500.

Nawrocki-Raby, B., C. Gilles, M. Polette, E. Bruyneel, J. Y. Laronze, N. Bonnet, J. M. Foidart, M. Mareel and P. Birembaut (2003). "Upregulation of MMPs by soluble E-cadherin in human lung tumor cells." *Int J Cancer* **105**(6): 790-795.

Nemeth, J. A., J. F. Harb, U. Barroso, Z. He, D. J. Grignon and M. L. Cher (1999). "Severe combined immunodeficient-hu model of human prostate cancer metastasis to human bone." *Cancer Res* **59**(8): 1987-1993.

Nemeth, J. A., R. Yousif, M. Herzog, M. Che, J. Upadhyay, B. Shekarriz, S. Bhagat, C. Mullins, R. Fridman and M. L. Cher (2002). "Matrix metalloproteinase activity, bone matrix turnover, and tumor cell proliferation in prostate cancer bone metastasis." *J Natl Cancer Inst* **94**(1): 17-25.

Nieswandt, B., M. Hafner, B. Echtenacher and D. N. Männel (1999). "Lysis of tumor cells by natural killer cells in mice is impeded by platelets." *Cancer Res* **59**(6): 1295-1300.

Nishimura, R., K. Hata, F. Ikeda, F. Ichida, A. Shimoyama, T. Matsubara, M. Wada, K. Amano and T. Yoneda (2008). "Signal transduction and transcriptional regulation during mesenchymal cell differentiation." *J Bone Miner Metab* **26**(3): 203-212.

Nohe, A., S. Hassel, M. Ehrlich, F. Neubauer, W. Sebald, Y. I. Henis and P. Knaus (2002). "The mode of bone morphogenetic protein (BMP) receptor oligomerization determines different BMP-2 signaling pathways." *J Biol Chem* **277**(7): 5330-5338.

Nohe, A., E. Keating, P. Knaus and N. O. Petersen (2004). "Signal transduction of bone morphogenetic protein receptors." *Cell Signal* **16**(3): 291-299.

O'dowd, G. J., M. C. Miller, R. Orozco and R. W. Veltri (2000). "Analysis of repeated biopsy results within 1 year after a noncancer diagnosis." *Urology* **55**(4): 553-559.

Oertel, H. (1926). "An Address on Involutionary Changes in Prostate and Female Breast in Relation to Cancer Development." *Can Med Assoc J* **16**(3): 237-241.

Okadome, T., E. Oeda, M. Saitoh, H. Ichijo, H. L. Moses, K. Miyazono and M. Kawabata (1996). "Characterization of the interaction of FKBP12 with the transforming growth factor-beta type I receptor in vivo." *J Biol Chem* **271**(36): 21687-21690.

Onichtchouk, D., Y. G. Chen, R. Dosch, V. Gawantka, H. Delius, J. Massague and C. Niehrs (1999). "Silencing of TGF-beta signalling by the pseudoreceptor BAMBI." *Nature* **401**(6752): 480-485.

ONS (2015). Cancer Registration Statistics, England: 2015.

Ottewell, P. D. (2016). "The role of osteoblasts in bone metastasis." *J Bone Oncol* **5**(3): 124-127.

Oxford, G. and D. Theodorescu (2003). "Ras superfamily monomeric G proteins in carcinoma cell motility." *Cancer Lett* **189**(2): 117-128.

Paget, S. (1889). "THE DISTRIBUTION OF SECONDARY GROWTHS IN CANCER OF THE BREAST." *The Lancet* **133**(3421): 571-573.

Palumbo, J. S., K. E. Talmage, J. V. Massari, C. M. La Jeunesse, M. J. Flick, K. W. Kombrinck, M. Jirousková and J. L. Degen (2005). "Platelets and fibrin(ogen) increase metastatic potential by impeding natural killer cell-mediated elimination of tumor cells." *Blood* **105**(1): 178-185.

Papanagiotou, M., Z. H. Dailiana, T. Karachalios, S. Varitimidis, M. Vlychou, M. Hantes and K. N. Malizos (2015). "RhBMP-7 for the treatment of nonunion of fractures of long bones." *Bone Joint J* **97-B**(7): 997-1003.

Pereira, R. C., A. N. Economides and E. Canalis (2000). "Bone morphogenetic proteins induce gremlin, a protein that limits their activity in osteoblasts." *Endocrinology* **141**(12): 4558-4563.

Phadke, P. A., R. R. Mercer, J. F. Harms, Y. Jia, A. R. Frost, J. L. Jewell, K. M. Bussard, S. Nelson, C. Moore, J. C. Kappes, C. V. Gay, A. M. Mastro and D. R. Welch (2006). "Kinetics of metastatic breast cancer cell trafficking in bone." *Clin Cancer Res* **12**(5): 1431-1440.

Pienta, K. J. and D. Bradley (2006). "Mechanisms underlying the development of androgen-independent prostate cancer." *Clin Cancer Res* **12**(6): 1665-1671.

Pignatti, E., R. Zeller and A. Zuniga (2014). "To BMP or not to BMP during vertebrate limb bud development." *Seminars in Cell & Developmental Biology* **32**: 119-127.

Pittenger, M. F., A. M. Mackay, S. C. Beck, R. K. Jaiswal, R. Douglas, J. D. Mosca, M. A. Moorman, D. W. Simonetti, S. Craig and D. R. Marshak (1999). "Multilineage potential of adult human mesenchymal stem cells." *Science* **284**(5411): 143-147.

Postma, R., M. Roobol, F. H. Schroder and T. H. van der Kwast (2004). "Lesions predictive for prostate cancer in a screened population: first and second screening round findings." *Prostate* **61**(3): 260-266.

Re'em-Kalma, Y., T. Lamb and D. Frank (1995). "Competition between noggin and bone morphogenetic protein 4 activities may regulate dorsalization during *Xenopus* development." *Proc Natl Acad Sci U S A* **92**(26): 12141-12145.

Reddi, A. H. (2001). "Interplay between bone morphogenetic proteins and cognate binding proteins in bone and cartilage development: noggin, chordin and DAN." *Arthritis Res* **3**(1): 1-5.

Reymond, N., B. B. d'Água and A. J. Ridley (2013). "Crossing the endothelial barrier during metastasis." *Nat Rev Cancer* **13**(12): 858-870.

Ridley, A. J. (2015). "Rho GTPase signalling in cell migration." *Curr Opin Cell Biol* **36**: 103-112.

Rosner, W., D. J. Hryb, M. S. Khan, A. M. Nakhla and N. A. Romas (1991). "Sex hormone-binding globulin: anatomy and physiology of a new regulatory system." J Steroid Biochem Mol Biol **40**(4-6): 813-820.

Roudier, M. P., C. Morrissey, L. D. True, C. S. Higano, R. L. Vessella and S. M. Ott (2008). "Histopathological assessment of prostate cancer bone osteoblastic metastases." J Urol **180**(3): 1154-1160.

Rucci, N. (2008). "Molecular biology of bone remodelling." Clinical Cases in Mineral and Bone Metabolism **5**(1): 49-56.

Salazar, V. S., L. W. Gamer and V. Rosen (2016). "BMP signalling in skeletal development, disease and repair." Nature Reviews Endocrinology **12**: 203.

Saraon, P., A. P. Drabovich, K. A. Jarvi and E. P. Diamandis (2014). "Mechanisms of Androgen-Independent Prostate Cancer." EJIFCC **25**(1): 42-54.

Sardana, G., K. Jung, C. Stephan and E. P. Diamandis (2008). "Proteomic analysis of conditioned media from the PC3, LNCaP, and 22Rv1 prostate cancer cell lines: discovery and validation of candidate prostate cancer biomarkers." J Proteome Res **7**(8): 3329-3338.

Scheufler, C., W. Sebald and M. Hulsmeyer (1999). "Crystal structure of human bone morphogenetic protein-2 at 2.7 Å resolution." J Mol Biol **287**(1): 103-115.

Schneyer, A. L., Q. Wang, Y. Sidis and P. M. Sluss (2004). "Differential distribution of follistatin isoforms: application of a new FS315-specific immunoassay." J Clin Endocrinol Metab **89**(10): 5067-5075.

Schwaninger, R., C. A. Rentsch, A. Wetterwald, G. van der Horst, R. L. van Bezooijen, G. van der Pluijm, C. W. Löwik, K. Ackermann, W. Pyerin, F. C. Hamdy, G. N. Thalmann and M. G. Cecchini (2007). "Lack of noggin expression by cancer cells is a determinant of the osteoblast response in bone metastases." Am J Pathol **170**(1): 160-175.

Sebald, W., J. Nickel, J. L. Zhang and T. D. Mueller (2004). "Molecular recognition in bone morphogenetic protein (BMP)/receptor interaction." Biol Chem **385**(8): 697-710.

Secondini, C., A. Wetterwald, R. Schwaninger, G. N. Thalmann and M. G. Cecchini (2011). "The role of the BMP signaling antagonist noggin in the development of prostate cancer osteolytic bone metastasis." PLoS One **6**(1): e16078.

Sekelsky, J. J., S. J. Newfeld, L. A. Raftery, E. H. Chartoff and W. M. Gelbart (1995). "Genetic characterization and cloning of mothers against dpp, a gene required for decapentaplegic function in *Drosophila melanogaster*." Genetics **139**(3): 1347-1358.

Selever, J., W. Liu, M. F. Lu, R. R. Behringer and J. F. Martin (2004). "Bmp4 in limb bud mesoderm regulates digit pattern by controlling AER development." Dev Biol **276**(2): 268-279.

Sengle, G., R. N. Ono, K. M. Lyons, H. P. Bächinger and L. Y. Sakai (2008). "A new model for growth factor activation: type II receptors compete with the prodomain for BMP-7." J Mol Biol **381**(4): 1025-1039.

Sepporta, M. V., F. M. Tumminello, C. Flandina, M. Crescimanno, M. Giammanco, M. La Guardia, D. di Majo and G. Leto (2013). "Follistatin as potential therapeutic target in prostate cancer." Target Oncol **8**(4): 215-223.

Sequeira, L., C. W. Dubyk, T. A. Riesenberger, C. R. Cooper and K. L. van Golen (2008). "Rho GTPases in PC-3 prostate cancer cell morphology, invasion and tumor cell diapedesis." Clin Exp Metastasis **25**(5): 569-579.

Shi, Y. and J. Massagué (2003). "Mechanisms of TGF-beta signaling from cell membrane to the nucleus." Cell **113**(6): 685-700.

Shibue, T. and R. A. Weinberg (2011). "Metastatic colonization: Settlement, adaptation and propagation of tumor cells in a foreign tissue environment." Seminars in Cancer Biology **21**(2): 99-106.

Shih, W. and S. Yamada (2012). "N-cadherin-mediated cell-cell adhesion promotes cell migration in a three-dimensional matrix." Journal of Cell Science **125**(15): 3661-3670.

Shimasaki, S., M. Koga, F. Esch, K. Cooksey, M. Mercado, A. Koba, N. Ueno, S. Y. Ying, N. Ling and R. Guillemin (1988). "Primary structure of the human follistatin precursor and its genomic organization." Proc Natl Acad Sci U S A **85**(12): 4218-4222.

Shimasaki, S., M. Koga, F. Esch, M. Mercado, K. Cooksey, A. Koba and N. Ling (1988). "Porcine follistatin gene structure supports two forms of mature follistatin produced by alternative splicing." *Biochem Biophys Res Commun* **152**(2): 717-723.

Shimizu, H., R. K. Ross, L. Bernstein, R. Yatani, B. E. Henderson and T. M. Mack (1991). "Cancers of the prostate and breast among Japanese and white immigrants in Los Angeles County." *Br J Cancer* **63**(6): 963-966.

Shweiki, D., A. Itin, D. Soffer and E. Keshet (1992). "Vascular endothelial growth factor induced by hypoxia may mediate hypoxia-initiated angiogenesis." *Nature* **359**(6398): 843-845.

Sieber, C., J. Kopf, C. Hiepen and P. Knaus (2009). "Recent advances in BMP receptor signaling." *Cytokine Growth Factor Rev* **20**(5-6): 343-355.

Siegel, R. L., K. D. Miller and A. Jemal (2018). "Cancer statistics, 2018." *CA Cancer J Clin* **68**(1): 7-30.

Sieh, S., A. V. Taubenberger, M. L. Lehman, J. A. Clements, C. C. Nelson and D. W. Hutmacher (2014). "Paracrine interactions between LNCaP prostate cancer cells and bioengineered bone in 3D in vitro culture reflect molecular changes during bone metastasis." *Bone* **63**: 121-131.

Slobodan, V. and K. T. Sampath (2002). *Bone Morphogenetic Proteins: From Laboratory to Clinical Practice*.

Smith, J. R., D. Freije, J. D. Carpten, H. Gronberg, J. Xu, S. D. Isaacs, M. J. Brownstein, G. S. Bova, H. Guo, P. Bujnovszky, D. R. Nusskern, J. E. Damber, A. Bergh, M. Emanuelsson, O. P. Kallioniemi, J. Walker-Daniels, J. E. Bailey-Wilson, T. H. Beaty, D. A. Meyers, P. C. Walsh, F. S. Collins, J. M. Trent and W. B. Isaacs (1996). "Major susceptibility locus for prostate cancer on chromosome 1 suggested by a genome-wide search." *Science* **274**(5291): 1371-1374.

Sneddon, J. B., H. H. Zhen, K. Montgomery, M. van de Rijn, A. D. Tward, R. West, H. Gladstone, H. Y. Chang, G. S. Morganroth, A. E. Oro and P. O. Brown (2006). "Bone morphogenetic protein antagonist gremlin 1 is widely expressed by cancer-associated stromal cells and can promote tumor cell proliferation." *Proc Natl Acad Sci U S A* **103**(40): 14842-14847.

Sopory, S., S. M. Nelsen, C. Degnin, C. Wong and J. L. Christian (2006). "Regulation of bone morphogenetic protein-4 activity by sequence elements within the prodomain." *J Biol Chem* **281**(45): 34021-34031.

Sottnik, J. L., S. Daignault-Newton, X. Zhang, C. Morrissey, M. H. Hussain, E. T. Keller and C. L. Hall (2013). "Integrin alpha2beta 1 (alpha2beta1) promotes prostate cancer skeletal metastasis." *Clin Exp Metastasis* **30**(5): 569-578.

Souchelnytskyi, S., T. Nakayama, A. Nakao, A. Moren, C. H. Heldin, J. L. Christian and P. ten Dijke (1998). "Physical and functional interaction of murine and Xenopus Smad7 with bone morphogenetic protein receptors and transforming growth factor-beta receptors." *J Biol Chem* **273**(39): 25364-25370.

Souchelnytskyi, S., K. Tamaki, U. Engstrom, C. Wernstedt, P. ten Dijke and C. H. Heldin (1997). "Phosphorylation of Ser465 and Ser467 in the C terminus of Smad2 mediates interaction with Smad4 and is required for transforming growth factor-beta signaling." *J Biol Chem* **272**(44): 28107-28115.

Spanjol, J., G. Djordjević, D. Markić, M. Klarić, D. Fuckar and D. Bobinac (2010). "Role of bone morphogenetic proteins in human prostate cancer pathogenesis and development of bone metastases: immunohistochemical study." *Coll Antropol* **34 Suppl 2**: 119-125.

Steinberg, G. D., B. S. Carter, T. H. Beaty, B. Childs and P. C. Walsh (1990). "Family history and the risk of prostate cancer." *Prostate* **17**(4): 337-347.

Stewart, A., H. Guan and K. Yang (2010). "BMP-3 promotes mesenchymal stem cell proliferation through the TGF-beta/activin signaling pathway." *J Cell Physiol* **223**(3): 658-666.

Stoletov, K., H. Kato, E. Zardoujian, J. Kelber, J. Yang, S. Shattil and R. Klemke (2010). "Visualizing extravasation dynamics of metastatic tumor cells." *J Cell Sci* **123**(Pt 13): 2332-2341.

Stone, K. R., D. D. Mickey, H. Wunderli, G. H. Mickey and D. F. Paulson (1978). "Isolation of a human prostate carcinoma cell line (DU 145)." *Int J Cancer* **21**(3): 274-281.

Sugino, K., N. Kurosawa, T. Nakamura, K. Takio, S. Shimasaki, N. Ling, K. Titani and H. Sugino (1993). "Molecular heterogeneity of follistatin, an activin-binding protein. Higher affinity of the

carboxyl-terminal truncated forms for heparan sulfate proteoglycans on the ovarian granulosa cell." *J Biol Chem* **268**(21): 15579-15587.

Sun, J., F. F. Zhuang, J. E. Mullersman, H. Chen, E. J. Robertson, D. Warburton, Y. H. Liu and W. Shi (2006). "BMP4 activation and secretion are negatively regulated by an intracellular gremlin-BMP4 interaction." *J Biol Chem* **281**(39): 29349-29356.

Sylva, M., A. F. M. Moorman and M. J. B. Hoff (2013). "Follistatin-like 1 in vertebrate development." *Birth Defects Research Part C: Embryo Today: Reviews* **99**(1): 61-69.

Szulcek, R., H. J. Bogaard and G. P. van Nieuw Amerongen (2014). "Electric cell-substrate impedance sensing for the quantification of endothelial proliferation, barrier function, and motility." *J Vis Exp*(85).

Sánchez-Tilló, E., Y. Liu, O. de Barrios, L. Siles, L. Fanlo, M. Cuatrecasas, D. S. Darling, D. C. Dean, A. Castells and A. Postigo (2012). "EMT-activating transcription factors in cancer: beyond EMT and tumor invasiveness." *Cell Mol Life Sci* **69**(20): 3429-3456.

Tae, B. S., S. Cho, H. C. Kim, C. H. Kim, S. H. Kang, J. G. Lee, J. J. Kim, H. S. Park, J. Cheon, M. M. Oh and S. G. Kang (2018). "Decreased expression of bone morphogenetic protein-2 is correlated with biochemical recurrence in prostate cancer: Immunohistochemical analysis." *Scientific Reports* **8**(1): 10748.

Tai, S., Y. Sun, J. M. Squires, H. Zhang, W. K. Oh, C. Z. Liang and J. Huang (2011). "PC3 is a cell line characteristic of prostatic small cell carcinoma." *Prostate* **71**(15): 1668-1679.

Taichman, R. S., C. Cooper, E. T. Keller, K. J. Pienta, N. S. Taichman and L. K. McCauley (2002). "Use of the stromal cell-derived factor-1/CXCR4 pathway in prostate cancer metastasis to bone." *Cancer Res* **62**(6): 1832-1837.

Takashima, A. and D. V. Faller (2013). "Targeting the RAS oncogene." *Expert opinion on therapeutic targets* **17**(5): 507-531.

Tarin, D., J. E. Price, M. G. Kettlewell, R. G. Souter, A. C. Vass and B. Crossley (1984). "Mechanisms of human tumor metastasis studied in patients with peritoneovenous shunts." *Cancer Res* **44**(8): 3584-3592.

Theriault, R. L. (2012). "Biology of bone metastases." *Cancer Control* **19**(2): 92-101.

Thiery, J. P. (2002). "Epithelial-mesenchymal transitions in tumour progression." *Nat Rev Cancer* **2**(6): 442-454.

Thiery, J. P., H. Acloque, R. Y. Huang and M. A. Nieto (2009). "Epithelial-mesenchymal transitions in development and disease." *Cell* **139**(5): 871-890.

Thomas, B. G. and F. C. Hamdy (2000). "Bone morphogenetic protein-6: potential mediator of osteoblastic metastases in prostate cancer." *Prostate Cancer Prostatic Dis* **3**(4): 283-285.

Thomas, R., W. A. Anderson, V. Raman and A. H. Reddi (1998). "Androgen-dependent gene expression of bone morphogenetic protein 7 in mouse prostate." *Prostate* **37**(4): 236-245.

Tumminello, F. M., G. Badalamenti, F. Fulfarò, L. Incorvaia, M. Crescimanno, C. Flandina, M. V. Sepporta and G. Leto (2010). "Serum follistatin in patients with prostate cancer metastatic to the bone." *Clin Exp Metastasis* **27**(8): 549-555.

Tylzanowski, P., L. Mebis and F. P. Luyten (2006). "The Noggin null mouse phenotype is strain dependent and haploinsufficiency leads to skeletal defects." *Dev Dyn* **235**(6): 1599-1607.

UICC (2017). *TNM Classification of Malignant Tumours*.

Vaarala, M. H., K. Porvari, A. Kyllonen and P. Vihko (2000). "Differentially expressed genes in two LNCaP prostate cancer cell lines reflecting changes during prostate cancer progression." *Lab Invest* **80**(8): 1259-1268.

van der Poel, H. G., C. Hanrahan, H. Zhong and J. W. Simons (2003). "Rapamycin induces Smad activity in prostate cancer cell lines." *Urol Res* **30**(6): 380-386.

Vesuna, F., P. van Diest, J. H. Chen and V. Raman (2008). "Twist is a transcriptional repressor of E-cadherin gene expression in breast cancer." *Biochem Biophys Res Commun* **367**(2): 235-241.

Walsh, D. W., C. Godson, D. P. Brazil and F. Martin (2010). "Extracellular BMP-antagonist regulation in development and disease: tied up in knots." *Trends Cell Biol* **20**(5): 244-256.

Wang, J., Y. Shiozawa, Y. Wang, Y. Jung, K. J. Pienta, R. Mehra, R. Loberg and R. S. Taichman (2008). "The role of CXCR7/RDC1 as a chemokine receptor for CXCL12/SDF-1 in prostate cancer." *J Biol Chem* **283**(7): 4283-4294.

Wang, R. N., J. Green, Z. Wang, Y. Deng, M. Qiao, M. Peabody, Q. Zhang, J. Ye, Z. Yan, S. Denduluri, O. Idowu, M. Li, C. Shen, A. Hu, R. C. Haydon, R. Kang, J. Mok, M. J. Lee, H. L. Luu and L. L. Shi (2014). "Bone Morphogenetic Protein (BMP) signaling in development and human diseases." *Genes Dis* **1**(1): 87-105.

Weiss, L. (1990). "Metastatic inefficiency." *Adv Cancer Res* **54**: 159-211.

Weiss, L., D. S. Dimitrov and M. Angelova (1985). "The hemodynamic destruction of intravascular cancer cells in relation to myocardial metastasis." *Proc Natl Acad Sci U S A* **82**(17): 5737-5741.

Wessely, O., E. Agius, M. Oelgeschlager, E. M. Pera and E. M. De Robertis (2001). "Neural induction in the absence of mesoderm: beta-catenin-dependent expression of secreted BMP antagonists at the blastula stage in *Xenopus*." *Dev Biol* **234**(1): 161-173.

Wirtz, D., K. Konstantopoulos and P. C. Searson (2011). "The physics of cancer: the role of physical interactions and mechanical forces in metastasis." *Nat Rev Cancer* **11**(7): 512-522.

Wood, M., K. Fudge, J. L. Mohler, A. R. Frost, F. Garcia, M. Wang and M. E. Stearns (1997). "In situ hybridization studies of metalloproteinases 2 and 9 and TIMP-1 and TIMP-2 expression in human prostate cancer." *Clin Exp Metastasis* **15**(3): 246-258.

Wordinger, R. J., G. Zode and A. F. Clark (2008). "Focus on molecules: gremlin." *Exp Eye Res* **87**(2): 78-79.

Wozney, J. M., V. Rosen, A. J. Celeste, L. M. Mitsock, M. J. Whitters, R. W. Kriz, R. M. Hewick and E. A. Wang (1988). "Novel regulators of bone formation: molecular clones and activities." *Science* **242**(4885): 1528-1534.

Wright, J. L. and P. H. Lange (2018). Prostate cancer in elderly patients.

Wrighton, K. H., X. Lin and X. H. Feng (2009). "Phospho-control of TGF-beta superfamily signaling." *Cell Res* **19**(1): 8-20.

Wu, M., G. Chen and Y. P. Li (2016). "TGF-beta and BMP signaling in osteoblast, skeletal development, and bone formation, homeostasis and disease." *Bone Res* **4**: 16009.

Wynder, E. L. (1979). "Dietary habits and cancer epidemiology." *Cancer* **43**(5 Suppl): 1955-1961.

Xing, L. and B. F. Boyce (2005). "Regulation of apoptosis in osteoclasts and osteoblastic cells." *Biochem Biophys Res Commun* **328**(3): 709-720.

Yamaguchi, A., T. Ishizuya, N. Kintou, Y. Wada, T. Katagiri, J. M. Wozney, V. Rosen and S. Yoshiki (1996). "Effects of BMP-2, BMP-4, and BMP-6 on osteoblastic differentiation of bone marrow-derived stromal cell lines, ST2 and MC3T3-G2/PA6." *Biochem Biophys Res Commun* **220**(2): 366-371.

Yamaji, N., A. J. Celeste, R. S. Thies, J. J. Song, S. M. Bernier, D. Goltzman, K. M. Lyons, J. Nove, V. Rosen and J. M. Wozney (1994). "A mammalian serine/threonine kinase receptor specifically binds BMP-2 and BMP-4." *Biochem Biophys Res Commun* **205**(3): 1944-1951.

Yamashita, H., P. ten Dijke, D. Huylebroeck, T. K. Sampath, M. Andries, J. C. Smith, C. H. Heldin and K. Miyazono (1995). "Osteogenic protein-1 binds to activin type II receptors and induces certain activin-like effects." *J Cell Biol* **130**(1): 217-226.

Yang, J., K. Fizazi, S. Peleg, C. R. Sikes, A. K. Raymond, N. Jamal, M. Hu, M. Olive, L. A. Martinez, C. G. Wood, C. J. Logothetis, G. Karsenty and N. M. Navone (2001). "Prostate cancer cells induce osteoblast differentiation through a Cbfa1-dependent pathway." *Cancer Res* **61**(14): 5652-5659.

Yang, S., L. K. Pham, C. P. Liao, B. Frenkel, A. H. Reddi and P. Roy-Burman (2008). "A novel bone morphogenetic protein signaling in heterotypic cell interactions in prostate cancer." *Cancer Res* **68**(1): 198-205.

Yang, S., C. Zhong, B. Frenkel, A. H. Reddi and P. Roy-Burman (2005). "Diverse biological effect and Smad signaling of bone morphogenetic protein 7 in prostate tumor cells." *Cancer Res* **65**(13): 5769-5777.

Yao, D., C. Dai and S. Peng (2011). "Mechanism of the mesenchymal-epithelial transition and its relationship with metastatic tumor formation." *Mol Cancer Res* **9**(12): 1608-1620.

Yao, H., C. M. Dashner, E. J. Fau - van Golen, K. L. van Golen, C. M. Fau - van Golen and K. L. van Golen "RhoC GTPase is required for PC-3 prostate cancer cell invasion but not motility." (0950-9232 (Print)).

Ye, L., J. M. Lewis-Russell, H. Kynaston and W. G. Jiang (2007). "Endogenous bone morphogenetic protein-7 controls the motility of prostate cancer cells through regulation of bone morphogenetic protein antagonists." *J Urol* **178**(3 Pt 1): 1086-1091.

Ye, L., J. M. Lewis-Russell, A. J. Sanders, H. Kynaston and W. G. Jiang (2008). "HGF/SF up-regulates the expression of bone morphogenetic protein 7 in prostate cancer cells." *Urol Oncol* **26**(2): 190-197.

Yin, J. J., C. B. Pollock and K. Kelly (2005). "Mechanisms of cancer metastasis to the bone." *Cell Res* **15**(1): 57-62.

Yuen, H. F., Y. P. Chan, W. L. Cheung, Y. C. Wong, X. Wang and K. W. Chan (2008). "The prognostic significance of BMP-6 signaling in prostate cancer." *Mod Pathol* **21**(12): 1436-1443.

Yuen, H. F., W. K. Kwok, K. K. Chan, C. W. Chua, Y. P. Chan, Y. Y. Chu, Y. C. Wong, X. Wang and K. W. Chan (2008). "TWIST modulates prostate cancer cell-mediated bone cell activity and is upregulated by osteogenic induction." *Carcinogenesis* **29**(8): 1509-1518.

Zabkiewicz, C., J. Resaul, R. Hargest, W. G. Jiang and L. Ye (2017). "Increased Expression of Follistatin in Breast Cancer Reduces Invasiveness and Clinically Correlates with Better Survival." *Cancer Genomics Proteomics* **14**(4): 241-251.

Zheng, Y., H. Zhou, C. R. Dunstan, R. L. Sutherland and M. J. Seibel (2013). "The role of the bone microenvironment in skeletal metastasis." *J Bone Oncol* **2**(1): 47-57.

Zhu, H., P. Kavsak, S. Abdollah, J. L. Wrana and G. H. Thomsen (1999). "A SMAD ubiquitin ligase targets the BMP pathway and affects embryonic pattern formation." *Nature* **400**(6745): 687-693.

Zhu, W., J. Kim, C. Cheng, B. A. Rawlins, O. Boachie-Adjei, R. G. Crystal and C. Hidaka (2006). "Noggin regulation of bone morphogenetic protein (BMP) 2/7 heterodimer activity in vitro." *Bone* **39**(1): 61-71.

Zimmerman, L. B., J. M. De Jesús-Escobar and R. M. Harland (1996). "The Spemann organizer signal noggin binds and inactivates bone morphogenetic protein 4." *Cell* **86**(4): 599-606.

Zou, H. and L. Niswander (1996). "Requirement for BMP signaling in interdigital apoptosis and scale formation." *Science* **272**(5262): 738-741.

Özen, H. and S. Sözen (2006). "PSA Isoforms in Prostate Cancer Detection." *European Urology Supplements* **5**(6): 495-499.

Coleman, R. E. (2006). "Clinical features of metastatic bone disease and risk of skeletal morbidity." *Clin Cancer Res* **12**(20 Pt 2): 6243s-6249s.

Coman, D. R. (1944). "Decreased Mutual Adhesiveness, a Property of Cells from Squamous Cell Carcinomas." *Cancer Research* **4**(10): 625-629.

David, J. M. and A. K. Rajasekaran (2012). "Dishonorable discharge: the oncogenic roles of cleaved E-cadherin fragments." *Cancer Res* **72**(12): 2917-2923.

de Caestecker, M. (2004). "The transforming growth factor- $\beta$  superfamily of receptors." *Cytokine & Growth Factor Reviews* **15**(1): 1-11.

De Craene, B. and G. Berx (2013). "Regulatory networks defining EMT during cancer initiation and progression." *Nat Rev Cancer* **13**(2): 97-110.

De Wever, O., L. Derycke, A. Hendrix, G. De Meerleer, F. Godeau, H. Depypere and M. Bracke (2007). "Soluble cadherins as cancer biomarkers." *Clin Exp Metastasis* **24**(8): 685-697.

Derynck, R. and Y. E. Zhang (2003). "Smad-dependent and Smad-independent pathways in TGF-beta family signalling." *Nature* **425**(6958): 577-584.

Draffin, J. E., S. McFarlane, A. Hill, P. G. Johnston and D. J. Waugh (2004). "CD44 potentiates the adherence of metastatic prostate and breast cancer cells to bone marrow endothelial cells." *Cancer Res* **64**(16): 5702-5711.

Ducy, P. and G. Karsenty (2000). "The family of bone morphogenetic proteins." Kidney Int **57**(6): 2207-2214.

Ebisawa, T., K. Tada, I. Kitajima, K. Tojo, T. K. Sampath, M. Kawabata, K. Miyazono and T. Imamura (1999). "Characterization of bone morphogenetic protein-6 signaling pathways in osteoblast differentiation." J Cell Sci **112** ( Pt **20**): 3519-3527.

Egeblad, M. and Z. Werb (2002). "New functions for the matrix metalloproteinases in cancer progression." Nat Rev Cancer **2**(3): 161-174.

Fainsod, A., K. Deissler, R. Yelin, K. Marom, M. Epstein, G. Pillemer, H. Steinbeisser and M. Blum (1997). "The dorsalizing and neural inducing gene follistatin is an antagonist of BMP-4." Mech Dev **63**(1): 39-50.

Feeley, B. T., S. C. Gamradt, W. K. Hsu, N. Liu, L. Krenek, P. Robbins, J. Huard and J. R. Lieberman (2005). "Influence of BMPs on the formation of osteoblastic lesions in metastatic prostate cancer." J Bone Miner Res **20**(12): 2189-2199.

Feeley, B. T., L. Krenek, N. Liu, W. K. Hsu, S. C. Gamradt, E. M. Schwarz, J. Huard and J. R. Lieberman (2006). "Overexpression of noggin inhibits BMP-mediated growth of osteolytic prostate cancer lesions." Bone **38**(2): 154-166.

Ferrara, N. and T. Davis-Smyth (1997). "The biology of vascular endothelial growth factor." Endocr Rev **18**(1): 4-25.

Fidler, I. J. (1970). "Metastasis: quantitative analysis of distribution and fate of tumor emboli labeled with 125 I-5-iodo-2'-deoxyuridine." J Natl Cancer Inst **45**(4): 773-782.

Fidler, I. J. (2005). "Cancer biology is the foundation for therapy." Cancer Biol Ther **4**(9): 1036-1039.

Gassmann, P., J. Haier, K. Schlüter, B. Domikowsky, C. Wendel, U. Wiesner, R. Kubitz, R. Engers, S. W. Schneider, B. Homey and A. Müller (2009). "CXCR4 regulates the early extravasation of metastatic tumor cells in vivo." Neoplasia **11**(7): 651-661.

Gazzerro, E. and E. Canalis (2006). "Bone morphogenetic proteins and their antagonists." Rev Endocr Metab Disord **7**(1-2): 51-65.

Gazzerro, E., V. Gangji and E. Canalis (1998). "Bone morphogenetic proteins induce the expression of noggin, which limits their activity in cultured rat osteoblasts." J Clin Invest **102**(12): 2106-2114.

Geraghty, S., J. Q. Kuang, D. Yoo, M. LeRoux-Williams, C. T. Vangsness and A. Danilkovitch (2015). "A novel, cryopreserved, viable osteochondral allograft designed to augment marrow stimulation for articular cartilage repair." J Orthop Surg Res **10**: 66.

Golimbu, M., P. Morales, S. Al-Askari and J. Brown (1979). "Extended Pelvic Lymphadenectomy for Prostatic Cancer." J Urol **121**(5): 617-620.

Govender, S., C. Csima, H. K. Genant, A. Valentin-Opran, Y. Amit, R. Arbel, H. Aro, D. Atar, M. Bishay, M. G. Börner, P. Chiron, P. Choong, J. Cinats, B. Courtenay, R. Feibel, B. Geulette, C. Gravel, N. Haas, M. Raschke, E. Hammacher, D. van der Velde, P. Hardy, M. Holt, C. Josten, R. L. Ketterl, B. Lindeque, G. Lob, H. Mathevon, G. McCoy, D. Marsh, R. Miller, E. Munting, S. Oevre, L. Nordsletten, A. Patel, A. Pohl, W. Rennie, P. Reynders, P. M. Rommens, J. Rondia, W. C. Rossouw, P. J. Daneel, S. Ruff, A. Rüter, S. Santavirta, T. A. Schildhauer, C. Gekle, R. Schnettler, D. Segal, H. Seiler, R. B. Snowdowne, J. Stapert, G. Taglang, R. Verdonk, L. Vogels, A. Weckbach, A. Wentzensen, T. Wisniewski and B.-E. i. S. f. T. T. B. S. Group (2002). "Recombinant human bone morphogenetic protein-2 for treatment of open tibial fractures: a prospective, controlled, randomized study of four hundred and fifty patients." J Bone Joint Surg Am **84-A**(12): 2123-2134.

Graham, T. R., K. C. Agrawal and A. B. Abdel-Mageed (2010). "Independent and cooperative roles of tumor necrosis factor-alpha, nuclear factor-kappaB, and bone morphogenetic protein-2 in regulation of metastasis and osteomimicry of prostate cancer cells and differentiation and mineralization of MC3T3-E1 osteoblast-like cells." Cancer Sci **101**(1): 103-111.

Gravdal, K., O. J. Halvorsen, S. A. Haukaas and L. A. Akslen (2007). "A switch from E-cadherin to N-cadherin expression indicates epithelial to mesenchymal transition and is of strong and

independent importance for the progress of prostate cancer." Clin Cancer Res **13**(23): 7003-7011.

Greenwald, J., J. Groppe, P. Gray, E. Wiater, W. Kwiatkowski, W. Vale and S. Choe (2003). "The BMP7/ActRII extracellular domain complex provides new insights into the cooperative nature of receptor assembly." Mol Cell **11**(3): 605-617.

Griffith, D. L., P. C. Keck, T. K. Sampath, D. C. Rueger and W. D. Carlson (1996). "Three-dimensional structure of recombinant human osteogenic protein 1: structural paradigm for the transforming growth factor beta superfamily." Proc Natl Acad Sci U S A **93**(2): 878-883.

Hamdy, F. C., P. Autzen, M. C. Robinson, C. H. Horne, D. E. Neal and C. N. Robson (1997). "Immunolocalization and messenger RNA expression of bone morphogenetic protein-6 in human benign and malignant prostatic tissue." Cancer Res **57**(19): 4427-4431.

Hanahan, D. and R. A. Weinberg (2011). "Hallmarks of cancer: the next generation." Cell **144**(5): 646-674.

Haudenschild, D. R., S. M. Palmer, T. A. Moseley, Z. You and A. H. Reddi (2004). "Bone morphogenetic protein (BMP)-6 signaling and BMP antagonist noggin in prostate cancer." Cancer Res **64**(22): 8276-8284.

Hazan, R. B., G. R. Phillips, R. F. Qiao, L. Norton and S. A. Aaronson (2000). "Exogenous expression of N-cadherin in breast cancer cells induces cell migration, invasion, and metastasis." J Cell Biol **148**(4): 779-790.

Hazan, R. B., R. Qiao, R. Keren, I. Badano and K. Suyama (2004). "Cadherin switch in tumor progression." Ann N Y Acad Sci **1014**: 155-163.

Haÿ, E., J. Lemonnier, O. Fromigué and P. J. Marie (2001). "Bone morphogenetic protein-2 promotes osteoblast apoptosis through a Smad-independent, protein kinase C-dependent signaling pathway." J Biol Chem **276**(31): 29028-29036.

Hemmati-Brivanlou, A. and G. H. Thomsen (1995). "Ventral mesodermal patterning in *Xenopus* embryos: Expression patterns and activities of BMP-2 and BMP-4." Developmental Genetics **17**(1): 78-89.

Hogan, B. L. (1996). "Bone morphogenetic proteins: multifunctional regulators of vertebrate development." Genes Dev **10**(13): 1580-1594.

Horoszewicz, J. S., S. S. Leong, E. Kawinski, J. P. Karr, H. Rosenthal, T. M. Chu, E. A. Mirand and G. P. Murphy (1983). "LNCaP model of human prostatic carcinoma." Cancer Res **43**(4): 1809-1818.

Hsu, D. R., A. N. Economides, X. Wang, P. M. Eimon and R. M. Harland (1998). "The *Xenopus* dorsalizing factor Gremlin identifies a novel family of secreted proteins that antagonize BMP activities." Mol Cell **1**(5): 673-683.

Iemura, S., T. S. Yamamoto, C. Takagi, H. Uchiyama, T. Natsume, S. Shimasaki, H. Sugino and N. Ueno (1998). "Direct binding of follistatin to a complex of bone-morphogenetic protein and its receptor inhibits ventral and epidermal cell fates in early *Xenopus* embryo." Proc Natl Acad Sci U S A **95**(16): 9337-9342.

Kaighn, M. E., K. S. Narayan, Y. Ohnuki, J. F. Lechner and L. W. Jones (1979). "Establishment and characterization of a human prostatic carcinoma cell line (PC-3)." Invest Urol **17**(1): 16-23.

Katayama, M., S. Hirai, K. Kamihagi, K. Nakagawa, M. Yasumoto and I. Kato (1994). "Soluble E-cadherin fragments increased in circulation of cancer patients." Br J Cancer **69**(3): 580-585.

Kessenbrock, K., V. Plaks and Z. Werb (2010). "Matrix metalloproteinases: regulators of the tumor microenvironment." Cell **141**(1): 52-67.

Key, M. E. (1983). "Macrophages in cancer metastases and their relevance to metastatic growth." Cancer Metastasis Rev **2**(1): 75-88.

Kim, I. Y., D. H. Lee, H. J. Ahn, H. Tokunaga, W. Song, L. M. Devereaux, D. Jin, T. K. Sampath and R. A. Morton (2000). "Expression of bone morphogenetic protein receptors type-IA, -IB and -II correlates with tumor grade in human prostate cancer tissues." Cancer Res **60**(11): 2840-2844.

Kim, M., S. Yoon, S. Lee, S. A. Ha, H. K. Kim, J. W. Kim and J. Chung (2012). "Gremlin-1 induces BMP-independent tumor cell proliferation, migration, and invasion." PLoS One **7**(4): e35100.

Kingsley, D. M. (1994). "The TGF-beta superfamily: new members, new receptors, and new genetic tests of function in different organisms." Genes Dev **8**(2): 133-146.

Kirschenbaum, A., X. H. Liu, S. Yao, A. Leiter and A. C. Levine (2011). "Prostatic acid phosphatase is expressed in human prostate cancer bone metastases and promotes osteoblast differentiation." Ann N Y Acad Sci **1237**: 64-70.

Kobayashi, T., K. M. Lyons, A. P. McMahon and H. M. Kronenberg (2005). "BMP signaling stimulates cellular differentiation at multiple steps during cartilage development." Proc Natl Acad Sci U S A **102**(50): 18023-18027.

Koenenman, K. S., F. Yeung and L. W. Chung (1999). "Osteomimetic properties of prostate cancer cells: a hypothesis supporting the predilection of prostate cancer metastasis and growth in the bone environment." Prostate **39**(4): 246-261.

Korenchuk, S., J. E. Lehr, M. C. L. Y. G. Lee, S. Whitney, R. Vessella, D. L. Lin and K. J. Pienta (2001). "VCaP, a cell-based model system of human prostate cancer." In Vivo **15**(2): 163-168.

Kretzschmar, M. and J. Massagué (1998). "SMADs: mediators and regulators of TGF- $\beta$  signaling." Current Opinion in Genetics & Development **8**(1): 103-111.

Kuefer, R., M. D. Hofer, J. E. Gschwend, K. J. Pienta, M. G. Sanda, A. M. Chinnaiyan, M. A. Rubin and M. L. Day (2003). "The role of an 80 kDa fragment of E-cadherin in the metastatic progression of prostate cancer." Clin Cancer Res **9**(17): 6447-6452.

Kumagai, T., K. Tomari, T. Shimizu and K. Takeda (2006). "Alteration of gene expression in response to bone morphogenetic protein-2 in androgen-dependent human prostate cancer LNCaP cells." Int J Mol Med **17**(2): 285-291.

Kwon, H., H. J. Kim, W. L. Rice, B. Subramanian, S. H. Park, I. Georgakoudi and D. L. Kaplan (2010). "Development of an in vitro model to study the impact of BMP-2 on metastasis to bone." J Tissue Eng Regen Med **4**(8): 590-599.

Lai, T. H., Y. C. Fong, W. M. Fu, R. S. Yang and C. H. Tang (2008). "Osteoblasts-derived BMP-2 enhances the motility of prostate cancer cells via activation of integrins." Prostate **68**(12): 1341-1353.

Lamouille, S., J. Xu and R. Derynck (2014). "Molecular mechanisms of epithelial-mesenchymal transition." Nat Rev Mol Cell Biol **15**(3): 178-196.

Larson, S. R., X. Zhang, R. Dumpit, I. Coleman, B. Lakely, M. Roudier, C. S. Higano, L. D. True, P. H. Lange, B. Montgomery, E. Corey, P. S. Nelson, R. L. Vessella and C. Morrissey (2013). "Characterization of osteoblastic and osteolytic proteins in prostate cancer bone metastases." Prostate **73**(9): 932-940.

Laurila, R., S. Parkkila, J. Isola, A. Kallioniemi and E. L. Alarmo (2013). "The expression patterns of gremlin 1 and noggin in normal adult and tumor tissues." Int J Clin Exp Pathol **6**(7): 1400-1408.

Lavery, K., P. Swain, D. Falb and M. H. Alaoui-Ismaili (2008). "BMP-2/4 and BMP-6/7 differentially utilize cell surface receptors to induce osteoblastic differentiation of human bone marrow-derived mesenchymal stem cells." J Biol Chem **283**(30): 20948-20958.

Lee, Y., E. Schwarz, M. Davies, M. Jo, J. Gates, J. Wu, X. Zhang and J. R. Lieberman (2003). "Differences in the cytokine profiles associated with prostate cancer cell induced osteoblastic and osteolytic lesions in bone." J Orthop Res **21**(1): 62-72.

Lee, Y. C., J. K. Jin, C. J. Cheng, C. F. Huang, J. H. Song, M. Huang, W. S. Brown, S. Zhang, L. Y. Yu-Lee, E. T. Yeh, B. W. McIntyre, C. J. Logothetis, G. E. Gallick and S. H. Lin (2013). "Targeting Constitutively Activated  $\beta$ (1) Integrins inhibits Prostate Cancer Metastasis." Molecular cancer research : MCR **11**(4): 405-417.

Li, G., K. Satyamoorthy and M. Herlyn (2001). "N-cadherin-mediated intercellular interactions promote survival and migration of melanoma cells." Cancer Res **61**(9): 3819-3825.

Livak, K. J. and T. D. Schmittgen (2001). "Analysis of relative gene expression data using real-time quantitative PCR and the 2(-Delta Delta C(T)) Method." Methods **25**(4): 402-408.

Logothetis, C. J. and S. H. Lin (2005). "Osteoblasts in prostate cancer metastasis to bone." Nat Rev Cancer **5**(1): 21-28.

Luu, H. H., W. X. Song, X. Luo, D. Manning, J. Luo, Z. L. Deng, K. A. Sharff, A. G. Montag, R. C. Haydon and T. C. He (2007). "Distinct roles of bone morphogenetic proteins in osteogenic differentiation of mesenchymal stem cells." J Orthop Res **25**(5): 665-677.

Luzzi, K. J., I. C. MacDonald, E. E. Schmidt, N. Kerkvliet, V. L. Morris, A. F. Chambers and A. C. Groom (1998). "Multistep nature of metastatic inefficiency: dormancy of solitary cells after successful extravasation and limited survival of early micrometastases." Am J Pathol **153**(3): 865-873.

Lynch, C. C. (2011). "Matrix metalloproteinases as master regulators of the vicious cycle of bone metastasis." Bone **48**(1): 44-53.

Massague, J. (1998). "TGF-beta signal transduction." Annu Rev Biochem **67**: 753-791.

Masuda, H., Y. Fukabori, K. Nakano, N. Shimizu and H. Yamanaka (2004). "Expression of bone morphogenetic protein-7 (BMP-7) in human prostate." Prostate **59**(1): 101-106.

Masuda, H., Y. Fukabori, K. Nakano, Y. Takezawa, T. CSuzuki and H. Yamanaka (2003). "Increased expression of bone morphogenetic protein-7 in bone metastatic prostate cancer." Prostate **54**(4): 268-274.

McCutcheon, M., D. R. Coman and F. B. Moore (1948). "Studies on invasiveness of cancer; adhesiveness of malignant cells in various human adenocarcinomas." Cancer **1**(3): 460-467.

Merino, R., J. Rodriguez-Leon, D. Macias, Y. Gañan, A. N. Economides and J. M. Hurlle (1999). "The BMP antagonist Gremlin regulates outgrowth, chondrogenesis and programmed cell death in the developing limb." Development **126**(23): 5515-5522.

Metheny-Barlow, L. J. and L. Y. Li (2003). "The enigmatic role of angiopoietin-1 in tumor angiogenesis." Cell Res **13**(5): 309-317.

Miyazaki, H., T. Watabe, T. Kitamura and K. Miyazono (2004). "BMP signals inhibit proliferation and in vivo tumor growth of androgen-insensitive prostate carcinoma cells." Oncogene **23**(58): 9326-9335.

Miyazono, K., S. Maeda and T. Imamura (2005). "BMP receptor signaling: transcriptional targets, regulation of signals, and signaling cross-talk." Cytokine Growth Factor Rev **16**(3): 251-263.

Mizrahi, O., D. Sheyn, W. Tawackoli, I. Kallai, A. Oh, S. Su, X. Da, P. Zarrini, G. Cook-Wiens, D. Gazit and Z. Gazit (2013). "BMP-6 is more efficient in bone formation than BMP-2 when overexpressed in mesenchymal stem cells." Gene Ther **20**(4): 370-377.

Mol, A. J., A. A. Geldof, G. A. Meijer, H. G. van der Poel and R. J. van Moorselaar (2007). "New experimental markers for early detection of high-risk prostate cancer: role of cell-cell adhesion and cell migration." J Cancer Res Clin Oncol **133**(10): 687-695.

Morrissey, C., L. G. Brown, T. E. Pitts, R. L. Vessella and E. Corey (2010). "Bone morphogenetic protein 7 is expressed in prostate cancer metastases and its effects on prostate tumor cells depend on cell phenotype and the tumor microenvironment." Neoplasia **12**(2): 192-205.

Mosig, R. A., O. Dowling, A. DiFeo, M. C. Ramirez, I. C. Parker, E. Abe, J. Diouri, A. A. Aqeel, J. D. Wylie, S. A. Oblander, J. Madri, P. Bianco, S. S. Apte, M. Zaidi, S. B. Doty, R. J. Majeska, M. B. Schaffler and J. A. Martignetti (2007). "Loss of MMP-2 disrupts skeletal and craniofacial development and results in decreased bone mineralization, joint erosion and defects in osteoblast and osteoclast growth." Hum Mol Genet **16**(9): 1113-1123.

Mueller, T. D. and J. Nickel (2012). "Promiscuity and specificity in BMP receptor activation." FEBS Lett **586**(14): 1846-1859.

Mundy, G. R. (2002). "Metastasis to bone: causes, consequences and therapeutic opportunities." Nat Rev Cancer **2**(8): 584-593.

Nabha, S. M., E. B. dos Santos, H. A. Yamamoto, A. Belizi, Z. Dong, H. Meng, A. Saliganan, A. Sabbota, R. D. Bonfil and M. L. Cher (2008). "Bone marrow stromal cells enhance prostate cancer cell invasion through type I collagen in an MMP-12 dependent manner." Int J Cancer **122**(11): 2482-2490.

Nagle, R. B., J. D. Knox, C. Wolf, G. T. Bowden and A. E. Cress (1994). "Adhesion molecules, extracellular matrix, and proteases in prostate carcinoma." J Cell Biochem Suppl **19**: 232-237.

Navone, N. M., M. Olive, M. Ozen, R. Davis, P. Troncoso, S. M. Tu, D. Johnston, A. Pollack, S. Pathak, A. C. von Eschenbach and C. J. Logothetis (1997). "Establishment of two human prostate cancer cell lines derived from a single bone metastasis." Clin Cancer Res **3**(12 Pt 1): 2493-2500.

Nawrocki-Raby, B., C. Gilles, M. Polette, E. Bruyneel, J. Y. Laronze, N. Bonnet, J. M. Foidart, M. Mareel and P. Birembaut (2003). "Upregulation of MMPs by soluble E-cadherin in human lung tumor cells." Int J Cancer **105**(6): 790-795.

Nemeth, J. A., J. F. Harb, U. Barroso, Z. He, D. J. Grignon and M. L. Cher (1999). "Severe combined immunodeficient-hu model of human prostate cancer metastasis to human bone." Cancer Res **59**(8): 1987-1993.

Nemeth, J. A., R. Yousif, M. Herzog, M. Che, J. Upadhyay, B. Shekarriz, S. Bhagat, C. Mullins, R. Fridman and M. L. Cher (2002). "Matrix metalloproteinase activity, bone matrix turnover, and tumor cell proliferation in prostate cancer bone metastasis." J Natl Cancer Inst **94**(1): 17-25.

Nieswandt, B., M. Hafner, B. Echtenacher and D. N. Männel (1999). "Lysis of tumor cells by natural killer cells in mice is impeded by platelets." Cancer Res **59**(6): 1295-1300.

Nohe, A., S. Hassel, M. Ehrlich, F. Neubauer, W. Sebald, Y. I. Henis and P. Knaus (2002). "The mode of bone morphogenetic protein (BMP) receptor oligomerization determines different BMP-2 signaling pathways." J Biol Chem **277**(7): 5330-5338.

Nohe, A., E. Keating, P. Knaus and N. O. Petersen (2004). "Signal transduction of bone morphogenetic protein receptors." Cell Signal **16**(3): 291-299.

Ottewell, P. D. (2016). "The role of osteoblasts in bone metastasis." J Bone Oncol **5**(3): 124-127.

Oxford, G. and D. Theodorescu (2003). "Ras superfamily monomeric G proteins in carcinoma cell motility." Cancer Lett **189**(2): 117-128.

Paget, S. (1889). "THE DISTRIBUTION OF SECONDARY GROWTHS IN CANCER OF THE BREAST." The Lancet **133**(3421): 571-573.

Palumbo, J. S., K. E. Talmage, J. V. Massari, C. M. La Jeunesse, M. J. Flick, K. W. Kombrinck, M. Jirousková and J. L. Degen (2005). "Platelets and fibrin(ogen) increase metastatic potential by impeding natural killer cell-mediated elimination of tumor cells." Blood **105**(1): 178-185.

Papanagiotou, M., Z. H. Dailiana, T. Karachalios, S. Varitimidis, M. Vlychou, M. Hantes and K. N. Malizos (2015). "RhBMP-7 for the treatment of nonunion of fractures of long bones." Bone Joint J **97-B**(7): 997-1003.

Pereira, R. C., A. N. Economides and E. Canalis (2000). "Bone morphogenetic proteins induce gremlin, a protein that limits their activity in osteoblasts." Endocrinology **141**(12): 4558-4563.

Pignatti, E., R. Zeller and A. Zuniga (2014). "To BMP or not to BMP during vertebrate limb bud development." Seminars in Cell & Developmental Biology **32**: 119-127.

Re'em-Kalma, Y., T. Lamb and D. Frank (1995). "Competition between noggin and bone morphogenetic protein 4 activities may regulate dorsalization during *Xenopus* development." Proc Natl Acad Sci U S A **92**(26): 12141-12145.

Reymond, N., B. B. d'Água and A. J. Ridley (2013). "Crossing the endothelial barrier during metastasis." Nat Rev Cancer **13**(12): 858-870.

Ridley, A. J. (2015). "Rho GTPase signalling in cell migration." Curr Opin Cell Biol **36**: 103-112.

Roodman, G. D. (2004). "Mechanisms of bone metastasis." N Engl J Med **350**(16): 1655-1664.

Roudier, M. P., C. Morrissey, L. D. True, C. S. Higano, R. L. Vessella and S. M. Ott (2008). "Histopathological assessment of prostate cancer bone osteoblastic metastases." J Urol **180**(3): 1154-1160.

Scheufler, C., W. Sebald and M. Hulsmeyer (1999). "Crystal structure of human bone morphogenetic protein-2 at 2.7 Å resolution." J Mol Biol **287**(1): 103-115.

Schwaninger, R., C. A. Rentsch, A. Wetterwald, G. van der Horst, R. L. van Bezooijen, G. van der Pluijm, C. W. Löwik, K. Ackermann, W. Pyerin, F. C. Hamdy, G. N. Thalmann and M. G. Cecchini (2007). "Lack of noggin expression by cancer cells is a determinant of the osteoblast response in bone metastases." Am J Pathol **170**(1): 160-175.

Sebald, W., J. Nickel, J. L. Zhang and T. D. Mueller (2004). "Molecular recognition in bone morphogenetic protein (BMP)/receptor interaction." *Biol Chem* **385**(8): 697-710.

Secondini, C., A. Wetterwald, R. Schwaninger, G. N. Thalmann and M. G. Cecchini (2011). "The role of the BMP signaling antagonist noggin in the development of prostate cancer osteolytic bone metastasis." *PLoS One* **6**(1): e16078.

Sekelsky, J. J., S. J. Newfeld, L. A. Raftery, E. H. Chartoff and W. M. Gelbart (1995). "Genetic characterization and cloning of mothers against dpp, a gene required for decapentaplegic function in *Drosophila melanogaster*." *Genetics* **139**(3): 1347-1358.

Selever, J., W. Liu, M. F. Lu, R. R. Behringer and J. F. Martin (2004). "Bmp4 in limb bud mesoderm regulates digit pattern by controlling AER development." *Dev Biol* **276**(2): 268-279.

Sengle, G., R. N. Ono, K. M. Lyons, H. P. Bächinger and L. Y. Sakai (2008). "A new model for growth factor activation: type II receptors compete with the prodomain for BMP-7." *J Mol Biol* **381**(4): 1025-1039.

Sepporta, M. V., F. M. Tumminello, C. Flandina, M. Crescimanno, M. Giammanco, M. La Guardia, D. di Majo and G. Leto (2013). "Follistatin as potential therapeutic target in prostate cancer." *Target Oncol* **8**(4): 215-223.

Sequeira, L., C. W. Dubyk, T. A. Riesenberger, C. R. Cooper and K. L. van Golen (2008). "Rho GTPases in PC-3 prostate cancer cell morphology, invasion and tumor cell diapedesis." *Clin Exp Metastasis* **25**(5): 569-579.

Shi, Y. and J. Massagué (2003). "Mechanisms of TGF-beta signaling from cell membrane to the nucleus." *Cell* **113**(6): 685-700.

Shibue, T. and R. A. Weinberg (2011). "Metastatic colonization: Settlement, adaptation and propagation of tumor cells in a foreign tissue environment." *Seminars in Cancer Biology* **21**(2): 99-106.

Shih, W. and S. Yamada (2012). "N-cadherin-mediated cell–cell adhesion promotes cell migration in a three-dimensional matrix." *Journal of Cell Science* **125**(15): 3661-3670.

Shweiki, D., A. Itin, D. Soffer and E. Keshet (1992). "Vascular endothelial growth factor induced by hypoxia may mediate hypoxia-initiated angiogenesis." *Nature* **359**(6398): 843-845.

Sieber, C., J. Kopf, C. Hiepen and P. Knaus (2009). "Recent advances in BMP receptor signaling." *Cytokine Growth Factor Rev* **20**(5-6): 343-355.

Sieh, S., A. V. Taubenberger, M. L. Lehman, J. A. Clements, C. C. Nelson and D. W. Huttmacher (2014). "Paracrine interactions between LNCaP prostate cancer cells and bioengineered bone in 3D in vitro culture reflect molecular changes during bone metastasis." *Bone* **63**: 121-131.

Sopory, S., S. M. Nelsen, C. Degnin, C. Wong and J. L. Christian (2006). "Regulation of bone morphogenetic protein-4 activity by sequence elements within the prodomain." *J Biol Chem* **281**(45): 34021-34031.

Sottnik, J. L., S. Daignault-Newton, X. Zhang, C. Morrissey, M. H. Hussain, E. T. Keller and C. L. Hall (2013). "Integrin alpha2beta 1 (alpha2beta1) promotes prostate cancer skeletal metastasis." *Clin Exp Metastasis* **30**(5): 569-578.

Spanjol, J., G. Djordjević, D. Markić, M. Klarić, D. Fuckar and D. Bobinac (2010). "Role of bone morphogenetic proteins in human prostate cancer pathogenesis and development of bone metastases: immunohistochemical study." *Coll Antropol* **34 Suppl 2**: 119-125.

Stewart, A., H. Guan and K. Yang (2010). "BMP-3 promotes mesenchymal stem cell proliferation through the TGF-beta/activin signaling pathway." *J Cell Physiol* **223**(3): 658-666.

Stoletov, K., H. Kato, E. Zardoujian, J. Kelber, J. Yang, S. Shattil and R. Klemke (2010). "Visualizing extravasation dynamics of metastatic tumor cells." *J Cell Sci* **123**(Pt 13): 2332-2341.

Stone, K. R., D. D. Mickey, H. Wunderli, G. H. Mickey and D. F. Paulson (1978). "Isolation of a human prostate carcinoma cell line (DU 145)." *Int J Cancer* **21**(3): 274-281.

Szulcek, R., H. J. Bogaard and G. P. van Nieuw Amerongen (2014). "Electric cell-substrate impedance sensing for the quantification of endothelial proliferation, barrier function, and motility." *J Vis Exp*(85).

Sánchez-Tilló, E., Y. Liu, O. de Barrios, L. Siles, L. Fanlo, M. Cuatrecasas, D. S. Darling, D. C. Dean, A. Castells and A. Postigo (2012). "EMT-activating transcription factors in cancer: beyond EMT and tumor invasiveness." *Cell Mol Life Sci* **69**(20): 3429-3456.

Takashima, A. and D. V. Faller (2013). "Targeting the RAS oncogene." *Expert opinion on therapeutic targets* **17**(5): 507-531.

Tarin, D., J. E. Price, M. G. Kettlewell, R. G. Souter, A. C. Vass and B. Crossley (1984). "Mechanisms of human tumor metastasis studied in patients with peritoneovenous shunts." *Cancer Res* **44**(8): 3584-3592.

Theriault, R. L. (2012). "Biology of bone metastases." *Cancer Control* **19**(2): 92-101.

Thiery, J. P. (2002). "Epithelial-mesenchymal transitions in tumour progression." *Nat Rev Cancer* **2**(6): 442-454.

Thiery, J. P., H. Acloque, R. Y. Huang and M. A. Nieto (2009). "Epithelial-mesenchymal transitions in development and disease." *Cell* **139**(5): 871-890.

Thomas, B. G. and F. C. Hamdy (2000). "Bone morphogenetic protein-6: potential mediator of osteoblastic metastases in prostate cancer." *Prostate Cancer Prostatic Dis* **3**(4): 283-285.

Thomas, R., W. A. Anderson, V. Raman and A. H. Reddi (1998). "Androgen-dependent gene expression of bone morphogenetic protein 7 in mouse prostate." *Prostate* **37**(4): 236-245.

Tomari, K., T. Kumagai, T. Shimizu and K. Takeda (2005). "Bone morphogenetic protein-2 induces hypophosphorylation of Rb protein and repression of E2F in androgen-treated LNCaP human prostate cancer cells." *Int J Mol Med* **15**(2): 253-258.

Tumminello, F. M., G. Badalamenti, F. Fulfarò, L. Incorvaia, M. Crescimanno, C. Flandina, M. V. Sepporta and G. Leto (2010). "Serum follistatin in patients with prostate cancer metastatic to the bone." *Clin Exp Metastasis* **27**(8): 549-555.

Tylzanowski, P., L. Mebis and F. P. Luyten (2006). "The Noggin null mouse phenotype is strain dependent and haploinsufficiency leads to skeletal defects." *Dev Dyn* **235**(6): 1599-1607.

UK, C. R. (2017). "<http://www.cancerresearchuk.org/about-cancer/secondary-cancer/secondary-bone-cancer/treatment>." Retrieved 9th May, 2018.

Vesuna, F., P. van Diest, J. H. Chen and V. Raman (2008). "Twist is a transcriptional repressor of E-cadherin gene expression in breast cancer." *Biochem Biophys Res Commun* **367**(2): 235-241.

Walsh, D. W., C. Godson, D. P. Brazil and F. Martin (2010). "Extracellular BMP-antagonist regulation in development and disease: tied up in knots." *Trends Cell Biol* **20**(5): 244-256.

Wang, R. N., J. Green, Z. Wang, Y. Deng, M. Qiao, M. Peabody, Q. Zhang, J. Ye, Z. Yan, S. Denduluri, O. Idowu, M. Li, C. Shen, A. Hu, R. C. Haydon, R. Kang, J. Mok, M. J. Lee, H. L. Luu and L. L. Shi (2014). "Bone Morphogenetic Protein (BMP) signaling in development and human diseases." *Genes Dis* **1**(1): 87-105.

Weiss, L. (1990). "Metastatic inefficiency." *Adv Cancer Res* **54**: 159-211.

Weiss, L., D. S. Dimitrov and M. Angelova (1985). "The hemodynamic destruction of intravascular cancer cells in relation to myocardial metastasis." *Proc Natl Acad Sci U S A* **82**(17): 5737-5741.

Wirtz, D., K. Konstantopoulos and P. C. Searson (2011). "The physics of cancer: the role of physical interactions and mechanical forces in metastasis." *Nat Rev Cancer* **11**(7): 512-522.

Wood, M., K. Fudge, J. L. Mohler, A. R. Frost, F. Garcia, M. Wang and M. E. Stearns (1997). "In situ hybridization studies of metalloproteinases 2 and 9 and TIMP-1 and TIMP-2 expression in human prostate cancer." *Clin Exp Metastasis* **15**(3): 246-258.

Wozney, J. M., V. Rosen, A. J. Celeste, L. M. Mitsock, M. J. Whitters, R. W. Kriz, R. M. Hewick and E. A. Wang (1988). "Novel regulators of bone formation: molecular clones and activities." *Science* **242**(4885): 1528-1534.

Wu, M., G. Chen and Y. P. Li (2016). "TGF-beta and BMP signaling in osteoblast, skeletal development, and bone formation, homeostasis and disease." *Bone Res* **4**: 16009.

Yamaguchi, A., T. Ishizuya, N. Kintou, Y. Wada, T. Katagiri, J. M. Wozney, V. Rosen and S. Yoshiki (1996). "Effects of BMP-2, BMP-4, and BMP-6 on osteoblastic differentiation of bone marrow-derived stromal cell lines, ST2 and MC3T3-G2/PA6." *Biochem Biophys Res Commun* **220**(2): 366-371.

Yamaji, N., A. J. Celeste, R. S. Thies, J. J. Song, S. M. Bernier, D. Goltzman, K. M. Lyons, J. Nove, V. Rosen and J. M. Wozney (1994). "A mammalian serine/threonine kinase receptor specifically binds BMP-2 and BMP-4." Biochem Biophys Res Commun **205**(3): 1944-1951.

Yamashita, H., P. ten Dijke, D. Huylebroeck, T. K. Sampath, M. Andries, J. C. Smith, C. H. Heldin and K. Miyazono (1995). "Osteogenic protein-1 binds to activin type II receptors and induces certain activin-like effects." J Cell Biol **130**(1): 217-226.

Yang, J., K. Fizazi, S. Peleg, C. R. Sikes, A. K. Raymond, N. Jamal, M. Hu, M. Olive, L. A. Martinez, C. G. Wood, C. J. Logothetis, G. Karsenty and N. M. Navone (2001). "Prostate cancer cells induce osteoblast differentiation through a Cbfa1-dependent pathway." Cancer Res **61**(14): 5652-5659.

Yao, H., C. M. Dashner, E. J. van Golen, K. L. van Golen, C. M. van Golen and K. L. van Golen (2009). "RhoC GTPase is required for PC-3 prostate cancer cell invasion but not motility." (0950-9232 (Print)).

Ye, L., J. M. Lewis-Russell, H. Kynaston and W. G. Jiang (2007). "Endogenous bone morphogenetic protein-7 controls the motility of prostate cancer cells through regulation of bone morphogenetic protein antagonists." J Urol **178**(3 Pt 1): 1086-1091.

Ye, L., J. M. Lewis-Russell, A. J. Sanders, H. Kynaston and W. G. Jiang (2008). "HGF/SF up-regulates the expression of bone morphogenetic protein 7 in prostate cancer cells." Urol Oncol **26**(2): 190-197.

Yin, J. J., C. B. Pollock and K. Kelly (2005). "Mechanisms of cancer metastasis to the bone." Cell Res **15**(1): 57-62.

Yuen, H. F., W. K. Kwok, K. K. Chan, C. W. Chua, Y. P. Chan, Y. Y. Chu, Y. C. Wong, X. Wang and K. W. Chan (2008). "TWIST modulates prostate cancer cell-mediated bone cell activity and is upregulated by osteogenic induction." Carcinogenesis **29**(8): 1509-1518.

Zabkiewicz, C., J. Resaul, R. Hargest, W. G. Jiang and L. Ye (2017). "Increased Expression of Follistatin in Breast Cancer Reduces Invasiveness and Clinically Correlates with Better Survival." Cancer Genomics Proteomics **14**(4): 241-251.

Zheng, Y., H. Zhou, C. R. Dunstan, R. L. Sutherland and M. J. Seibel (2013). "The role of the bone microenvironment in skeletal metastasis." J Bone Oncol **2**(1): 47-57.

Zhu, W., J. Kim, C. Cheng, B. A. Rawlins, O. Boachie-Adjei, R. G. Crystal and C. Hidaka (2006). "Noggin regulation of bone morphogenetic protein (BMP) 2/7 heterodimer activity in vitro." Bone **39**(1): 61-71.

Zimmerman, L. B., J. M. De Jesús-Escobar and R. M. Harland (1996). "The Spemann organizer signal noggin binds and inactivates bone morphogenetic protein 4." Cell **86**(4): 599-606.

Zou, H. and L. Niswander (1996). "Requirement for BMP signaling in interdigital apoptosis and scale formation." Science **272**(5262): 738-741.

# Appendix

	PC-3	DU-145	LNCaP
BMP-7	Very low Moderately high (3) Moderately high (4)	Very high Very high (3) Higher (4)	High (2) Very low (1) Very low (3) Very low (4)
BMP-2	High (1) Moderately high (2) Very low (3)	Moderately high (1) Very low (3)	Very low (1) Very high (2) Moderately high (3)
BMP-4	Very high (1) High (2) High (3)	High (1) Very high (2) Very low (3)	High Very high (3)
BMP-6	Very low (1) Moderately high (3)	Moderately high (1) (3)	High (1) Very low (3)
Noggin	Very high (3)	Very high (3)	Very high (3)
Follistatin	Very high (3)	High (3)	Very high (3)
BMPRII	High (1) Very low (2) High (3)	High (1) Extremely high (2) High (3)	Very high (1) Extremely high (2) Moderately high (3)
ActRI	High (2)	Very high (2)	Very high (2)
ActRII	Higher (1) High (2)	High (1) Extremely high (2)	High (1) Extremely high (2)
ActRIIB	High (1) Very high (2)	Higher (1) Extremely high (2)	Moderately high (1) Very high (2)
ALK1	Very low (1)	Very low (1)	Very low (1)
ALK2	Higher (1)	Higher (1)	High (1)
ALK3 (BMPRI-1A)	Very high (1) High (2)	Very high (1) Extremely high (2)	High (1) Very high (2)
ALK4	High (1)	Higher (1)	High (1)
ALK5 (TGF- $\beta$ RI)	High (1)	Higher (1)	High (1)
ALK6 (BMPRI-1B)	Very high (1) Higher (2) Extremely high (3)	Moderately high (1) Very high (2) Extremely high (3)	Very low (1) Very high (2) High (3)
Smad1	Higher (1)	Higher (1)	High (1)
Smad2	Higher (1)	Very high (1)	Very high (1)
Smad3	High (1)	Very high (1)	Moderately high (1)
Smad4	High (1)	Moderately high (1)	Very high (1)
Smad5	Very high (1)	Extremely high (1)	Very high (1)
Smad6			
Smad7			
Smad8/9	Moderately high (1)	Extremely high (1)	High (1)

References: 1 – Miyazaki, Watabe et al. 2002; 2 – Yang, Zhong et al. 2003; 3 – Ye, Lewis-Russell et al. 2007; 4 – Ye, Lewis-Russell et al. 2008

**Table A1: Expression of BMPs and their signalling components in different studies.** The table lists some of the different results obtained from studies that assessed the expression of BMP and their signalling components in different prostate cancer cell lines.

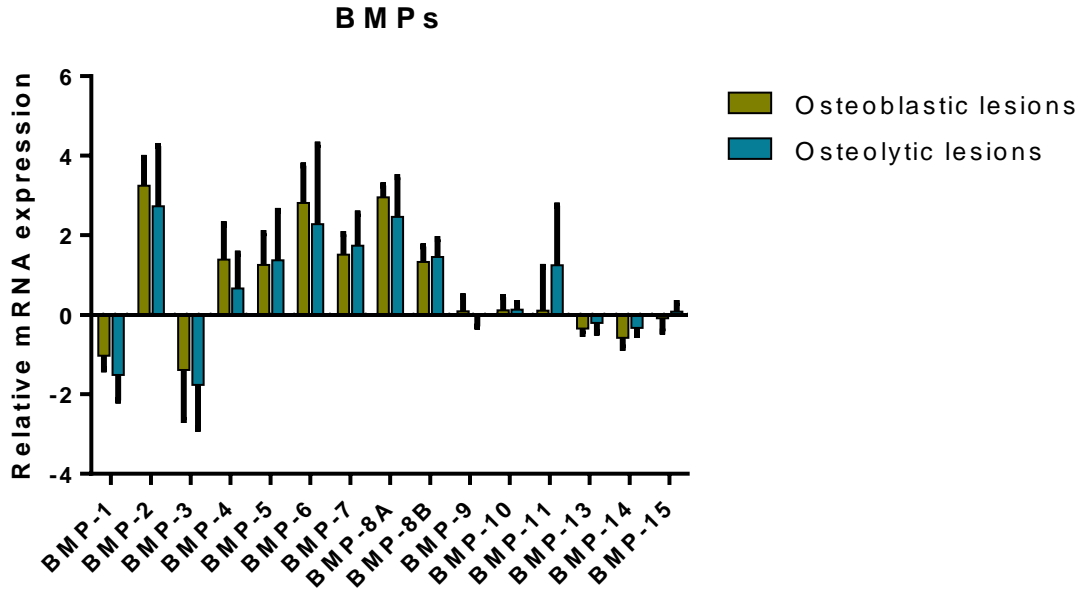


**Figure A1: Differential expression of BMPs in osteoblastic and osteolytic prostate cancer bone lesions.** The data represents mean + SD of BMP expression results from a microarray study by Larson et al (2003; GSE41619). Significance was assessed by t-test using the Holm-Sidak method.

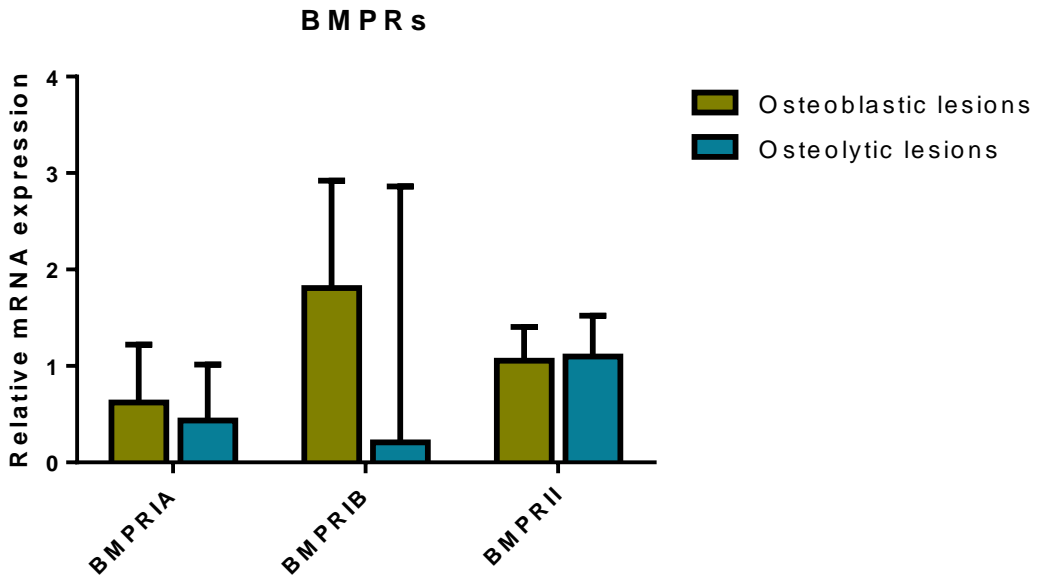


**Figure A2: Differential expression of BMPRs in osteoblastic and osteolytic prostate cancer bone lesions.** The data represents mean + SD of BMP expression results from a microarray study by Larson et al (2003; GSE41619). Significance was assessed by t-test using the Holm-Sidak method.

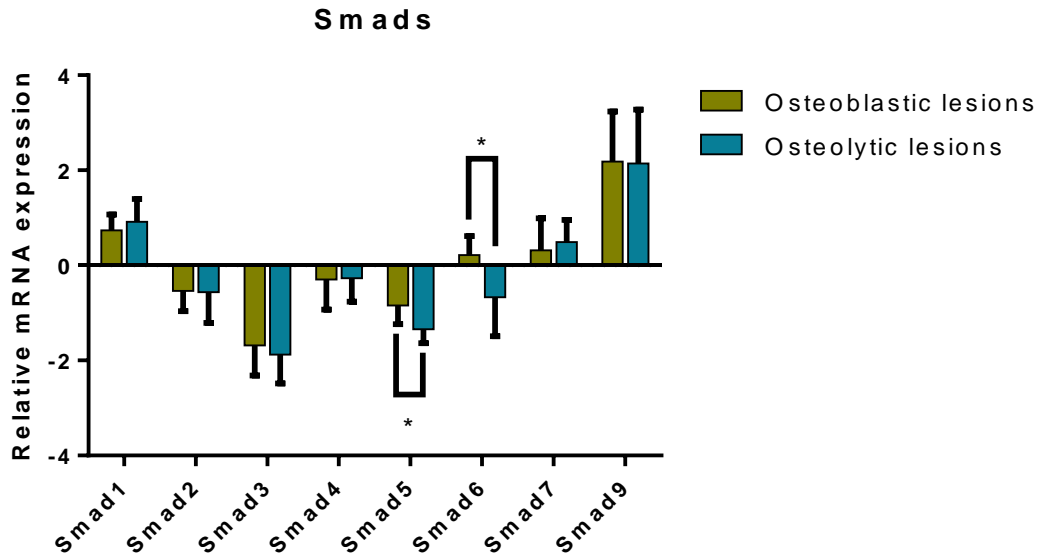


**Figure A3: Differential expression of Smads in osteoblastic and osteolytic prostate cancer bone lesions.** The data represents mean + SD of BMP expression results from a microarray study by Larson et al (2003; GSE41619). Significance was assessed by t-test using the Holm-Sidak method (\* $p \leq 0.05$ ).

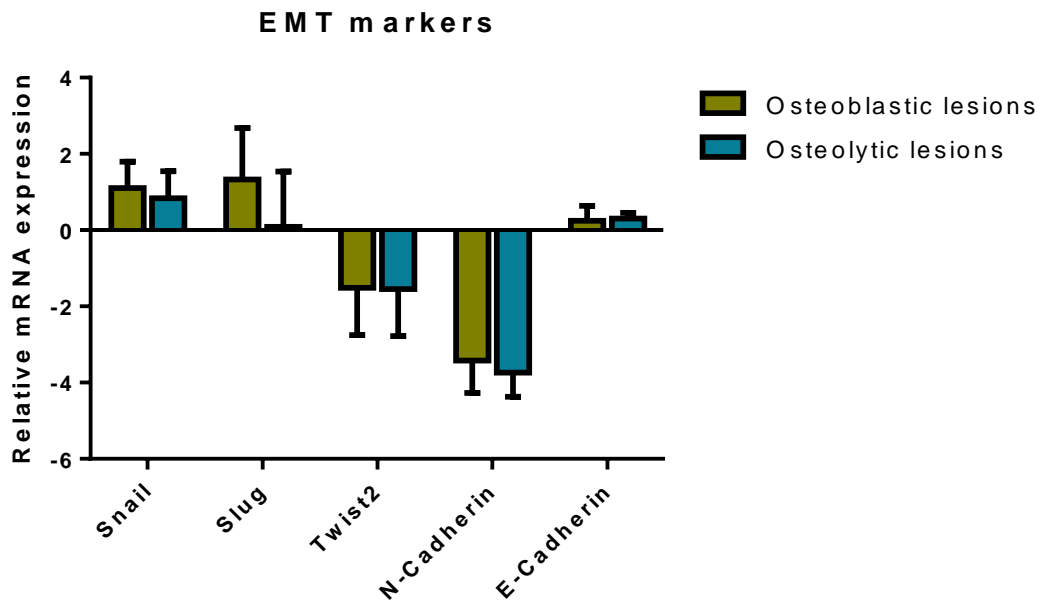


**Figure A4: Differential expression of EMT markers in osteoblastic and osteolytic prostate cancer bone lesions.** The data represents mean + SD of BMP expression results from a microarray study by Larson et al (2003; GSE41619). Significance was assessed by t-test using the Holm-Sidak method.

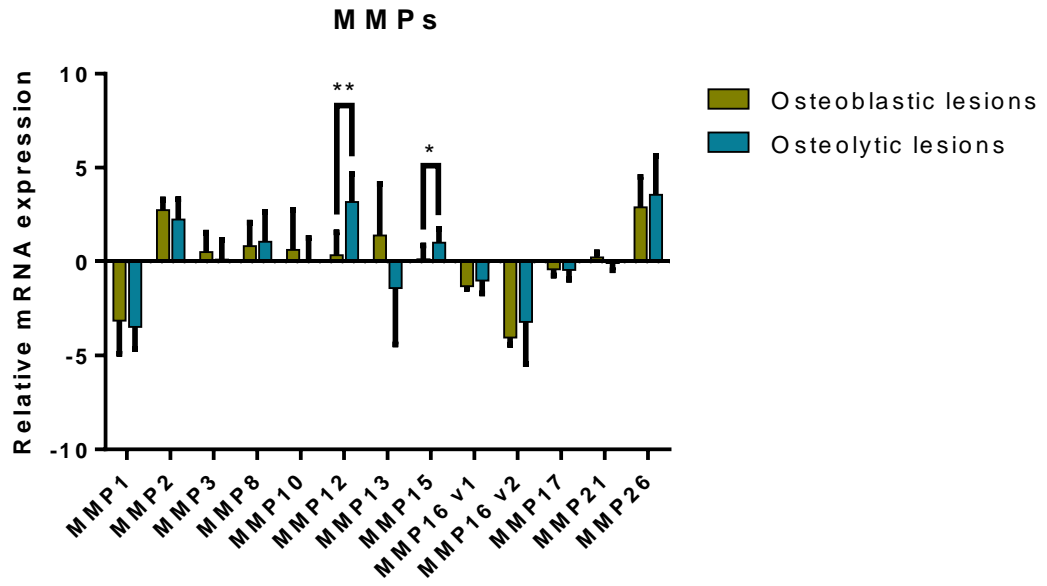


**Figure A5: Differential expression of MMPs in osteoblastic and osteolytic prostate cancer bone lesions.** The data represents mean + SD of BMP expression results from a microarray study by Larson et al (2003; GSE41619). Significance was assessed by t-test using the Holm-Sidak method (\*  $p \leq 0.05$ , \*\*  $p \leq 0.01$ ).

